HYDROLOGICAL STUDY FOR REVIVAL AND RESTORATION OF TRADITIONAL WATER BODIES IN BIKANER, RAJASTHAN

STUDY TEAM

Dr. A. K. Lohani, Sc-G, *Project Coordinator*
Dr. L. N. Thakural, Sc-E, *Lead PI*
Sh. J. P. Patra, Sc-E, *PI*
Dr. M. K. Shama, Sc-F, *PI*
Dr. Rahul Kumar Jaiswal, Sc-F, *PI*
Dr. P. K. Mishra, Sc-D, *PI*
Dr. Nitesh Patidaar, Sc-C, *PI*
Sh. N. K. Bhatnagar, Sc-B, *Co-PI*
Sh. Jatin Malhotra, SRA, *Co-PI*
Abhishek Agrawal, *Resource Person*

NATIONAL INSTITUTE OF HYDROLOGY
JALVIGIYAN BHAVAN, ROORKEE
(2024-25)

Preface

Small traditional waterbodies including ponds and tanks are the most important water sources especially in rural areas. These waterbodies are increasingly recognized for their role in meeting rural water needs, aquifer recharge, providing livelihood opportunity, maintaining ecological balance and ecosystem services (Biggs et al., 2016). Small waterbodies are playing vital role in socio-cultural, economic and environmental development. Often, tanks and ponds support rural livelihoods of the marginalized community in rural, urban, coastal and tribal areas. There are about 5,00,000 tanks in India and mostly situated in semi-arid parts of India. As per 5th Census of Minor Irrigation Schemes Report, in surface flow schemes, tanks/ ponds have largest share of 41% followed by reservoir (14%) and temporary diversions (10%). These tanks help in capturing the runoff during monsoon and providing water for irrigation and other multiple uses for the community. However, continued unsustainable exploitation, increasing negligence and lack of conservation and urban growth resulting in huge adverse impact on these small waterbodies. Waterbodies are the lifeline for human existence and always the backbone of water resource sustainability in any urban area. They are going to disappear around the world. Solid waste dumping, industrial pollution, sewage pollution, encroachments, commercial fish farming and other practices are the main causes of this situation. Urbanization and industrialization have increased the intensity of pollution to such an extent that waterbodies' self-healing capacities are no longer enough to counter these multiple onslaughts. Flood mitigation, groundwater recharge, biodiversity enhancement, industrial development and water security are just a few of the benefits that waterbodies provide to a city. It is time their role is properly evaluated in the urban economy and effective actions are initiated for their rejuvenation. Bikaner city has a number of water bodies since ancient time, which has been disappeared due to ignorance and non-maintenance of these water bodies. Bikaner city will be studied followed by broad recommendations on site-specific approaches for revival and restoration.

The study entitled 'Hydrological study for revival and restoration of traditional water bodies in Bikaner, Rajasthan', being carried out at Surface Water Hydrology Division, National Institute of Hydrology, Roorkee. The study group comprises of Dr. L. N. Thakural, Sc-E, Dr. A. K. Lohani, Sc-G, Sh. J. P. Patra, Sc-E, Dr. M. K. Shama, Sc-F, Dr. Rahul Kumar Jaiswal, Sc-F, Dr. P. K. Mishra, Sc-D, Dr. Nitesh Patidaar, Sc-C, Dr. Anil Kumar Chhangani, Professor, Sh. N. K. Bhatnagar, Sc-B, Sh. Jatin Malhotra, SRA, Abhishek Agrawal, Resource Person

(M. K. Goel)
Director

Abstract

Bikaner city has a number of water bodies since ancient time, which has been disappeared due to ignorance and non-maintenance of these water bodies. Due to over exploitation and increasing pressure on the natural resource and biodiversity, water bodies are declining. The study focuses on revival and restoration of traditional water bodies in Bikaner, Rajasthan with the objectives including mainly inventory of water bodies in Bikaner, Long-term spatio-temporal analysis of rainfall and temperature variables, Landuse/Land cover (LULC) change detection, Trend analysis of groundwater levels and assessment of recharge to groundwater, surface water availability, soil loss assessment, and both quantitative and water quality assessment of pilot water bodies for the selected water bodies. Finally suggesting ameliorative measures to restore and mitigation measures for rejuvenation and sustenance of water bodies.

In the present study 13 pilot waterbody are identified. The catchment area of all the waterbodies are delineated and land use land cover map are also prepared. The climate trend detection is conducted for different climatic variables (Rainfall, maximum temperature, minimum temperature) on annual and seasonal basis for the duration 1951-2020 using Mann-Kendall test and Sen slope test. Soil samples are collected from seven different locations in Bikaner district and Infiltration test was performed at four different locations using double ring infiltrometer. Trend in groundwater level is analysed utilizing groundwater level data acquired from CGWB. Total 17 water samples from these surface water bodies and 2 groundwater samples were collected for physico-chemical parameters, demand parameters, heavy metals and pesticides. The analysis of physico-chemical parameters DO, BOD, COD were performed as per standard methods (APHA, 2017). Major Cations (Na, K, Ca, Mg), Major Anions (HCO_3, Cl, SO_4, NO_3), and Minor Ions (F, PO_4) were analysed using Ion Chromatograph. Results showed a non-significant increasing trend in rainfall and maximum temperature, whereas a significant increasing trend is observed in minimum temperature over the Bikaner district. Assessment of decadal change in land use land cover change (2010-2020) in the study area showed a notable reduction in barren land, significant increase in built-up, and substantial increases in tree cover in most catchments, whereas waterbodies remained relatively stable, with only minor changes observed, suggesting that water resources were largely unchanged over the decade. Soil sample analysis showed a sandy texture soil over the study area with the infiltration rate varying from 16 to 19 mm/hr, except in the lake near RD-507. Groundwater trend analysis showed a rising trend (in 43% wells) towards the IGNP canal, Falling trend is found in the southern parts of

district (in 21% wells), whereas, approximately 35% wells show no-trend in groundwater levels. Water quality assessment showed that almost all physico-chemical parameters in almost all water bodies except Dharnidhar (SW4) were observed within the permissible limit of BIS (2012) for drinking water (IS: 10500). Safe BOD level (>2.0 mg/L) is observed in almost all water bodies. Heavy metal concentrations show Al, Fe, Mn, Pb and B exceeded the prescribed permissible limit of BIS (2012) for drinking water (IS: 10500) in few of the samples. The runoff analysis from 2001 to 2020 reveals significant variability across catchments, influenced by factors like soil, vegetation, and topography. Years of intense rainfall, such as 2018 and 2012, saw high runoff, while dry years like 2002 showed minimal runoff. Each catchment's unique conditions affect its runoff patterns, emphasizing the need for effective water management. Similarly, pond data show periods of overflow and deficit, highlighting the impact of precipitation and water management practices.

Table of Contents

Chapter 1 1
INTRODUCTION 1
Present Status of Water Resources 2
Water Availability 2
Water Consumptive Patterns 3
Need of traditional waterbodies rejuvenation 4
Study objectives 6
CHAPTER 2 7
REVIEW OF LITERATURE 7
General 7
Homogeneity and Trend assessment 7
Waterbodies Inventory 11
Land Use Land Cover Detection 13
Runoff Estimation using Curve Number 15
Water Quality Assessment 18
Rejuvenation & Sustainable Management of waterbodies 21
CHAPTER 3 24
STUDY AREA AND DATA USED 24
Location: 24
Administrative Set-up 24
Topography 25
Geology and Minerals 25
Geomorphology 26
Soil 26
Rainfall & Climate 27
Agriculture 28
CHAPTER 4 29
METHODOLOGY USED 29
INVENTORY AND MAPPING OF SURFACE WATERBODIES 29
Catchment delineation 29
DECADAL LAND USE LAND COVER CHANGE DETECTION 30
CLIMATE TREND ANALYSIS 31
3.4.1 Mann–Kendall test 32
3.4.2 Sen's Slope test 33
SOIL LOSS ASSESSMENT 34

Estimation of soil loss using USLE 34
Rainfall Erosivity Factor (R) 35
Soil Erodibility Factor (K) 35
Slope length and steepness factor (LS) 36
Cover management factor (C) 36
Conservation practice factor (P) 37
RUNOFF ESTIMATION 37
SCS Curve Number Method 38
Curve Number 38
Hydrologic Soil Groups 40
Land Use 41
Antecedent Soil Moisture Condition (AMC) 42
Estimation of Direct Runoff 43
SITE SURVEY AND DISCUSSIONS WITH THE LOCAL COMMUNITY 44
Water Sampling and Analysis 44
 DETERMINATION OF pH 44
Apparatus required 44
Chemical required 45
Procedure 45
 DETERMINATION OF ELECTRICAL CONDUCTIVITY 45
Principle 45
Apparatus required 45
Chemicals required 45
Procedure 45
DETERMINATION OF OXIDATION-REDUCTION POTENTIAL (ORP) 46
Apparatus required 46
Procedure 46
 DETERMINATION OF TOTAL SUSPENDED SOLID (TSS) 47
Apparatus required 47
Procedure 47
 DETERMINATION OF DISSOLVED OXYGEN (DO) 48
Apparatus required: 48
Reagent List: 48
Starch solution preparation: 48
Procedure 48

DETERMINATION OF BIO-CHEMICAL OXYGEN DEMAND (BOD):.....49
Reagents.....49
Equipment.....49
Procedure.....49
Chapter 5.....51
Results and Discussions.....51
WATERBODIES INVENTORY.....51
Land Use Land Cover Change Detection.....59
Land Use Land Cover Change Detection.....65
Climate Trend Analysis.....71
Evaluation of Rainfall Dataset.....71
Evaluation of Temperature Dataset.....73
Temporal Variability in Long Term Trend of Rainfall.....75
Monthly analysis.....75
Seasonal and annual analysis.....76
Spatial Variability in Long-Term Trend of Rainfall Time Series.....78
Temporal variability in Long Term Trend of Temperature.....79
Monthly analysis.....79
Seasonal and annual analysis.....80
Spatial Variability in Long-Term Trend of Temperature Time Series.....83
CHAPTER – 6.....85
PRESENT STATUS OF GROUNDWATER RESOURCES AND RECHARGE TO GROUNDWATER.....85
5.1 General.....85
5.2 Present GW Scenario in the Study Area.....85
5.2.1 Analysis of GW level data.....85
Data pre-processing.....85
Interpolation.....86
Trend analysis.....86
5.2.2 Present scenario of depth to GW.....87
Pre-monsoon season.....89
Monsoon season.....90
Post-monsoon Kharif (POMKH).....91
Post-monsoon Rabi (POMRB).....91
Annual average.....92
5.2.3 Trends in GW levels during past two decades.....92

Pre-monsoon season 93
Post-monsoon season 93
Annual 94
5.3 Recharge to groundwater from precipitation and irrigation 95
5.4 Recharge/percolation from canal 98
5.5 Estimates of CGWB 98
Runoff assessment 99
Rainfall data 99
Hydrological soil group classification 100
Land Use Land Cover analysis 101
Estimation of curve number 102
Potential Maximum Retention (S) 105
Initial Abstraction (I_a) 106
Estimation of Direct Runoff 106
Sonsolav catchment 106
Harsolav catchment 108
Foolnath catchment 109
Darbari catchment 111
Gajner catchment 112
Diyatra catchment 114
Kodamdesar catchment 115
Kolayat catchment 117
Swarupdesar catchment 118
Miscellaneous 120
Soil Loss Assessment 122
Development of a database for USLE 122
Rainfall Erosivity factor (R) 122
Soil Erodibilty Factor (K) 124
Topographic Factor (LS) 126
Crop management factor (C) 129
Conservation practice factor (P) 131
Assessment of annual rate of soil erosion 132
Soil loss from Sonsolav catchment 133
Soil loss from Harsolav catchment 134
Soil loss from Foolnath catchment 136

Soil loss from Kodamdesar catchment 137
Soil loss from Darbari catchment 138
Soil loss from Gajner catchment 139
Soil loss from Kolayat catchment 140
Soil loss from Diyatra catchment 141
Soil loss from Swarupdesar catchment 142
Conclusion 143
Water Quality Assessment 144
CHAPTER 7 147
STRATEGIES AND MEAURES ON POND REJUVENATION 147
Chapter 8 162
CONCLUSION AND SUMMARY 162
Limitations 163
REFERENNCES 164

Table of Figures

Figure 1. Location map of Bikaner District 24
Figure 2:Soil map of the Bikaner District 27
Figure 3:Location of waterbodies in Bikaner District 53
Figure 4:Location map of pilot waterbodies 54
Figure 5:Catchment boundary and pictorial view of Sonsolav waterbody 55
Figure 6: Catchment boundary and pictorial view of Harsolay waterbody 55
Figure 7: Catchment boundary and pictorial view of Foolnath waterbody 55
Figure 8:Catchment boundary and pictorial view of Kodamdesar waterbody 55
Figure 9:Catchment boundary and pictorial view of Darbari waterbody 56
Figure 10:Catchment boundary and pictorial view of Gajner waterbody 56
Figure 11:Catchment boundary and pictorial view of Kolayat waterbody 56
Figure 12:Catchment boundary and pictorial view of Diyatra waterbody 57
Figure 13:Catchment boundary and pictorial view of Swarupdesar waterbody 57
Figure 14:Land Use land cover changes over Harsolav catchment between year 2010 & 2020 61
Figure 15: Land Use land cover changes over Foolnath catchment between year 2010 & 2020 62
Figure 16:Land Use land cover changes over Kodamdesar catchment between year 2010 & 2020 62
Figure 17:Land Use land cover changes over Darbari catchment between year 2010 & 2020 63
Figure 18:Land Use land cover changes over Gajner catchment between year 2010 & 2020 64
Figure 19:: Land Use land cover changes over Kolayat catchment between year 2010 & 2020 64
Figure 20:Land Use land cover changes over Diyatra catchment between year 2010 & 2020 65
Figure 21:Land Use land cover changes over Swarupdesar catchment between year 2010 & 2020 65
Figure 22:Land Use land cover changes over Harsolav catchment between year 2010 & 2020 68
Figure 23:Land Use land cover changes over Foolnath catchment between year 2010 & 2020 68
Figure 24:Land Use land cover changes over Kodamdesar catchment between year 2010 & 2020 69
Figure 25:Land Use land cover changes over Darbari catchment between year 2010 & 2020 69
Figure 26:Land Use land cover changes over Gajner catchment between year 2010 & 2020 70
Figure 27:Land Use land cover changes over Kolayat catchment between year 2010 & 2020 70
Figure 28:Land Use land cover changes over Diyatra catchment between year 2010 & 2020 71
Figure 29:Land Use land cover changes over Swarupdesar catchment between year 2010 & 2020 71
Figure 30:Monthly characteristics of long term (1951–2023) rainfall 72
Figure 31:Spatial distribution of mean annual rainfall over the district 73
Figure 32:Monthly characteristics of (A) Maximum Temperature (B) Minimum Temperature 74
Figure 33:(A) Spatial distribution of mean annual maximum temperature (Tmax) 75
Figure 34:(B) Spatial distribution of mean annual minimum temperature (Tmin) 75
Figure 35:Graphical representation of annual and seasonal rainfall trend 78
Figure 36:Spatial distribution of MK test Z statistics and Sen's slope over the Bikaner district 78
Figure 37:Graphical representation of annual and seasonal Tmax trend 82
Figure 38:Graphical representation of annual and seasonal Tmin trend 83
Figure 39:Spatial distribution of Z statistics and Sen's slope for Tmax over the Bikaner district 84
Figure 40:Spatial distribution of Z statistics and Sen's slope for Tmin over the Bikaner district 84
Figure 41:Temporal variations in depth to GW in the study area 88
Figure 42:Spatial variation in depth to GW in pre-monsoon season during the period from 2011 - 2020 90
Figure 43:Spatial variation in depth to GW in monsoon season during the period from 2011 – 2020. 90
Figure 44:Spatial variation in depth to GW during post-monsoon Kharif (POMKH) and post-monsoon Rabi (POMRB) during the period from 2011 – 2020. 91

Figure 45:Spatial variation in depth to GW at annual scale during 2011 - 2020 92
Figure 46:Trend in GW levels during pre-monsoon season 93
Figure 47:Trend in GW levels during post-monsoon Kharif season 94
Figure 48:Trend in GW levels at annual time scale 95
Figure 49:Potential recharge to groundwater from precipitation and irrigation in Bikaner district 95
Figure 50:Annual average precipitation from 2012 to 2020 in Bikaner District 96
Figure 51:LAI for Bikaner District 96
Figure 52:Percolation losses from canal in stage-I of IGNP. 98
Figure 53:Groundwater Recharge in Bikaner District (2023-2024) ..... **Error! Bookmark not defined.**
Figure 54:Annual rainfall (2001-2020) over the Bikaner district 100
Figure 55:Hydrologic Soil group in different catchments over Bikaner district 101
Figure 56:Status of water availability in Sonsolav pond 108
Figure 57:Status of water availability in Harsolav pond 109
Figure 58:Status of water availability in Foolnath pond 111
Figure 59:Status of water availability in Darbari pond 112
Figure 60:Status of water availability in Diyatra pond 115
Figure 61:Status of water availability in Kodamdesar pond 117
Figure 62:Status of water availability in Kolayat pond 118
Figure 63:Status of water availability in Swarupdesar pond 120
Figure 64:Spatial distribution of R-Factor values over different catchments 124
Figure 65:Soil map of the study area 125
Figure 66:Digital elevation model (DEM) of study area 127
Figure 67:Slope map of the study area 128
Figure 68:Spatial distribution of Topographic factor (LS) map of study area. 129
Figure 69:Spatial distribution of crop management factor 130
Figure 70:Spatial distribution of Conservation practice factor 132
Figure 71:Spatial distribution of soil loss from Sonsolav catchment 134
Figure 72:Spatial distribution of soil loss from Harsolav catchment 135
Figure 73:Spatial distribution of soil loss from Foolnath catchment 137
Figure 74:Spatial distribution of soil loss from Kodamdesar catchment 138
Figure 75:Spatial distribution of soil loss from Darbari catchment 139
Figure 76:Spatial distribution of soil loss from Gajner catchment 140
Figure 77:Spatial distribution of soil loss from Kolayat catchment 141
Figure 78:Spatial distribution of soil loss from Diyatra catchment 142
Figure 79:Spatial distribution of soil loss from Diyatra catchment 143

Lists of Figures

Table 1List of various acts and laws related to water bodies restoration (Singh et al., 2021) 22
Table 2 Basic statistics of the district at block level. 24
Table 3 Details elevation of blocks 25
Table 4 Crop Statistics (2018-2019) 28
Table 5 CN for different hydrologic soil group and hydrologic soil condition 39
Table 6 Multiplying factor for converting AMCII to I or III conditions 40
Table 7 Description of soil group 41
Table 8 Classification of Antecedent Moisture Conditions 43
Table 9 Waterbodies over the Bikaner district 51
Table 10 Details of Pilot waterbodies 57
Table 11 Land Use Land Cover statistics between the year 2010 & 2020 60
Table 12 Land Use Land Cover statistics between the year 2010 & 2020 66
Table 13 Descriptive statistics of annual rainfall (1951-2023) over the Bikaner District 72
Table 14 Descriptive statistics of annual Tmax and Tmin (1951-2023) over the Bikaner District 74
Table 15 MK-test statistic and Sen's slope values for 70 years monthly rainfall 75
Table 16 MK-test statistic and Sen's slope values for 70 years seasonal and annual rainfall 77
Table 17 MK-test statistic and Sen's slope values for 70 years monthly Tmax 79
Table 18 MK-test statistic and Sen's slope values for 70 years monthly Tmin 79
Table 19 MK-test statistic and Sen's slope values for 70 years seasonal and annual Tmax 81
Table 20 MK-test statistic and Sen's slope values for 70 years seasonal and annual Tmin 81
Table 21 Recharge due to precipitation and irrigation 97
Table 22 Figure 53:Groundwater Recharge in Bikaner District (2023-2024) 99
Table 23 Statistical characteristics of monthly rainfall during the period 2001-2020 100
Table 24 LULC statistics of the year 2020 over Different catchment (All value in 'Hectare') 102
Table 25 Area for each CN value 102
Table 26 Curve Number for AMC II condition 104
Table 27 Curve Number for AMC I and AMC III condition 104
Table 28 S' values over different catchments 105
Table 29 Annual rainfall and runoff over the Sonsolav catchment 107
Table 30 Annual rainfall and runoff over the Harsolav catchment 108
Table 31 Annual rainfall and runoff over the Foolnath catchment 110
Table 32 Annual rainfall and runoff over the Darbari catchment 111
Table 33 Annual rainfall and runoff over the Gajner catchment 113
Table 34 Annual rainfall and runoff over the Diyatra catchment 114
Table 35 Annual rainfall and runoff over the Kodamdesar catchment 116
Table 36 Annual rainfall and runoff over the Kolayat catchment 117
Table 37 Annual rainfall and runoff over the Swarupdesar catchment 119
Table 38 Proportion of sand, silt, clay, and OC 125
Table 39 K-Factor over different catchments 125
Table 40 Crop management factor for different land use/land cover classes 130
Table 41 Conservation practice factor for different land use/land cover classes 131
Table 42 Priority scales for soil erosion 133

Chapter 1

INTRODUCTION

Water is a natural resource, fundamental to life, livelihood, food security and sustainable development. Water is indeed most essential for human life and an absolute necessity for all multi activities like drinking/ domestic purposes, agriculture and industry, and allied sectors; it is also a vital element in the development of the economy of a country or region. It would not be an exaggeration to say that no life on the earth is possible without water. Ancient India has witnessed river valley civilization where human settlements flourished near flowing water. This is because the dependency on water was high for agricultural activity. In a healthy ecosystem for surface water, the dependency is not only with the quantity of water, but it has a direct relation with the quantity, quality, and timing of water available for sustainable use by living beings. Nowadays, rapid urbanization, increasing infrastructure projects, and anthropogenic activities have modified the surface as well as groundwater from its original state. Alteration to the natural movement of the water impacts the ecosystem adversely. This not only has an impact on water quantity but also has an adverse impact on its quality in turn health impact on various living species having a dependency on the same. The Abstraction of water changes the natural system significantly. The natural health of all such water bodies is very much required and important to sustain a wide range of social and economic benefits and values. Various social, cultural, and economic values can be sustained if water bodies can be protected or restored in their natural environment. Surface water bodies like lakes and ponds, reservoirs, tanks play a vital role in bridging the gap between the demand for groundwater and its natural availability by storage of rainwater, river flow water, etc. Water bodies are quite abundant in rural areas as well as in urban areas. However, due to poor management, the count of the water bodies is getting reduced or their capacity to store water is getting reduced. This results in low penetration of water to the ground led to the depletion of the groundwater table. If we identify the specific water requirement for a healthy ecosystem in its original form, then effective management of water can be planned. This can be done by the restoration of lakes, ponds, tanks by increasing their water storage capacity, regular cleaning, maintaining the source of water throughout the year. Once restoration gets completed then planning the volume of water abstraction for domestic, industrial, and agricultural purposes without impacting on the natural course of the water system can be done.

Present Status of Water Resources

Rajasthan is located in the Thar desert, and it has only 1 % of country's water resources on account of limited erratic and unpredictable nature of monsoon climate (Meena et al., 2023). Bikaner district has acute shortage of water along with the average monsoon and non-monsoon season rainfall of 26.37 cm and 7.58 cm, respectively (Ali et al., 2015). The Bikaner district has no river system therefore, it has acute shortage of surface as well as ground water resources. Ground water resources are not adequate to fulfill the ever-growing needs of water resources of the region. Therefore, canal facilities (IGNP) were developed in 1961. After inception of canal irrigation in the north-western Rajasthan, surface water resources are also being used for drinking, agriculture and industrial uses. In the north-western part of Bikaner district which is served by canal irrigation system, the surface water is also used in drinking as well as agricultural purposes. In north-eastern, eastern, central and southern part of the district which is covering about 84083 ha. area, the ground water is used for irrigation purposes. The district has total irrigated area of about 194098 ha. out of which 43.32% area is irrigated by ground water resources. Presently Bikaner district's 56.81% (438) villages are depended on ground water resources and the remaining 43.19% (333) villages (Poogal, Khajuwala, Chhattargarh) are served by canal water services (Ali et al., 2015). The villages of Nokha and dungargarh tehsils are fully dependent of ground water resources. The villages of Bikaner, Kolayat, Lunkaransar are served by surface as well as ground water resources.

Water Availability

Underground water, which is the main source for drinking, agriculture and other purposes in Bikaner district. It is generally found at a depth of about 80 to 120 metres below the ground level. The discharge from the well varies from 18,200 litres per hour to 91,000 litres per hour (Sharma et al., 2023). In Bikaner district, there are four major hydrological units viz., *Bilara limestone, Nagaur sandstone, tertiary sandstone* and the *quaternary alluvium* (Sharma et al., 2022). The study area has about 227.1 MCM ground water resources and presently 214.9 MCM water is being exploited. The percentage of ground water availability of the different blocks of the study area varies from 11.8% (Kolayat) to 27.8% (Nokha) blocks. Therefore, Nokha block has maximum (63.2 MCM) available ground water resources. The ground water availability for irrigation purposes is about 17.1 MCM and the ground water development rate is about 94.65% in the study area (CGWB, 2023). The alluvium formations cover major part (north-western part) of the district but due to saline ground water and thick sequence small area in north-eastern and south-western part in Lunkaransar and Kolayat blocks have been delineated as ground water potential. In these geological formations depth to water table

ranges from 100 to 140 meter and these formations occupy about 14% potential area. The general depth to water table increases from south-west to north-east direction. The water table contours indicate that the general direction of ground water flow is south-east to north-west (Hydrological Atlas of Bikaner, 2013). The ground water studies indicate that hydraulic gradient generally varies from 1.1 to 2.5 m/km. The quality of ground water is suitable for irrigation and drinking purposes. In southern part gradient become more steep (4.5 to 5.0 m/km). In Bikaner and Kolayat blocks quality of ground water is saline (Sharma et al., 2022).

Water Potability

Bikaner district's 55.22 % area (16779.24 sq.km.) contains saline ground water, and the remaining part of the district (44.78 %) has potable water, which is used for domestic as well as non-domestic uses (Industrial Potential Survey, 2015). The Bikaner district has about 749 villages, about 62.08 % (465) villages have potable water resources and the remaining 37.92 % (284) villages have saline water (Mohammad.and Ranga, 2023) As far as the spatial distribution pattern of ground water resources is concerned, the northern and western (Kolayat, Khajuwala, Chhattargarh, Pugal and Lunkaransar) part, have saline ground water and remaining more than half part of southern and eastern parts (Bikaner, small portion of Lunkaransar, Dungargarh and Nokha tehsils) have potable water. The availability of ground water in the Bikaner district ranges from 11.12 to 135.15 metres. Geohydrologically, Kolayat and Lunkaransar tehsils are safe ground water zones, where potable water is found at the depth of about 37.85 m to 135.15 m and 20.53 m to 66.15 m, respectively (CGWB, 2013).

As far as potability of ground water resources is concerned blockwise percentage ranges from 24.13 % (Kolayat) to 97.68 % (Nokha block). The south-eastern part of the district where Nokha and Sridungargarh block are situated the percentage of potability of water is above 90% (Hydrological Atlas of Bikaner, 2013). On the other hand, western part of the district (Kolayat, Bikaner, Lunkaransar) has very little percentage of potable water, the percentage of saline ground water ranges from 65.61 % in the Bikaner block to 75.87 % in the Kolayat block (CGWB, 2013).

Water Consumptive Patterns

Water demand in Rajasthan is fast increasing with increase in population, urbanization and industrialization. Water in Rajasthan is mainly consumed for irrigation purpose, and second and third priorities are for drinking and industrial purposes, respectively. About 63.3% of the net irrigated area exists underground water irrigation. At present the water supply should be

3952.73 lac gallons for 13205444 persons of urban area according to central norms of water supply but actual supply of water is only 2672.11 lac gallons (Singh et al., 2022). Thus, a wide gap exists between the water demand and supplied to the people. The gap may be widening when our future demand of water would be raised to 6723.85 lac gallons for urban population of 226.61 lac in 2021 (Ali et al., 2015). Likewise, for rural population, the water demand according to central norms would raised to 10843.15 lac gallons in 2021 (Ali et al., 2015).

In 1901, the population of Rajasthan was 1,02,94,090 and it increased to 1,59,70,774 in 1951 but during the same duration, the population of Bikaner district also increased from 1,90,457 to 3,43,091 (Population Census, 2011). On account of increasing population, water demand also increased in the state from 1721 lac GPCD (gallon per capita per day) to 2719 lac GPCD and in the Bikaner district 33 lac GPCD to 65 lac GPCD (Ali et al., 2015). If we compare the population growth and water demand of urban and rural areas for the above mentioned period of data analysis indicates that urban population in the Rajasthan state for the first five decades increased almost double (15.5 lac to 29.5 lac), consequently water demand also increased approximately in the same ratio (375 LGPCD (lac gallon per capita per day) to 715 LGPCD). But in the study area, the urban population of Bikaner district increased three times during the same period. Consequently, water demand in the urban areas also increased three times (12 LGPCD to 36 LGPCD) (Ali et al., 2015). The overall population migration trend is from rural to urban areas, therefore demographic pressure is continuously increasing in the urban area on account of better infrastructural facilities. Consequently, the water demand also increased in the urban areas.

Need of traditional waterbodies rejuvenation

The water bodies in Bikaner district are facing significant challenges exacerbated by climate change. With decreasing precipitation and rising temperatures, these arid landscapes are experiencing intensified water scarcity, leading to dwindling water levels in rivers, lakes, and reservoirs. Prolonged droughts further exacerbate water stress, posing threats to both human populations and the ecological health of aquatic ecosystems. Additionally, unsustainable groundwater extraction practices contribute to groundwater depletion, compounding the challenges faced by water bodies in the region. Climate change also impacts water quality, with increased temperatures and altered hydrological regimes affecting parameters such as pH, dissolved oxygen levels, and pollution levels, further compromising the suitability of water for various uses. The ecological impacts of these changes are significant, disrupting habitats and threatening the survival of aquatic species and biodiversity. To address these

challenges, holistic and adaptive strategies are required, including rainwater harvesting, groundwater recharge, watershed management, and the restoration of traditional water bodies. Community participation and awareness-raising efforts are crucial for fostering sustainable water management practices and building resilience to climate change impacts in Bikaner district.

The rejuvenation of water bodies in Bikaner district would have several significant impacts, positively contributing to sustainable water management in the region. Firstly, restoring and enhancing the health of water bodies would increase the availability of water resources, mitigating the impacts of water scarcity exacerbated by climate change. By improving water availability, communities in Bikaner would have greater access to clean water for domestic, agricultural, and industrial purposes, thus supporting livelihoods and economic development. Moreover, rejuvenated water bodies play a crucial role in groundwater recharge, replenishing aquifers and helping to stabilize groundwater levels. This recharge process is essential for sustaining both surface water and groundwater resources, thereby enhancing the resilience of water supplies to fluctuations in precipitation and climate variability. Rejuvenating water bodies preserves and restores ecosystems and biodiversity, fostering ecological balance and resilience to environmental shifts. Revived wetlands, rivers, and lakes offer crucial ecosystem services like flood regulation, water purification, and habitat provision, benefiting both communities and wildlife. Moreover, revitalized water bodies serve as recreational and cultural hubs, improving local residents' quality of life and drawing tourism, thereby stimulating economic growth and environmental stewardship. This strengthens communities' bond with their environment, underscoring the importance of safeguarding water resources for posterity.

Overall, the rejuvenation of water bodies in Bikaner district would have so many benefits for sustainable water management, including increased water availability, enhanced groundwater recharge, ecosystem restoration, and socio-economic development. By prioritizing the conservation and restoration of water resources, communities can build resilience to climate change and ensure the long-term sustainability of water supplies for current and future generations. Therefore, in the present study the hydrological investigation is conducted for revival and restoration of traditional waterbodies in the Bikaner district of Rajasthan.

Study objectives

- To prepare inventory of water bodies in Bikaner and to understand the role of the water bodies in the human survival, livestock and livelihood sustainable and in biodiversity conservation.
- Long-term spatio-temporal analysis of meteorological variables (rainfall and temperature)
- Land use/Land cover (LULC) change detection in the study area and selection of pilot water bodies (ponds).
- Trend analysis of groundwater levels and assessment of recharge to groundwater in Bikaner district
- Surface water availability analysis of pilot water bodies.
- Identification of various issues both quantitative and water quality assessment of pilot water bodies.
- To understand the socio-economical role of the water bodies to meet the daily requirement of community for water and other natural resources in and around water body.
- To understand the existing governance and management practices of water bodies by the local community or any other authorities.
- Suggesting ameliorative measures to restore water quality of water bodies and adaptive and mitigation measures for rejuvenation and sustenance of water bodies.

CHAPTER 2

REVIEW OF LITERATURE

This section focuses on reviewing previous research conducted in India and other countries to address the objectives of the present study. A thorough examination of relevant research is conducted in alignment with the objectives of the study to facilitate the development of an appropriate approach for addressing the research problem. The literature supporting the current research are carefully reviewed, and the most pertinent reviews are presented in the following section.

General

The Hydrological study for the revival and restoration of water bodies in Bikaner district aims to address the pressing water scarcity challenges in the arid landscapes of Rajasthan, India. Through comprehensive analysis of hydrological dynamics and community engagement, the study seeks to assess the current state of water resources and propose sustainable solutions for the conservation and rejuvenation of water bodies. By integrating scientific research with local knowledge, the study aims to identify key intervention areas and develop tailored strategies for water management, including the restoration of traditional waterbodies and the promotion of nature-based solutions.

Homogeneity and Trend assessment

The analysis of change point, trend and time series modelling of climatological variables are important areas of research in climatology (Baseville & Nikiforov, 1993; Lai, 1995; Chen & Gupta, 2001; Liao, 2005; Silvestrini & Veredas, 2008). The variability of climate is not uniform globally and vary with respect to time and space. The spatial and temporal variation is larger and considerable on the regional scale in comparison to continental scale (Yue & Hashino, 2003). In the past, many parametric and nonparametric tests have been proposed and investigated for detection of underlying magnitude and direction of trend along with change point by many researchers throughout the world (Hawkins, 1977; Buishand, 1984; Serra et al., 2001; Basher et al., 2018; Patakamuri et al., 2020; Yildirim et al., 2022).

Trends analysis of climatological variables is a crucial focus within the field of climatology, as highlighted by various researchers. The uniformity of climate across the globe is not consistent and varies across both time and space. Specifically, the regional scale exhibits more notable spatial and temporal variations compared to the continental scale (Yue and Hashino, 2003). Over time, researchers worldwide have proposed and explored numerous parametric and

nonparametric tests aimed at detecting the underlying magnitude and direction of trends in climatic variables. Parametric tests rely on population distribution assumptions, while nonparametric tests, commonly applied in climatic studies, avoid such assumptions. Examples of various tests include the t-test (Marengo & Camargo, 2008), Mann Kendall's test (Mann, 1945; Kendall, 1957), Mann-Whitney and Pettitt test (Mauget, 2004), linear regression test (Su et al., 2008), cumulative sum analysis test (Fealy & Sweeney, 2005), Markov chain Monte Carlo method (Elsner et al., 2004), and nonparametric regression test (Bates et al., 2010). The Mann Kendall's test is a nonparametric statistical method designed for analyzing trends in independent time series that follow a normal distribution. This test, recommended by the World Meteorological Organization for public application, finds extensive application in examining trends within climatological and hydrological time series (Hirsch et al., 1982). Two notable advantages of the Mann-Kendall test are its independence from the requirement of normal distribution in data and its low sensitivity to abrupt breaks caused by inhomogeneous time series.

Parthasarathy and Dhar (1974) studied the secular variations of regional rainfall over India for the period 1901-1960. They have shown that the yearly rainfall data for western part in Indian Peninsula to central parts of the country follow a positive trend. The yearly rainfall data for some sub-divisions, namely Punjab, Himachal Pradesh and Assam follow and increasing trend. However, south Assam is the only sub-division where rainfall data show a negative trend.

Intergovernmental Panel on Climate Change (IPCC) (2001) assessment warned the potential increases in the vulnerabilities and adaptation possibilities of human populations to future climate change, including sea-level rise and changes in the frequency and intensity of climate extremes such as floods, droughts, heat waves and windstorms and taking into account potential impacts on water resources scarcity, agriculture and food security, human health and other economic activities by major region of the world.

Martnez et al. (2010) applied three location specific homogeneity tests - the standard normal homogeneity test (SNHT), the Buishand range test and the Pettitt test to detect break year in annual maximum temperature and annual minimum temperature series of Spain. When two out of three tests detect the same year at a certain confidence level, the year was assumed as the breaking year. Tests for trends for climatic data are of great importance. There are a number of statistical tests. Mann-Kendall test, regression test for linear trend, turning point test, etc. have been widely used to analyze trends by climatologists and researchers.

Salarijazi et al. (2012) have analyzed annual maximum, minimum and mean stream-flow series at Ahvaz hydromet station as representative for Karun watershed to determine the change point and trend. The Pettitt's test has been applied for change point detection, while the trend in the annual stream-flow series of this station was evaluated by the Mann Kendall's test. The Pettitt's test didn't detect any change point in these series, but Mann Kendall'stest showed an increasing trend. However, this increasing trend has no fitness with observed data in the recent decade.

Adarsh et al. (2015) examined long-term rainfall trends in four southern Indian regions—Tamil Nadu, Kerala, Telangana, and North Interior Karnataka. Linear regression, the Mann–Kendall test, and Sen's slope estimator methods were employed for analysis. Results indicated an increasing trends in Tamilnadu, NI Karnataka, and Telangana, while Kerala exhibits a decreasing trend. Sequential change in annual and seasonal rainfall trends is analyzed using the sequential Mann–Kendall method, revealing early divergence in post-monsoon rainfall in Kerala and winter rainfall in Telangana. Notably, post-monsoon rainfall in Kerala has seen a statistically significant increase. Further analysis using discrete wavelet transform and sequential Mann– Kendall identifies short-term periodicity of less than a decade in Kerala's post-monsoon rainfall.

Chakraborty et al. (2017) assessed the variations in mean air temperature (Tavg) in the eastern Himalayan regions encompassing Naga, Khashi, and Lusai hills, spanning seven northeastern Indian states. A statistically significant increase in annual Tavg across the majority of meteorological stations in the northeast was identified. Monthly values show significant rises in Basar, Gangtok, and Imphal for most months, followed by Kolasib, Umiam, and Kailashahar. Despite spatial differences, the overall temperature increase ranged from 0.2°C to 1.6°C per decade across the study area. Notably, five out of seven locations experience a significant rise in Tavg during winter.

Deoli et al. (2019) examined the trend analysis of monthly rainfall in the Udaipur district of Rajasthan from 1975 to 2013. Both parametric (linear regression) and non-parametric (Mann-Kendall and Sen's slope estimator) tests were employed to determine rainfall characteristics. Linear regression revealed six months with a negative rainfall trend and four months with a positive trend, while no trend was found in March and September. Whereas, Mann-Kendall test showed increasing trends in April, May, June, July, and September, with decreasing trends in January, February, March, August, October, November, and December.

Sharma et al. (2021) analyzed temperature and rainfall trends in five divisional headquarters of Rajasthan: Jaipur, Kota, Jodhpur, Bikaner, and Udaipur. Trend detection and magnitude change analysis were conducted using the Mann–Kendall (MK) test and Sen's slope, respectively. The results revealed a significant increase in both minimum and maximum temperatures across all five stations. However, rainfall exhibited a non-significant increasing trend for Kota and Udaipur, while Bikaner, Jaipur, and Jodhpur showed a negative trend.

Mehta et al. (2022) conducted trend analysis of rainfall data during 1871 to 2016 and temperature from 1901 to 2002 for the Rajasthan state. To detect the existing trend, Mann-Kendall test was performed and to detect the magnitude of trend, Sen's slope estimator test was employed. Trend analysis of rainfall over 146 years showed increasing trend in pre monsoon, southwest monsoon and annual precipitation in west Rajasthan while the result shows increasing trend in pre monsoon, post monsoon and annual rainfall in the east Rajasthan. Trend analysis of temperature over 102 years shows increasing trend in annual temperature in both regions.

Mehta and Yadav (2022) investigated trend in rainfall data from 1871 to 2016 and temperature data from 1901 to 2002 for the Rajasthan state. The Mann-Kendall and Sen's slope estimator test were employed to identify existing trends and determine the magnitude of trends respectively. Over 146 years, the trend analysis revealed an increasing trend in pre-monsoon, monsoon, and annual precipitation in west Rajasthan, while the east Rajasthan region experienced an increasing trend in pre-monsoon, post-monsoon, and annual rainfall. The temperature trend analysis over 102 years indicated a rising trend in annual temperature in both regions.

Nath et al. (2023) analyzed trend in average monsoon rainfall and summer temperature in four diverse-climate Indian states: Rajasthan, Gujarat, Karnataka, and Maharashtra. Utilizing Mann-Kendall test, Sen's slope estimator, Kendall tau, and Mann-Whitney-Pettitt (MWP), trend was examined from 1951 to 2000 at a 5% significance level. Linear regression was also employed for identifying climatic pattern. Results revealed both positive and negative trend in average monsoon rainfall and summer temperature across all states. The rainfall trend decreased in all states except Maharashtra, which showed a slightly negative trend despite an overall positive annual temperature trend. Conversely, temperature trend increased in all states except Maharashtra. Examination of urban centres within these states indicated a general decline in yearly monsoon precipitation across most regions, coupled with recorded temperature changes. Karnataka exhibited a stronger positive correlation between rainfall and

temperature trends, while Maharashtra and Gujarat showed a positive correlation at a moderate level. In contrast, Rajasthan displayed a very weak correlation (tau = 0.079), suggesting no significant relationship between these two climatic parameters.

Waterbodies Inventory

Mapping and monitoring of surface water bodies is necessary as they are dynamic in nature in terms of water spread area and volume of water. The dynamic nature results into inter/intra annual/ seasonal/ monthly variations in surface water spread and there by the availability of water for agricultural use varies (Roberts et al., 1993, Voeroesmarty et al., 1997, Bastiaanssen et al., 2000). The utilisation of satellite images for the inventory, mapping and monitoring of surface water bodies would lead to the assessment of inter and intra seasonal as well as annual surface water spread dynamics. Several studies focus on utilizing remote sensing and Geographic Information System (GIS) techniques to map and classify waterbodies at different scales, from local to national levels. These efforts have contributed significantly to the understanding of waterbody distribution, dynamics, and changes over time. Additionally, research has emphasized the importance of integrating traditional ecological knowledge with scientific approaches to enhance the accuracy and relevance of waterbody inventories.

Prasad et al. (2002) studied the distribution of wetlands and causes and consequences of wetland losses. The study provided an overview of the use of Remote Sensing and Geographic Information System (GIS). They found that the dynamic nature of wetlands necessitates the widespread and consistent use of satellite based remote sensors and low cost, affordable GIS tools for effective management and monitoring.

Verpoorter et al. (2014) used high-resolution satellite imagery to produce a GLObal WAter BOdies database (GLOWABO), comprising all lakes greater than 0.002 km^2. GLOWABO contains geographic and morphometric information for ~117 million lakes with a combined surface area of about 5×10^6 km^2, which is 3.7% of the Earth's non-glaciated land area. Large and intermediate-sized lakes dominate the total lake surface area. Overall, lakes are less abundant but cover a greater total surface area relative to previous estimates based on statistical extrapolations.

Suresh et al. (2016) describes the need for spatio-temporal information on surface water bodies, brief overview of the existing scenario of popular satellite data interpretation / image processing / classification / methods for extraction of surface water bodies, need for development of automated image processing methods for extraction of surface water bodies

from satellite images etc. The results showed that, the automated methods for consistent information generation on surface water bodies can be operationally utilized. Though, the study was done for three months representing 3 seasons namely Kharif, Rabi and summer, the same can be extended at higher frequency with the combination of microwave and optical datasets.

Terasmaa et al. (2019) used combination of GIS-based methods (satellite, orthophoto, ground validation) to evaluate regional estimates of standing water body (SWB) inventories in two geographically different parts of Europe – France, and Estonia. In this study the SWBs surface area threshold limit was 0.00001 km2, exceeding the limits of previous studies (>0.002 km2). The total number of SWBs in Estonia is 111552 (2.5 per km2) and in France 598371 (1.1 per km2). Findings showed that the median size of SWBs in Estonia and France is 0.0003 km2 and 0.0007 km2 respectively, meaning that most of the SSWBs are not included in the global inventories, and their number is therefore underestimated. SSWBs (area below 0.01 km2) form a significant share of the total shoreline length of SWBs, 70.3% in Estonia and 58.8% in France.

Tyagi and Sahoo (2022) attempt to (a) study current geographical and historical background of water bodies/wetlands for the district. It aims to assess long-term (1917–2018) and short-term (pre and post-monsoon) changes in the water bodies of Gorakhpur District; (b) provide changes in the regime of water bodies and their conversion to different types of land use/land cover classes, which inundates a large extent of the area every year; (C) assess the channel characteristics and morphometric analysis of main rivers of the region during the last hundred years. Remote sensing and GIS have been used to prepare the inventory and to perform change detection, using land use/land cover maps. The floodplain areas of water bodies have almost changed their morphological characters due to encroachment by the nearby areas. Canals, drainage channels, and lakes are the most affected water bodies in the region, which have recorded − 65.38% and 43.37% loss in their area. Even permanent rivers have recorded a decrease of − 16.96% in the area. As per the seasonal change, agriculture land suffered the greatest conversion (18.33%) due to floodwater inundation.

Subramaniam et al. (2011) developed a new knowledge-based algorithm using multi-temporal spectral information available in four bands of Advanced Wide Field Sensor (AWiFS) on board ResourceSat-1 (with spatial resolution of 56 m) namely Green (G), Red (R), Near Infrared (NIR) and Short Wave Infrared (SWIR) for inventorying and monitoring of various types water bodies. The algorithm has been applied for the data obtained from other space-borne sensors with similar spectral bands such as Landsat ETM, IRS LISS III and ASTER and

found to be working satisfactorily. Results were validated by comparing the results reported from other popular methods.

Land Use Land Cover Detection

With the advent of the first remote sensing satellite (Landsat 1) in 1972 many land cover land use study has been undertaken. These studies were conducted in various areas including urban areas, agricultural area, mining area.

Singh et al. (1997) conducted detail study on the impact of coal mining and thermal power industry on land use pattern in and around Singrauli coalfields using Remote Sensing data and GIS. Database for land use was prepared for multispectral, multi-temporal data of years 1975, 1986 and 1991 of LANDSAT MSS and TM using PAMAP GIS software. The study revealed that areas mining and build up land increased from 1975 to 1991. There was substantial loss in agricultural and forest land which was due to rapid industrialization of the area.

Sharma et al. (2005) worked on coal mining impact on land use/land cover in Jaintia hills district of Meghalaya, India using remote sensing and GIS technique used LANDSAT data of 1975, 1987, 1999 and 2007 to conclude that there was four fold times increase in mining area from 1975 to 2007 accompanied by three times decrease in forest area. Visual interpretation technique was used for land use/land cover mapping for the different data of four years.

Mundia and Aniya (2006) analyzed LULC changes, dynamics of unplanned urbanization, and urban sprawl causes gigantic loss of forest of Nairobi, Kenya. The post-classification change detection method was implemented using an unsupervised classification iso-data algorithm to assess the LULC change of individually classified images. The overall accuracy and kappa indices above 80%.

Abbasi et al. (2011) analyzed decadal LULC change of riverine forest of Sindh, Pakistan using landsat satellite imagery. Supervised classification was applied to detect changes quantitatively by the post-classification comparison technique. This study revealed that continuous loss of sub-tropical forest was mainly due to anthropogenic activities that drive riverine forest to dry barren land.

Elhag et al. (2013) assessed Land use changes and its impacts on water resources in Nile Delta region using remote sensing techniques. Three temporal data sets of images were used: Landsat-5 Thematic Mapper (TM) acquired in 1984, and Landsat-7 enhanced Thematic Mapper acquired in 2000 and 2005 consequently. Two different supervised classification algorithms were implemented to produce classification maps in thematic form. Support

vector machine showed higher classification accuracies in comparison with maximum likelihood classification. The results indicated that the rapid imbalance changes occurred among three land cover classes (urban, desert, and agricultural land). These changes powered the land degradation and land fragmentation processes over the agricultural land exclusively due to urban encroachment.

Vorovencii (2014) compared change detection techniques and detected LULC changes in south-east Transilvania, Romania. Image differencing, NDVI differencing, principal component analysis (PCA), and post-classification change detection techniques were used to detect LULC changes. In the comparison of four change detection methods, the results revealed that NDVI differencing achieved a high overall accuracy of 83.80% and kappa value 0.6323. The post-classification results in 83.20% overall accuracy and 0.6206 kappa. While the PC2 difference and TM band 4 difference achieve overall accuracy of 81.60% and 79.40 and kappa value of 0.5759 and 0.5243.

Patra et al. (2018) assessed the impacts of urbanization on LULC change and groundwater depth level. K-mean unsupervised classification approach was used to assess LULC classes. And Inverse Distance Weighting (IDW) interpolation method was applied for the spatial distribution of temperature, rainfall, and groundwater level analysis. This study reveals that during the study period huge urban expansion up to 58% causes loss in vegetation, biodiversity, wetlands, and a rise in groundwater depth, temperature, and low rainfall in the area.

Vivekananda et al. (2021) focuses on the usage of the geographic information system (GIS) and land usage to identify the changes in Ananthapuramu, which is located in the Ananthapur district of Andhra Pradesh (AP) state, South India. This paper mainly focuses on the classification and identification of the changes in LULC in the period of 1999–2019 based on a survey of India's topographic map and temporal images gathered from the satellite. The experimental results indicate that over the specified period of study, the rate of increment and decrement in the built-up area, rate of underwater bodies, forest bodies that may demonstrate a significant impact on the environmental ecosystem.

Gupta et al. (2023) investigated the Spatial temporal changes of LULC in Mathura district of Uttar Pradesh, India, over the past 30 years (1990 to 2020). The study uses Landsat-5, Landsat-7 as well as Landsat-8 OLI images and GIS technique. The images were classified into LULC classes using a random forest classifier. The LULC changes were analyzed using a change detection analysis. The results of the change detection analysis were visualized using GIS. Confusion matrix was used for comparing the Crop classification during 1990–

2020. User accuracy, consumer accuracy, producer accuracy, overall accuracy and kappa coefficient were used to compare the study of approximately three decades from 1990 to 2020. The classification of LULC is done into six classes i.e., urban, water bodies, vegetation, wheat, mustard and other crops. The results showed that there were significant changes in LULC over the past 30 years. In the year 1990, 70.1 % accuracy and kappa 61.61 were obtained. In the year 2000, 70.8 % accuracy and kappa 63.02 were obtained. In the year 2010, 71.3% accuracy and kappa 64.8 is obtained. In the year 2020, 84% accuracy and kappa 80 are obtained.

Chauhan et al. (2022) analyzed the change in LULC of Rajsamand urban area. Various temporal Landsat imagery (Thematic Mapper) has been used for this study, particularly Landsat 5 TM and Landsat 7 Enhanced Thematic Mapper (ETM+) images from 1991 and 2021. Remote sensing is used to detect and measure land use pattern changes in the city. A Supervised Classification method by maximum likelihood method has been used to classify and map land use pattern types. The Kappa coefficient and the overall accuracy percentage have been measured to assess the accuracy of the research. Land use was found to change as a result of rapid urbanization in Rajsamand urban area, results showed that in the last 30 years, humanized land area i.e., buildings and construction structures has increased, which is more classify as urban area.

Patel et al. (2024) utilized the Geographic Information System (GIS) and Google Earth Engine (GEE) to track and examine changes in LULC over the last ten years (2013-2023). Modifications in LULC have a significant impact on both urban and environmental planning, especially in light of the fast urbanisation cycle. This study used a comprehensive approach to monitor and analyze Landsat imagery changes in LULC over the past ten years, leveraging the powerful capabilities of GEE and GIS. With a notable 0.85 Kappa and 89 % accuracy in LULC classification, the resulting LULC classifications cover settlements, vegetation, water bodies, arid land, and other relevant features. Results show that over the previous ten years, Ahmedabad has seen a noteworthy decrease in agricultural lands of 13.74 % and a reduction in barren areas of 4.78 %. Meanwhile, the total LULC patterns have shown a significant expansion of 23.56 %.

Runoff Estimation using Curve Number

Estimation of direct runoff, which is also called the effective rainfall, as response to heavy rainfall is often required for both: agricultural and urban catchment flood management (Banasik, 1994; Chormanski et al., 2011). Among the various methods for estimating runoff in ungauged catchments, the curve number method introduced by the USDA Soil

Conservation Service in the 1950s has gained significant recognition (SCS, 1972; Schneiderman, et al., 2007). The Natural Resources Conservation Service curve number (NRCS-CN) method, earlier called the SCS-CN method, represents an event-based lumped conceptual approach and is often used due to its simplicity and practical design. Despite its simplification of complex hydrological processes, the CN method has gained empirical validity through extensive calibration and validation against observed data, instilling confidence in its reliability (Sarangi et al., 2004; Ali et al., 2010; Sahu et al., 2012; Williams et al., 2012; Kim et al., 2018; Verma et al., 2020). Widely accepted and used by hydrologists, engineers, and researchers worldwide, the Curve Number method continues to serve as a valuable tool in water resource management and engineering applications.

With a number of applications world over, it forms an integral part of several standard software packages, dealing with physically based, distributed rainfall-runoff modelling, such as Hydrologic Engineering Center (HEC-HMS) (USACOE 1998), Soil and Water Assessment Tool (SWAT) (Neitsch et al. 2002; Arnold et al., 2012; Gassman et al., 2014; Krysanova and White, 2015, etc.). It is frequently employed in most remote sensing and geomorphological information system (GIS)-coupled packages.

Chaing (1975) developed an equation for flood volume estimation from small watershed by using number of wetness curve (NWC) instead of CN. Result showed that S value for each soil cover complex under AMC -I and III were too limiting and therefore recommended the use of SCS curve number approach via NWC. The antecedent soil moisture, initial base now and five days antecedent maximum daily temperature was found to be best predictor of optimal NWC.

Hawkins (1979) assumed an input error of 110% and found that runoff prediction is more sensitive to CN chosen for a considerable precipitation range upto 9 inches. These results showed the importance of accurate curve number in estimation of storm runoff.

Hjelmfelt (1983) discussed the problems associated with checking the validity of curve number, runoff equation and of using observation of rainfall and runoff to determine CN. The curve number S' derived from rainfall-runoff observation show much scatter. Attempt to correlate this scatter with AMC have not been fruitful due to other confounding factors such as storm conditions. Treatment of CN values as random values leads to interpretation of AMC I and AMC III as measure of dispersion around AMC II values. Acceptance of CN values as random variables permit and explanation of the reason that CN determined from rainfall -runoff data often yield values higher than expected.

Boughton (1989) evaluated the USDA, SCS curve number method for estimating runoff from small unguaged rural catchment. When the method is expressed as an infiltration equation, the infiltration rates become dependent on both total storm rainfall and rainfall intensity regardless of antecedent moisture. when expressed as a spatially varied saturation overland flow model, the method implies that some part of any catchment has infinite surface storage capacity. The lack of physical reality in the formulation of the method is an inherent limitation to any further development. A major weakness is the sensitivity of estimated runoff to errors in the selection of curve number.

Jadhav and Satpute (2001) observed that the CNs were not only varies according to antecedent moisture condition (AMC) but also according to storm size. The available 68 rainfall-runoff events were grouped and sub-grouped according to AMC and storm size respectively. The CNs were estimated for each sub-grouped by lognormal, least square and asymptotic method. They observed that performance of calibrated CNs is quite good over the Table CNs and calibrated CNs for only large storm events were matching with Table CNs.

Bhola and Singh (2010) calculated the runoff of Kosi river basin using ANN and NRCS CN method. The NRCS CN method requires the rainfall, soil information and vegetative cover properties while the ANN technique has the ability to learn from examples. Normalization of data was done to limit the range in between 0 and 1 before introducing the ANN model for training. The sigmoid function is selected as activation function. The coefficient of determination (R^2) was found to be 0.82 and 0.89 for NRCS CN method and ANN respectively.

Somashekar et al. (2011) estimated surface runoff of Hesaraghatta watershed. The analysis was carried using IRSID LISS III satellite images in the form of FCC using SCS curve number method and found that the runoff estimated by SCS method showed reasonable good result.

Nagarajan et al. (2013) found that from the runoff values estimated by the curve number technique, it is possible to assess which month has more runoff, which month has a moderate runoff and which month has a low runoff. With the help of these values, irrigation scheduling, rotation of cropping pattern and selection of suitable crops can be suggested.

Dwivedi et al (2017) calculated the surface runoff of upper Bhopal Lake by using curve number method. Around 80% of the catchment area was agricultural land, whereas 5% was

forest area and rest was urban area. From the starting of the monsoon season itself it was found that the lake was receiving runoff. The water scarcity problem of the basin can be reduced since the region has good surface hydrologic environment. The study helped in proper planning and implementing runoff control measures.

Luiz Claudio et al. (2018) estimated the runoff from 37000 ha area of Guariroba basin, Brazil. The rainfall-runoff events were measured during the year 2015 to 2017 for different land use pattern. The initial abstraction and curve number were computed using rainfall and runoff data. The 30 observed rainfall and runoff events were used with rainfall depth greater than 25 mm to derive associated CN values using statistical methods. The initial abstraction values ranged from 0.005 to 0.455. The findings suggested that CN was inappropriate to compute surface runoff in the studied basin because of the runoff mechanisms in the Guariroba basin may be dominated by subsurface runoff.

A significant research dealing with several issues (Ponce and Hawkins 1996; Mishra and Singh 2003) related with the SCS-CN method's capabilities, limitations, uses, and possible advancements have been published in the recent past. Specific to the subject matter suggested procedures for determining curve numbers for a watershed using field data (Hjelmfelt, 1991; Hawkins, 1993; Bonta, 1997). Neitsch et al. (2002) provided an empirical relation to account for the effect of watershed slope on CN. Hjelmfelt (1991), Svoboda (1991), and Mishra and Singh (1999) provided analytical treatments of the SCS-CN methodology. Jain et al. (2006) incorporated the storm duration and a nonlinear relation for initial abstraction (Ia), to enhance the SCS-CN-based model.

Water Quality Assessment

In the present era of modernization, a wide array of pollutants that are discharged into aquatic environment may have physico-chemical, biological, toxic and pathogenic effects. The life of aquatic ecosystem is directly or indirectly dependant on the water quality. Water pollution is a major threat to human population and dumping of pollutants into water body resulted in rapid deterioration of water quality and effect the ecological balance in the long run. The bacteriological and physico-chemical parameters of different river systems have been studied by various groups (Fokmare and Musaddiq 2001; Sood et al 2008; Rajkumar and Sharma, 2016).

Bartoneet al. (1992) examined that spatial concentration of individuals, industry, commerce, vehicles, energy consumption, water use, waste generation, and different environmental stresses are vital variables causing urban environmental issues as a result of

the sheer magnitude of increment of population. Uncontrolled, non-segregated dumping of municipal solid waste, hazardous/industrial wastes, and clinical/medical wastes in peri urban areas and near illegal tenants will increase the chance of injury and exposure to other health hazards.

Sharma (2003) studied the effects of population growth and climate change on the quantity and quality of water resources in the northeast of India, it was discovered that as more land is cultivated due to population pressure and that pesticides and fertilizers are used more frequently in an effort to increase crop productivity, the water quality in the area is degrading.

Robertson (2006) investigated the impact of farm land use systems on water quality in Jones Creek, Alberta, Canada. Results showed a significant impact of agriculture land use. Poor land management practices cause runoff including extra fertilizers, herbicides, pesticides, and animal wastes to pollute local rivers.

Sood et al. (2008) conducted detailed water quality analysis in the Gangetic river system of Uttarakhand during summer, rainy and winter seasons. Samples were subjected to bacteriological analyses, i.e. total viable count, total coliform count and faecal streptococcal count. The physico-chemical analyses of the water samples included pH, temperature, specific conductance, total dissolved solids (TDS), dissolved oxygen (DO), biological oxygen demand (BOD) and chemical oxygen demand (COD). All the physico-chemical properties, except BOD, were found to be within the permissible limits. The study confirmed the presence of bacterial indicators of faecal origin at various altitudes in every stretch of Gangetic river system. A huge bacterial gene pool was obtained during the study which was indicative of immense bacterial diversity in the region.

Pandey et al. (2010) evaluated the Ganga River's heavy metal contamination in Varanasi and reported that winter season had the highest concentrations of Cd, Cr, Cu, Ni, and Pb, whereas the summer season saw the highest concentrations of Zn. Heavy metal concentration trends were found to be Zn>Ni>Cr>Pb>Cu>Cd overall. While Cd and Ni levels were higher than acceptable limits, metal concentrations were below the limits allowed by Indian regulations.

Rout and Sharma (2011) in the Ambala Cantonment area assessed the ground water quality for different physico-chemical properties such as pH, EC, TDS, calcium, magnesium, total hardness (TH), sodium, potassium, carbonate, bicarbonate, total alkalinity (TA), chloride, fluoride and sulphate concentrations. The results were compared with the standards

prescribed by World Health Organization (WHO) and Bureau of Indian Standard (BIS). All the physico-chemical parameters were found to be within the prescribed permissible limit.

Khan and Hazarika (2012) examined samples of water from two sites of the River Kolong in Nagaon district, Assam for various physico-chemical parameters during the pre-monsoon and post-monsoon seasons. The pH during pre-monsoon and post-monsoon were 7.9 to 8.2 and 7.1 to 8.0 at site I; 8.2 to 8.6 and 6.5 to 7.1 at site II, respectively. DO of the river water ranged from 7.0 to 7.5 mg/l (pre-monsoon); 7.6 to 8.5 mg/l (post-monsoon) at site I and 7.0 to 7.3 mg/l (pre-monsoon); 7.1 to 7.9 mg/l (post-monsoon) at site II. The BOD was found highest at site I as compared to site II whereas the COD of river samples were found more than 400 mg/l during both the seasons. Based on the results, the water of River Kolong was found to be highly contaminated at both the selected sites during the course of study and was unfit for consumption and domestic purposes.

Arora et al (2013) assessed the water quality of River Ganga at mass bathings during Maha Kumbh Mela in Haridwar. The samples were collected during Makar Sankranti and Shath Poornima and assessed for faecal indicator bacteria along with Standard Plate Count (SPC). During the nine days of sample collection, the day of main royal bath (Baisakhi) displayed maximum SPC (log 6.79 CFU/ml) and Most Probable Number (MPN) of 210 and 150/100 ml for total coliforms and faecal coliforms, respectively. On the basis of the physico-chemical analysis: pH, TDS and TSS ranged between 8.1-8.5, 60.6-137.6 mg/l and 37-7-96.8 mg/l, respectively. The results clearly indicated that the mass bathing coupled with ritual activities performed by bathers were the main cause for the deterioration of water quality.

Huang et al. (2013) reported in a case study conducted in the China Chaohu Lake basin that there is a significant poor relationship between grassland and water pollution, as well as between built-up areas and water quality. However, the effect of cultivated land on water quality is much more complicated

Ghosh et al. (2013) studied water quality at Sirsakala village, Bhilai-3, Chhattisgarh, India, on pond and ground water and reported a significant concentrations of contaminants in some of the samples. These water samples were unfit for use for drinking, bathing, or household purposes, thus it was necessary to cleanse the water before it could be used for human consumption and safeguard the sources from pollution.

Lawniczak et al. (2016) reported that agriculture affected the nitrogen contamination of surface and ground water in central-western Poland. In the regions with heavy nitrogen application, there was a high concentration of nitrogen. Due to the plants' restricted ability

to consume the applied fertilizers' severe phosphorus and potassium shortages, nitrogen was leached.

Chauhan and Bhardwaj (2017) studied the impact of various land uses on the water quality in Himachal Pradesh's Solan block. According to their findings, industrial land use was associated with the highest levels of parameters including EC, COD, Ca2+, and pH, while rural and agricultural land use was associated with the lowest levels of EC, Ca2+, and Cl-. Low pH and Mg2+ levels were seen in urban and semi-urban land use.

Dev and Bali (2018) evaluated the Kangra region of Himachal Pradesh's groundwater quality and its suitability for drinking and irrigation. In addition to other physiochemical characteristics, samples were examined for pH, EC, TDS, Ca, Mg, Na, K, HCO3-, CO32-, SO42-, Cl-, NO3- . The factors were compared to established regional and global standards for drinking water. Significantly varied investigated variables were found in the groundwater at various places.

Saini and Dube (2018) studied quality of Narmada River in Jabalpur, MP, India discovered that COD and BOD both were highest during the summer and lowest during the rainy season, respectively. These findings were caused by human activity and the discharge of effluents into the river.

Chen et al. (2019) analyzed the levels and health risk of heavy metals of Taizihe River in China. The investigation's findings revealed that the average concentrations of the various elements were in the following order Pb>Cr Cu Zn Cd, and that Zn and Cu concentrations were significantly higher in the rainy season than the dry season while Pb, Cr, and Cd concentrations were comparable in both.

Singh et al. (2020) presents an outline of the current status of urbanisation as well as water in security in the HKH region of Bangladesh, India, Nepal and Pakistan which are undergoing rapid urbanization. The interlinkages of critical state of water resources, supply systems, rapid urbanisation and demand regime, aggravated by tourism leading to increasing water insecurity in the Hindu Kush Himalaya (HKH). Therefore, in order to avoid coping up with short-term strategies we must find solutions with long-term investments for sustainability which could lead to a water-secure future for the fragile urban centres of the HKH region.

Rejuvenation & Sustainable Management of waterbodies

Ponds are the biodiversity hotspots that collectively support far more species, including rare and threatened species than other freshwater habitats. They cover more earth’s surface than lakes) and provide a variety of ecosystem services such as food alleviation, aquifer recharge,

nutrient retention, carbon sequestration, mitigating urban heat islands (Downing et al. 2006). Nevertheless, the increased anthropogenic stresses (e.g., urban expansion, and agriculture intensification) driven by population overgrowth and resource demand declined the number of pond ecosystems. The emerging risks of bio invasion (invasive species) and climate change are also threatening the provision of the pond's ecosystem services. In the UK, the number of ponds declined by 75% between the 19th century and 1980 (Riley et al. 2018). In India, the loss of 80,128 pond/tanks (2006-2007) resulted in the loss of 1.95 million hectares of irrigation potential (Ministry of Jal Shakti, 2023). Loss of ponds is particularly threatening to the water and food security of the developing nations, where the freshwater bodies coverage is ≤1.4% of the land than the developed countries with 3.5% (UNESCO 2018). Restoration and management efforts are primarily directed towards the larger water bodies and the wetlands of national importance, or are part of a national protected area network (Ramsar-Convention on Wetlands 2018). The increasing number of scientific studies on ponds in recent decades indicates the growing concern of the global community. A large number of studies focused on the physicochemical characteristic (Yadav et al. 2017; Wang et al. 2022), specific species-based biodiversity conservation (Guareschi et al., 2020; Doi et al., 2023), and enhancing targeted ecosystem services of ponds (Moore et al., 2012; Oertli and Parris, 2019; Yadav and Goyal, 2022). The list of various acts and laws which are indirectly related to water bodies restoration, listed below in chronological manner.

Table 1List of various acts and laws related to water bodies restoration (Singh et al., 2021)

S. No.	Timeline	Acts
1.	1897	Indian Fisheries Act
2.	1927	Indian forest Act : conservation of lakes which come under these 4 categories reserved forests, village forest, protected forests, non-government forests.
3.	1974-1977	Water (prevention and control of pollution) Act : control sewage and industrial effluent discharges in the water bodies Water (prevention and control of pollution) Cess Act(1977)
4.	1980	Forest Conservation Act
5.	1982	Ramsar Convention on Wetlands came in India
6.	1985-1990	MoEF Notification, EPA (1986). NWP(1987), National Conservation Programme (1987)

7.	1995-2001	National river conservation plan (1995) National Lake conservation Plan
8.	2005	National project for repair, renovation and restoration
9.	2006	EIA guidelines
10.	2009	National Water Mission under National Action Plan on climate change
11.	2010	Wetlands (C & M) rules
12.	2013	2014 URDPFI guidelines Advisory on conservation and restoration of WBS in urban areas
13.	2015	Atal Mission for Rejuvenation and Urban Transformation (AMRUT)
14.	2016	National Plan for Conservation of Aquatic Eco-systems (NPCA)

CHAPTER 3

STUDY AREA AND DATA USED

Location:

Bikaner is located in the northwestern part of Rajasthan. It is bounded in the North by Ganganagar district, in the East by Hanumangarh, Churu and Nagaur districts, South by Jodhpur and Jaisalmer districts and Pakistan in the West. It stretches between 27º 09' 31.05" to 29º 03' 14.17" North atitude and 71º 50' 59.01'' to 74º 21' 59.21'' East longitude covering an approximate area of 30,279 km^2.

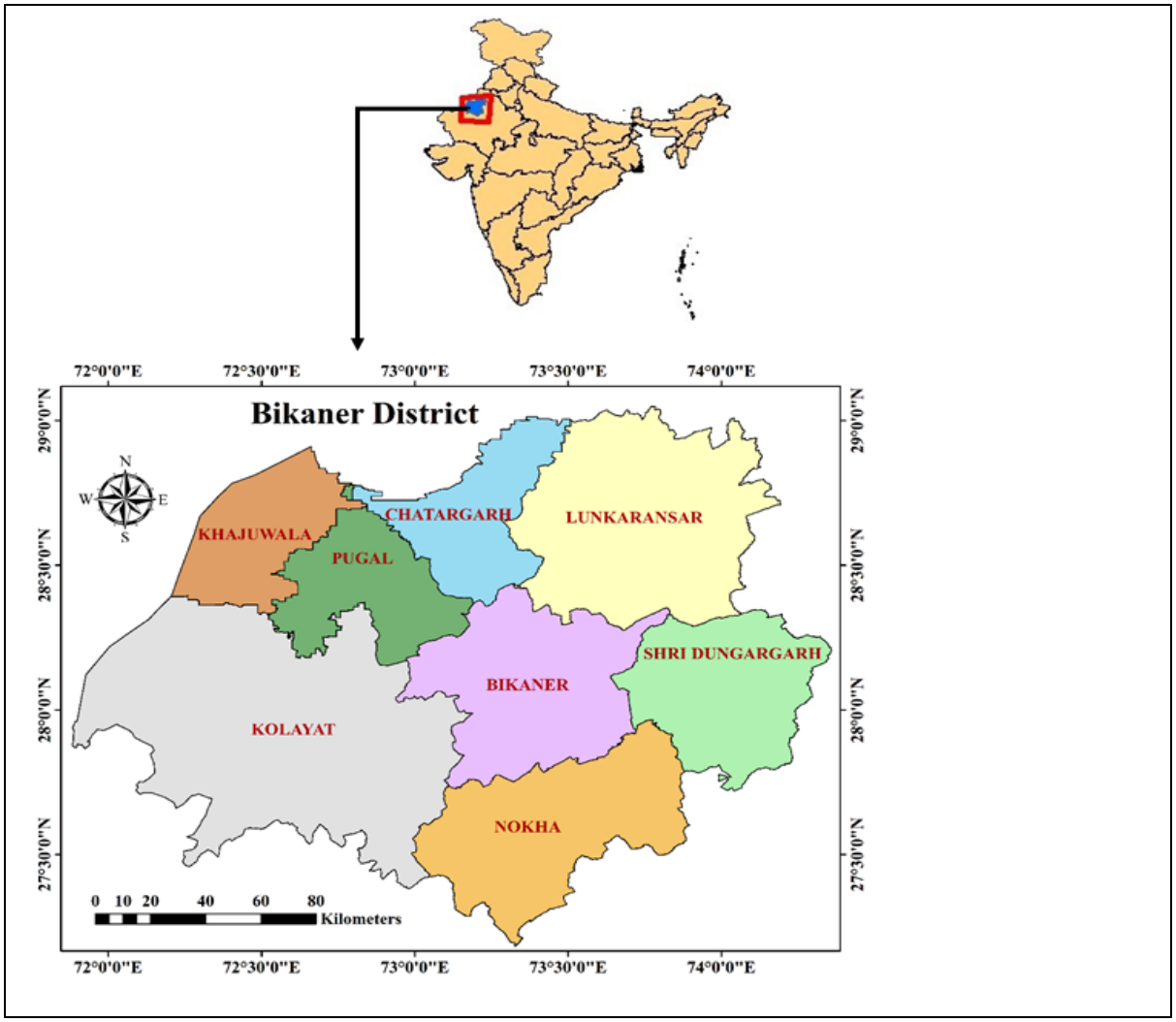

Figure 1. Location map of Bikaner District

Administrative Set-up

Administratively Bikaner district is part of Jodhpur division. This district is divided into 8 blocks.

Table 2 Basic statistics of the district at block level.

S. No.	Block name	Area (km^2)	% of District area
1.	Bikaner	3767.37	12.45
2.	Shri Dungargarh	2991.77	9.89
3.	Khujwal	2023.74	6.69
4.	Kolayat	8293.31	27.41
5.	Lunkaransar	5095.29	16.84
6.	Nokha	3798.7	12.56
7.	Chatargarh	2109.38	6.97
8.	Pugal	21774.92	7.19

Topography

Bikaner district is conspicuous of vast sandy areas and lack of hills. The topography is undulating interspersed with dunes of eolian origin. The table3.1 below reveals that the minimum elevation in the district is 103.7m above mean sea level (amsl) as found in Kolayat block whereas the maximum elevation is 349.1 m amsl in Nokha block where rocks of Tertiary sandstone are exposed. General slope of the terrain is from southeast to northwest.

Table 3 Details elevation of blocks

S. No.	Block Name	Minimum Elevation (meter)	Maximum Elevation (meter)
1.	Bikaner	123.2	298.6
2.	Dungargarh	200.2	347.3
3.	Khujwal	107.9	163
4.	Kolayat	103.7	315.3
5.	Lunkaransar	149.5	246.8
6.	Nokha	261.6	349.1
7.	Chatargarh	85.8	190.8
8.	Pugal	81.5	176.5

Geology and Minerals

Almost the entire district is devoid of rock exposures except near Kolayat and at a few places in the southern parts of Nokha and Dulmera. The district Bikaner is thus a vast sandy track except Kolayat are covered with sand of Rock locally known as “Magra” are found is parts

Kolayat tehsil. In the magra areas various types of sand stone, clay and lime stone are found are different levels. Fuller's earth viz Multani Miti, Clay lignite and gypsum, white clay, yellow ochre and grit and important economic minerals being produced in the district. Gypsum beds up to 30 meters thick and of the best quality available in India are found in Loonkaransar, Dulmera and Dheerera. There are deposits of fuller earth at Village Palana (Bikaner tehsil) and Mudh (Kolayat tehsil). Red sand-stone quarries are located near Dulmera village (Loonkaransar tehsil). Simultaneously impure lime stone is excavated all over the district. Glass sand is found near Madh and lignite is available at various places in Kolayat tehsil and Palana. Sand stone lime stone, Bajri and grit and Kankar are the main building materials found in the district.

Geomorphology

Geomorphologically, the district can broadly be divided into ten units viz. (1) flat aggraded older alluvial plains, (2) sandy undulating aggraded alluvial plains, (3) flat interdunal plains, (4) sandy undulating interdunal plains, (5) flood plains and aeolian complex, (6) stabilised sand dunes, (7) active sand dunes, (8) gravelly aggraded alluvial plains, (9) eroded rocky surface and (10) saline depressions. The western, south-western, northern and north eastern parts of the district are largely covered with dunes of different types and magnitudes with flat to undulating interdunal plains. The central eastern and southern parts of the district constitute largely flat and undulating aggraded alluvial plains. The general trend of the regional slope in the area is from SSE (275 mamsl) to NNW (152 mamsl). There are only a few small hill outcrops of about 1-2 mheight near Kolayat in the district. The district has no major river system except for a few short intermittent and ephemeral channels near Kolayat. A few natural lakes or depressions are observed near Gajner, Kolayat, Nal and Lunkaransar.

The main Rajasthan Canal enters the area somewhere north of village Bhansar and leaves the district in the southern boundary near village Gogliala. The main canal has a number of branches and distributaries like (1) Naushera Branch, (2) Dathar Branch, (3) Birsipur Branch, and (4) Charanwala branch. Besides the main Rajasthan canal command area, there are other command areas of lift canals. The Indira Gandhi Nahar Pariyoajna receives water from barrage at Hari Ka Pattan in Amritsar district of Punjab through 204 km. The IGNP canal command area is 591000 hectares in the district (Stage-I 179000 hectares and Stage-II 412000 hectares).

Soil

The soils of Bikaner district are predominantly light textured, weak – structured, sand to sandy loam with the clay content (**Fig.**). Arid climate with low rainfall, high temperature and high

evaporation losses has resulted in physical and mechanical disintegration of the parent material giving rise to predominance of coarse fraction in the soil. Very little chemical weathering has taken place and the development of soil is mostly indistinct. Soils are generally of desertic type with poor fertility status and very low water retention capacity. Soil profile studied during UNDP Project (1971-74) shows that the hydraulic conductivity in the soil profile reaches upto 10.9 cm/hr while the maximum available moisture in the soil profile remains to the extent of 1.13%. In general the soils have good porosity (40%) and good to very good permeability.

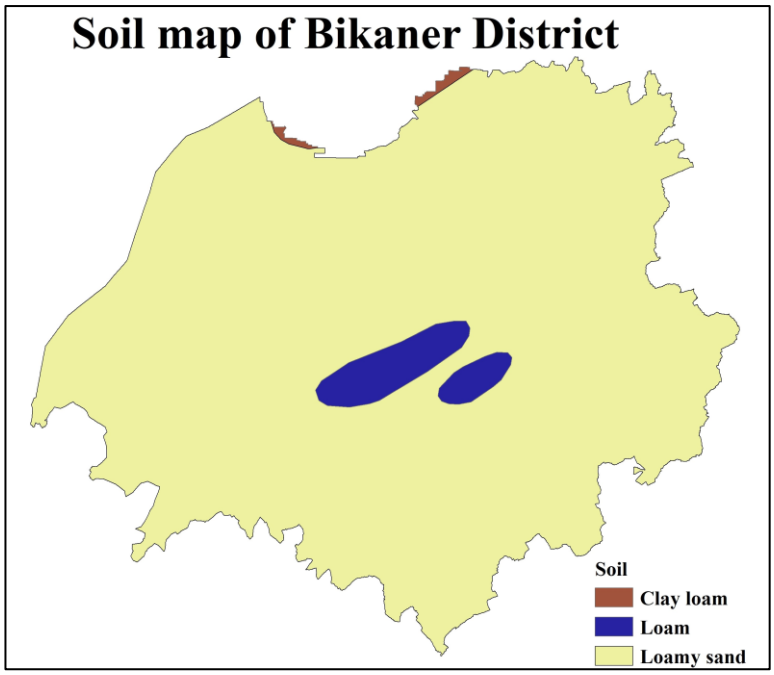

Figure 2:Soil map of the Bikaner District

Rainfall & Climate

The climate of the district is characterized by very high temperature, uncertain rainfall and dryness. The district experiences arid type of climate in the east to extremely arid in the west. Mean annual rainfall (1991-2010) of the district is 277.55 mm whereas normal rainfall (1901-1971) is lower than average rainfall and placed at 257.8 mm. Almost 90% of the total annual rainfall is received during the southwest monsoon, which enters the district in the first week of July and withdraws in the mid of September. As the district lies in the desert area, extremes of heat in summer and cold in winter are the characteristics of the desert. Both day and night temperatures increase gradually and reach their maximum values in April, May and June. The temperature varies from 48 degree in summer to 1 degree in winter. Atmosphere is generally dry except during the monsoon period. The humidity is the highest in August with mean daily relative humidity of 71% in the morning and 52% in the evening.

Agriculture

Bikaner district lies in the Hyper and Partial Irrigated Western Plains Agro-Climatic Zone, according to the classification by Department of Agriculture, Government of Rajasthan. Soils is desert soils and sand dunes aeilian soil, loamy coarse in texture & calcareous. Commonly grown crops in this zone in kharif season are pearl millet, Moth bean and Cluster bean and in rabi season are wheat, mustard and gram. In 2018-19, total sown area was 2091270 hectares, of which 596933 ha was sown in the Rabi season and 1494337 ha was sown in Kharif season.

Table 4 Crop Statistics (2018-2019)

Crops	**Area (Ha)**	**Production (MT)**	**Yield (kg/ha)**
Pearl millet	124132	43645	352
Moth	304188	85862	282
Wheat	105603	287989	2727
Gram	244225	244478	1001
Groundnut	238558	531099	2223
Mustard	161496	202522	1254
Source: Department of Agriculture (Government of Rajasthan)			

CHAPTER 4

METHODOLOGY USED

INVENTORY AND MAPPING OF SURFACE WATERBODIES

Surface water bodies are essential water storage units and play an important role in efficient tapping of huge water quantities from rainfall, runoff events. For irrigated agriculture in India, water is drawn from surface water bodies such as major/medium reservoirs, all irrigation tanks, river reaches where lifting of water is possible, etc. Huge infrastructure / establishments were created in India for creation of irrigation facilities. Identification of location of waterbodies and their catchment mapping is necessary as they are dynamic in nature in terms of water spread area and volume of water. The utilisation of satellite images for the inventory, mapping and monitoring of surface water bodies would lead to the assessment of various process occurring in the catchment such as land use change, hydrological modelling, soil loss assessment, etc.

Catchment delineation

Watershed delineation on a geographical location is simply a process to identify the ridge boundary surrounding a water body or runoff outlet. Basics of watershed delineation by using toposheet (based on contours and runoff outlet) are understood. The use of latest and modern technologies and tools like GPS or DGPS for (used for surveys), Remote Sensing Imageries and GIS is helpful for improving the precision quality and automating the process. By using Digital Elevation Model utility in GIS directly provides delineated boundaries of catchment. Following are the steps to delineate a catchment.

i. Download Digital Elevation Model (DEM)

Digital Elevation Models (DEM's) store topographic data in the form of grid cells. Typically, these grid cells have a resolution of 30 meters or less and elevation intervals of 1 meter. Using a DEM within a Geographical Information System (GIS), we can perform digital terrain analysis (DTA) such as calculating slopes, flow lengths, and delineate watershed boundaries and stream networks. Various sources of DEM are Space Shuttle Radar Topography Mission (SRTM), CartoSat, ALOS PALSAR, Copernicus, etc.

ii. Filling of DEM

After getting the DEM, there is need to fill the depressions if any in the DEM to get avoid false routings

- Open the hydrology tool box in the spatial analyst extension

- Open the fill tool and give the DEM as the input file. It fills the sinks in the surface raster and removes small imperfections in the data

iii. Flow Direction Raster generation

The filled DEM is used to prepare the Flow Direction map

- Flow direction tool is available in the hydrology tool box in spatial analyst extension
- It creates the raster with flow direction to the steepest neighbouring cell down the slope It is used to determine the direction of flow of water in the given topography
- Direction of flow must be known for each cell, because it is direction of flow that determines the ultimate destination of water flowing across the surface.

iv. Flow Accumulation Raster

It is done using hydrology tool box

- It shows the drainage path based on the flow direction raster.
- It shows the accumulation of flow in each cell.
- The maximum accumulated path gives the drainage path

v. Determining Pour Points

After getting the flow accumulation raster, pour points are required to determine watershed pertaining to the flow path

- We create a point shape file for determining the pour points
- These pour points are determined in the path using flow accumulation raster
- Care should be taken that the pour point lies in the line of flow accumulation

vi. Catchment Delineation

Using the watershed tool in hydrology tool box, a watershed is delineated

- The input required are the flow direction raster and the pour point shape file
- If there are multiple watersheds in a toposheet the If there are multiple watersheds in a toposheet, the watersheds corresponding to the drainage paths also can be determined

DECADAL LAND USE LAND COVER CHANGE DETECTION

Land cover change denotes a change in certain continuous characteristics of the land such as vegetation type, soil properties, and so on, whereas land-use change consists of an alteration in the way certain area of land is being used or managed by humans (Patel et al., 2019). This involves the transformation in the natural landscape due to urban growth. It is interesting to note that this change is responsible for a number of local and global effects, including biodiversity loss and its associated effects on human health, and the loss of habitat and

ecosystem services (Patel et al., 2019). Land use and land cover (LULC) changes have profound impacts on waterbodies, influencing their quantity, quality, and ecological health. Urbanization increases impervious surfaces, leading to higher runoff, reduced infiltration, and greater flood risks, while agricultural expansion can introduce sediments, nutrients, and pesticides into waterbodies, causing pollution and eutrophication. Deforestation accelerates soil erosion, increasing sediment loads in rivers and lakes, which can degrade aquatic habitats. Conversely, practices like afforestation and wetland restoration can enhance water quality and stabilize hydrological processes. Effective LULC management is essential to safeguard waterbodies from the adverse effects of these changes, ensuring sustainable water resource management. In the present study land use land cover change over three decades (2000s, 2010s, and 2020s) is analysed for whole Bikaner district. Moreover, LULC change analysis is also carried out over the catchment of each waterbody included in the study.

Literature offers studies comparing different classification algorithms/approaches to prepare LULC maps. However, when considering the cost-effectiveness and mapping accuracy, selection of a proper data source and an image classification technique has become a challenge, especially for researchers in the developing countries. On screen digitization with visual interpretation technique is an exact, cost-effective and highly suitable method for small study area as recommended by different researchers (Madarasinghe et al., 2020; Anitha 2022). In the present study, visual interpretation technique has been used to prepare a map and investigate LULC changes over an interval. High resolution (5 m) satellite image IRS-R2A LISS-IV FMX are employed for LULC map preparation for the year 2011 and 2020. LISS4 FMX satellite image consists of three spectral channels, green (0.52-0.59 μm), red (0.62-0.68 μm) and near infra-red (0.77-0.86 μm) with a temporal resolution of 5 days revisit for any given ground area and 70 km swath width. Different land uses were identified using image attributes and the image was classified into five classes; waterbodies, agriculture, trees, builtup, and barren land. False colour composite was also taken into consideration to identify different land use/land cover types. Area statistics of each land use class was estimated for the detection of change in LULC over the study area.

CLIMATE TREND ANALYSIS

Trends assessment proves to be a valuable tool for efficient planning and management of water resources. This is because it provides insights into the fluctuations of hydro-meteorological patterns over a specific period. Notably, significant shifts in hydrological or meteorological patterns may be linked to industrial and economic development or changes in observation

locations. During the analysis, two statistical tests were employed to evaluate trends in rainfall, T_{max}, and T_{min}. This assessment is conducted on annual, seasonal (including pre-monsoon, monsoon, post-monsoon, and winter), and monthly basis with the aim of identifying the impact of climate change. The following section outlines the various statistical tests applied to meteorological parameters.

Mann–Kendall test

Mann-Kendall stands out as one of the most widely adopted non-parametric tests for trend detection in time series, capable of identifying trends regardless of their nature (linear or non-linear). Mann (1945) originally documented the application of this test, and Kendall (1975) subsequently developed the distribution for the test statistic. This test has proven to be an outstanding tool for detecting trends, with numerous researchers employing it to evaluate the significance of trends in hydro-meteorological time series data, covering areas such as rainfall, temperature, stream flow, water quality, water level, etc. (Jaiswal et al., 2015; Ahmadi et al., 2017; Asfaw et al., 2018; Malik et al., 2020; Kumar et al., 2021; Gumus et al., 2022).

In this test, each element within the series is systematically compared to others in sequential order. When dealing with multiple data points for a given time period, the median value is employed. The Mann-Kendall statistic S starts with an initial assumption of 0. If a data value from a subsequent time period exceeds a data value from an earlier period, S is incremented by 1. Conversely, if the data value from the later period is lower than a previously sampled data value, S is decremented by 1. The final value of S is determined by the cumulative outcome of these increments and decrements. The Mann Kendall's statistic (S) can be expressed as follows:

$$S = \sum_{i=1}^{n-1} \sum_{j=i+1}^{n} sign(X_j - X_i)$$

where, n representing the overall length of the data, and X_i and X_j standing for two consecutive data values, the function $sign(X_i\text{-}X_j)$ assumes the subsequent values:

$$sign(X_j - X_k) = \begin{cases} +1, \text{if } X_j - X_k > 1 \\ 0\ , \text{if } X_j - X_k = 0 \\ -1, \text{if } X_j - X_k < 1 \end{cases}$$

In this test, the test statistic S exhibits a normal distribution, and the mean $E(S)$ and variance $Var(S)$ can be determined as follows:

$$E(S) = 0$$

$$Var(S) = \frac{1}{18}\left[n(n-1)(2n+5) - \sum_{k=1}^{n} tk(tk-1)(2tk+5)\right]$$

here, *n* represents the length of the time series, and *t* signifies the range of any specific tie, with *Σt* representing the sum of all ties. The standardized test statistics Z for this examination can be determined using the following equation:

$$Z = \begin{cases} \frac{s-1}{\sqrt{var(s)}} \ldots if\ s > 0 \\ 0 \ldots if\ s = 0 \\ \frac{s+1}{\sqrt{var(s)}} \ldots if\ s < 0 \end{cases}$$

In this test, the null hypothesis H_0 assumes the absence of a trend, indicating that the data is independent and randomly arranged. This hypothesis is contrasted with the alternative hypothesis H_1, which assumes the presence of a trend. A positive *Z* value indicates an ascending trend, while a negative *Z* value signifies a descending trend. The absolute value of the computed *Z* is then compared with the standard normal cumulative value of *Z(1-p/2)* at a significance level of *p%* from a standard table. This comparison is crucial for accepting or rejecting the null hypothesis, ultimately determining the significance of the observed trend (Partal and Kahya 2006).

Sen's Slope test

The Sen's Slope test is commonly applied for assessing the trend line's magnitude. This method involves calculating slopes for each pair of ordinal time points, and the median of these slopes is used as an estimate for the overall slope. Sen's approach computes the slope as the change in measurement per change in time. In this technique, the slope (T_i) for all data pairs can be determined using the equation:

$$T_i = \frac{x_j - x_k}{j-k} \quad for\ i = 1,2,3, \ldots., n, j > k$$

Where x_j and x_k denote the values at time points *j* and *k*, respectively, with *j* being greater than *k*. The median (β) of these *N* values of T_i serves as Sen's estimator of slope, which can be determined by using equation.

$$\beta = \begin{cases} T_{\frac{n+1}{2}} & n\ is\ odd \\ \frac{1}{2}\left(T_{\frac{n}{2}} + T_{\frac{n+2}{2}}\right) & n\ is\ even \end{cases}$$

SOIL LOSS ASSESSMENT

Soil erosion is a gradual process that occurs when the impact of water detaches and removes soil particles, causing the soil to deteriorate (Ni et al. 2004). Soil erosion in catchment area and the subsequent deposition in rivers, lakes and reservoirs are of great concern for two reasons. Firstly, rich fertile soil is eroded from the catchment areas. Secondly, there is a reduction in reservoir capacity as well as degradation of downstream water quality (European Environment Agency 1995). The rate of soil erosion from an area strongly depends upon rainfall, topographic characteristics, soil and vegetation. Therefore, a method that takes these factors into account while estimating soil erosion is expected to produce realistic estimate of rates of soil erosion (Das, 2008). For a long time, the Universal Soil Loss Equation (USLE) has been the most widely used model in predicting soil erosion loss and these equations take factors such as rainfall, topography, soil, and land use into consideration while assessing soil erosion.

Traditionally, these models were used for local conservation planning at an individual property level. The factors used in these models were usually estimated or calculated from field measurements. The methods of quantifying soil loss based on erosion plots possess many limitations in terms of cost, representative-ness, and reliability of the resulting data. They cannot provide the spatial distribution of soil erosion loss due to the constraint of limited samples in complex environments. So, mapping soil erosion in large areas is often very difficult using these traditional methods. The use of remote sensing and geographical information system (GIS) techniques makes soil erosion estimation and its spatial distribution feasible with reasonable costs and better accuracy in larger areas (Millward et al., 1999; Wang et al., 2003).

Estimation of soil loss using USLE

Soil loss assessment from the catchments of different waterbodies has been conducted using the Universal Soil Loss Equation (USLE) (Wishmeier and Smith 1978). The USLE is an erosion model for prediction of long-term average annual soil loss from specified area in specified cover and management conditions. The equation predicts losses from sheet and rill erosion only. According to the USLE, soil loss is the function of six different factors as shown in the following equation. The preparations of data for input to the equation are discussed here under:

$A = R \times K \times LS \times C \times P$

Where;

A= Computed annual soil loss rate (tons ha^{-1} $year^{-1}$)

R= Rainfall erosivity factor (MJ·mm/ha·hr·year)

K= Soil erodibility factor (ton·ha·hr/MJ·mm·ha)

LS= Topographic factor

C= Cover types factor

P= Land management and conservation practice factors

Rainfall Erosivity Factor (R)

The R factor reflects the impacts of various rainfall characteristics such as duration and intensity and soil erosion. This factor represents the driving force of sheet and rill erosion by rainfall and runoff (Naqvi et al. 2013). For the study area, the Rainfall erosivity (R) factor was calculated from available daily rainfall data of last 20 years over the Bikaner district of Rajasthan. Moreover, sub-hourly rainstorm data was not available for Jodhpur region to calculate the summative kinetic energy rainstorm events in a year. Instead, we used an empirical equation relating R factor with Fournier index (F) developed for arid region in having annual rainfall less than 600 mm (Irvem et al., 2007).

$R=0.1215\times (F)^{2.2421}$

$F=\sum 12(p_m)^2/P$

Where,

F = the modified Fournier coefficient

P_m = the precipitation/month

P = the precipitation/year (mm)

Rainfall erosivity map was generated by applying the IDW interpolation technique.

Soil Erodibility Factor (K)

Soil erodibility factor (K) is a measure of the total effect of a particular combination of soil properties. Some of these properties influence the soil's capacity to infiltrate rain, and therefore, help to determine the amount of rate of runoff; some influence its capacity to resist detachment by the erosive forces of falling raindrops and flowing water and thereby determine soil content of the runoff. The inter-relation of these variables is highly complex. The K factor in USLE model relates to the rate at which different soils erode. The soil map obtained from FAO, have been used to identify soil types in the study area. A formula relying on the proportions of sand, silt, clay, and organic carbon content was employed to estimate the K factor (Sharpley and Williams, 1990). This approach for K factor estimation in soil erosion

modeling has also been utilized by other researchers (Yang et al., 2018). The computation of the K factor utilized the following equation

$$K_{USLE} = f_{Csand} \times f_{cl-si} \times f_{org} \times f_{hisand}$$

$$f_{csand} = \left\{0.2 + 0.3 * exp\left[-0.256 * m_s\left(1 - \frac{m_{silt}}{100}\right)\right]\right\}$$

$$f_{cl-si} = \left(\frac{m_{silt}}{m_c + m_{silt}}\right)^{0.3}$$

$$f_{org} = \left\{1 - \frac{0.25 * orgC}{orgC + exp * \{3.72 - 2.95 * orgC\}}\right\}$$

$$f_{hisand} = \left\{1 - \frac{0.7 * \frac{m_s}{100}}{1 - \frac{m_s}{100} + exp * \left[-5.51 + 22.9 * \left(1 - \frac{m_s}{100}\right)\right]}\right\}$$

where, $f_{c\ sand}$ is high-coarse sand content, f_{cl-si} is clay and silt content, f_{org} is organic carbon content, and $f_{hi\ sand}$high sand content. The variables m_s and m_{silt} respectively represent the percentage of sand and silt fractions within the soil layer.

Slope length and steepness factor (LS)

The LS factor shows the impact of both slope length (L) and slope steepness (S) on slope erosion. LS factor signifies the ratio of soil loss occurring on a specific slope's length and steepness to the total soil loss from that slope (Wu et al., 2012). The LS factor is unitless, having value equal to or more than zero. To compute the slope length (LS) factor, Shuttle Radar Topographic Mission (SRTM) images sourced from the USGS Earth Explorer website (https://earthexplorer.usgs.gov/) were utilized. In this study, the combined LS factor is determined using the equation proposed by Moore and Burch (1986) (Equation 8).

$$LS = \left(\frac{\text{flow accumulation} \times \text{cell size}}{22.13}\right)^{0.4} \times \left(\frac{\sin Slope}{0.0896}\right)^{1.3}$$

LS represents the combined factor incorporating both slope length and steepness. Flow accumulation refers to the accumulated upslope contributing area for a specific cell, while cell size denotes the grid size (30 meter for present study). Additionally, "sin slope" refers to the sine of the slope angle measured in degrees.

Cover management factor (C)

The C-factor, as defined by Wischmeier and Smith (1978), represents the ratio of soil loss from a specifically cultivated area to that from an identical area under continuous fallow conditions. It includes the cumulative impact of various factors such as crop cover, crop rotation, growing period, tillage methods, productivity status, residue management, and the temporal distribution of erosive rainstorms concerning seeding and harvesting dates in the area. It is dimensionless parameters and falls within the range of 0 to 1. A value of 0 indicates

minimal erosion, typically associated with ample vegetation cover, while a value of 1 indicates significant soil loss occurring in the area. This reduction in soil loss subject to the specific combination of crop cover, sequence, and management practices employed (Mhangara et al., 2012). Researchers have employed various methods to estimate the C factor, particularly for croplands, often relying on field experiments. The choice of method depends on the availability of data, given that many of the parameters involved are challenging and expensive to assess across large spatial domains. Consequently, there has been extensive utilization of satellite imagery-based land use land cover (LULC) classification for C factor estimation (Koirala et al., 2019). The present study involves assigning C values from existing literature or those derived from field-based studies to different LULC classes, for the creation of C factor map

Conservation practice factor (P)

The P factor is defined as the ratio of soil erosion under a particular soil conservation practice to the erosion under conditions of tillage and cultivation on slopes (Wischmeier and Smith, 1978). It captures the impact of different conservation and support practices on reducing soil erosion by affecting flow velocity, concentration, and flow direction, as well as the hydraulic forces acting on the soil (Renard et al., 1997). The P factor includes the collective impact of various management practices, including contour farming, strip cropping, ridge planting, bunding and terracing, aimed at reducing both the rate and volume of runoff, consequently lowering soil erosion rates. Adoption of these practices leads to a decrease in the P factor, facilitating increased sediment deposition. Similar to the challenges encountered with the C factor, acquiring information on many of these parameters over large spatial extents proves to be difficult and costly. In this study, we employed an approach utilizing the LULC map of the area. The P factor was assigned to various LULC classes based on a literature review of studies conducted in large areas with similar characteristics, supplemented by expert opinion (Jena et al., 2018). These finalized P values were then allocated to different LULC classes, and subsequently reclassified to generate P factor maps of the study area.

RUNOFF ESTIMATION

Surface runoff quantification is a prerequisite of integrated watershed management. A direct method for this is watershed gauging. However, installations of gauging stations are not always feasible due to inaccessible terrains and the cost involved in construction, maintenance and periodic data retrieval. In this context, development of appropriate models to simulate the rainfall runoff responses over ungauged watersheds is an alternative. There are various

methods available for the estimation of runoff i.e. Rational method, SCS-Curve Number method, Cooks method, Rational formula, etc. Among them Curve Number method developed by the soil conservation service (SCS) of the U.S. department is the widely used methods for surface runoff estimation based on recharge capacity.

SCS Curve Number Method

The SCS curve number method was developed by the soil conservation service (SCS) of the U.S. department of agriculture for use in rural areas. The procedure has been modified to permit its application to urban areas and has been further adapted to a computerized simulation technique which become routing of hydrographs. The SCS curve number method is a simple, widely used and efficient method for determining the approximate amount of runoff from a rainfall even in a particular area. Although the method is designed for a single storm event, it can be scaled to find average annual runoff values. The requirements for this method are very low, rainfall amount and curve number. The curve number is based on the areas hydrologic soil group, land use, treatment and hydrologic condition (Randkivi, 1978).

Curve Number

The determination of the CN value for a watershed is a function of soil characteristics, hydrologic condition and cover or land use. Its value varies from minimum zero for the most permeable surface to the maximum 100 for impervious (concrete) surface. The values of CN are given in Table. These values are applied to the antecedent moisture condition II only, i.e., for average condition. To get the CN values for other AMCs (i.e. I and III), the correction factors are applied. The values of correction factors for other antecedent moisture conditions are given in Table.

Table 5 CN for different hydrologic soil group and hydrologic soil condition

Land use pattern	Treatment /practice adopted	Hydrologic condition	Hydrologic soil group			
			A	B	C	D
Fallow-row crops	Straight row	-	77	86	91	94
		Poor	72	81	88	91
		Good	67	78	85	89
	Contoured	Poor	70	79	84	88
		Good	65	75	82	86
	Contoured +Terraced	Poor	66	74	80	82
Small Grains	Straight Row	Poor	65	76	84	88
		Good	63	75	83	87
	Contoured	Poor	63	74	82	85
		Good	63	75	83	87
	Contoured +Terraced	Poor	61	72	79	82
		Good	59	70	78	81
Seeded	Straight Row	Poor	66	77	85	89
Legumes		Good	58	72	81	85
	Contoured	Poor	64	75	83	85
		Good	55	69	78	83
	Contoured +Terraced	Poor	63	73	80	83
		Good	61	67	76	80
Pastured Land	Contoured	Poor	47	67	81	88
		Fair	25	59	75	83
		Good	60	35	70	79
Farm Woodland		Poor	45	66	77	83
		Fair	36	60	73	79
		Good	25	55	70	77
Hard surface			74	84	90	92
Meadow			30	58	71	78

Table 6 Multiplying factor for converting AMCII to I or III conditions

S No.	Curve number/weighted curve number for AMC II	Factors to convert from AMC II to	
		AMC I	AMC III
1.	10	0.40	2.22
2.	20	0.45	1.85
3.	30	0.50	1.67
4.	40	0.55	1.50
5.	50	0.62	1.40
6.	60	0.67	1.30
7.	70	0.73	1.21
8.	80	0.79	1.14
9.	90	0.87	1.07
10.	100	1.00	1.00

Hydrologic Soil Groups

Study of hydrologic soil classification is done with a view to study overland flow characteristics of runoff. Hydrologic soil classes are of great use in estimating the runoff for any given watershed as soil properties influence the process of generation of runoff from rainfall. Soils may be classified into four hydrologic groups (A, B, C and D), (USDA,1985), depend on infiltration, soil classification and other criteria. The hydrologic soil groups, as defined by SCS soil scientists, are as follows:

Group A (lowest runoff potential): Soils having high infiltration rates even if it wetted, and consisting deep sands with very little silt and clay, also deep, rapidly permeable loess.

Group B (moderately low runoff potential): Soils having moderate infiltration rates, mostly sandy soils less deep than A, less aggregated than A, and consisting chiefly of moderately well to well drained soils with moderately fine to moderately coarse textures.

Group C (moderately high runoff potential): Soils having slow infiltration rates when thoroughly wetted and consisting chiefly of soil with moderately fine to fine texture. Comprise shallow soils and soils containing considerable clay and colloids, though less than group those of D.

Group D (high runoff potential): Soils having very slow infiltration rates when thoroughly wetted includes mostly clays of high swelling percent, soils with a permanent high water table, and soils with clay layer at or near the surface and shallow soils. (Randkivi, 1978).

Soils are also classified into four soil groups (A, B, C and D) according to their minimum infiltration rate, which is obtained for a bare soil after prolonged wetting. A description of these groups is shown in Table 4.3

Table 7 Description of soil group

Soil Group	**Description**	**Final Infiltration Rate (mm/hour)**
A	Lowest runoff potential. Includes deep sands with very little silt and clays, also deep, rapidly permeable loess.	8-12
B	Moderately low runoff potential. Mostly sandy soils less deep than A, and less deep or less aggregated than A, but the group as a whole has above average infiltration thorough wetting.	4-8
C	Moderately high runoff potential. Comprises shallow soils and soils containing considerable clay and colloids, though less than those of group D. The group has below average infiltration after pre-saturation	1-4
D	Highest runoff potential. Includes mostly clays of high swelling percent, but the group also includes some shallow soils with nearly impermeable sub horizons near the surface.	0.1

Land Use

Land use and treatment classes are used in the preparation of hydrological soil-cover complex, which in turn are used in estimating direct runoff. Types of land use and treatment are classified on a flood runoff producing basis. Below are a few extracts of the land use classification (USDA,1985):

i. Crop rotations: The sequence of crops on a watershed must be evaluated on the basis of its hydrologic effects. Rotations range from poor to good largely in proportion to the amount of

dense vegetation in the rotation. Poor rotations are those in which a row crop or small gain is planted in the same field year after year. Good rotations will contain alfalfa or other close seeded legumes or grasses, to improve tilth and increase infiltration.

ii. Farm woodlots: Poor woodlots are heavily grazed and regularly burned in a manner that destroys litter, small trees, and brush. Fair woodlots are grazed but not burned and may have some litter, but usually these woods are not protected. Good woodlots are protected from grazing so that litter and shrubs cover the soil.

iii. Native pasture or range: Poor pasture or range is heavily grazed, has no much or has plant cover on less than about 50% of the area. Fair pasture or range has between 50% and 75% of the area with plant cover and is not heavily grazed. Good pasture or range has more about 75% of the area with plant cover. And is lightly grazed.

iv. Commercial forest: The hydrologic condition classes are determined on the basis of depth and quality of litter, humus, and compactness of humus.

v. Miscellaneous: Usually only very small parts of a watershed are farmsteads, roads, and urban areas. When this is so, the areas may be included with one of the other land use cover types (such as fallow or small grain) in the computation of runoff.

vi. Straight row farming: This class includes up and down and cross slope farming in straight rows.

vii. Contouring: Contour furrows used with small grains and legumes are made while planting, are generally small and disappear due to climatic action.

Antecedent Soil Moisture Condition (AMC)

AMC is an indicator of watershed wetness and availability of soil moisture storage prior to a storm, and can have a significant effect on runoff volume. Recognizing its significance, SCS developed a guide for adjusting CN according to AMC based on the total rainfall in the 5-day period preceding a storm (USDA-SCS, 1985).For purpose of practical application, SCS suggests three levels of AMC as follows:

i. AMC I: This includes the lowest runoff potential, because the soils are dry enough for satisfactory cultivation to take place.

ii. AMCII: It includes average condition of the soil regarding runoff generating potential.

iii. AMCIII: This includes the features favourable to develop highest runoff potential of the soil, when areas of watershed are saturated from antecedent rains.

Table 8 Classification of Antecedent Moisture Conditions

AMC	Total 5-days Antecedent Rainfall (mm)	
	Dormant Season	**Growing Season**
I	<12.7	<35.6
II	12.7-27.9	35.6-53.3
III	>27.9	>53.3

The CN values documented for the case of AMC-II (USDA, 1985). To adjust the CN for the cases of AMC-I and AMC-III, the following equations are used (Chow, 2002):

$$CN_I = \frac{4.2 \times CN_{II}}{10 - (0.058 \times CN_{II})}$$

$$CN_{II} = \frac{23 \times CN_{II}}{10 + (0.13 \times CN_{II})}$$

Where,

$CN_{(II)}$ = curve number for normal condition

$CN_{(I)}$ = curve number for dry condition

$CN_{(III)}$ = curve number for wet condition.

Estimation of Direct Runoff

For the estimation of the peak runoff rate by SCS CN method, the following equation is given below:

$$Q_P = \frac{0.0208 \times A \times Q}{T_P}$$

Where Q_p is the peak runoff rate (m^3/s), A is the area of the watershed (ha), Q is the runoff depth (mm) and T_P is the Time to peak (hr). Here Q is calculated as

$$Q = \frac{(P - 0.2S)^2}{(P + 0.8S)}$$

Where, Q = direct runoff, P = daily rainfall, S = retention parameter, all in the unit of mm.

S is related to curve number (CN) and can be estimated as

$$S = \frac{25400}{CN} - 254$$

SITE SURVEY AND DISCUSSIONS WITH THE LOCAL COMMUNITY

Field investigations were carried out during October (2022), July (2023), and February (2024) and the information regarding waterbodies was collected. The filed investigations included (i) Identification of location of ponds (ii) assessment of the present status of the pond (ii) Soil infiltration test (iii) water sample collection of the pond (v) discussion with the local community to understand causal factors of water quality changes and the social perspective of the pond.

Water Sampling and Analysis

Hand held GPS was used for recording the geographical coordinates of sampling locations and also to map the boundary of the pond. Field investigations were carried out to find out the status of the pond and also the sources of contamination (if any). Water samples were collected in disinfected sampling bottles. These bottles were thoroughly washed and rinsed with deionised water. The samples were then carried to the lab and were analysed for different parameters according to Standard protocol (APHA AWWA WEF, 2000). Water samples were analysed for pH (pH probe), water temperature (temperature probe), Total Dissolved Solids (TDS) (TDS probe), salinity (salinity probe), conductivity (conductivity probe), dissolved oxygen (iodometry), Oxidation Reduction Potential (ORP), turbidity (turbidometer), total alkalinity (titrimetry), total hardness, Ca, Mg (complexometric titration), Na, K (flame photometer), chlorides (argentometric method), nitrates (phenol disulphonic acid method), phosphates (stannous chloride method), chemical oxygen demand (dichromate oxidation with open reflux) and BOD (5-d BOD).

❖ DETERMINATION OF pH :

"pH" refers to the measurement of hydrogen ion activity in the solution. pH is measured on a scale of 0 to 14, with lower values indicating high H+ (more acidic) and higher values indicating low H+ ion activity (less acidic). A pH of 7 is considered as neutral. pH is measured using pH meter, which comprises a detecting unit consisting of a glass electrode, reference electrode, usually a calomel electrode connected by KCl Bridge to the pH sensitive glass electrode and an indicating unit which indicates the pH corresponding to the electromotive force is then detected. Before measurement, pH meter is calibrated by using at least two buffers.

Apparatus required

pH Meter with Electrode, Standard flask, Measuring jar, Beaker, Funnel, Tissue Paper

Chemical required

Buffer solutions (pH 4 and 7)

Procedure

i. Plug in the pH meter to power source and allow warm up for 5 to 10 minutes

ii. Wash the glass electrode with distilled water and clean it using soft tissue/cloth.

iii. Place the electrode in pH 7 buffer solution and set the value of 7 on the pH meter by turning the calibrate knob on the meter.

iv. Take out the electrode, wash with distilled water and clean it.

v. Dip the electrode in the pH 4 buffer solution. Adjust the value of 4 on the pH meter. Repeat with pH 7 and pH4 buffers till a correct and stable reading is displayed.

vi. Now place the electrode in the water sample whose pH is to be determined.

❖ DETERMINATION OF ELECTRICAL CONDUCTIVITY

The electrical conductivity can be expressed as mhos (Reciprocal of ohms) or as siemens. The conductivity of water is a measure of the ability of water to carry an electric current. In most water, the conductivity is very low, so milli Siemens or micro Siemens are used as units for water conductivity. The conductivity of water is directly linked to the concentration of the ions and their mobility. The conductivity depends on the value of the pH, on the temperature of measurement and on the amount of CO_2 which has been dissolved in the water to form ions.

Principle

Conductivity is measured with a probe and a meter. A voltage is applied between the two electrodes in the probe immersed in the sample water. The drop in voltage caused by the resistance of the water is used to calculate the conductivity per centimetre.

Apparatus required

Conductivity Meter with Electrode, Standard flask, Measuring jar, Beaker, Funnel, Tissue Paper

Chemicals required

Potassium Chloride, Distilled Water

Procedure

1. Preparation of Potassium Chloride Solution (0.1N):

i. Switch on the Electronic balance, keep the weighing pan, set the reading to zero.

ii. Measure 50 mL of distilled water and transfer it to the beaker.

iii. Weigh 0.7456g of Potassium chloride.

iv. Transfer the 0.7456g of potassium chloride to the beaker contains distilled water and mix it by the glass rod until it dissolves thoroughly.

v. Transfer the contents to the 100 mL standard flask.

vi. Make up the volume to 100 mL, by adding distilled water and shake the contents well. This solution is used to calibrate the conductivity meter.

2. EC meter calibration and testing of water sample

i. Switch on the conductivity meter for at least 30 minutes before starting the experiment so that the instrument gets stabilizes.

ii. Prepare 0.1N Potassium chloride solution (calibration reagent).

iii. Rinse the glass electrode with distilled water and clean slowly with a soft tissue.

iv. Place the electrode inside the solution.

v. Calibrate the conductivity meter to 14.13 mhos using the standard solution of 0.1 KCl by adjusting the calibration knob.

vi. Read the conductivity meter by inserting the electrode into water samples one by one and note the reading.

DETERMINATION OF OXIDATION-REDUCTION POTENTIAL (ORP)

Oxidation-reduction potential (ORP) measures the ability of a lake or river to cleanse itself or break down waste products, such as contaminants and dead plants and animals. ORP is measured in millivolts (mV) and the more oxygen that is present in the water, the higher the ORP reading is. ORP can either be above zero or below zero. In healthy waters, ORP should read high between 300 and 500 millivolts.

Apparatus required

Conductivity Meter with Electrode, Standard flask, Measuring jar, Beaker, Funnel, Tissue Paper

Procedure

i. Rinse the probe with distilled water. Dry the probe with a tissue paper.

ii. Put the probe in a beaker that contains the solution. Do not let the probe touch the stir bar, bottom or sides of the container. Remove the air bubbles from under the probe tip. Stir the sample at a slow to moderate rate.

iii. Push Read button. A progress bar is shown. When the measurement is stable, the lock icon is shown.

iv. When the value is stable, store or record the mV value.

❖ DETERMINATION OF TOTAL SUSPENDED SOLID (TSS)

Total Suspended Solids can be referred to materials which are not dissolved in water and are non-filterable in nature. It is defined as residue upon evaporation of non-filterable sample on a filter paper.

Apparatus required

Oven, Desiccators, weighing balance, Graduated Cylinders, Filter paper and assembly, Vacuum Pump, Petri dish.

Procedure

i. Collect 1 sample in a HDPE 1 L container.

ii. Put filters paper into petri dish and place it in oven set to 104 ± 1ºC for 1 hour.

iii. Remove filters from the oven and place them into a desiccator until they have cooled to balance temperature.

iv. Weight each filter using weighing balance and note the readings.

v. Set up the filtration apparatus and connect it to vacuum pump.

vi. Place filtration apparatus with pre-weighted filter paper in filter mask.

vii. Mix the sample well and pour into a graduated cylinder to the selected volume.

viii. Pour selected volume into filtration apparatus.

ix. Draw sample through filter in to filter flask.

x. Carefully transfer the filter paper to petri dish. Follow same steps for all water samples.

xi. Place petri dishes into an oven set to 104 ± 1ºC and dry for a minimum of one hour.

xii. Remove petri dishes from oven and transfer them to a desiccator to cool to room temperature.

xiii. Weight the filter paper one by one and note the readings.

xiv. Calculate TSS using the formula as described below.

$$TSS\ (m\dot{g}/L) = \frac{(A - B)}{V}$$

Where: A = mass of filter + dried residue (mg), B = mass of filter (tare weight) (mg), and V = volume of sample filtered (L)

❖ DETERMINATION OF DISSOLVED OXYGEN (DO)

Dissolved oxygen (DO) is a measure of how much oxygen is dissolved in the water - the amount of oxygen available to living aquatic organisms. Two methods are commonly used to determine DO concentration: (1) The iodometric method which is a titration-based method and depends on oxidizing property of DO and (2) The membrane electrode procedure, which works based on the rate of diffusion of molecular oxygen across a membrane. In the present study iodometric method is used.

Apparatus required:

Burette, conical flask, pipette, measuring cylinder.

Reagent List:

Manganese sulphate, Alkali-iodide-azide, Conc. sulfuric acid, starch solution, Sodium thiosulfate

Starch solution preparation:

Dissolve 2 g laboratory-grade soluble starch and 0.2 g salicyclic acid as preservative in 100 mL hot distilled water.

Procedure

i. Fill a 300-mL glass Biological Oxygen Demand (BOD) stoppered bottle upto brim with sample water.

ii. Immediately add 2mL of manganese sulfate to the collection bottle by inserting the pipette just below the surface of the liquid. Squeeze the pipette slowly so no bubbles are introduced via the pipette.

iii. Add 2 mL of alkali-iodide-azide reagent in the same manner.

iv. Stopper the bottle with care to be sure no air is introduced. Mix the sample by inverting several times.

v. Add 2 mL of concentrated sulfuric acid via a pipette held just above the surface of the sample. Stopper the bottle again and mix well. The brown precipitate will completely dissolve leaving a brown coloured solution.

vi. Fill the burette with 0.052N sodium thiosulfate ($Na_2SO_4O_3$).

vii. Add 2 mL of starch solution so a blue colour forms. Titrate this solution against 0.025N sodium thiosulfate ($Na_2SO_4O_3$).

viii. Continue slowly titrating until the sample turns clear.

ix. Calculate DO using the formula described below.

$$\mathbf{DO}\left(\frac{\mathbf{mg}}{\mathbf{L}}\right) = \frac{(\mathbf{Volume\ of\ Na2SO4O3\ used}) \times (\mathbf{Normality\ of\ Na2SO4O3}) \times (\mathbf{Eq.weight\ of\ oxygen})}{\mathbf{Volume\ of\ sample\ taken}}$$

❖ DETERMINATION OF BIO-CHEMICAL OXYGEN DEMAND (BOD):

Biochemical oxygen demand (BOD) is the amount of dissolved oxygen (DO) needed by aerobic biological organisms to break down organic material present in a given water sample at a certain temperature over a specific time period. The BOD value is most commonly expressed in milligrams of oxygen consumed per liter of sample during 5 days of incubation at 20 °C. It indicates the amount of organic pollution present in an aquatic ecosystem. It indicates the amount of organic pollution present in an aquatic ecosystem. High BOD levels are caused by high consumption of dissolved oxygen by microorganisms. It indicates that the water is highly polluted with organic matter.

Reagents

Phosphate buffer solution, Magnesium sulphate solution (MgSO4.7H2O), Calcium chloride solution (CaCl2), Ferric chloride solution (FeCl3), Sulfuric acid (H2SO4), 1 N, Starch indicator solution, Manganese sulphate, Alkali-iodide-azide, 0.025N sodium thiosulphate, Distilled water.

Equipment

300 mL BOD bottles, Incubator, graduated cylinders, measuring pipettes, beaker, Dilution water bottle

Procedure

i. Preparation of dilution water. Fill the desired volume of distilled water in a suitable bottle and add 1ml each of Phosphate buffer solution, Magnesium sulphate solution (MgSO4 7H2O), Calcium chloride solution (CaCl2), Ferric chloride solution (FeCl3) solution per litre. Add 2 mL settled sewage per Litre and aerate for 2 hours.

ii. Samples may be prepared at different dilution percentage. In the present study BOD test is conducted at 10% dilution.

iii. Carefully fill a BOD bottle with sample water at 10% dilution.

iv. Add 2ml of manganese sulfate to the BOD bottle carefully by inserting the pipette just below the surface of water. So that formation of air bubbles can be avoided.

v. Add 2 mL of alkali-iodide-azide reagent in the same manner.

vi. Close the bottle and mix the sample by inverting many times. A brownish cloud will appear in the solution as an indicator of the presence of Oxygen.

Chapter 5

Results and Discussions

WATERBODIES INVENTORY

Water bodies are the most precious and life-sustaining resources. Availability of reliable and updated information about water bodies is necessary for their sustainable management and planning. An inventory of water bodies has been created for Bikaner district of Rajasthan using semi-automatic method including field visit, literature review, Remote Sensing and GIS for mapping of water bodies. Google earth imagery has been used for deriving information on various waterbodies. In addition, Survey of India topographical maps at 1:50, 000 scale, and published maps and reports were also used as collateral information. The total 61 waterbodies have been identified over the Bikaner district and their location coordinates were noted. The list of all the waterbodies is given in **Table** 5.1

Table 9 Waterbodies over the Bikaner district

S. No.	Ponds	Latitude	Longitude	S. No.	Ponds	Latitude	Longitude
1	Mahanand	28.0028	73.2886	32	Chimpolai	28.0223	73.2890
2	Pir talai	28.0030	73.2865	33	Kandolai	28.0050	73.2877
3	Sutharon ki Talai	28.0054	73.2905	34	Kukh sagar	28.0252	73.3036
4	Harolai	28.0061	73.2891	35	Kasaiyon ki talai	28.0215	73.2975
5	Jatolai	28.0072	73.2906	36	Gop talai	28.0051	73.2851
6	Naathsagar	28.0087	73.2885	37	Dhobi talai	28.0098	73.3136
7	Dharnidhar	28.0028	73.2920	38	Lalniyon ki talai	28.0190	73.2915
8	Kishnani vyason ki talai	27.9876	73.2875	39	Bhaktolai	28.0172	73.2895
9	Farsolai talai	28.0082	73.2943	40	Bagolai	28.0009	73.2911
10	Jasolai talai	28.0130	73.2976	41	Nishani ki talai	28.0129	73.2748
11	Ratneshwar talai	28.0129	73.2902	42	Krupalbhairun ki talai	28.0435	73.2943

12	Chetolai	28.0127	73.2871	43	Radholai	28.0167	73.2973
13	Bhatolai	28.0158	73.2884	44	Darjiyon ki talai	28.0026	73.2885
14	Thingaal bhairun ki talai	28.0078	73.2769	45	Choge ri talai	27.9953	73.3327
15	Karmisar talai	28.0038	73.2756	46	Hinglaj talab	28.0215	73.3027
16	Gujrolai	28.0046	73.3070	47	Naaiyon ki talai	28.0031	73.2844
17	Kharnada	28.0134	73.3078	48	Garolai	27.9828	73.3182
18	Mirzamal ji ki talai	28.0008	73.2998	49	Darbari	27.9760	73.1069
19	Bharolai	27.9945	73.3041	50	Gajner	27.9506	73.0552
20	Savalakhi talai	27.9916	73.3057	51	Daytra	27.7826	72.8169
21	Bagdiyon ki talai	27.9902	73.3077	52	Kolayat	27.8421	72.9539
22	Bahktsagar	28.9977	73.3039	53	RD-507	28.8035	73.2454
23	Rangolai	28.0181	73.2777	54	RD-750	28.3240	72.7775
24	Brahm sagar	28.0236	73.2816	55	Kodamdesar	28.0467	73.0811
25	Binnani talai	28.0220	73.2907	56	Swarupdesar	27.8915	73.2067
26	Nrusingh sagar	28.0307	73.2988	57	Harsholav	28.0002	73.2850
27	Gabolai talai	28.0241	73.2960	58	Sansolav	28.0096	73.2848
28	Ghadsisar	27.9829	73.0353	59	Foolnath	28.0091	73.2758
29	Shiv bari	27.9988	73.3563	60	Sursagar	28.0233	73.3200
30	Devi kund sagar	28.0171	73.3900	61	Kalyan sagar	28.0210	73.3919
31	Akherajpuri talai	28.0014	73.3044				

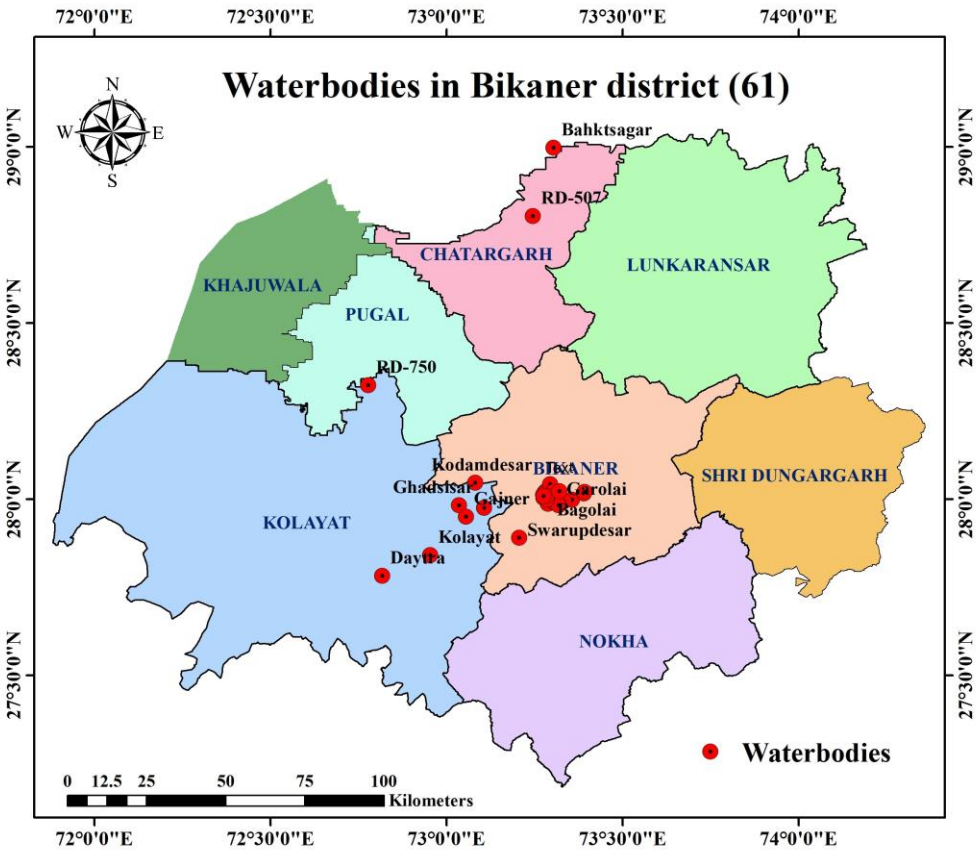

Figure 3:Location of waterbodies in Bikaner District

Out of these 61 waterbodies, 9 waterbodies namely Sonsolav, Harsolav, Foolnath, Darbari, Dayatra, Kolayat, Kodamdesar, Swarupdesar, and Gajner. were considered as pilot waterbodies for further analysis. Out of 9 waterbodies, 6 are located in rural area Sonsolav, Harsolav, Foolnath) and 3 are located in urban area (Darbari, Dayatra, Kolayat, Kodamdesar, Swarupdesar, and Gajner). The location map of pilot waterbodies is shown in **Fig.**

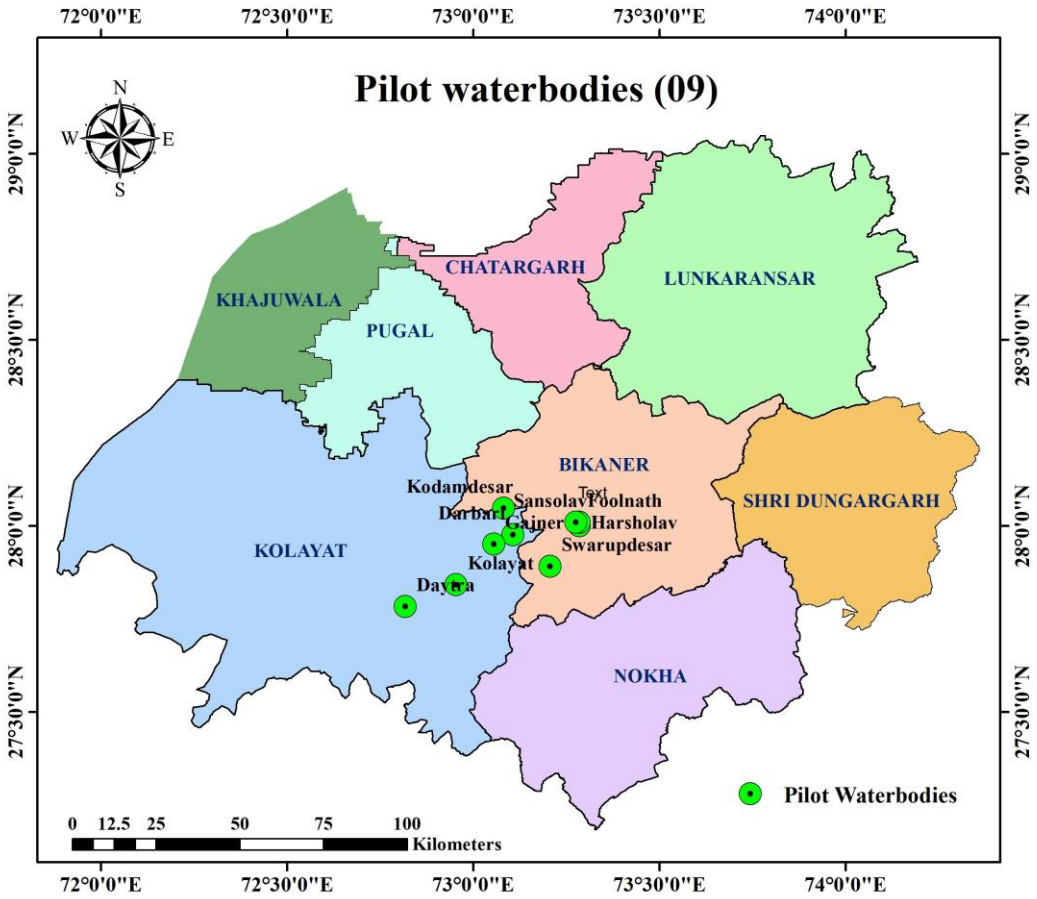

Figure 4:Location map of pilot waterbodies

The catchment area of all pilot waterbodies was delineated by following the methodology as mentioned in **section** by inserting CartoSat DEM as input. After catchment delineation, it has found that Gajner has largest (4845.34 Ha) catchment area, whereas, Foolnath has smallest (10.71 Ha) catchment area. The width of waterbodies has been recorded based on interaction with local people. The catchment boundary and pictorial view of all the pilot waterbodies is shown in **Fig**. The details of these pilot waterbodies are given in **Table**.

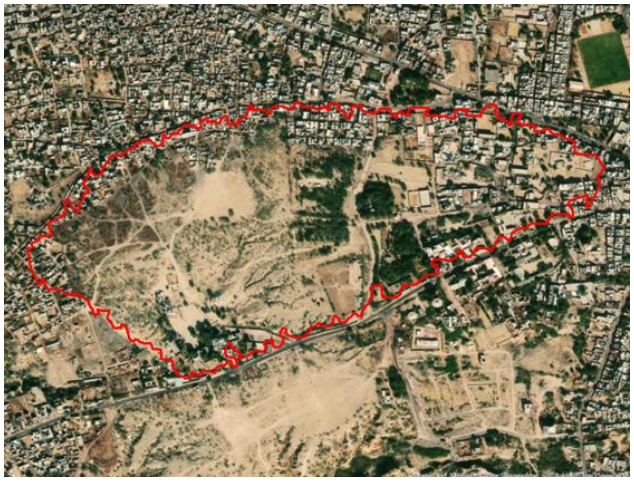

Figure 5:Catchment boundary and pictorial view of Sonsolav waterbody

Figure 6: Catchment boundary and pictorial view of Harsolay waterbody

Figure 7: Catchment boundary and pictorial view of Foolnath waterbody

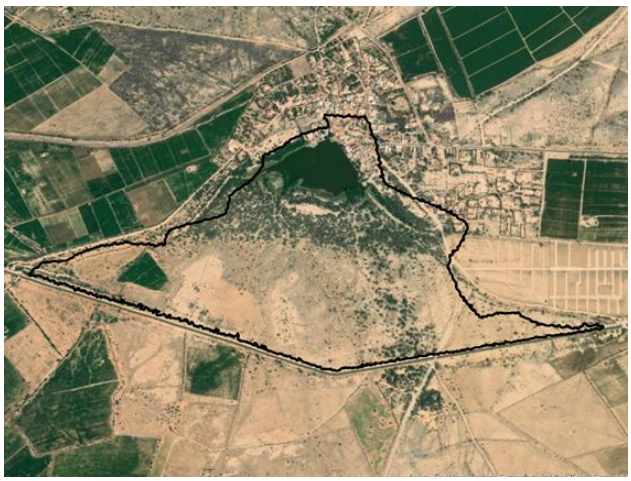

Figure 8:Catchment boundary and pictorial view of Kodamdesar waterbody

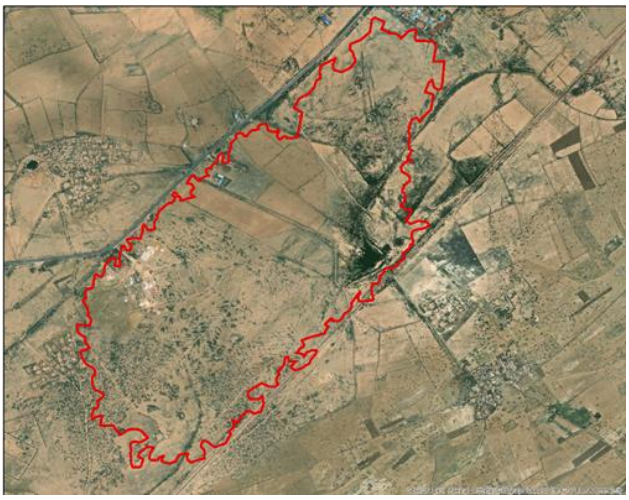

Figure 9:Catchment boundary and pictorial view of Darbari waterbody

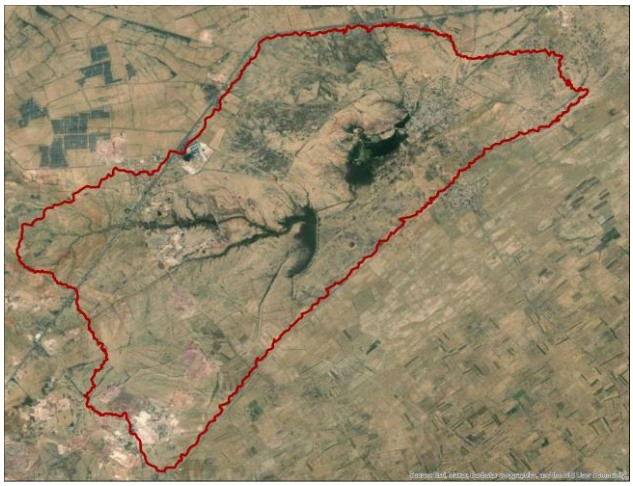

Figure 10:Catchment boundary and pictorial view of Gajner waterbody

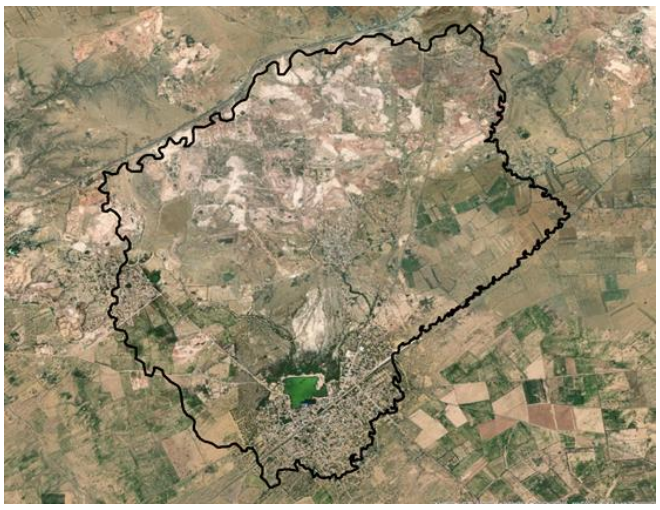

Figure 11:Catchment boundary and pictorial view of Kolayat waterbody

Figure 12:Catchment boundary and pictorial view of Diyatra waterbody

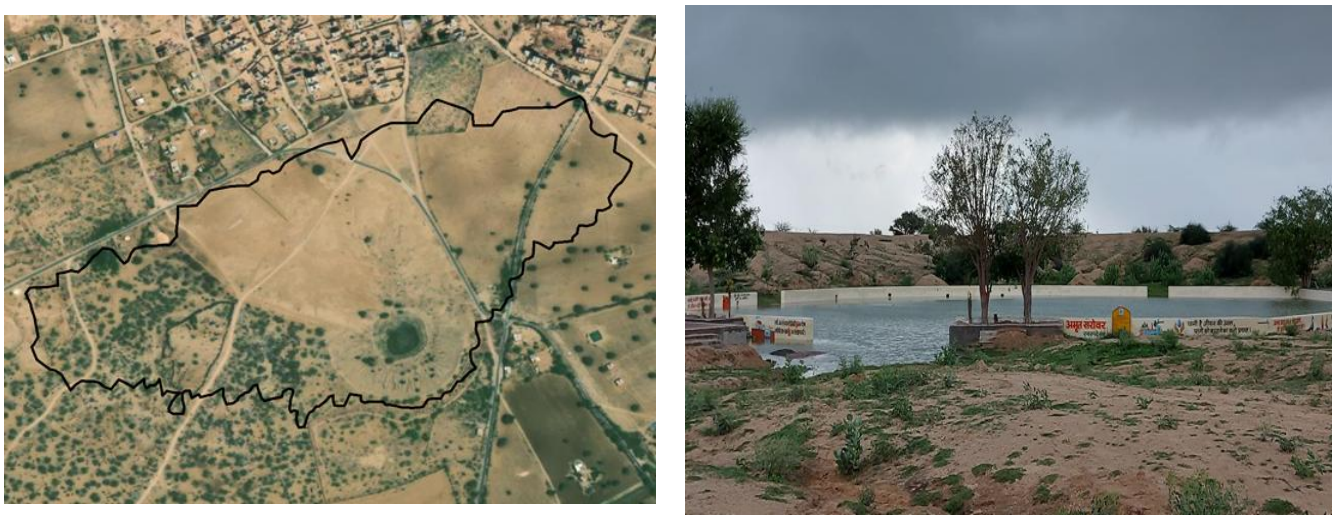

Figure 13:Catchment boundary and pictorial view of Swarupdesar waterbody

Table 10 Details of Pilot waterbodies

S. No.	Pond Name	Latitude/ Longitude	Type	Depth (Ft)	Catchment Area (Ha)	Description
1	Sonsolav	28.0096/ 73.2848	Urbanized	20	40.01	• Within the premise of Vishwanath temple, • Source: Rainfall and runoff from catchment, • Problem : Encroachment in the catchment and Garbage dumping
2	Harsolav	28.0002/ 73.2850	Urbanized	40	82.19	• Source: Rainfall and runoff from catchment,

						• Problem : Encroachment in the catchment and Garbage dumping
3	Foolnath	28.0091/ 73.2758	Urbanized	18	10.71	• In temple premise, • Source: Rainfall and runoff from catchment, • Encroachment problem, • Surrounded by boundary wall
4	Kodamdesar	28.0467/ 73.0811	Rural	20	80.973	• Within the premise of Bherunath temple, • Source: Rainfall and runoff from catchment, • Use: For irrigation and drinking, • Problem : Mining in the catchment,
5	Darbari	27.9760/ 73.1069	Rural	23	637.06	• Near railway track, • Source: Rainfall and runoff from catchment, Linked with Jal Shakti abhiyan
6.	Gajner	27.9506/ 73.0552	Rural	43	4845.34	• Resort built near lake • Three lakes in series, Source: Rainfall and runoff from catchment
7.	Kolayat	27.8421/ 72.9539	Rural	30	2561.83	• Within temple premise, • Source: Rainfall and runoff from catchment, • Problem :Mining in the catchment
8.	Diyatra	27.7826/ 72.8169	Rural	35	1206.92	• Source: Rainfall and runoff from catchment, • Used for drinking and irrigation,

						• Linked with Jal Shakti Abhiyan
9.	Swarupdesar	27.8915/ 73.2067	Rural	18	21.58	• Clean and well maintained Pond, Good catchment condition, • Source: Rainfall and runoff from catchment, • Linked with Jal Shakti Abhiyan

Land Use Land Cover Change Detection

The preparation of accurate LULC is of great importance as it is used in various studies ranging from change detection to geospatial modelling. In this study, high resolution (5 m) satellite image IRS-R2A LISS-IV FMX are employed for LULC map preparation for the year 2011 and 2020. In the present study, on screen digitization with visual interpretation technique was used to prepare a map and investigate LULC changes over an interval in ArcMap v.10.2. Different land uses were identified using image attributes and the image was classified into five classes; waterbodies, agriculture, trees, builtup, and barren land. Finally, area statistics were derived for each land use class. Area estimation of each land use class was carried out using the same GIS software.

The analysis revealed land use and land cover changes between 2010 and 2020 across various catchments. In Harsolav, barren land decreased by 6.64%, trees by 3.13%, and waterbodies by 0.25%, while built-up areas increased by 10.03%. Foolnath experienced a 9.79% reduction in barren land and 7.08% decrease in tree cover, but built-up areas grew significantly by 16.79%. In Kodamdesar catchment, a decrease of 12.60% in barren land and a slight increase in agriculture (0.17%) and built-up areas (1.00%) was observed, while tree cover increased substantially by 11.90%. Darbari had the most dramatic changes, with barren land decreasing by 16.32%, tree cover by 12.71%, and a substantial increase in built-up areas by 29.35%. In Gajner catchment, barren land reduced by 3.98%, while agriculture and built-up areas slightly increased by 0.55% and 0.73%, respectively. In Kolayat, barren land decreased by 9.09%, tree cover increased by 6.56%, and built-up areas by 1.49%. In Diyatra a significant decrease of 15.59% in barren land and an increase in agriculture by 16.63% was observed, while tree cover

decreased by 1.58% and built-up areas grew slightly by 0.59%. Swarupdesar experienced minimal changes, with a slight decrease in barren land (2.13%) and minor increases in tree cover (1.39%) and built-up areas (0.32%). Decadal change in land use statistics are given in **Table.**

Table 11 Land Use Land Cover statistics between the year 2010 & 2020

	Time	**Barren land**	**Agriculture**	**Trees**	**Builtup**	**Waterbodies**
Harsolav	**2010**	57.62	0	16.01	7.91	0.66
	2020	52.16	0	13.43	16.16	0.45
Foolnath	**2010**	6.44	0	3.43	0.81	0.04
	2020	5.39	0	2.67	2.61	0.04
Kodamdesar	**2010**	57.96	1.22	16.24	1.1	4.45
	2020	47.75	1.36	25.88	1.91	4.08
Darbari	**2010**	423	112	96	1	5
	2020	319	110	15	188	5
Gajner	**2010**	3666.65	180.24	917.33	41.7	39.43
	2020	3473.67	207.35	1054.04	77.43	32.85
Kolayat	**2010**	1915.36	404.23	122.47	95.86	23.92
	2020	1686.45	438.42	291.35	134.44	17.33
Diyatra	**2010**	796.59	305.52	47.74	52.79	4.29
	2020	608.35	506.35	28.66	60	3.55
Swarupdesar	**2010**	16.31	0	4.98	0	0.29
	2020	15.85	0	5.28	0.07	0.38

Overall, a notable reduction in barren land is evident in most catchments, suggesting a shift towards more productive land uses or natural vegetation recovery. Concurrently, there has been a significant increase in built-up areas across nearly all regions, indicating ongoing urbanization and infrastructure development. Changes in agricultural land varied, with some catchments like Diyatra and Kolayat experiencing increases, while others showed minimal or no change **(Fig.)**. Tree cover dynamics also differed, with significant increases in some areas such as Kodamdesar, while others like Foolnath and Darbari saw decreases, pointing to differing regional practices or environmental conditions **(Fig.)**. Waterbodies remained relatively stable, with only minor changes observed, suggesting that water resources were

largely unchanged over the decade. Each catchment displayed unique trends, emphasizing the role of localized factors in land use changes. For instance, Darbari experienced a substantial increase in built-up areas, whereas Gajner and Kolayat showed modest increases in agricultural land **(Fig.)**. Overall, the analysis indicates a trend of decreasing barren land and increasing urbanization, with varied changes in agricultural land and tree cover depending on the catchment, highlighting the dynamic nature of land use and the impact of regional development and environmental policies.

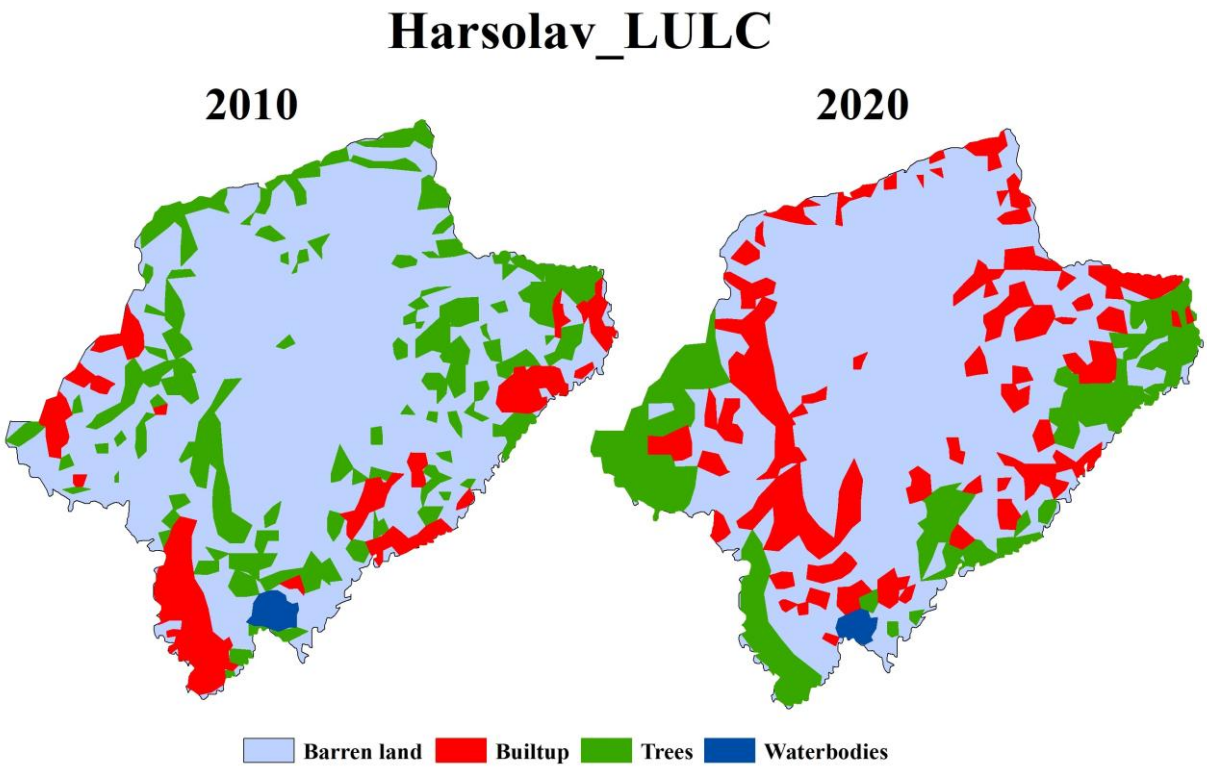

Figure 14:Land Use land cover changes over Harsolav catchment between year 2010 & 2020

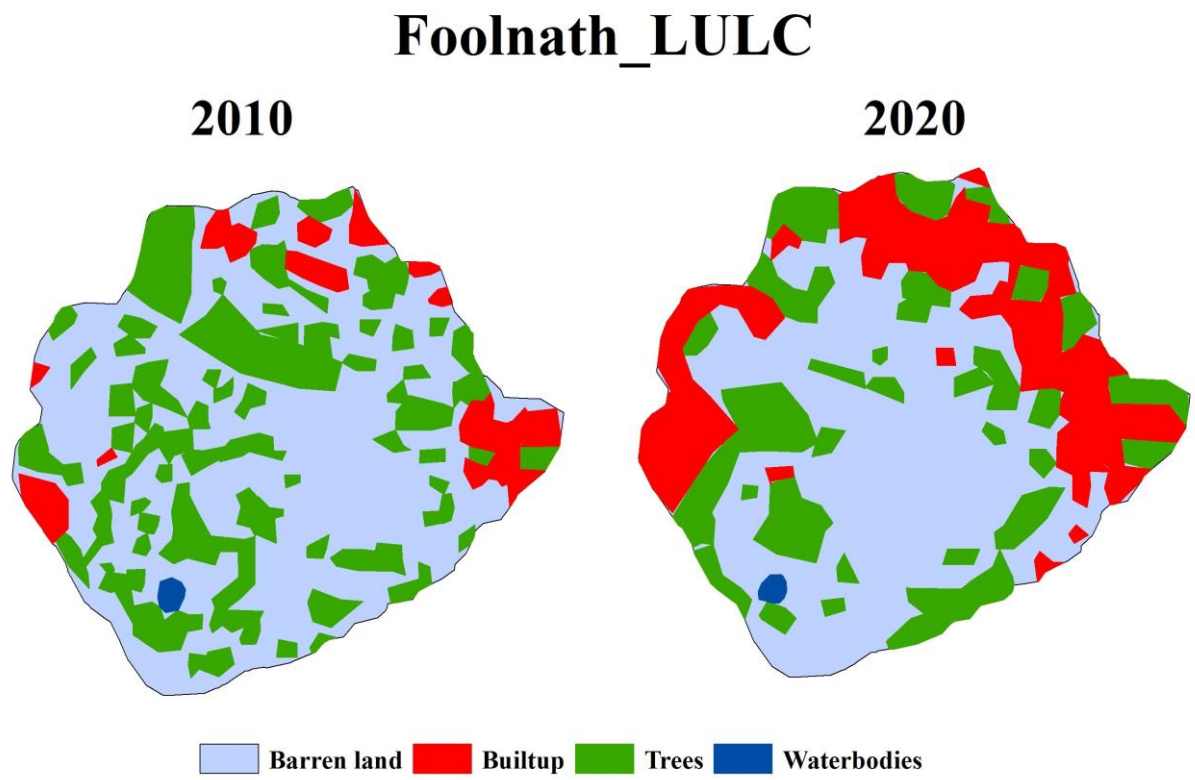

Figure 15: Land Use land cover changes over Foolnath catchment between year 2010 & 2020

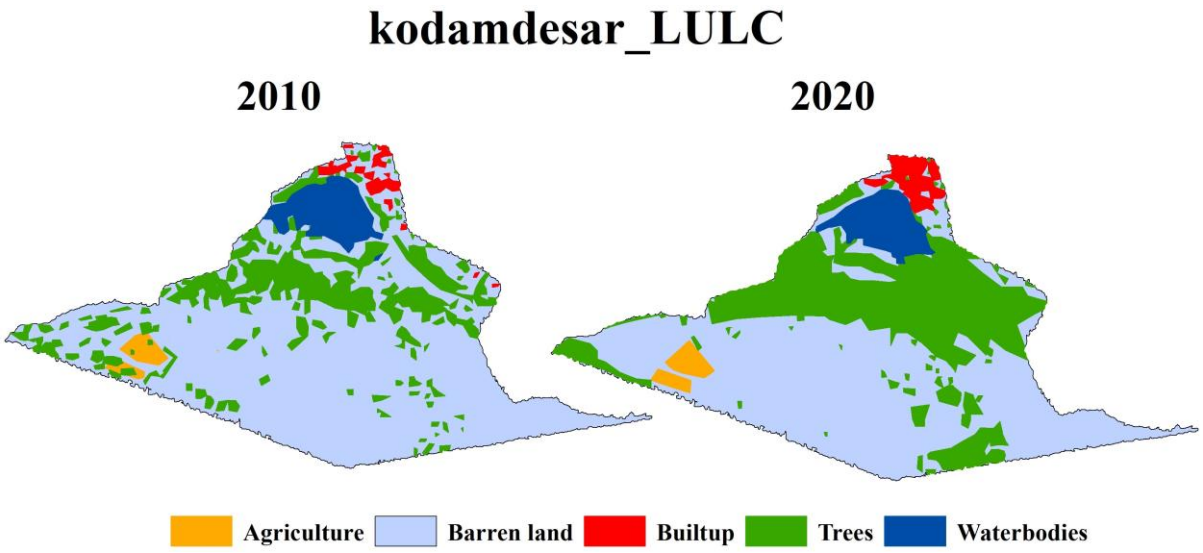

Figure 16:Land Use land cover changes over Kodamdesar catchment between year 2010 & 2020

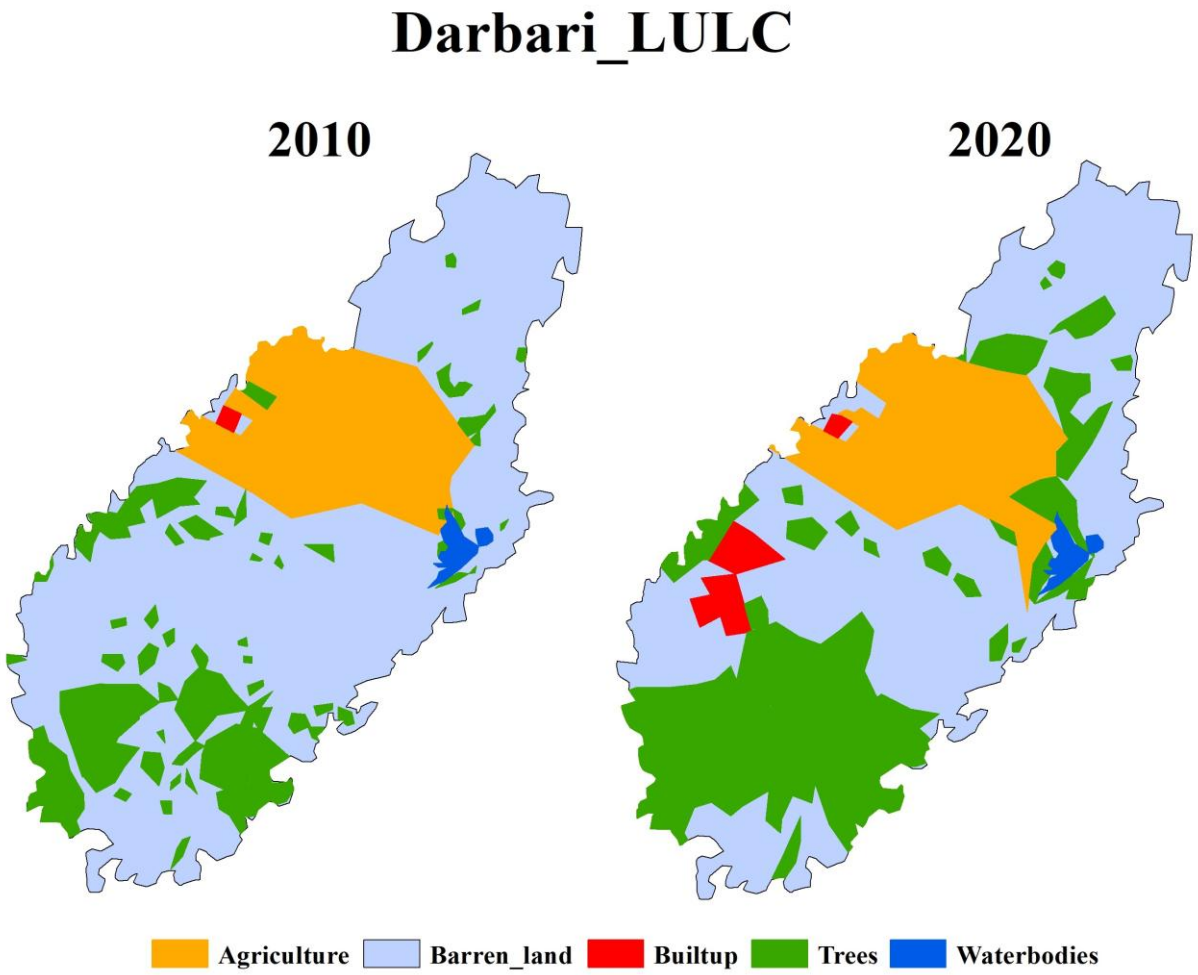

Figure 17:Land Use land cover changes over Darbari catchment between year 2010 & 2020

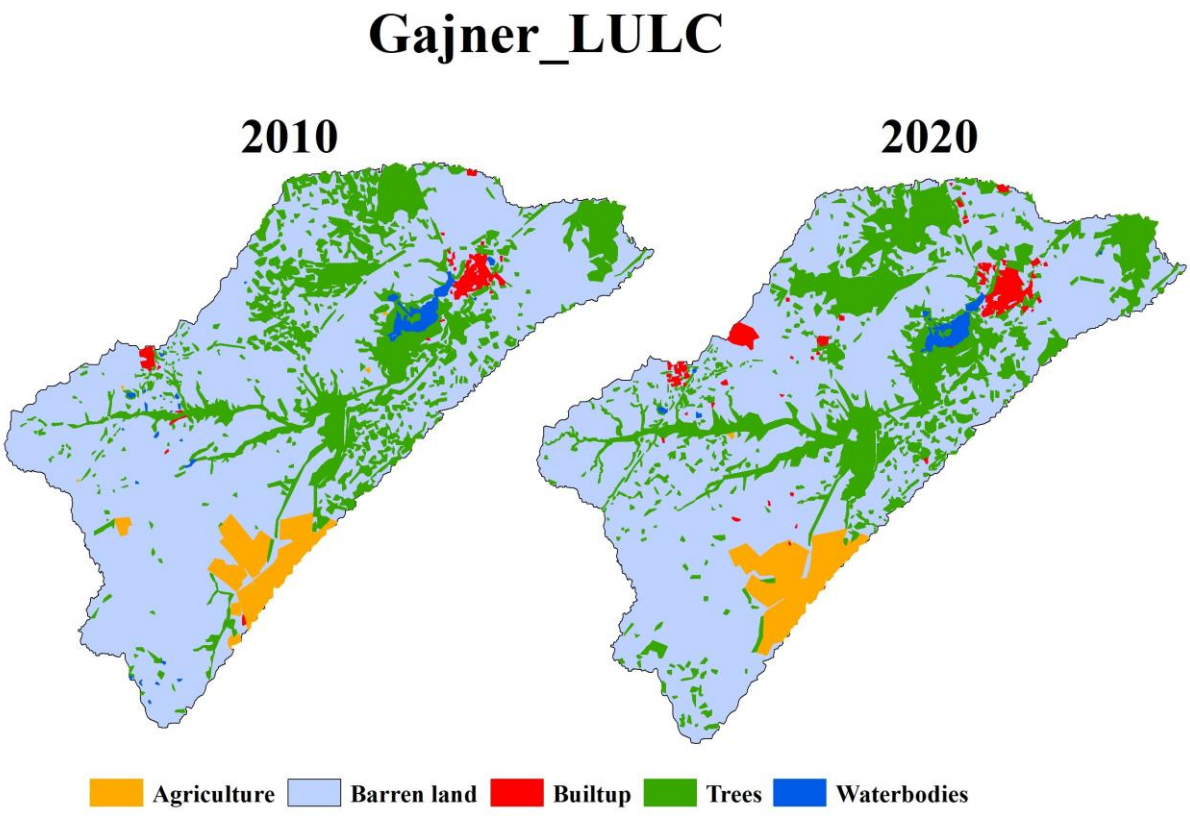

Figure 18:Land Use land cover changes over Gajner catchment between year 2010 & 2020

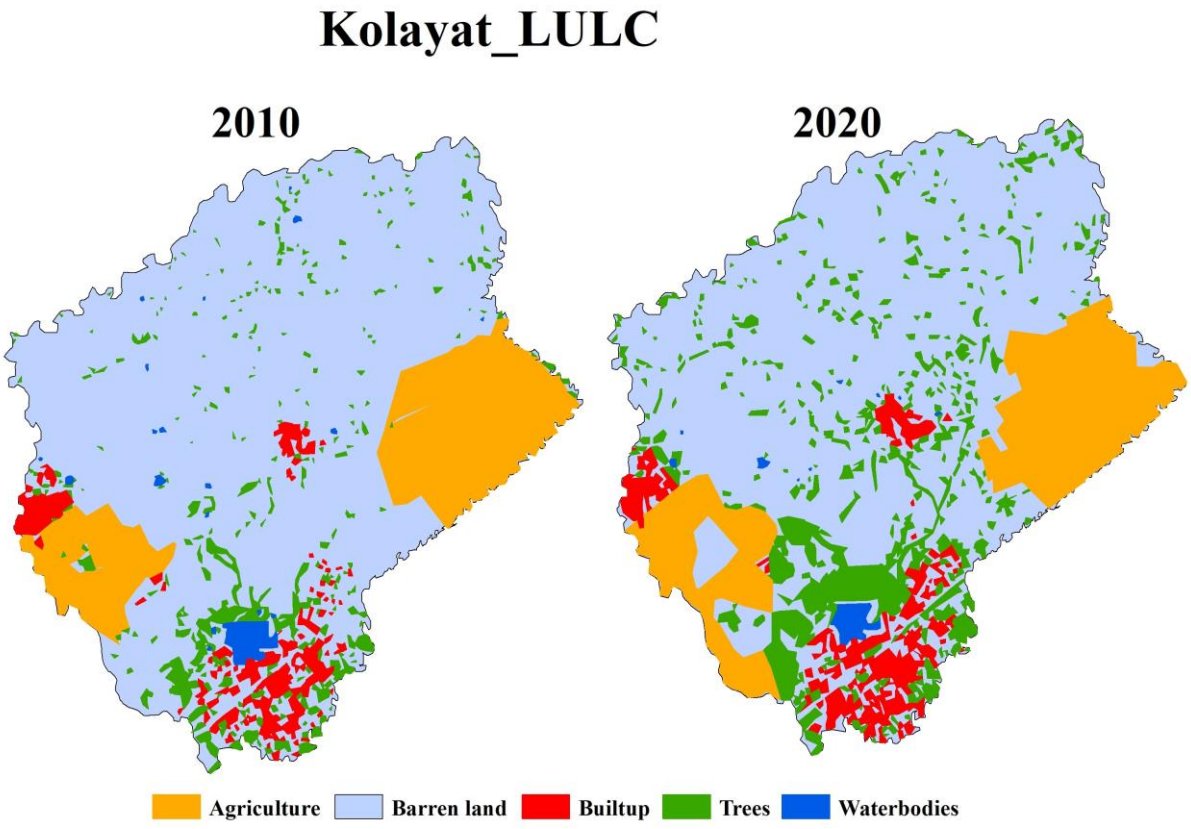

Figure 19:: Land Use land cover changes over Kolayat catchment between year 2010 & 2020

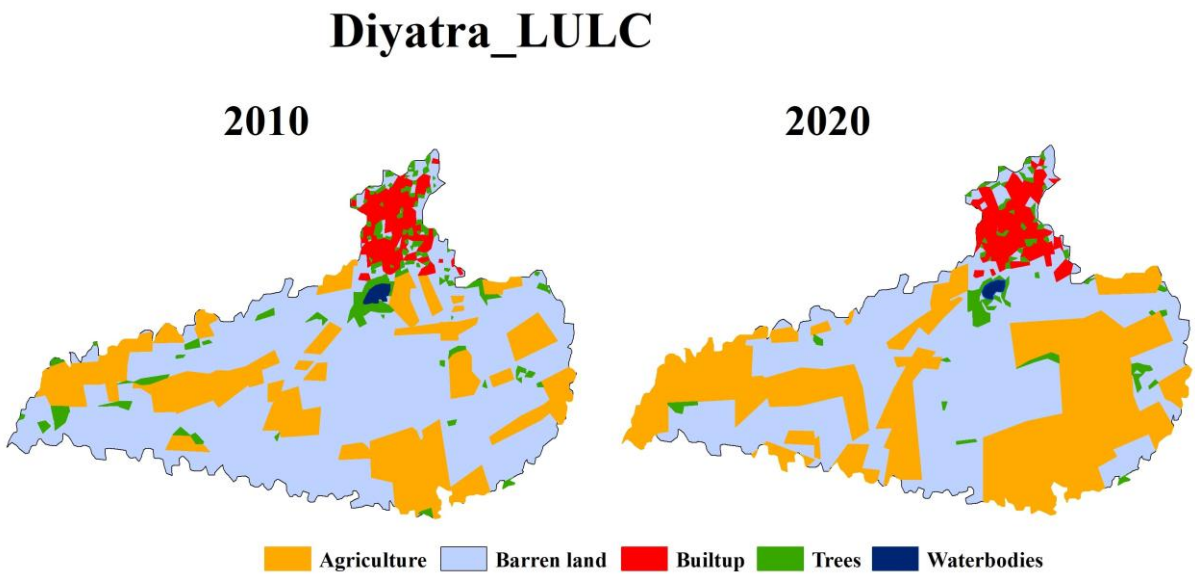

Figure 20:Land Use land cover changes over Diyatra catchment between year 2010 & 2020

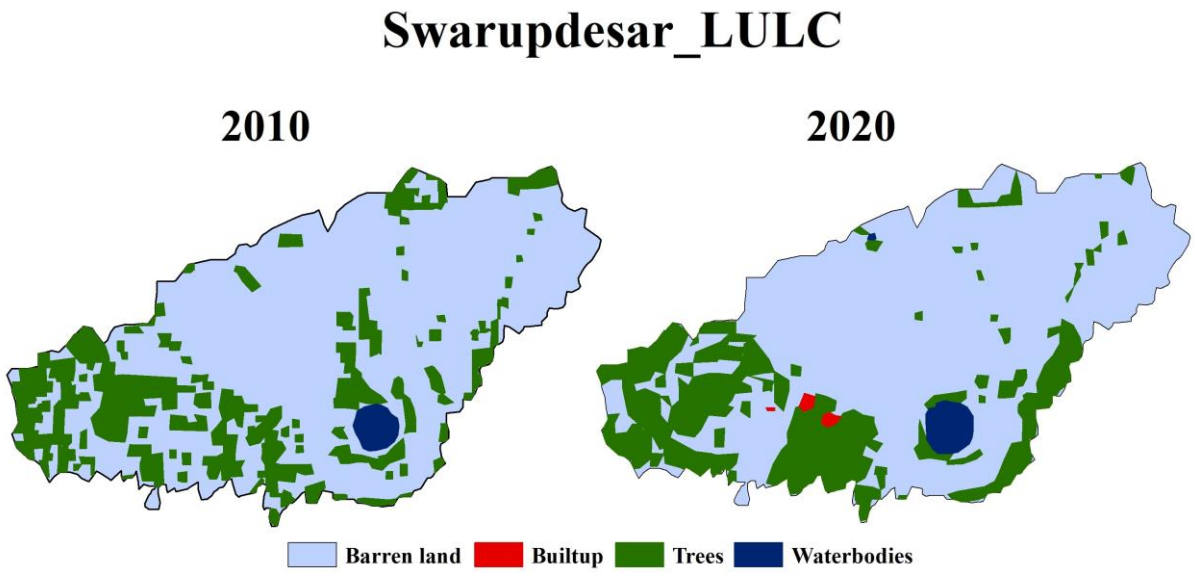

Figure 21:Land Use land cover changes over Swarupdesar catchment between year 2010 & 2020

Land Use Land Cover Change Detection

The preparation of accurate LULC is of great importance as it is used in various studies ranging from change detection to geospatial modelling. In this study, high resolution (5 m) satellite image IRS-R2A LISS-IV FMX are employed for LULC map preparation for the year 2011 and 2020. In the present study, on screen digitization with visual interpretation technique was used to prepare a map and investigate LULC changes over an interval in ArcMap v.10.2. Different land uses were identified using image attributes and the image was classified into five classes; waterbodies, agriculture, trees, builtup, and barren land. Finally, area statistics were derived for each land use class. Area estimation of each land use class was carried out using the same GIS software.

The analysis revealed land use and land cover changes between 2010 and 2020 across various catchments. In Harsolav, barren land decreased by 6.64%, trees by 3.13%, and waterbodies by 0.25%, while built-up areas increased by 10.03%. Foolnath experienced a 9.79% reduction in barren land and 7.08% decrease in tree cover, but built-up areas grew significantly by 16.79%. In Kodamdesar catchment, a decrease of 12.60% in barren land and a slight increase in agriculture (0.17%) and built-up areas (1.00%) was observed, while tree cover increased substantially by 11.90%. Darbari had the most dramatic changes, with barren land decreasing by 16.32%, tree cover by 12.71%, and a substantial increase in built-up areas by 29.35%. In Gajner catchment, barren land reduced by 3.98%, while agriculture and built-up areas slightly increased by 0.55% and 0.73%, respectively. In Kolayat, barren land decreased by 9.09%, tree cover increased by 6.56%, and built-up areas by 1.49%. In Diyatra a significant decrease of 15.59% in barren land and an increase in agriculture by 16.63% was observed, while tree cover decreased by 1.58% and built-up areas grew slightly by 0.59%. Swarupdesar experienced minimal changes, with a slight decrease in barren land (2.13%) and minor increases in tree cover (1.39%) and built-up areas (0.32%). Decadal change in land use statistics are given in **Table.**

Table 12 Land Use Land Cover statistics between the year 2010 & 2020

	Year	Barren land (Ha)	Agriculture (Ha)	Trees (Ha)	Builtup (Ha)	Waterbodies (Ha)
Harsolav	**2010**	57.62	0	16.01	7.91	0.66
	2020	52.16	0	13.43	16.16	0.45
Foolnath	**2010**	6.44	0	3.43	0.81	0.04
	2020	5.39	0	2.67	2.61	0.04
Kodamdesar	**2010**	57.96	1.22	16.24	1.1	4.45
	2020	47.75	1.36	25.88	1.91	4.08
Darbari	**2010**	423	112	96	1	5
	2020	319	110	15	188	5
Gajner	**2010**	3666.65	180.24	917.33	41.7	39.43
	2020	3473.67	207.35	1054.04	77.43	32.85
Kolayat	**2010**	1915.36	404.23	122.47	95.86	23.92
	2020	1686.45	438.42	291.35	134.44	17.33
Diyatra	**2010**	796.59	305.52	47.74	52.79	4.29
	2020	608.35	506.35	28.66	60	3.55

Swarupdesar	**2010**	16.31	0	4.98	0	0.29
	2020	15.85	0	5.28	0.07	0.38

Overall, a notable reduction in barren land is evident in most catchments, suggesting a shift towards more productive land uses or natural vegetation recovery. Concurrently, there has been a significant increase in built-up areas across nearly all regions, indicating ongoing urbanization and infrastructure development. Changes in agricultural land varied, with some catchments like Diyatra and Kolayat experiencing increases, while others showed minimal or no change **(Fig.)**. Tree cover dynamics also differed, with significant increases in some areas such as Kodamdesar, while others like Foolnath and Darbari saw decreases, pointing to differing regional practices or environmental conditions **(Fig.)**. Waterbodies remained relatively stable, with only minor changes observed, suggesting that water resources were largely unchanged over the decade. Each catchment displayed unique trends, emphasizing the role of localized factors in land use changes. For instance, Darbari experienced a substantial increase in built-up areas, whereas Gajner and Kolayat showed modest increases in agricultural land **(Fig.)**. Overall, the analysis indicates a trend of decreasing barren land and increasing urbanization, with varied changes in agricultural land and tree cover depending on the catchment, highlighting the dynamic nature of land use and the impact of regional development and environmental policies.

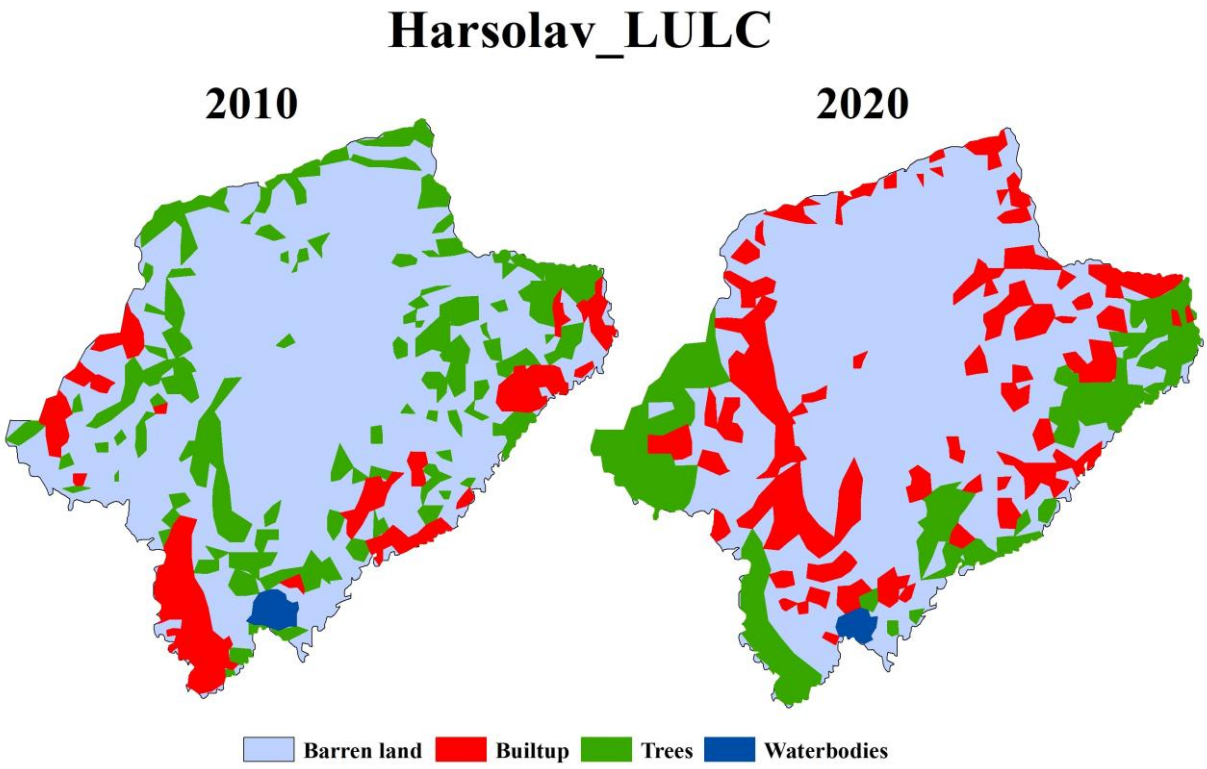

Figure 22:Land Use land cover changes over Harsolav catchment between year 2010 & 2020

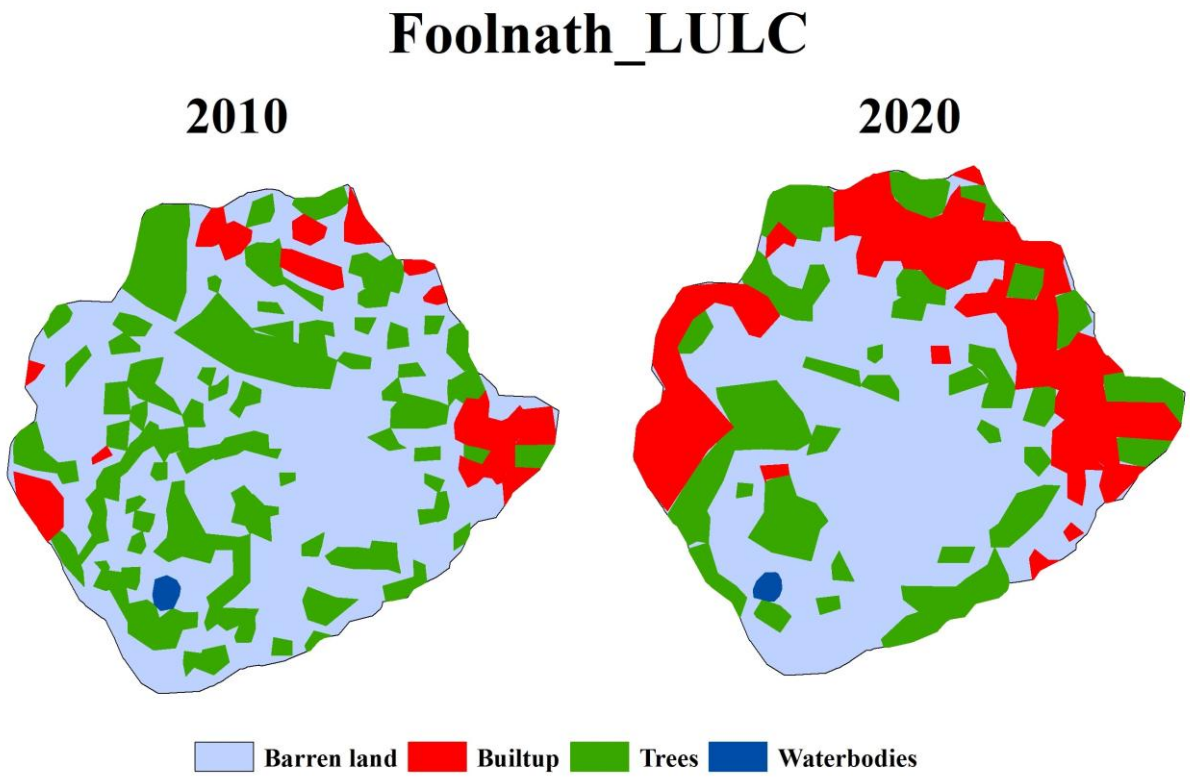

Figure 23:Land Use land cover changes over Foolnath catchment between year 2010 & 2020

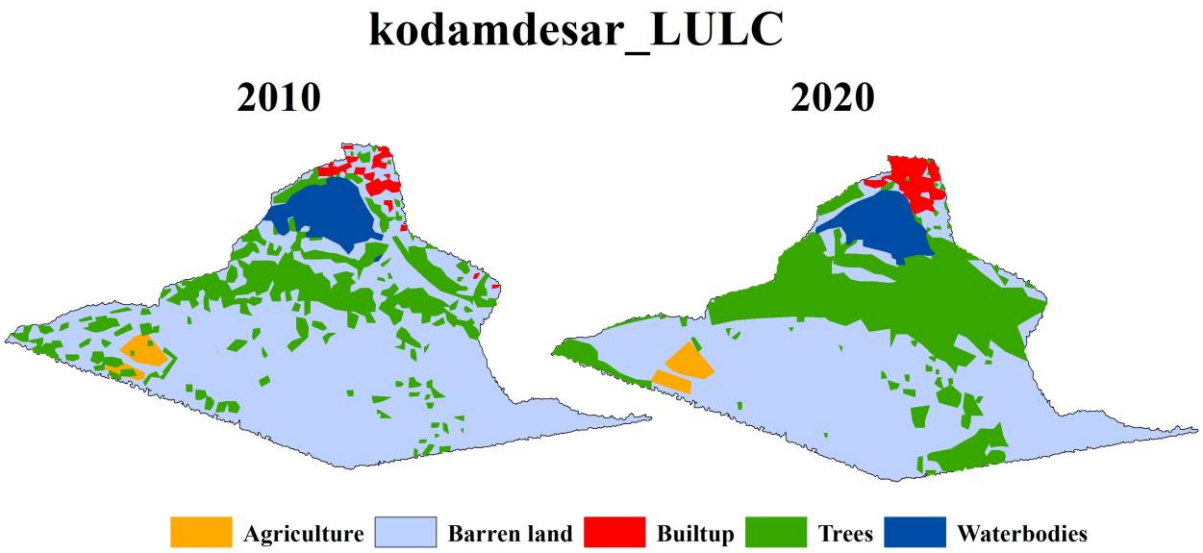

Figure 24:Land Use land cover changes over Kodamdesar catchment between year 2010 & 2020

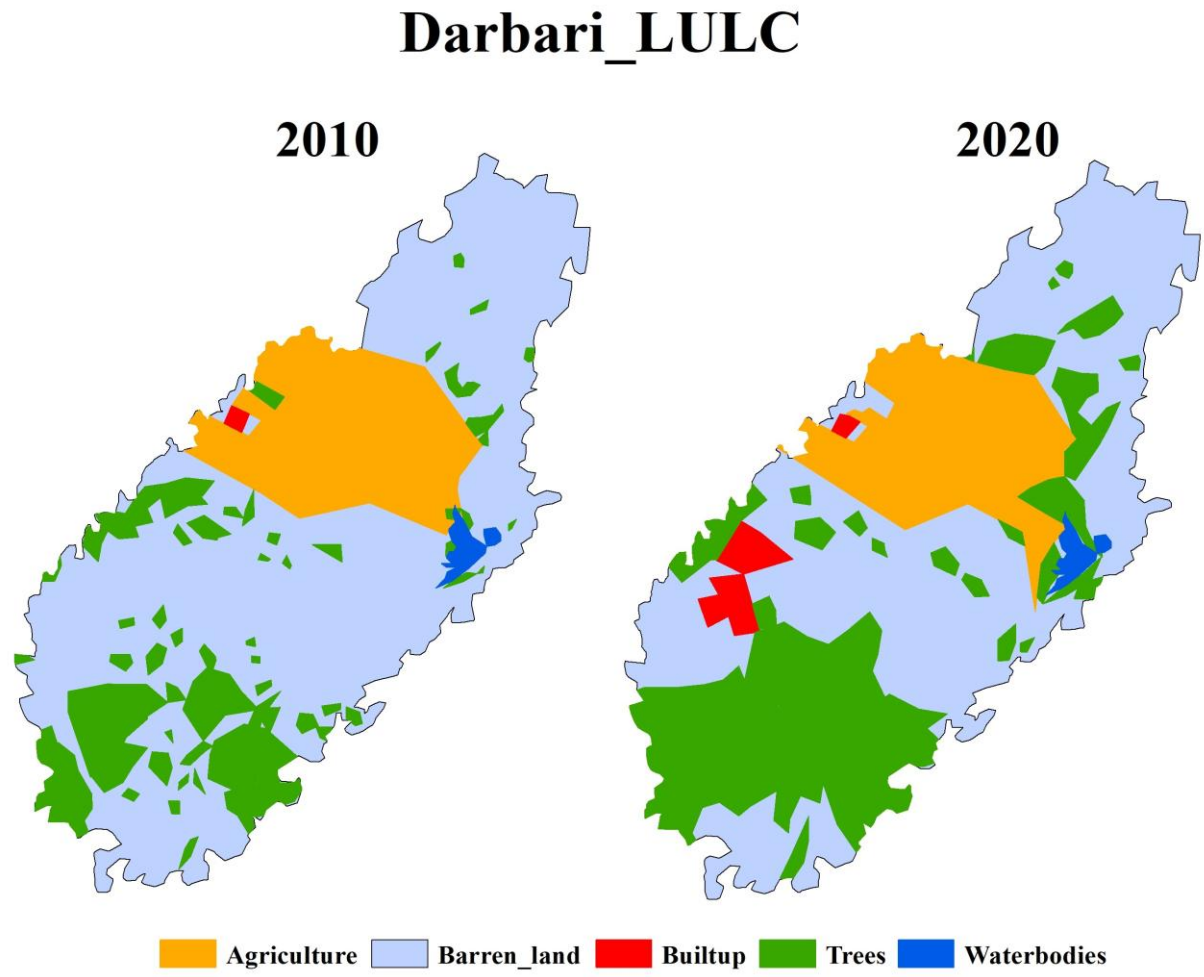

Figure 25:Land Use land cover changes over Darbari catchment between year 2010 & 2020

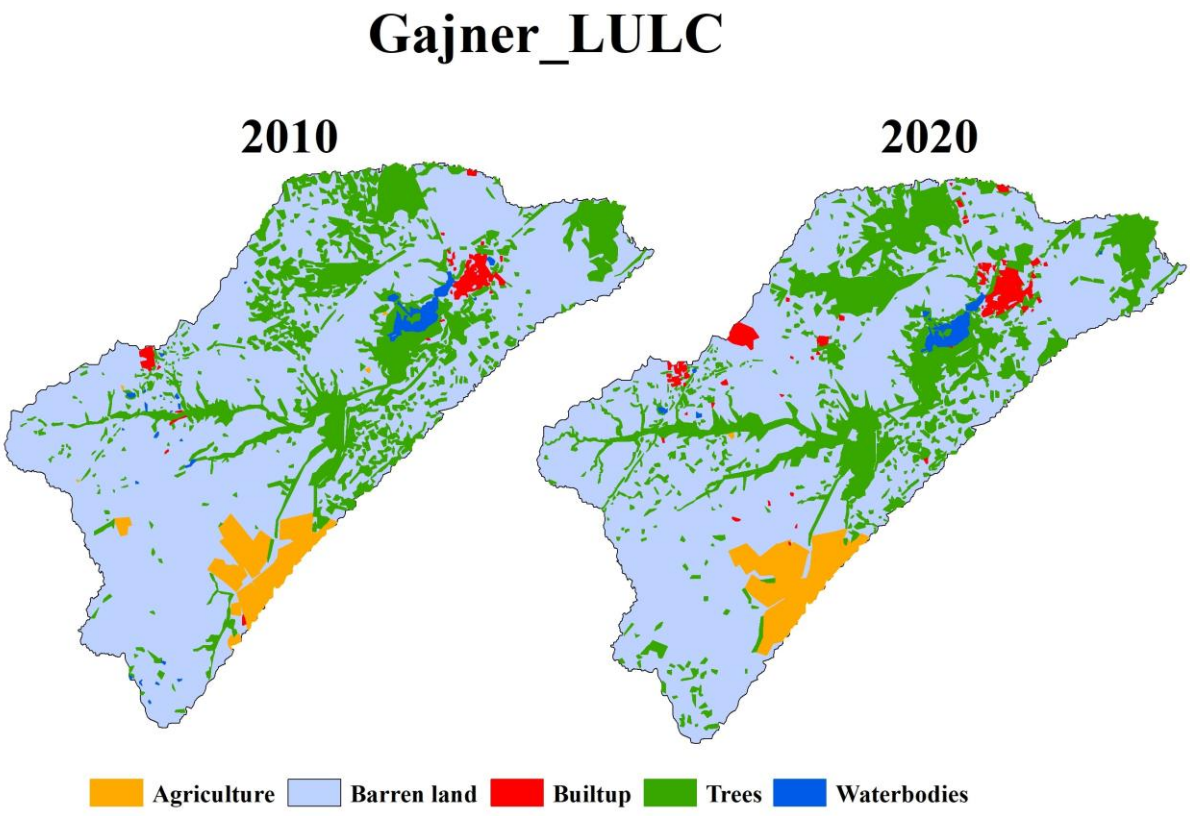

Figure 26:Land Use land cover changes over Gajner catchment between year 2010 & 2020

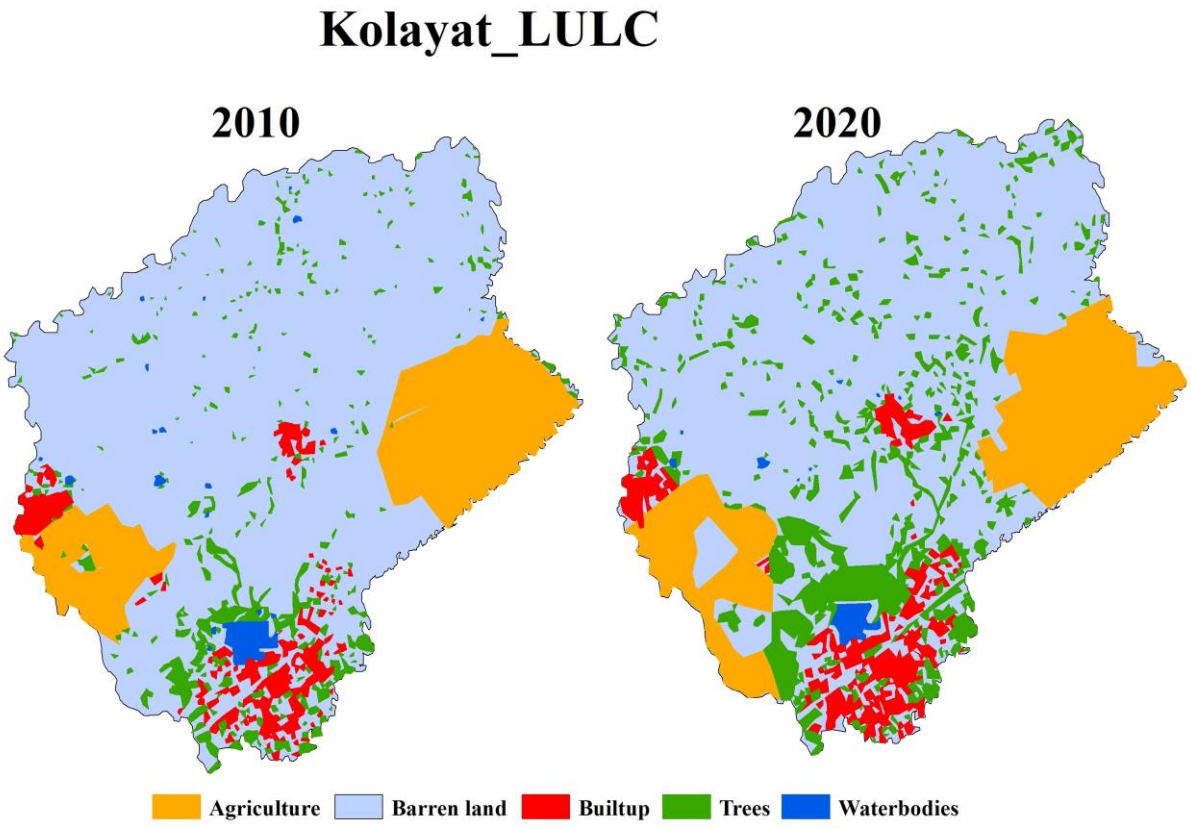

Figure 27:Land Use land cover changes over Kolayat catchment between year 2010 & 2020

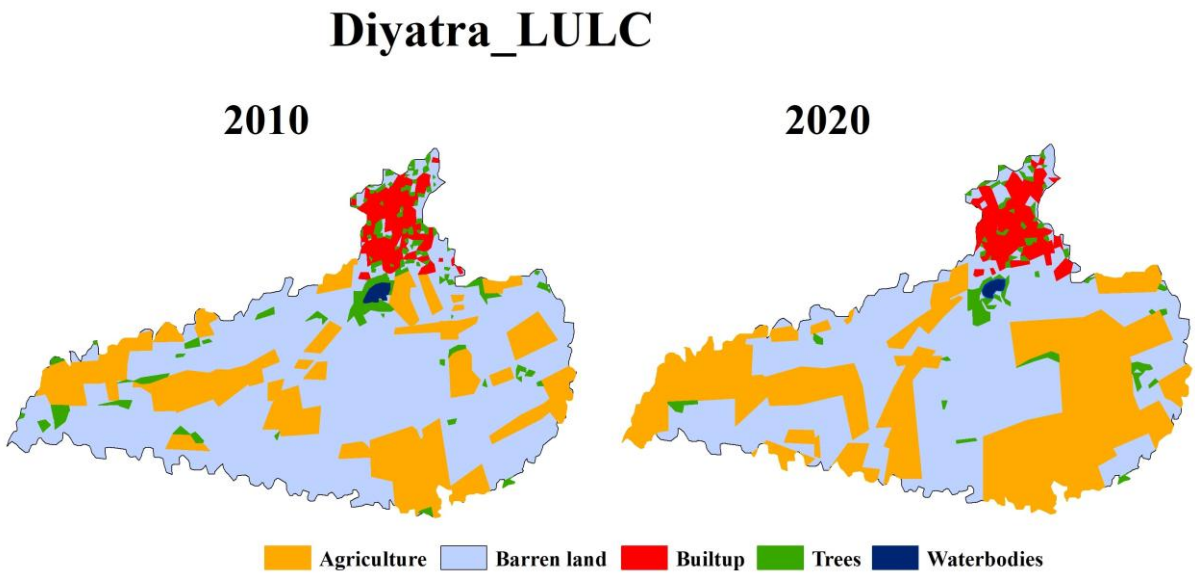

Figure 28:Land Use land cover changes over Diyatra catchment between year 2010 & 2020

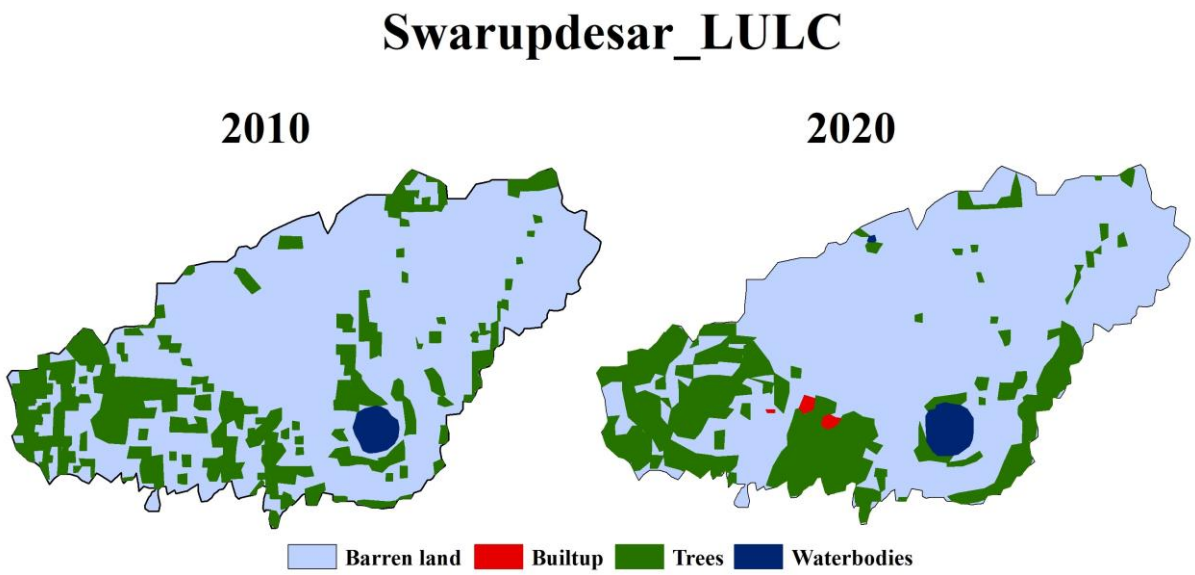

Figure 29:Land Use land cover changes over Swarupdesar catchment between year 2010 & 2020

Climate Trend Analysis

Evaluation of Rainfall Dataset

The rainfall statistics based on 73 years (1951-2023) data provided useful insights into the spatial-temporal distribution across the entire district. It is seen that the district experienced a significant rainfall during the monsoon season (June - September). Notably, the maximum annual rainfall of 584.52 mm occurred in the year 1962, while the minimum of 53.68 mm was recorded in the year 2002. Table 1 displays the descriptive statistics of the annual rainfall over the district. The mean annual rainfall over the district estimated as 267.23 mm. Skewness value of the annual rainfall estimated as 0.72, indicating a tail extending to the right in the rainfall distribution. Similarly, kurtosis of 1.13, indicating a higher peak than the normal distribution.

Values of coefficient of variation (CV) estimated as 37.55%, which indicates high rainfall variability over the area. Mean monthly rainfall was observed maximum in July (82.62mm) followed by August (71.27 mm) and September (34.80 mm) and minimum in December (2.13 mm). Standard deviation is found maximum for July and minimum for November. Spatial distribution of mean annual rainfall, illustrates declination in rainfall from the East to West of the district. The rainfall in the district varies from 222.58 to 311.91 mm/year (Figure). Maximum rainfall of 872.5 mm in year 1975 was occurred in Nokha division. Whereas, minimum rainfall of 32.3 mm in year 1999 was occurred in Bikaner division.

Table 13 Descriptive statistics of annual rainfall (1951-2023) over the Bikaner District

Parameters	**Rainfall**
Mean (mm)	267.23
Minimum (mm)	53.68
Maximum (mm)	584.52
Standard Deviation (mm)	100.35
Kurtosis	1.13
Skewness	0.72
CV (%)	37.55

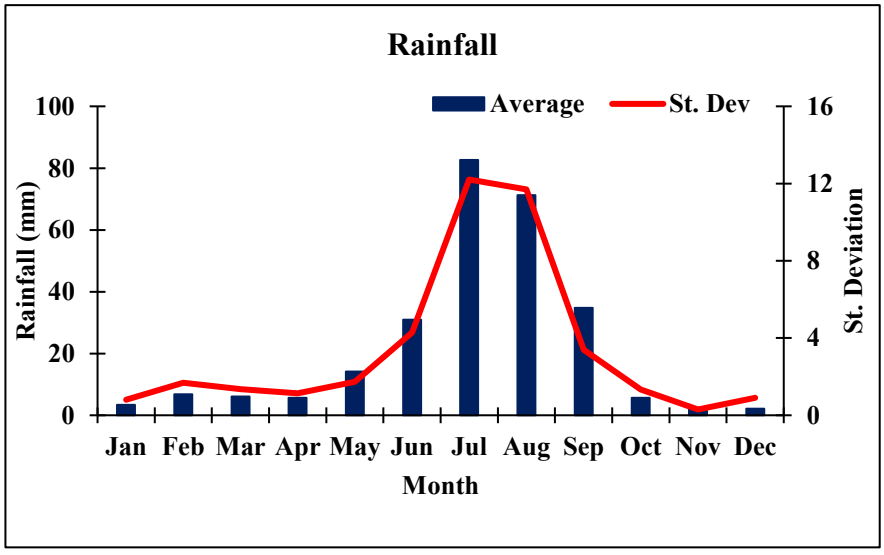

Figure 30:Monthly characteristics of long term (1951–2023) rainfall

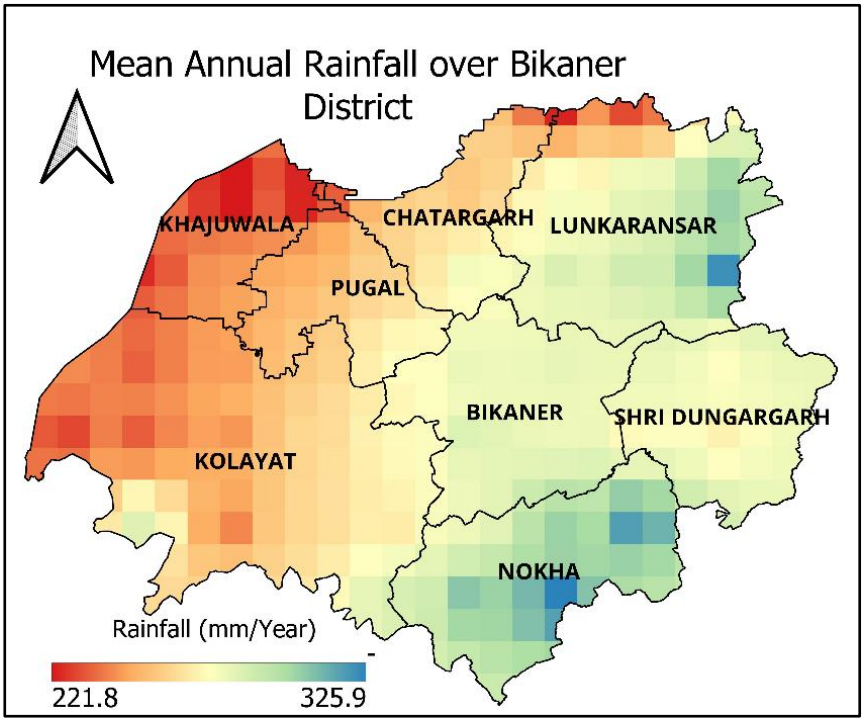

Figure 31:Spatial distribution of mean annual rainfall over the district

Evaluation of Temperature Dataset

The maximum temperature (T_{max}) and minimum temperature (T_{min}) statistics based on 73 years (1951-2023) data provided useful insights into the spatial-temporal distribution across the entire district. It is seen that the district experienced a highest Tmax and Tmin in the month of May and June respectively and Lowest in the month of January. Notably, the highest annual Tmax of 34.60 °C occurred in the year 2002, while the lowest Tmax of 31.47 °C was recorded in the year 1997. Similarly, the highest annual Tmin of 20 °C occurred in the year 2010, while the lowest value of 17.15 °C was recorded in the year 1974. Table 1 displays the descriptive statistics of the annual rainfall over the district. The mean annual Tmax and Tmin over the district estimated as 33.12°C and 18.42 °C respectively. Values of coefficient of variation (CV) estimated as 1.88% and 3.58% for Tmax and Tmin respectively, which indicates slight variability in temperature over the area. Mean monthly Tmax was observed maximum in May (41.04 °C) followed by June (40.63 °C) and April (37.67 °C) and minimum in January (22.71 °C). Standard deviation is found maximum for March and minimum for November. Similarly, mean monthly Tmin was observed maximum in June (27.50 °C) followed by July (26.58 °C) and August (25.51 °C) and minimum in January (6.67 °C). Standard deviation is found maximum for April and minimum for August. Spatial distribution of mean annual Tmax and Tmin, illustrates a slight declination in from the East to West of the district. The mean Tmax

over the district varies from 33.05 °C to 33.19 °C, whereas, mean Tmin varies from 18.23°C to 18.61°C (Figure).

Table 14 Descriptive statistics of annual Tmax and Tmin (1951-2023) over the Bikaner District

Parameters	**T_{max}**	**T_{min}**
Mean (°C)	33.12	18.42
Minimum (°C)	31.47	17.15
Maximum (°C)	34.60	20.00
Standard Deviation (°C)	0.62	0.66
Kurtosis	0.15	-0.52
Skewness	0.12	0.26
CV (%)	1.88	3.58

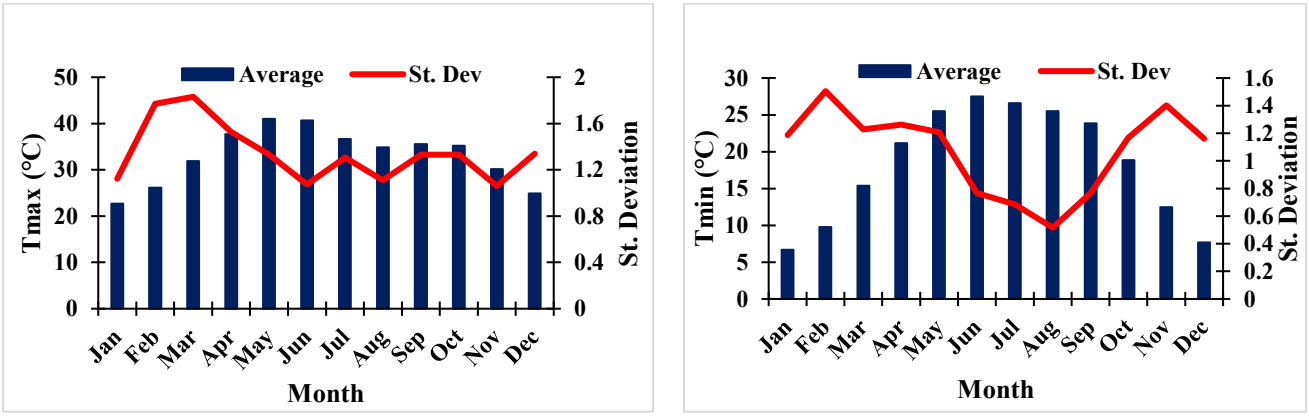

(A) **(B)**

Figure 32:Monthly characteristics of (A) Maximum Temperature (B) Minimum Temperature

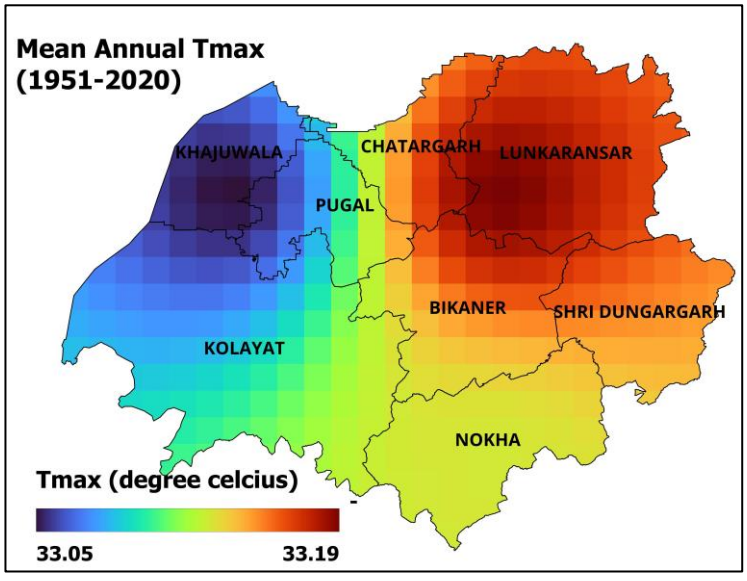

Figure 33:(A) Spatial distribution of mean annual maximum temperature (Tmax)

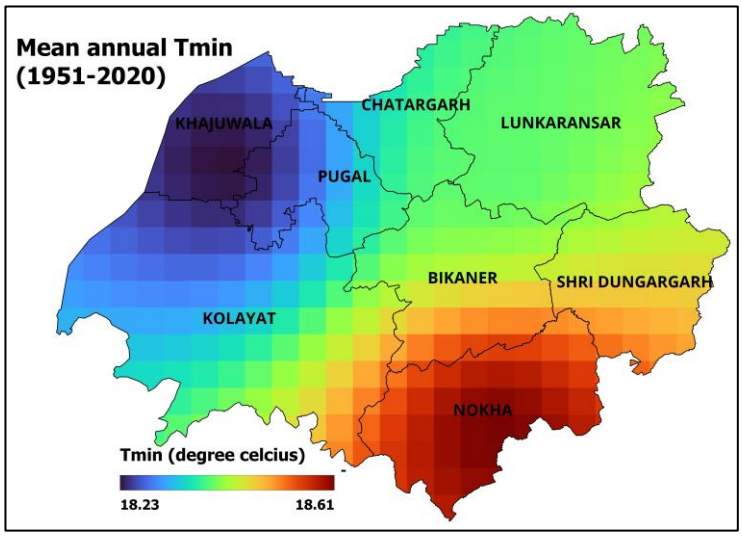

Figure 34:(B) Spatial distribution of mean annual minimum temperature (Tmin)

Temporal Variability in Long Term Trend of Rainfall

Monthly analysis

The non-parametric MK test together with Sen's slope was applied individually to each month of the 70 years rainfall time series at 95% significance level. If the value of z-calculated is more than z-tabulated i.e. 1.96 (for 95% confidence interval), then there is a rejection of null hypothesis (H_0). Rejection of hypothesis H_0 shows that a trend is exist in the series of time, while accepting H_0 shows no trend. The test is said to be statistically significant if there is a rejection of null hypothesis. The results of the monthly rainfall trend in terms of z statistics and slope are depicted in **Table**. The results showed considerable fluctuation, but there were non-significant trends throughout the months except April and June, which is consistent with the previous findings. The declined rainfall trend at rates of −0.005 mm/year and −0.149 mm/year was observed for the months of January and August, respectively. The higher increase in rainfall was observed in the month of April, June, and July with the rate of 0.214 mm/year, 0.296 mm/year, and 0.296 mm/year respectively. However, the months October, November, and December showed a very low increasing trend (~0 mm/year). Among the monthly trend, the maximum negative magnitude was observed in August (−0.149 mm/year), while the positive magnitude were seen for the month of June and July (0.296 mm/year).

Table 15 MK-test statistic and Sen's slope values for 70 years monthly rainfall

Time Scale	Z-value	Sen's slope (mm/year)	Trend
January	-0.07	0.005	Non-significant (↓)
February	1.28	0.005	Non-significant (↑)

March	1.12	0.012	Non-significant (↑)
April	3.07	0.214	Significant (↑)
May	1.68	0.107	Non-significant (↑)
June	2.58	0.296	Significant (↑)
July	1.01	0.296	Non-significant (↑)
August	-0.48	-0.149	Non-significant (↓)
September	0.49	0.056	Non-significant (↑)
October	-0.12	0	Non-significant (↓)
November	-0.35	0	Non-significant (↓)
December	-0.51	0	Non-significant (↓)

Seasonal and annual analysis

In addition to the month-wise trend analysis, the seasonal and annual trend analysis of the 70 years of rainfall was carried out using the MK test and Sen's slope estimator for the magnitude of the trend. The results of the trend analysis of annual and seasonal rainfall are shown in **Table**. The analysis results revealed that a significant increasing trend of rainfall is observed during pre-monsoon season, whereas, non-significant increasing trend is observed during monsoon, post-monsoon, and winter season. The pre-monsoon season is showing a positive change with z statistic value of 3.18 and Sen's slope of 0.289 mm/year.

For the annual trend, the z statistic and Sen's slope were estimated as 1.86 and 0.968 mm/year respectively. Graphical representations of the trends in annual and seasonal rainfall over the 70 years (1951-2020) are provided in the **Fig**. These changes in the rainfall pattern suggest a need to develop better irrigation management strategies for crop planning in the study area. A similar non-significant increasing trend of rainfall at annual and monsoon scales was also reported by Mehta and Yadav (2021) over the Bikaner district, although the time period and data source were different. These results are found in agreement with the findings reported by Mehta and Yadav (2021), where increasing trends of rainfall were detected at some stations in the western part of Rajasthan. The upward trend in the annual rainfall could be due to the extreme heat flows and consequent rainfall under the changing climate (Bandyopadhyay et al., 2015). Additionally, local land use changes including agricultural practices and expansion of irrigation are the potential causes that increased the humidity levels locally and contributed to more frequent rainfall (Mahmoud & Gan, 2018; Ortiz et al., 2022; Pant et al., 2024). It is evident that the widespread use of canal for irrigation in western Rajasthan might have enhanced local

evapotranspiration and must have added moisture to the atmosphere that potentially led to increased rainfall (Pathak et al., 2013).

Table 16 MK-test statistic and Sen's slope values for 70 years seasonal and annual rainfall

Time Scale	Z-value	Sen's slope (mm/year)	Trend
Pre-monsoon	3.18	0.289	Significant (↑)
Monsoon	1.3	0.578	Non-significant (↑)
Post-monsoon	0.1	0	Non-significant (↑)
Winter	0.19	0.006	Non-significant (↑)
Annual	1.86	0.968	Non-significant (↑)

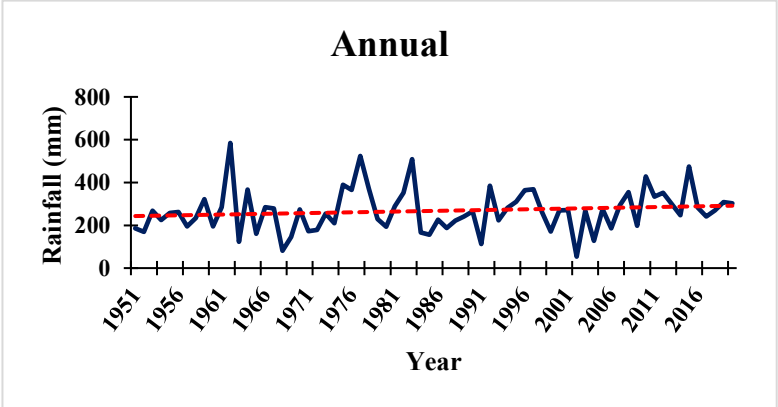

(A)

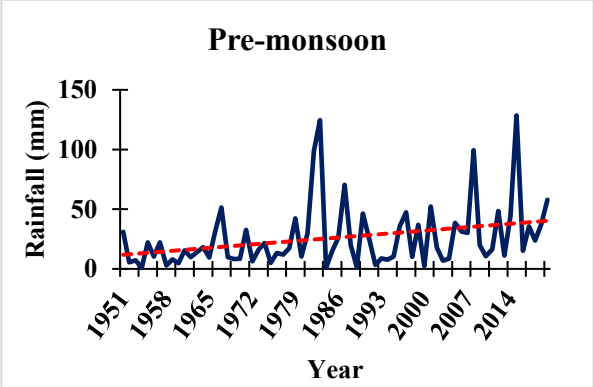

(B)

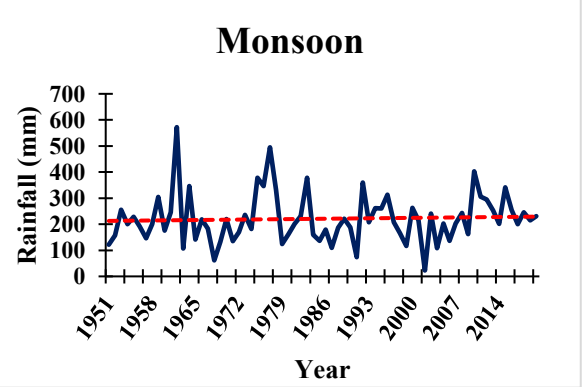

(C)

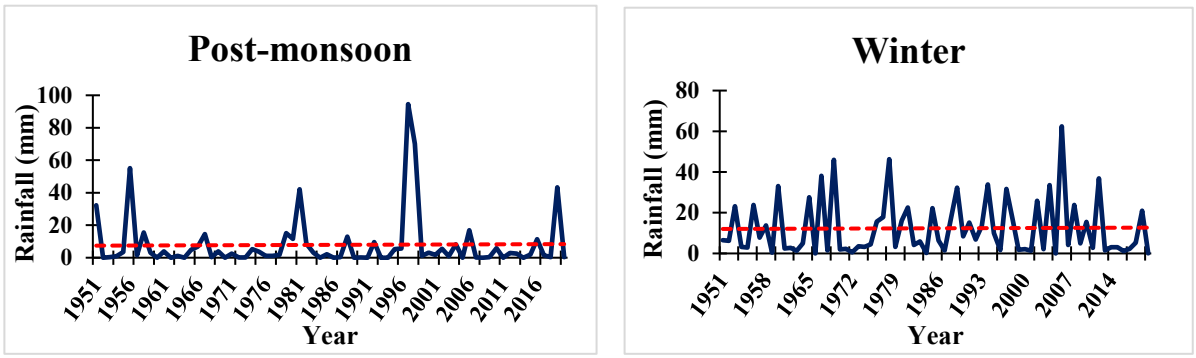

(D) **(E)**

Figure 35:Graphical representation of annual and seasonal rainfall trend

Spatial Variability in Long-Term Trend of Rainfall Time Series

The spatial distribution of z-values as shown in **Fig.** revealed that out of 43 grids, 13 grids showed a significant increasing trend over the Bikaner district, whereas remaining grids showed a non-significant increasing trend. In a Bikaner block, all 4 grids showed a significant increasing trend, whereas, in the Khajuwala and Nokha block, all the grids showed a non-significant increasing trend. The spatial distribution of Sen's slope (magnitude of change) over the district is shown in **Fig**. It can also be clearly observed that highest rate of increase in magnitude (1.91 mm/year) was witnessed in the Bikaner block, whereas the lowest increasing rate was observed in Khajuwala and Shri Dungargarh block. Moreover, a complicated variation in rainfall trend pattern was observed, which may impact or be impacted by the climate change in the basin. Improved understanding of the spatio-temporal distribution and variability in rainfall trends has paramount importance for the planning and management of water resources in the basin.

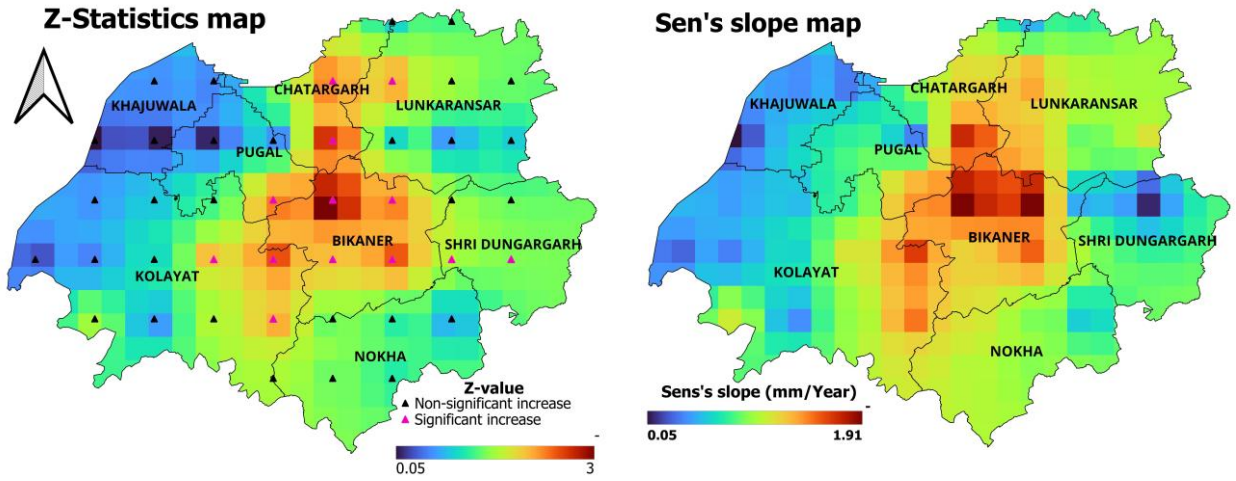

(A) **(B)**

Figure 36:Spatial distribution of MK test Z statistics and Sen's slope over the Bikaner district

Temporal variability in Long Term Trend of Temperature

Monthly analysis

The non-parametric MK test together with Sen's slope was applied individually to each month of the 70 years Tmax and Tmin time series. The results of the monthly Tmax trend in terms of z statistics and slope are depicted in **Table**. The results showed considerable fluctuation, but there was non-significant increasing trend throughout the months except April, May, August, and September. Sen's slope estimator showed the increase in Tmax between the rate of 0.001 °C/year to 0.013 °C/year. Highest rate of increase was observed in the month of July and August, whereas, lowest rate of increase was observed in the month of January. Likewise, the results of the monthly Tmin trend in terms of z statistics and slope are depicted in **Table**. The results showed high fluctuation, and there was significant increasing trend throughout the months except June and September. Sen's slope estimator showed the increase in Tmin between the rate of 0.005 °C/year to 0.031 °C/year. Highest rate of increase was observed in the month of November, whereas, lowest rate of increase was observed in the month of June.

Table 17 MK-test statistic and Sen's slope values for 70 years monthly Tmax

Time scale	Z-value	Sen's slope (mm/year)	Trend
January	0.01	0	Non-significant (↑)
February	0.5	0.006	Non-significant (↑)
March	0.74	0.007	Non-significant (↑)
April	3.02	0.027	Significant (↑)
May	2.73	0.021	Significant (↑)
June	0.91	0.006	Non-significant (↑)
July	1.81	0.013	Non-significant (↑)
August	2.37	0.013	Significant (↑)
September	2.27	0.02	Significant (↑)
October	1.6	0.012	Non-significant (↑)
November	1.34	0.009	Non-significant (↑)
December	0.87	0.006	Non-significant (↑)

Table 18 MK-test statistic and Sen's slope values for 70 years monthly Tmin

Time scale	Z-value	Sen's slope (mm/year)	Trend
January	3.19	0.022	Significant (↑)

February	3.22	0.029	Significant (↑)
March	2.17	0.023	Significant (↑)
April	3.34	0.027	Significant (↑)
May	2.84	0.021	Significant (↑)
June	1.03	0.005	Non-significant (↑)
July	2.26	0.01	Significant (↑)
August	3.33	0.01	Significant (↑)
September	1.91	0.011	Non-significant (↑)
October	3.01	0.025	Significant (↑)
November	3.14	0.031	Significant (↑)
December	3.2	0.02	Significant (↑)

Seasonal and annual analysis

In addition to the month-wise trend analysis, the seasonal and annual trend analysis of the 70 years of Tmax and Tmin was carried out using the MK test and Sen's slope estimator for the magnitude of the trend. The results of the trend analysis of annual and seasonal Tmax are shown in **Table**. The analysis results revealed that a significant increasing trend of Tmax is observed during monsoon and post-monsoon season, whereas, non-significant increasing trend is observed during pre-monsoon and winter season. The monsoon season showed a positive change with z statistic value of 2.6 and Sen's slope of 0.017 °C/year, whereas post-monsoon season showed a positive change with z statistic value of 2.5 and Sen's slope of 0.012 °C/year. Likewise, the results of the trend analysis of annual and seasonal Tmin are shown in **Table**. The analysis results revealed a significant increasing trend of Tmin during all four seasons with the rate varying between 0.009°C/year during post-monsoon season and 0.023 °C/year during pre-monsoon and monsoon season.

For the annual trend Tmax, the z statistic and Sen's slope were estimated as 2.41 and 0.011 °C/year respectively. Graphical representations of the trends in annual and seasonal Tmax and Tmin over the 70 years (1951-2020) are provided in the **Fig**. Likewise, For the annual trend Tmin, the z statistic and Sen's slope were estimated as 2.34 and 0.019 °C/year respectively. It can also be clearly observed from **Figure** that there is increasing trend in both the annual and seasonal Tmax between the period 1951 to 2020. These findings are found consistent with previous studies conducted by different researchers in the western Rajasthan (Sharma et al., 2021; Mehta et al., 2022). These findings clearly indicate that the global trend of climate change is persisting over the Bikaner district, whose major area already falls under hot and dry climatic conditions, and this is a matter of great concern for all. Increasing temperature is already a

major concern for environmentalist, climatologists, farmers, policy makers, and society at large, and in such situation, the above findings are very imperative for an agrarian economy like India.

Table 19 MK-test statistic and Sen's slope values for 70 years seasonal and annual Tmax

Time scale	**Z-value**	**Sen's slope (mm/year)**	**Trend**
Pre-monsoon	0.2	0.002	Non-significant (↑)
Monsoon	2.6	0.017	Significant (↑)
Post-monsoon	2.5	0.012	Significant (↑)
Winter	1.56	0.011	Non-significant (↑)
Annual	2.41	0.011	Significant (↑)

Table 20 MK-test statistic and Sen's slope values for 70 years seasonal and annual Tmin

Time scale	**Z-value**	**Sen's slope (mm/year)**	**Trend**
Pre-monsoon	2.71	0.023	Significant (↑)
Monsoon	2.4	0.023	Significant (↑)
Post-monsoon	2.15	0.009	Significant (↑)
Winter	3.35	0.029	Significant (↑)
Annual	2.34	0.019	Significant (↑)

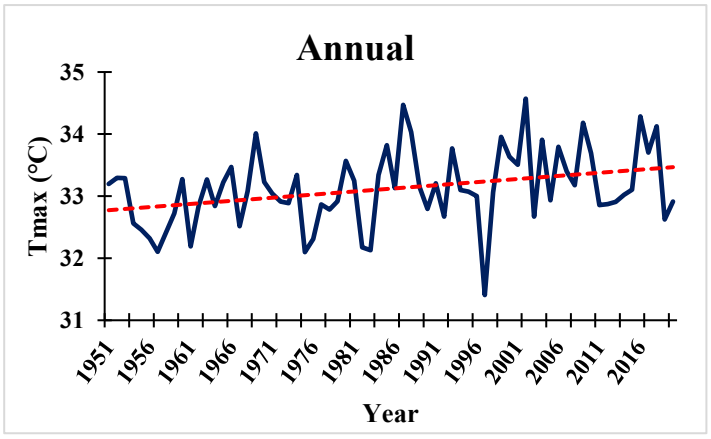

(A)

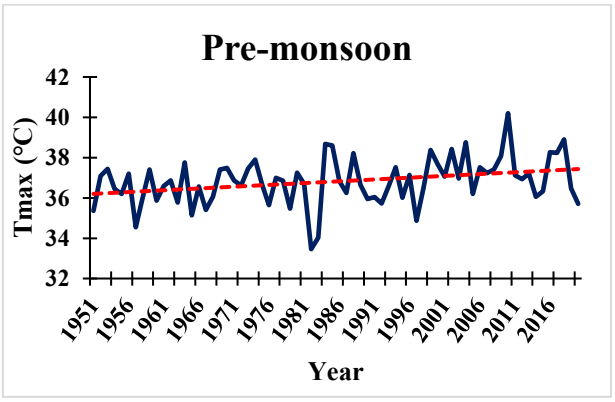

(B)

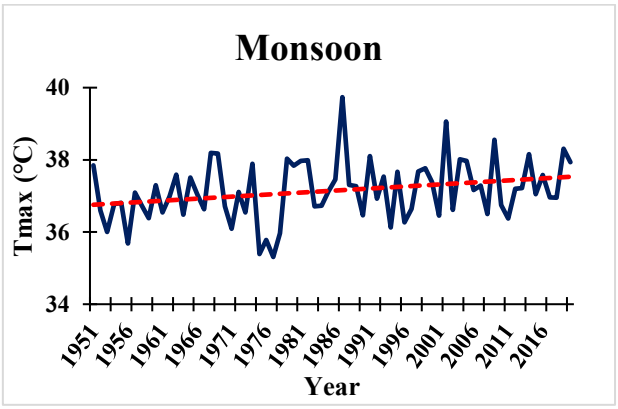

(C)

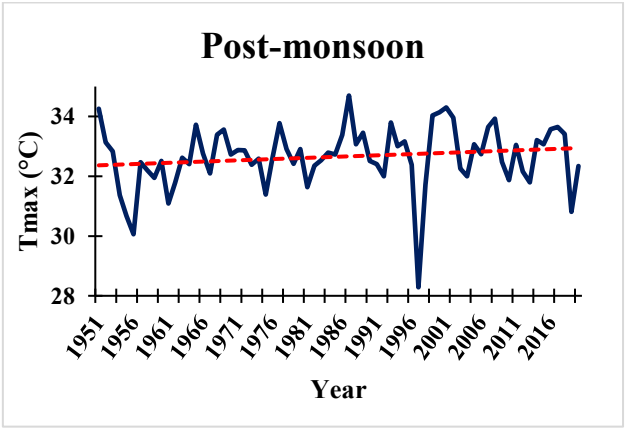

(D)

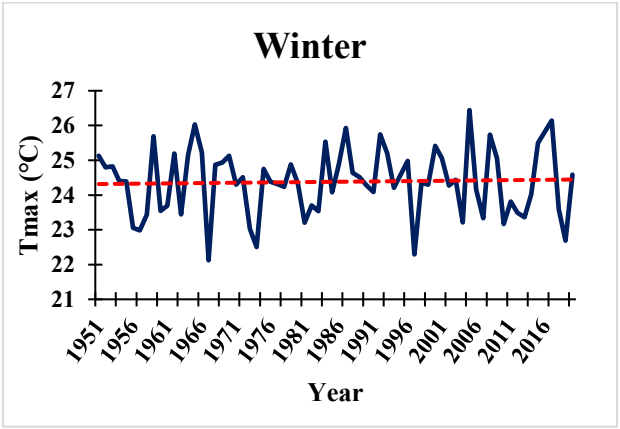

(E)

Figure 37:Graphical representation of annual and seasonal Tmax trend

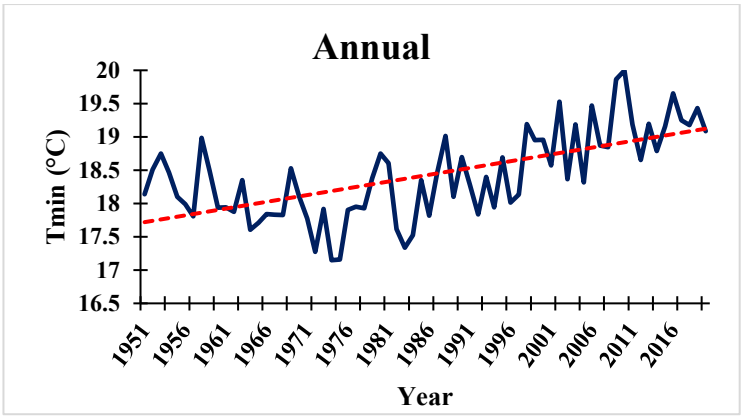

(A)

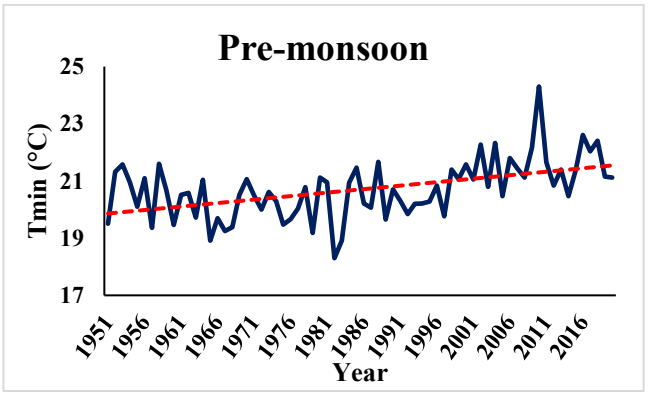

(B)

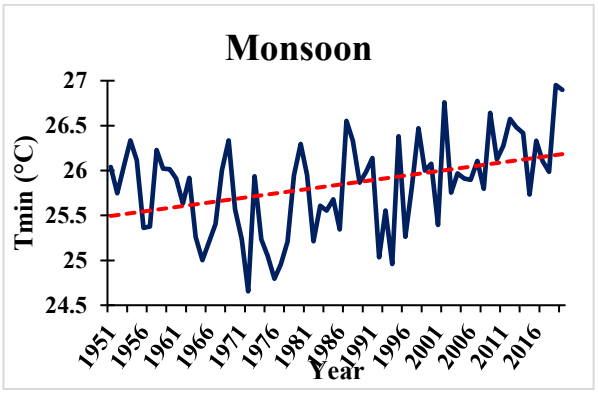

(C)

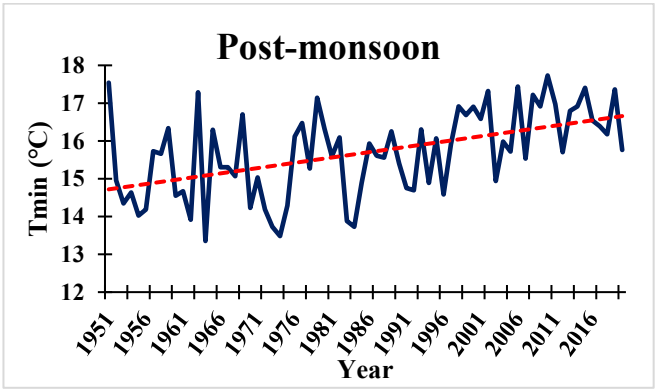

(E)

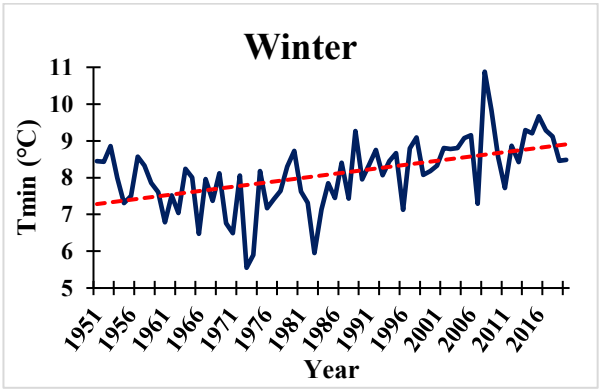

(F)

Figure 38:Graphical representation of annual and seasonal Tmin trend

Spatial Variability in Long-Term Trend of Temperature Time Series

The spatial distribution of z-values for Tmax as shown in **Fig.** revealed that all three grids over the districts showed a significant increasing trend with Z- value varying in the range of 2.02 to 2.64. The spatial distribution of sen's slope value showed the increase in the rate of Tmax by 0.010 to 0.013 °C/year. The highest rate of increase is observed in Nokha block, whereas lowest rate of increase is observed in the Khajuwala block of Bikaner district**. Similarly,** the spatial distribution of z-values for Tmin as shown in **Fig.** revealed that all three grids over the districts

showed a significant increasing trend with Z- value varying in the range of 2.19 to 2.65. The spatial distribution of sen's slope value showed the increase in the rate of Tmax by 0.017 to 0.022 °C/year. The highest rate of increase is observed in Lunkaransar block, whereas lowest rate of increase is observed in the Khajuwala block of Bikaner district**.**

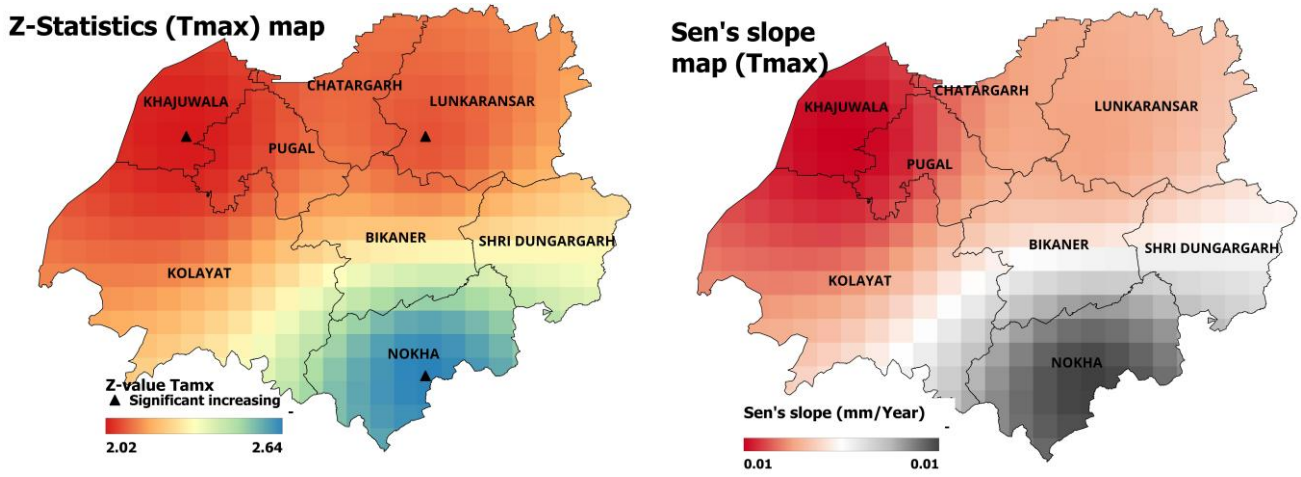

(A) **(B)**

Figure 39:Spatial distribution of Z statistics and Sen's slope for Tmax over the Bikaner district

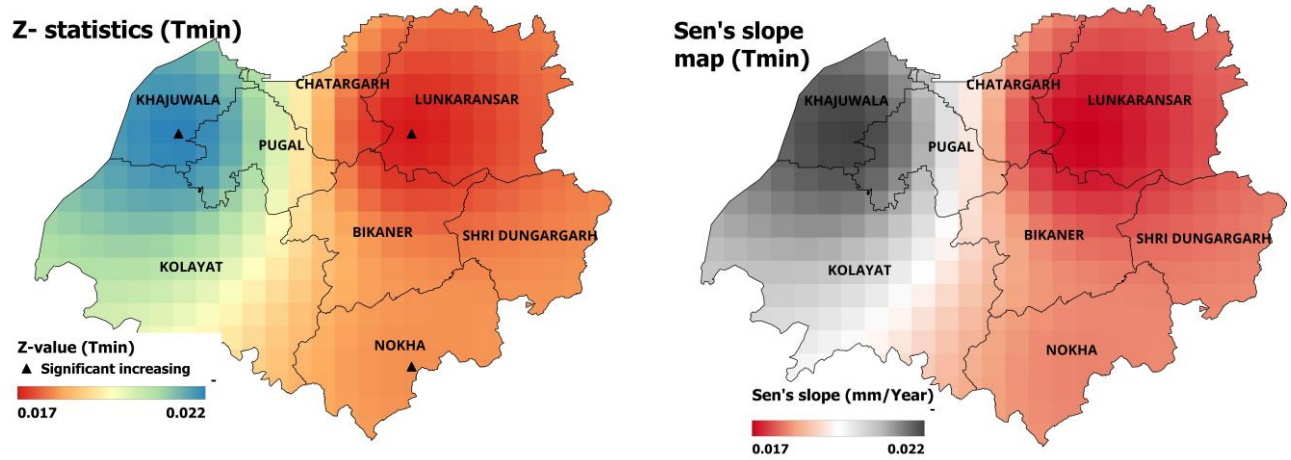

(A) **(B)**

Figure 40:Spatial distribution of Z statistics and Sen's slope for Tmin over the Bikaner district

CHAPTER – 6

PRESENT STATUS OF GROUNDWATER RESOURCES AND RECHARGE TO GROUNDWATER

5.1 General

The analysis of present status of groundwater (GW) in the Bikaner District is crucial for understanding currently available groundwater and past changes due to various interventions. Bikaner, located in the arid Thar Desert of Rajasthan, has a rich tradition of rainwater harvesting to combat harsh climate. The analysis of present GW status is performed using the observed GW level data of CGWB. Analysis was performed by conducting Mann-Kendall trend analysis on each observation well and by generating spatial maps using interpolation at seasonal and annual scales. In order to estimate recharge from various sources, integrated hydrologic model (NIH's Web-based Integrated Catchment Modelling System for Decision Making (WISDOM)) was used. The methodology used and results obtained are detailed in the following sections.

5.2 Present GW Scenario in the Study Area

Groundwater levels indicate the overall GW balance of an area. In this study, GW level data acquired from CGWB were analysed for the period from 2001 to 2020 to assess the current GW scenario and changes that have occurred during the past two decades. These datasets are available at different observation wells for four seasons. Through interpolation between datasets at different stations, it is possible to determine the characteristics of elements at any point in the region. CGWB measures depth to GW during April (pre-monsoon), August (monsoon), November (post-monsoon Kharif) and January (Post-monsoon Rabi). These datasets were obtained from India Water Resources Information System (INDIA-WRIS).

5.2.1 Analysis of GW level data

Data pre-processing

GW level data are processed to check the consistency of observations. For analysis, wells for which consistent data is available were selected. Wells with more 30% missing values were eliminated before analysis. A total of 82 selected wells were used in trend analysis and for creating spatial maps.

Interpolation

In order to derive groundwater level maps, data of observation wells was interpolated using Kriging, a geo-statistical interpolation technique. Kriging estimates interpolated surface from a spatially scattered set of points with z-values. The z-value, in this case, was the groundwater level from observation wells. To obtain the interpolated surface, kriging goes through a two-step process: first, it obtains spatial autocorrelation values using variograms and covariance functions, and second, it predicts the z-values. Kriging was applied to groundwater levels using a python program. The interpolated groundwater levels were used in analysing the spatial variability of groundwater in the study command.

In order to investigate the seasonal fluctuations, groundwater level maps for four seasons, i.e. post-monsoon Rabi (January to March), Pre-monsoon (April to June), monsoon (July to September) and post-monsoon Kharif (October to December), were created and examined.

Trend analysis

Trend analysis was performed on the selected 82 wells, on seasonal and annual scales using modified Mann-Kendall (M-K) test (Hamed and Rao, 1998). The Mann-Kendall test is a non-parametric test for identifying trends in time series data. Being non-parametric, it allows to perform trend analysis on any distribution of data. The data values are evaluated as an ordered time series. Each data value is compared to all subsequent data values. The initial value of the Mann-Kendall statistic, S, is assumed to be 0 (e.g., no trend). If a data value from a later time period is higher than a data value from an earlier time period, S is incremented by 1. On the other hand, if the data value from a later time period is lower than a data value sampled earlier, S is decremented by 1. The net result of all such increments and decrements yields the final value of S. Further, in order to test the significance level, a probability test is integrated with the M-K test.

In this study, the modified Mann-Kendall (M-K) test developed by Hamed and Rao (1998) was used. For each season, an annual time series from 2001 to 2020 of depth to GW was created and used in the modified M-K test. Wells with rising and falling GW level were identified at a significance level of 0.05.

5.2.2 Present scenario of depth to GW

Bikaner district, which comprises sub-divisions such as Kolayat, Nokha, Lunkaransar, Chhatargarh, Poogal, Dungargarh, and Bikaner city, shows varied groundwater depth trends across its monitoring stations. The groundwater levels range from as shallow as 10 meters in some locations to over 80 meters in others. The trends observed in the last two decades reveal areas of severe depletion, moderate decline, and relative stability, highlighting the need for region-specific groundwater management interventions.

Kolayat sub-division, covering GW stations such as Kolayat, Bajju, Bhikampur, Godu, Modayat, and Ranjitpura, exhibits diverse groundwater trends. In Bhikampur, groundwater levels remain between 8 and 12 meters, showing stability over the years with seasonal fluctuations. However, in Bajju and Godu, the water table has deepened from 35 meters in the 1990s to over 45 meters in recent years, indicating excessive withdrawal. Kolayat town itself shows moderate depletion, with levels declining from around 20 meters in the mid-1990s to nearly 30 meters. Ranjitpura, another important location in Kolayat sub-division, has seen fluctuating trends but a general decline, with groundwater levels ranging from 30 to 35 meters. Lunkaransar sub-division, which includes stations Amarpura, Lakhanasar, and Malkisar, faces serious groundwater depletion. In Amarpura, groundwater depth has increased from approximately 15 meters in 1994 to over 25 meters in 2018, demonstrating continuous depletion. Similarly, in Lakhanasar and Malkisar, levels have dropped significantly, with groundwater now at depths exceeding 30 meters in most seasons.

Chhatargarh and Poogal sub-divisions exhibit both stable and declining trends. In Chhatargarh, groundwater levels have dropped from 40 meters in 1994 to over 50 meters, making it one of the most affected areas in the district. Baderan experiences highly irregular trends, with groundwater depth fluctuating between 30 and 45 meters. Manaria, in contrast, shows relatively stable groundwater conditions, with levels consistently ranging between 50 and 55 meters over the past two decades. Nokha sub-division, with GW monitoring stations such as Kodamdesar, Lakhusar, Lakhasar2, and Kasturia, displays moderate to stable groundwater trends. Kodamdesar and Lakhusar show steady depletion, with water tables dropping from 35 meters in the late 1990s to over 45 meters today. However, Lakhasar2 and Kasturia show minimal change, with groundwater levels fluctuating within a 40 to 45 meter range. The mixed trends in Nokha suggest that certain areas may have better recharge conditions, while others rely heavily on groundwater extraction. Dungargarh sub-division has some of the deepest groundwater levels in the district. In Dungargarh town, water depth has

remained consistently between 60 and 70 meters, with slight fluctuations in different seasons. The persistently deep water table indicates that groundwater recharge is limited in this region. Bikaner city and its nearby locations, including Tanwar Wala, Mankasar, and Modayat, show moderate stability with some gradual declines. Tanwar Wala has seen a slow but steady drop in water levels, from around 18 meters in 1994 to nearly 25 meters in 2018. Mankasar shows more pronounced depletion, with levels increasing from around 12 meters to over 20 meters, suggesting a growing reliance on groundwater. Modayat, however, remains relatively stable, with levels fluctuating between 20 and 25 meters over the years. The conditions in and around Bikaner city indicate that while groundwater extraction is increasing, the presence of alternative water sources such as surface water supply may be slowing the rate of decline.

The seasonal variations observed across the district indicate that groundwater levels generally improve slightly after the monsoon, with post-monsoon Rabi and Kharif seasons showing minor recharge effects. However, the recharge is not sufficient to counteract the long-term depletion in heavily affected regions. Some locations, such as Khara1 and Baderan, show extreme fluctuations, with groundwater depths varying widely from year to year, suggesting localized influences of rainfall, groundwater pumping, and aquifer recharge. The analysis highlights that Kolayat, Lunkaransar, and Chhatargarh sub-divisions are the most affected, with groundwater depths exceeding 40 meters in multiple locations. Bikaner city and its surrounding areas have relatively stable levels, while Dungargarh continues to have the deepest groundwater levels in the district.

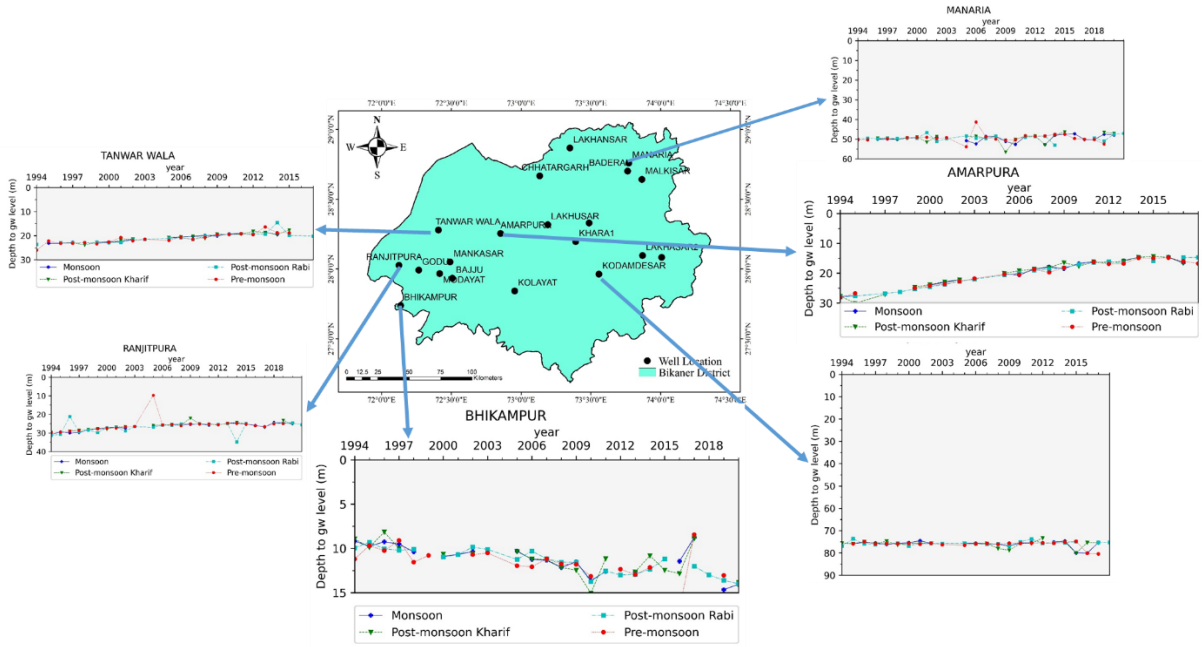

Figure 41:Temporal variations in depth to GW in the study area

The overall analysis highlights that in the northern part of the district, groundwater levels remain relatively stable, as observed in Manaria and Amarpura, with only minor fluctuations over time. Moving toward the central region, locations like Tanwar Wala and Ranjitpura show a gradual decline in groundwater levels, reflecting increased groundwater extraction and seasonal variations. In contrast, the southern region, particularly Bhikampur, exhibits a significant decline in groundwater levels over the years, indicating persistent groundwater depletion. This suggests over-reliance on groundwater resources, likely due to irrigation and domestic water demand.

Overall, the groundwater level trends indicate a more stable condition in the north, gradual depletion in the central part, and severe decline in the south. The data highlights the need for groundwater conservation strategies such as artificial recharge and efficient water management to mitigate depletion across Bikaner district.

Pre-monsoon season

The spatial map generated using well observations from the recent decade (2011-2020) illustrates the groundwater depth variations across Bikaner district during the pre-monsoon period. The grey lines represent the canal network, which plays a crucial role in influencing groundwater recharge in the region. The western and north-western subdivisions, including Khajuwala and Chhatargarh, exhibit relatively shallow groundwater levels, with depths ranging from approximately 20 to 40 meters below ground level (m-bgl). Moving southeast towards Kolayat and Nokha, the depth to groundwater gradually increases, ranging from 40 to 60 m-bgl. The deepest groundwater levels, exceeding 60 m-bgl, are observed in the south-eastern subdivisions, such as Dungargarh and parts of Lunkaransar. This spatial trend indicates a progressive decline in groundwater levels from the north-western to south-eastern parts of Bikaner. The influence of canals is more prominent in the western regions, where groundwater is relatively shallower, while the south-eastern areas, which are farther from major canals, continue to experience deeper water tables.

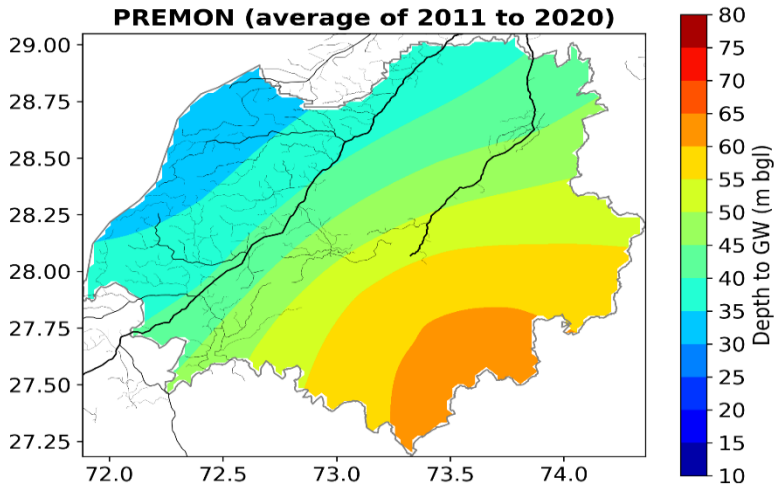

Figure 42:Spatial variation in depth to GW in pre-monsoon season during the period from 2011 - 2020

Monsoon season

The north-western and western subdivisions, including Khajuwala and Chhatargarh, show relatively shallow groundwater levels, with depths ranging from 20 to 40 meters below ground level (m-bgl), indicating some recharge from monsoon rainfall. Moving towards the central region, including Kolayat and parts of Lunkaransar, groundwater levels range between 40 to 60 m-bgl. The south-eastern parts, particularly around Dungargarh and Nokha, exhibit the deepest groundwater levels, exceeding 70 m-bgl, suggesting limited recharge and higher rates of groundwater extraction. This seasonal shift highlights the impact of monsoon rainfall on groundwater availability, with recharge occurring primarily in the north-western canal-fed areas, while the south-eastern regions remain under significant groundwater stress.

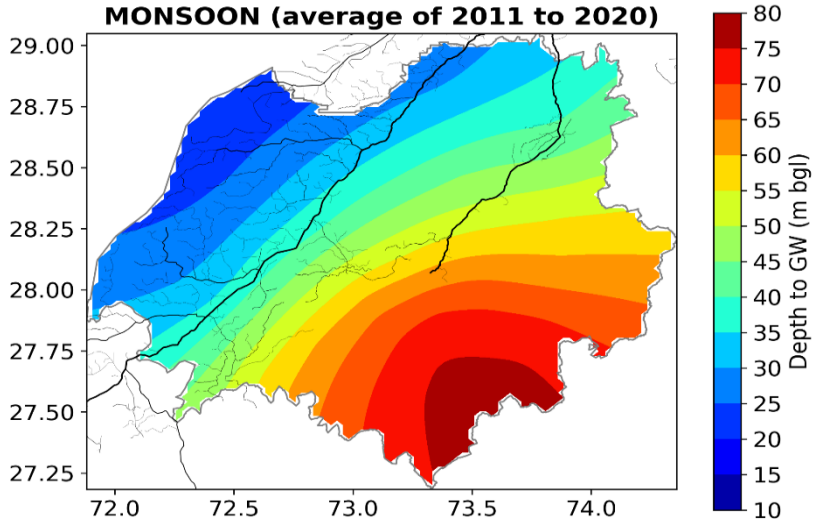

Figure 43:Spatial variation in depth to GW in monsoon season during the period from 2011 – 2020

Post-monsoon Kharif (POMKH)

The depth to GW during the post-monsoon Kharif season (2011-2020) across Bikaner district reveals a pattern influenced by monsoonal recharge and canal recharge. The north-western and western subdivisions, including Khajuwala and Chhatargarh, continue to exhibit relatively shallow groundwater levels, with depths ranging from 20 to 40 meters below ground level (m-bgl). This indicates a sustained recharge effect from the monsoon season, aided by proximity to canals. Moving towards the central region, including Kolayat and parts of Lunkaransar, the depth to groundwater falls between 40 to 60 m-bgl. The south-eastern areas, particularly around Dungargarh and Nokha, still show the deepest groundwater levels, exceeding 70 m-bgl, similar to the monsoon season. The post-monsoon groundwater levels suggest that while certain areas benefit from seasonal recharge, particularly in the north-western and western canal-fed regions, the south-eastern parts of Bikaner remain under significant groundwater stress.

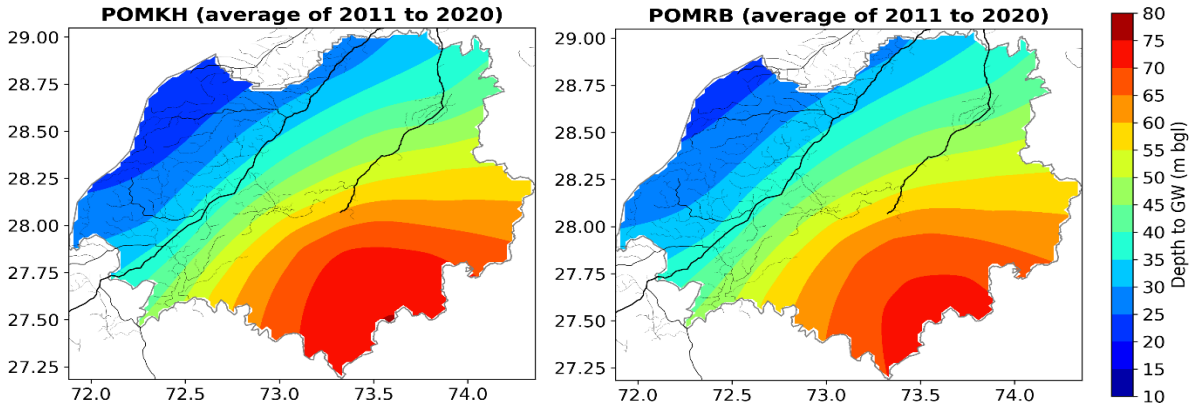

Figure 44:Spatial variation in depth to GW during post-monsoon Kharif (POMKH) and post-monsoon Rabi (POMRB) during the period from 2011 – 2020.

Post-monsoon Rabi (POMRB)

During the post-monsoon Rabi season (2011-2020) across Bikaner district a trend influenced by the preceding monsoon recharge and subsequent groundwater utilization is seen. The north-western and western subdivisions, including Khajuwala and Chhatargarh, continue to have relatively shallow groundwater levels, ranging from 20 to 40 meters below ground level (m-bgl), indicating a retention of monsoon recharge. In the central region, including Kolayat and parts of Lunkaransar, groundwater depths range between 40 to 60 m-bgl, reflecting a gradual decline due to post-monsoon extraction. The south-eastern parts, particularly around Dungargarh and Nokha, exhibit the deepest groundwater levels, exceeding 70 m-bgl, signifying high groundwater abstraction for Rabi cultivation. The seasonal pattern suggests that while monsoon recharge benefits parts of the district, continued groundwater depletion in the south-

eastern regions underscores the need for sustainable water management, particularly in high-extraction zones.

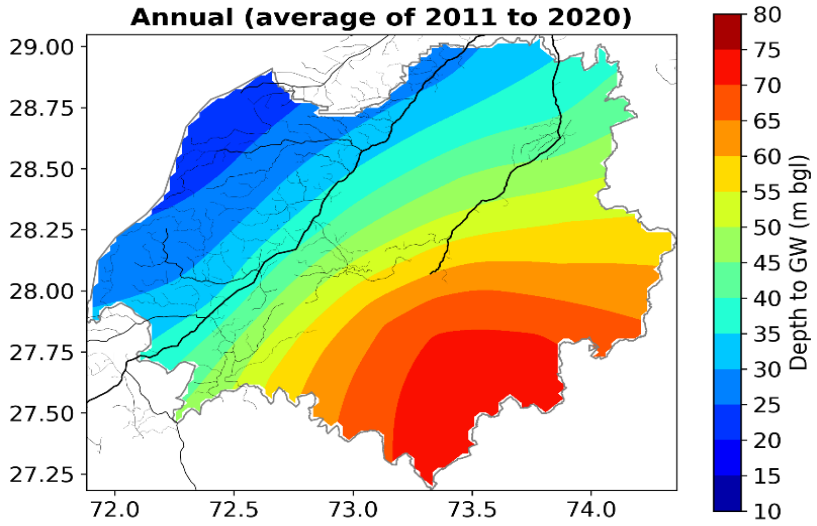

Figure 45:Spatial variation in depth to GW at annual scale during 2011 - 2020

Annual average

The annual average groundwater depth map (2011-2020) for Bikaner district highlights a persistent spatial pattern of groundwater availability. The north-western and western subdivisions, including Khajuwala and Chhatargarh, maintain relatively shallow groundwater levels, ranging from 20 to 40 meters below ground level (m-bgl. These areas benefit from seasonal recharge and canal seepage, helping to sustain groundwater levels. The central regions, including Kolayat and parts of Lunkaransar, exhibit moderate groundwater depths between 40 to 60 m-bgl, showing a balance between recharge and withdrawal. In contrast, the south-eastern parts, particularly around Dungargarh and Nokha, consistently display the deepest groundwater levels, exceeding 70 m-bgl, indicating prolonged groundwater stress. This annual trend underscores the necessity for targeted groundwater management strategies, especially in the south-eastern regions, to mitigate depletion and enhance recharge efficiency for sustainable water use in Bikaner district.

5.2.3 Trends in GW levels during past two decades

Modified M-K test was performed on 82 observation wells at seasonal and annual time scale for the period 2001 to 2020. Figures - 5.5, 5.6 and 5.7 show the locations of selected wells and the significant trend during pre-monsoon and monsoon seasons and at annual scale. The rising and falling trends during pre- and post-monsoon seasons and annual time scale are enumerated below.

Pre-monsoon season

The pre-monsoon groundwater trend analysis (2001-2020) for Bikaner district reveals distinct spatial and temporal variations in groundwater levels. 42.2% of the observation wells show a rising groundwater trend, while 20.5% exhibit a falling trend, and 37.3% display no significant trend. The spatial distribution of these trends highlights that the north-western and northern parts of Bikaner predominantly show a rising groundwater trend, suggesting some recharge influence. In contrast, the southern and south-eastern regions, particularly around Dungargarh and Nokha, exhibit a falling trend indicating persistent groundwater depletion due to over-extraction and limited recharge. The central region, including Kolayat and parts of Lunkaransar, has a mix of rising, falling, and stable trends, suggesting localized variations in groundwater dynamics.

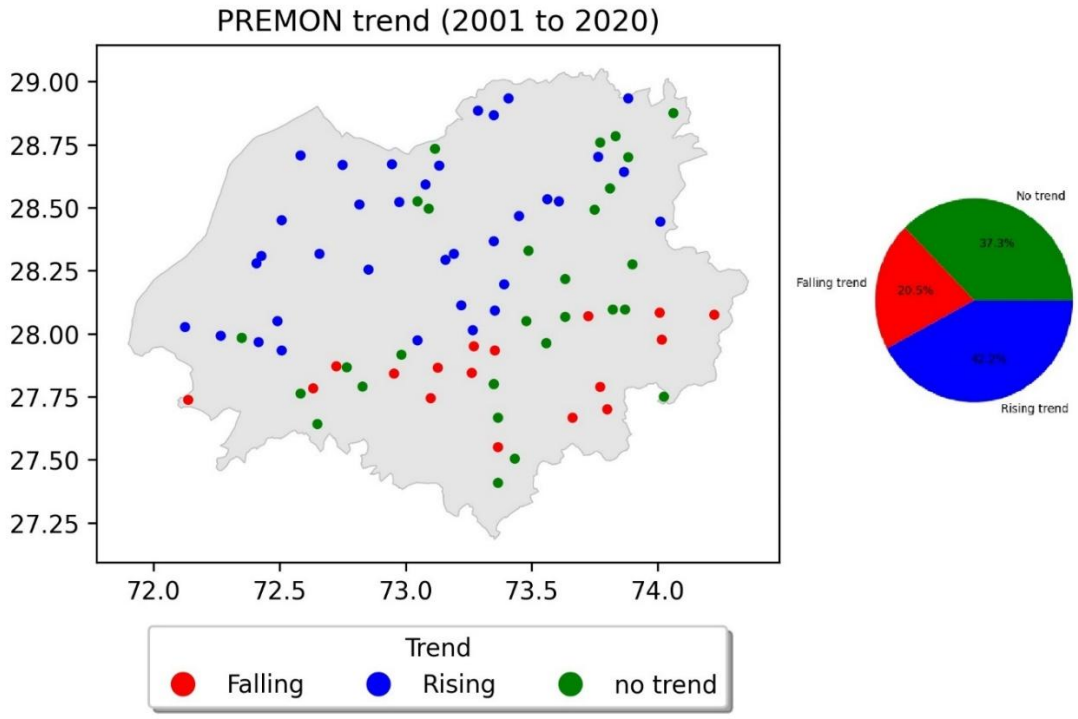

Figure 46:Trend in GW levels during pre-monsoon season

Post-monsoon season

For Post-monsoon season 45.8% of the observation wells show a rising groundwater trend, 20.5% indicate a falling trend, and 33.7% have no significant trend. The spatial distribution map reveals that the northern and north-western regions, particularly around Khajuwala and Chhatargarh, show a rising groundwater trend, indicating recharge effects from monsoon precipitation and possibly reduced extraction during this period. However, the southern and south-eastern areas, particularly around Dungargarh and Nokha, exhibit a falling

trend, suggesting continued groundwater depletion due to excessive post-monsoon withdrawal, likely for Rabi cultivation. The central parts, including Kolayat and Lunkaransar, display a mix of rising, falling, and stable trends, reflecting localized variations in groundwater dynamics based on recharge and abstraction rates. The observed trends indicate that while monsoon recharge positively influences groundwater levels in some areas, other regions continue to experience depletion.

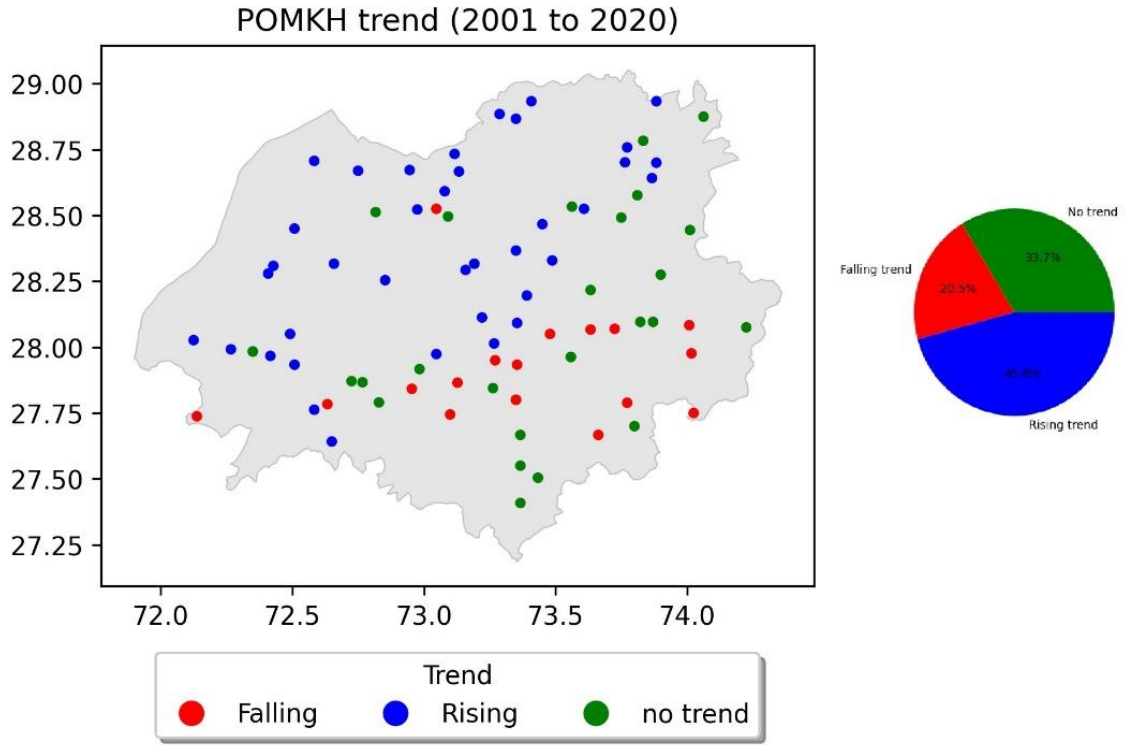

Figure 47:Trend in GW levels during post-monsoon Kharif season

Annual

On annual scale, 43.4% of the observation wells exhibit a rising groundwater trend, while 21.7% show a falling trend, and 34.9% display no significant trend. The spatial distribution of these trends highlights that the northern and north-western regions, including Khajuwala and Chhatargarh, predominantly exhibit a rising trend, suggesting improved groundwater conditions, possibly due to controlled extraction and irrigation return flow. Conversely, the southern and south-eastern areas, particularly around Dungargarh and Nokha, show a falling trend, indicating persistent groundwater depletion. The central regions, including Kolayat and parts of Lunkaransar, display a mix of rising, falling, and stable trends, reflecting localized groundwater fluctuations based on varying extraction and recharge patterns.

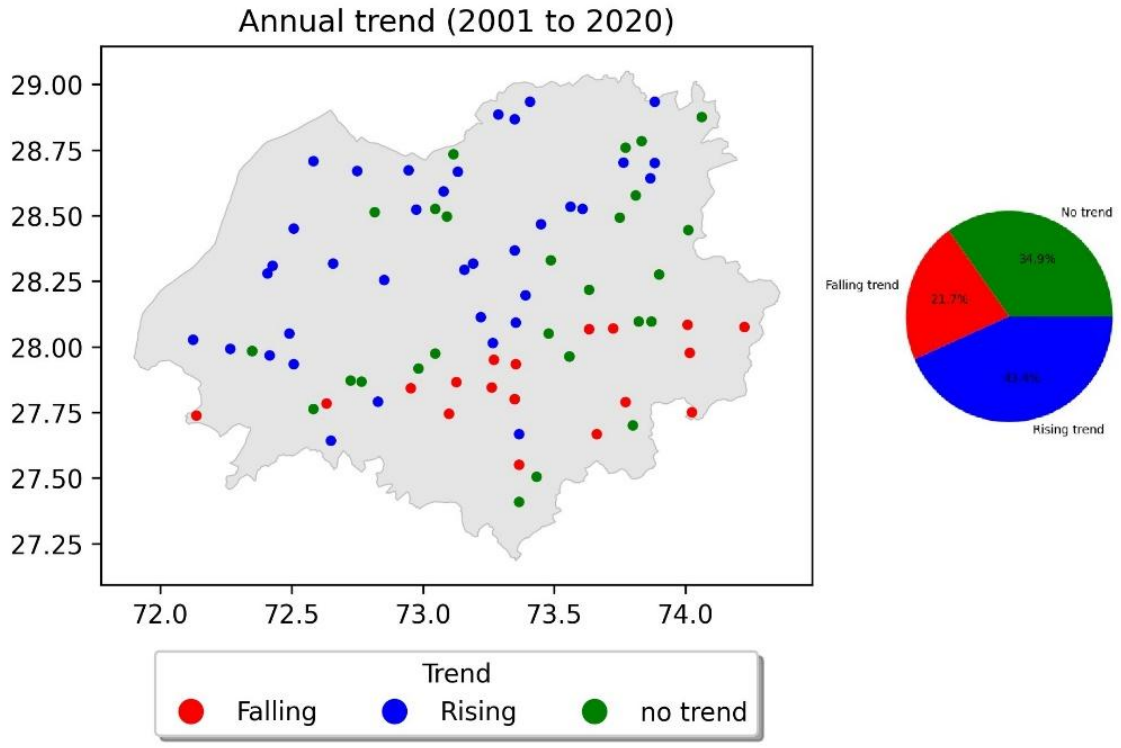

Figure 48:Trend in GW levels at annual time scale

5.3 Recharge to groundwater from precipitation and irrigation

The analysis of precipitation and percolation patterns in Bikaner district reveals that natural rainfall alone is insufficient for groundwater recharge, and irrigation-induced percolation plays a dominant role. Recharge to groundwater due to rainfall and irrigation is estimated using RZF module of NIH-WISDOM.

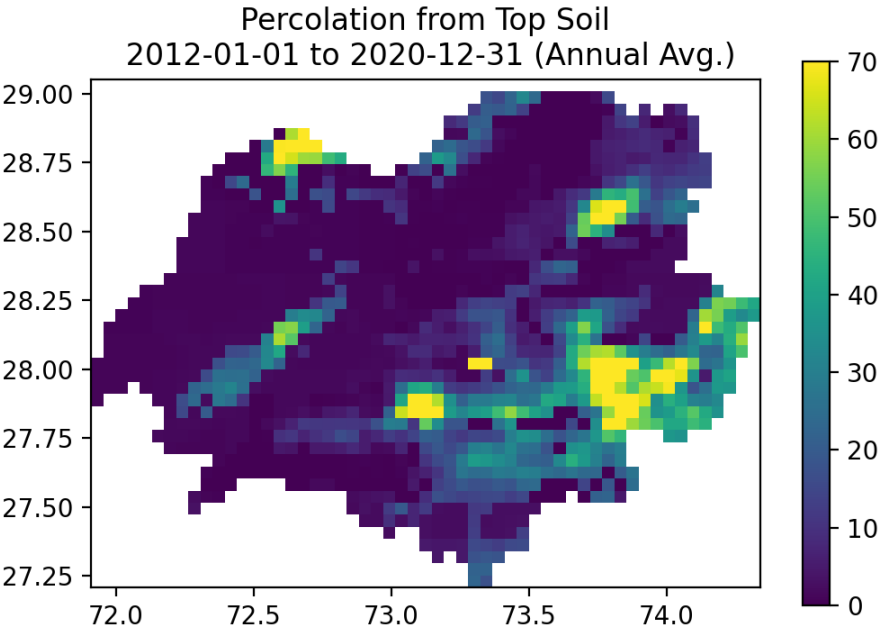

Figure 49:Potential recharge to groundwater from precipitation and irrigation in Bikaner district.

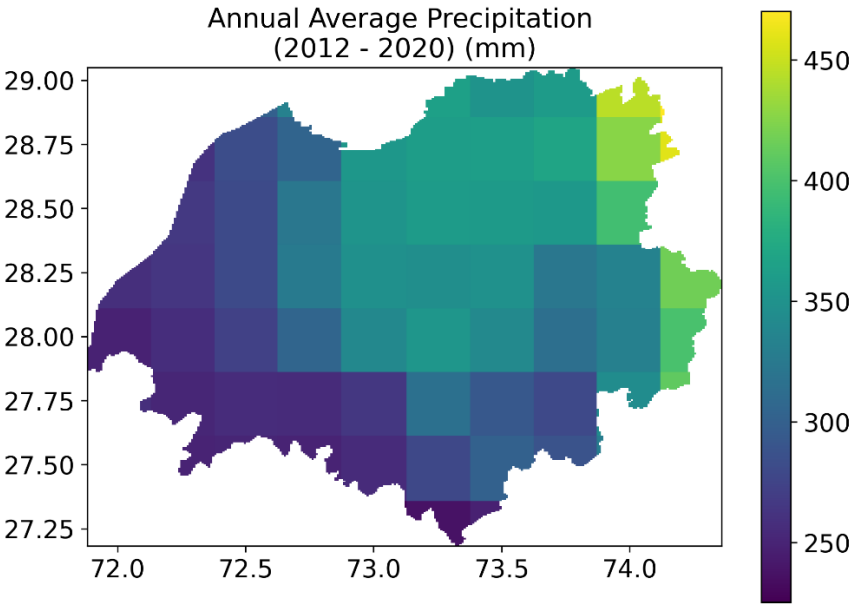

Figure 50:Annual average precipitation from 2012 to 2020 in Bikaner District

The precipitation and potential recharge maps highlight significant spatial variations in rainfall and recharge to groundwater, while the Leaf Area Index (LAI) map indicate cropping and irrigation. It is observed that the recharge is considerably high in the irrigated areas, located towards Southeast.

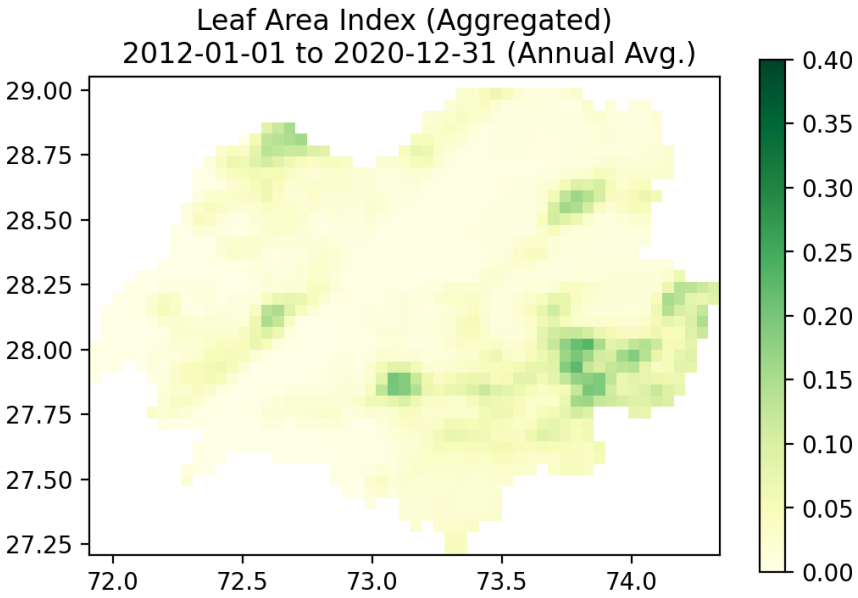

Figure 51:LAI for Bikaner District

The precipitation map (2012–2020) shows that annual rainfall varies between less than 250 mm in the southwest to over 400 mm in the northeast. However, the recharge map indicates that the contribution of rainfall to recharge is lesser than that caused by irrigation. Irrigation plays a crucial role in groundwater recharge, particularly in the eastern and south-eastern

regions. The bright yellow and green zones in the recharge map suggest that irrigation enhances groundwater recharge, particularly in areas with intensive cultivation.

In the south-western and western parts of the district, including Kolayat, Bajju, and Bhikampur, both precipitation and LAI values are low, leading to minimal groundwater recharge. The percolation map confirms that these regions experience high evaporation rates, poor water retention, and limited infiltration. Conversely, in the eastern and north-eastern regions, such as Lunkaransar, Malkisar, and Manaria, where LAI is relatively higher due to irrigated agriculture, percolation rates are also higher, suggesting a strong correlation between vegetation, soil moisture conservation, and groundwater recharge.

Another key observation is that areas with moderate vegetation cover and irrigation show a balanced percolation rate, whereas regions with excessively high LAI (dense vegetation) may experience increased evapotranspiration losses, which could offset some of the potential groundwater recharge. Therefore, while vegetation helps improve soil moisture retention and reduces surface runoff, excessive transpiration from dense crops may limit groundwater recharge in certain areas.

Year	2012	2013	2014	2015	2016	2017	2018	2019	2020
GW Recharge (MCM)	217.5	275.1	248.7	295.2	318.9	357.6	453.3	333.6	303.6

Table 21 Recharge due to precipitation and irrigation

The groundwater recharge in Bikaner district, influenced by both precipitation and irrigation, has exhibited fluctuations over the years from 2012 to 2020 as shown in **Table 5.1**. The data reflects a general upward trend with certain years experiencing significant increases or declines. In 2012, the recharge stood at 217.5, which rose to 275.1 MCM in 2013, indicating a positive change. However, in 2014, a slight decline to 248.7 MCM was observed, likely due to variations in annual rainfall or irrigation patterns. A remarkable increase occurred in 2015, with groundwater recharge reaching 295.2 MCM, followed by further growth in subsequent years. The recharge values in 2016 and 2017 stood at 318.9 MCM and 357.6 MCM, respectively, reflecting a steady rise. The peak recharge was recorded in 2018 at 453.3 MCM, marking the highest level in the observed period. However, from 2019 onwards, a decline in groundwater recharge is evident. In 2019, the recharge dropped to 333.6 MCM, followed by a further reduction to 303.6 MCM in 2020.

5.4 Recharge/percolation from canal

The Indira Gandhi Nahar Pariyojana (IGNP) has significantly altered the hydrological conditions of Bikaner district by introducing surface water through its extensive canal network. While the project has brought much-needed irrigation water to the region, the percolation from the IGNP canal system has also played a crucial role in recharging groundwater. The percolation losses from the canal contribute to groundwater recharge. A detailed study of canal losses in stage-I of IGNP was conducted by NIH wherein an integrated model was employed to estimate canal percolation losses. The estimated canal supply and losses in stage-I of IGNP are shown in Figure 5.10.

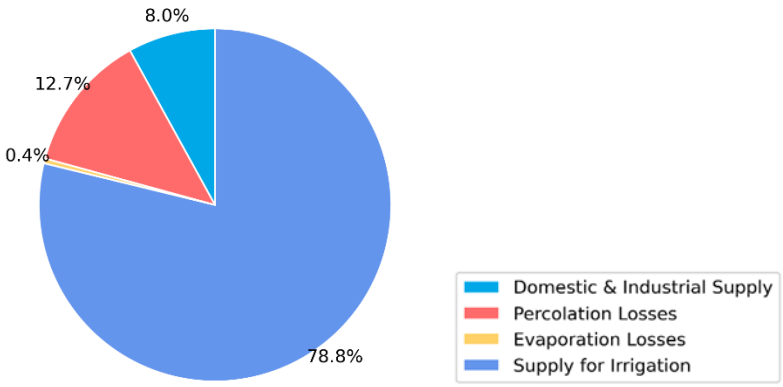

Figure 52:Percolation losses from canal in stage-I of IGNP.

The Stage-I of IGNP receives about 2000 MCM of water annually, this translates to an estimated 254 MCM (12.7%) of groundwater recharge due to canal percolation. A portion of IGNP Stage-I lies within the Bikaner district. These figures, although derived from modelling of Stage-I IGNP, help contextualize the indirect hydrological impact of the canal even beyond its immediate command boundaries. Groundwater recharge in Bikaner is not limited to the canal-aligned zones, as seepage-induced lateral groundwater movement can also benefit adjacent areas. CGWB also estimates a considerable recharge from canal in Bikaner district. A total of 5.11 MCM of recharge is fed by canal percolation in the district.

5.5 Estimates of CGWB

The estimates of CGWB are shown in **Table 5.2**. The estimates of the total annual groundwater recharge in Bikaner district is 312.27 MCM. The primary contributor to this recharge is rainfall, accounting for 287.03 MCM, which reflects the district's heavy reliance on precipitation for groundwater replenishment.

Source	Recharge (MCM)
Rainfall Recharge	287.03
Canal Recharge	5.11
Irrigation Recharge	20.13
Total	**312.27**

Table 22 Figure 53:Groundwater Recharge in Bikaner District (2023-2024)

Irrigation recharge adds an additional 20.13 MCM, indicating the role of agricultural practices in supplementing groundwater reserves. A smaller but notable contribution of 5.11 MCM comes from canal water seepage, which, although limited in extent, still supports localized recharge.

Overall, the figures highlight the importance of rainfall in sustaining groundwater levels in Bikaner, while irrigation and canal systems serve as secondary yet supportive sources of recharge.

Runoff assessment

The runoff potential of watershed is a major tool for planning and design of soil and water conservation structures. In the SCS method a basic parameter to be calculated was the curve number (CN), the descriptive of runoff potential of watershed is mostly used by researchers and engineers for runoff estimation. The value of which depends mainly on the, hydrological soil group, and antecedent moisture class. The results of these parameters for different catchments were described below; and the values of curve number was calculated and used for estimating the runoff depth from the study area.

Rainfall data

Rainfall is the important climatic factor which affects the runoff (Mohamadi and Kavian, 2015). There was no runoff for rainfall depths less than or equal to initial abstractions, provided initial abstraction is 0.2 times of potential maximum retention for Indian conditions. In the present study, the rainfall data was obtained from Indian Meteorological Department for the period 2001 –2020 was 300.1 mm, there were considerable variations in the quantity of the annual rainfall from year to year **(Fig.)**. Notably, the maximum annual rainfall of 472.9 mm occurred in the year 2015, while the minimum of 43 mm was recorded in the year 2002. The mean annual rainfall over the district estimated as 300.1 mm. Values of coefficient of variation (CV) estimated as 32.62%, which indicates high rainfall variability over the area. The average monthly rainfall showed more than 60% of the rainfall occurs during South-West monsoon.

The maximum average rainfall was observed in the month of July and minimum in the December. The statistical characteristics of monthly rainfall during the period 2001-2020 are given in **Table.**

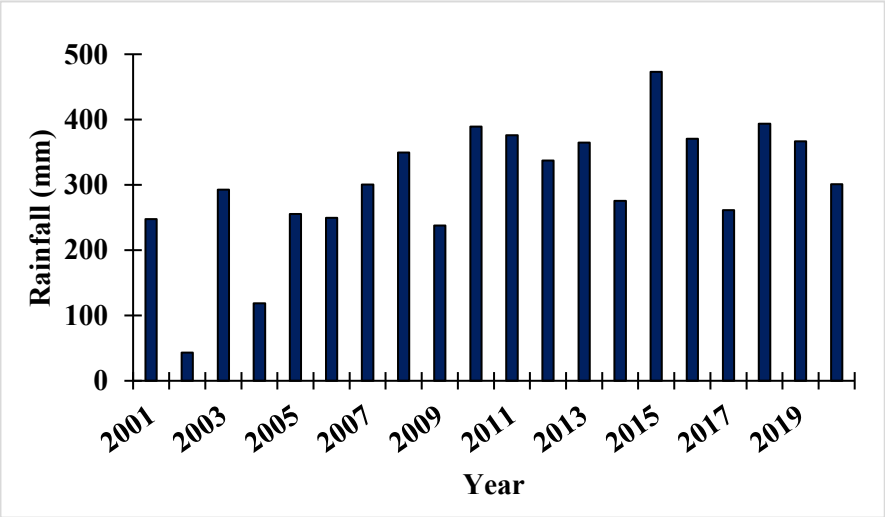

Figure 53:Annual rainfall (2001-2020) over the Bikaner district

Table 23 Statistical characteristics of monthly rainfall during the period 2001-2020

	Maximum	**Minimum**	**Average**	**St. Dev**
January	4.46	1.56	3.35	0.80
February	9.67	3.90	6.82	1.68
March	7.82	3.65	6.06	1.35
April	7.78	3.70	5.66	1.14
May	18.80	10.07	14.19	1.74
June	38.28	20.99	30.94	4.28
July	109.75	61.59	82.62	12.21
August	101.11	55.97	71.27	11.70
September	41.07	26.35	34.80	3.39
October	8.75	2.50	5.70	1.33
November	2.70	1.52	2.18	0.30
December	4.07	0.90	2.13	0.90

Hydrological soil group classification

In the determination of CN, the hydrological soil classification is adopted. The important soil characteristics that influence hydrological classification of soils are infiltration characterstics

and average clay content of soil. The slope of the soil surface is not considered when assigning hydrologic soil groups (USDA,2002). It has been observed that HSG-C is present in Sonsolav, Harsolav, Foolnath, Kodamdesar, and Sonsolav catchments, while both HSG-B and HSG-C are found in Dayatra, Darbari, Gajner, and Kolayat catchments. HSG-C composed of shallow loams, or soils with a moderate low infiltration rate when thoroughly wet. HSG-B have moderate infiltration rate and are of coarse texture such as sandy loam.

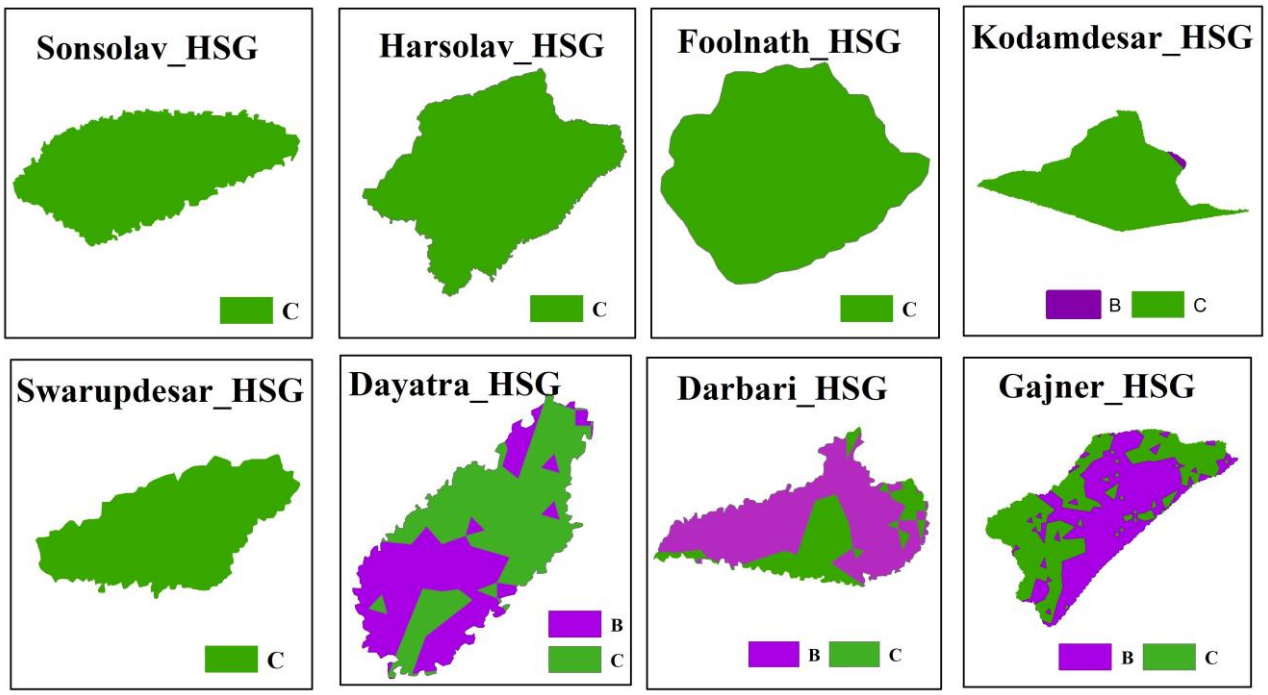

Figure 54:Hydrologic Soil group in different catchments over Bikaner district

Land Use Land Cover analysis

LULC analysis is vital for understanding and predicting hydrological processes, managing water resources, assessing environmental impacts, and developing sustainable land use strategies. LULC analysis forms the foundation for effective hydrological modeling and decision-making in water resource management. In the present study LULC analysis revealed a diverse distribution of classes across different catchments. Barren land is most extensive in Gajner, covering 3,473.67 hectares, whereas Foolnath has only 5.39 hectares. Agricultural land is predominantly found in Diyatra with 506.35 hectares, while it is absent in Sonsolav, Harsolav, Foolnath, and Swarupdesar. Tree cover is highest in Gajner, where it spans 1,054.04 hectares, and lowest in Foolnath with 2.67 hectares. Built-up areas are most significant in Darbari, comprising 188 hectares, and least in Swarupdesar, with only 0.07 hectares. Waterbodies are mainly present in Gajner, totaling 32.85 hectares, whereas Foolnath has only 0.04 hectares. Overall, Gajner stands out for its extensive barren land and tree cover, Diyatra for its agricultural land, and Darbari for its built-up areas. Waterbodies are relatively scarce

across all catchments, except Gajner and Kolayat. The LULC statistics of different catchments over the Bikaner district for the year 2020 are given in **Table.**

Table 24 LULC statistics of the year 2020 over Different catchment (All value in 'Hectare')

Catchment	Barren land	Agriculture	Trees	Builtup	Waterbodies
Sonsolav	22.24	0	6.912	10.168	0.68
Harsolav	52.16	0	13.43	16.16	0.45
Foolnath	5.39	0	2.67	2.61	0.04
Kodamdesar	47.75	1.36	25.88	1.91	4.08
Darbari	319	110	15	188	5
Gajner	3473.67	207.35	1054.04	77.43	32.85
Kolayat	1686.45	438.42	291.35	134.44	17.33
Diyatra	608.35	506.35	28.66	60	3.55
Swarupdesar	15.85	0	5.28	0.07	0.38

Estimation of curve number

The NRCS curve number (CN) is a parameter which shows the ability of soils in terms of infiltration of water with respect to antecedent moisture condition (Amutha and Porchelvan, 2009). Direct runoff estimates are more sensitive to changes in the CN than to rainfall variability. Boughton (1989) has shown that a 15-20%increase in CN almost doubles direct runoff predictions, while a similar extent of CN reduction predicts nearly half of it.

To create and detect the CN values for each classified area; the hydrological soil group and the land use results were used. Curve number for each area corresponding to land use classes and HSGs are represented in Table.

Table 25 Area for each CN value

Catchment	Land Use	Area of Land Use class (%)	Area of HSG (%)		CN	
			B	C	B	C
Sonsolav	Barren land	55.6	0	100	77	85
	Agriculture	0	0	100	81	88
	Trees	17.28	0	100	66	77
	Builtup	25.42	0	100	92	94
	Waterbody	1.7	0	100	98	98
Harsolav	Barren land	63.45	0	100	77	85

	Agriculture	0	0	100	81	88
	Trees	16.33	0	100	66	77
	Builtup	19.65	0	100	92	94
	Waterbody	0.54	0	100	98	98
Foolnath	Barren land	50.27	0	100	77	85
	Agriculture	0	0	100	81	88
	Trees	24.90	0	100	66	77
	Builtup	24.34	0	100	92	94
	Waterbody	0.37	0	100	98	98
Kodamdesar	Barren land	58.97246	99.5	0.5	77	85
	Agriculture	1.67	99.5	0.5	81	88
	Trees	31.96	99.5	0.5	66	77
	Builtup	2.35	99.5	0.5	92	94
	Waterbody	5.03	99.5	0.5	98	98
Swarupdesar	Barren land	73.44	0	100	77	85
	Agriculture	0	0	100	81	88
	Trees	24.46	0	100	66	77
	Builtup	0.32	0	100	92	94
	Waterbody	1.76	0	100	98	98
Diyatra	Barren land	50.40	27	73	77	85
	Agriculture	41.95	27	73	81	88
	Trees	2.37	27	73	66	77
	Builtup	4.97	27	73	92	94
	Waterbody	0.29	27	73	98	98
Darbari	Barren land	50.07	43	57	77	85
	Agriculture	17.26	43	57	81	88
	Trees	2.35	43	57	66	77
	Builtup	29.51	43	57	92	94
	Waterbody	0.78	43	57	98	98
Gajner	Barren land	71.69	77	85	50	50
	Agriculture	4.27	81	88	50	50
	Trees	21.75	66	77	50	50
	Builtup	1.59	92	94	50	50

	Waterbody	0.67	98	98	50	50

The composite curve number was found by using the following equation, (USDA, A985)

$$CN = \frac{\sum A_i CN_i}{\sum A_i}$$

Where,

CN = composite curve number

A_i = Area for each land use class

The composite curve number under normal condition (AMC II) for different catchment varies in the range of 76.18 (Gajner) and 86.12 (Sonsolav) as given in Table.

Table 26 Curve Number for AMC II condition

Catchment	**CN II value**
Sonsolav	86.12
Harsolav	85.25
Foolnath	83.88
Kodamdesar	84.26
Darbari	80.98
Gajner	76.18
Kolayat	85.37
Diyatra	85.22
Swarupdesar	83.58

The CN was founded for the normal condition (AMCII), CN for the other two condition i.e. the dry condition (AMC I) and the wet condition (AMC III) were

Table 27 Curve Number for AMC I and AMC III condition

Catchment	**CN I value**	**CN III value**
Sonsolav	73.12	93.56
Harsolav	71.70	93.12
Foolnath	69.53	92.42
Kodamdesar	70.12	92.61

Darbari	65.12	90.89
Gajner	58.37	88.22
Kolayat	71.89	93.18
Diyatra	71.66	93.10
Swarupdesar	69.05	92.26

Potential Maximum Retention (S)

The potential maximum retention (S) represents the maximum amount of water the soil can hold before runoff occurs, reflecting the soil's infiltration ability and the catchment area's land cover characteristics. This parameter is determined using the NRCS-CN method. The retention capacity across different catchments varies significantly, indicating diverse water retention capabilities. Gajner has the highest retention capacity, ranging from 27 to 144, highlighting its superior ability to retain moisture and effectively support vegetation while reducing runoff. Darbari closely follows with a range of 25 to 136, showcasing strong retention capabilities. Swarupdesar and Foolnath also exhibit high retention capacities, ranging from 21 to 113 and 20 to 111, respectively. Kodamdesar shows a retention range of 20 to 108, while Harsolav and Dayatra have ranges from 18 to 100, indicating moderate retention abilities that could benefit from improved land management practices. Kolayat and Sonsolav have the lowest retention capacities, with ranges of 18 to 99 and 17 to 93, respectively, suggesting these areas may require interventions to enhance their water retention potential. The ‘S’ values over different catchments are given below.

Table 28 S’ values over different catchments

Catchment	**S1**	**S2**	**S3**
Darbari	136	59	25
Dayatra	100	44	18
Foolnath	111	48	20
Gajner	144	63	27
Harsolav	100	43	18
Kodam	108	47	20
Sonsolav	93	40	17
Swarup	113	49	21
Kolayat	99	43	18

Initial Abstraction (I_a)

Runoff yield is very sensitive to initial abstraction ratio and the amount of water before runoff, such as rainfall interception by vegetation, infiltration etc. will constitutes the initial abstractions in an area. Generally, it is assumed as a part of potential maximum retention. For the larger channel area and finer soil, the initial abstractions will be lesser. The effect of initial abstraction ratio on runoff estimation increases with decreasing CNs (Yuan et al, 2012). The initial abstraction is taken as 0.2 times of potential maximum retention for the study area. Analysis revealed Darbari and Gajner have the highest ranges, from 5 to 27.2 and 5.4 to 28.8, respectively, suggesting diverse soil types and vegetation that enhance water retention. Foolnath and Swarupdesar also show moderate retention capabilities, with ranges of 4 to 22.2 and 4.2 to 22.6. Dayatra, Harsolav, and Kolayat exhibit similar ranges (3.6 to 20), indicating comparable hydrological conditions. Kodam and Sonsolav have slightly lower ranges of 4 to 21.6 and 3.4 to 18.6, reflecting less permeable surfaces and faster runoff initiation. Overall, these variations highlight the influence of soil, vegetation, and land use on water retention, providing insights essential for effective water management and conservation.

Estimation of Direct Runoff

The NRCS CN method was used to estimate the runoff occurring from the different catchments over the study area. The NRCS CN equation is widely used due to its simplicity and flexibility in estimation of runoff. Catchment wise description of simulated runoff during the period 2001 to 2020 is given below.

Sonsolav catchment

The rainfall and runoff data analysis for the Sonsolav catchment from 2001 to 2020 provide insights into the hydrological behavior of this region. Over the two decades, the average annual rainfall was 300.1 mm, with an average runoff of 80.7 mm, indicating indicating a runoff-rainfall ratio of approximately 26.9%. The year 2015 having highest recorded rainfall of 472.9 mm and a significant runoff of 135 mm. This suggests a strong response of the catchment to heavy rainfall events, likely due to soil saturation and reduced absorption capacity. Similarly, 2018 witnessed high rainfall of 393.6 mm and the maximum recorded runoff of 171.7 mm, reinforcing the pattern of increased runoff following substantial rainfall. Conversely, in 2002, the catchment experienced the lowest rainfall of 43 mm, resulting in no measurable runoff, indicating drought conditions. In the year 2017, despite a moderate rainfall of 261.1 mm, the runoff was only 17.9 mm, which might be attributed to dry soil conditions. The data also reveals years with moderate rainfall but significant runoff, such as 2012, which had a rainfall of 337.1

mm and a high runoff of 152.9 mm. This could suggest factors like antecedent wet conditions or catchment characteristics that favor runoff generation. Similarly, in 2010 and 2011, both years had rainfall around 380 mm, with runoff over 129 mm, indicating a period of high runoff efficiency, possibly due to favorable hydrological conditions or minimal water retention by the soil.

Table 29 Annual rainfall and runoff over the Sonsolav catchment

Year	Rainfall (mm)	Runoff (mm)	Year	Rainfall (mm)	Runoff (mm)
2001	247.4	40.2	**2012**	337.1	152.9
2002	43	0.0	**2013**	364.5	131.3
2003	292.6	76.0	**2014**	275.5	66.4
2004	118.6	6.0	**2015**	472.9	135.0
2005	255.6	62.6	**2016**	370.4	95.6
2006	249.3	69.7	**2017**	261.1	17.9
2007	300.3	85.6	**2018**	393.6	171.7
2008	349.4	59.3	**2019**	366.9	96.0
2009	237.8	46.4	**2020**	300.8	41.1
2010	389	129.0	**Average**	300.1	80.7
2011	376.2	131.5			

The runoff analysis to the pond having a capacity of 28,341.6 m^3 between the period 2001 to 2020 showed fluctuations between overflow and deficit. The pond experienced overflow in several years, with the most significant overflow occurring in 2018, when the runoff exceeded the pond capacity by 40,351.5 m^3. Other years with notable overflow include 2012, 2011, and 2010, with overflows of 32,828.1 m3, 24,266.7 m^3, and 23,280.1 m^3, respectively. Conversely, the years 2002, 2004, 2009, and 2017 witnessed significant deficits, with 2002 having the largest deficit of 28,336.8 m^3 due to no runoff **(Fig.)**. These findings highlight the variability in water availability, underscoring the need for effective water management strategies to handle both excess and deficit situations, ensuring sustainable water use and mitigating flood risks.

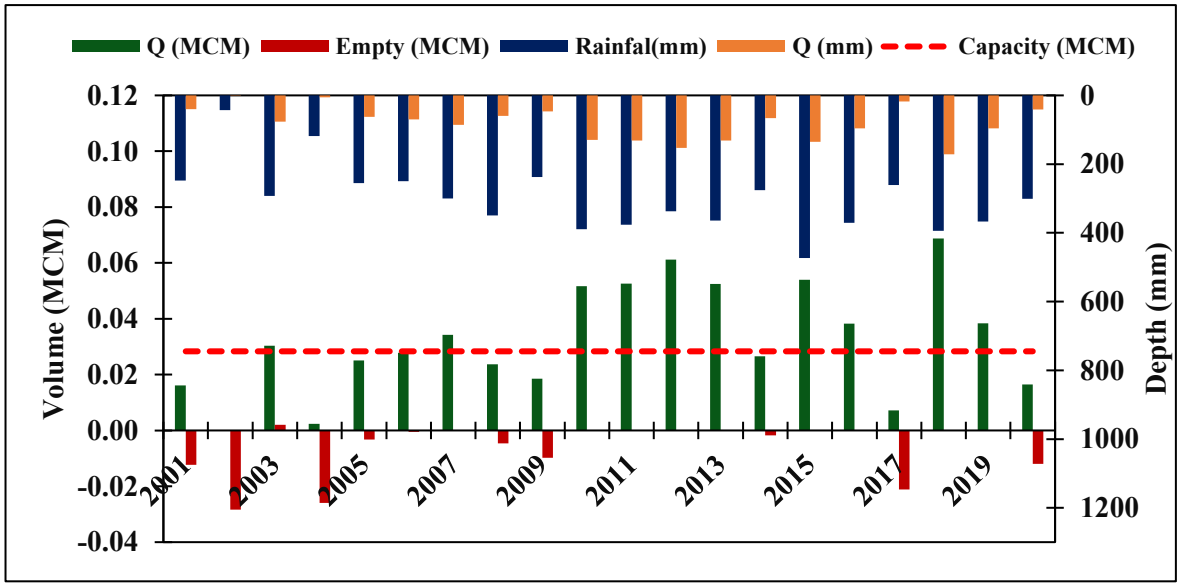

Figure 55:Status of water availability in Sonsolav pond

Harsolav catchment

The rainfall and runoff data for the Harsolav catchment from 2001 to 2020 demonstrates a notable relationship between these two hydrological parameters. The average annual rainfall over the two decades is 300.1 mm, with an average runoff of 78.2 mm (**Table**). Generally, higher rainfall years correspond to increased runoff, as seen in years like 2010, 2011, 2012, 2013, 2015, and 2018. For instance, 2018, which had one of the highest rainfalls at 393.6 mm, also saw the highest runoff of 167.6 mm, indicating a direct response of runoff to intense rainfall events. Conversely, years with lower rainfall, such as 2002 and 2004, resulted in minimal runoff, reflecting the limited capacity for water accumulation when rainfall is sparse. In some years, such as 2008 and 2014, where despite higher than average rainfall, the runoff was relatively moderate at 56.2 mm and 64.1 mm, respectively. This suggests other influencing factors like soil absorption capacity and temporal distribution of rainfall events, which can mitigate or delay runoff. Similarly, in 2017, despite a rainfall of 261.1 mm, the runoff was significantly lower at 16.6 mm, which may indicate a year where the catchment retained more water due to antecedent moisture conditions or other environmental factors.

Table 30 Annual rainfall and runoff over the Harsolav catchment

Year	Rainfall (mm)	Runoff (mm)	Year	Rainfall (mm)	Runoff (mm)
2001	247.4	38.2	**2012**	337.1	148.9
2002	43	0.0	**2013**	364.5	127.6
2003	292.6	73.7	**2014**	275.5	64.1

2004	118.6	5.7	**2015**	472.9	129.8
2005	255.6	60.1	**2016**	370.4	91.6
2006	249.3	67.8	**2017**	261.1	16.6
2007	300.3	83.6	**2018**	393.6	167.6
2008	349.4	56.2	**2019**	366.9	94.0
2009	237.8	44.5	**2020**	300.8	39.5
2010	389	125.2	**Average**	300.1	78.2
2011	376.2	128.9			

The data from 2001 to 2020 for a pond with a capacity of 98,365.7 m^3 indicates a pattern of deficits, with only a few years of overflow, reflecting variability in water availability. Most years experienced a deficit, where runoff was insufficient to fill the pond to capacity. Significant deficits occurred in 2002, 2004, and 2017, with 2002 experiencing the largest shortfall of 98,365.5 m^3 due to almost no runoff. Years such as 2001, 2003, and 2009 also faced considerable deficits, showing consistent underperformance in filling the pond. However, the years 2010, 2011, 2012, 2013, 2015, and 2018 (**Fig.**). The most substantial overflow happened in 2018, with a surplus of 39,380.7 m^3, while 2012 also saw a significant overflow of 24,011.0 m^3, highlighting periods of excess runoff amid generally deficit conditions.

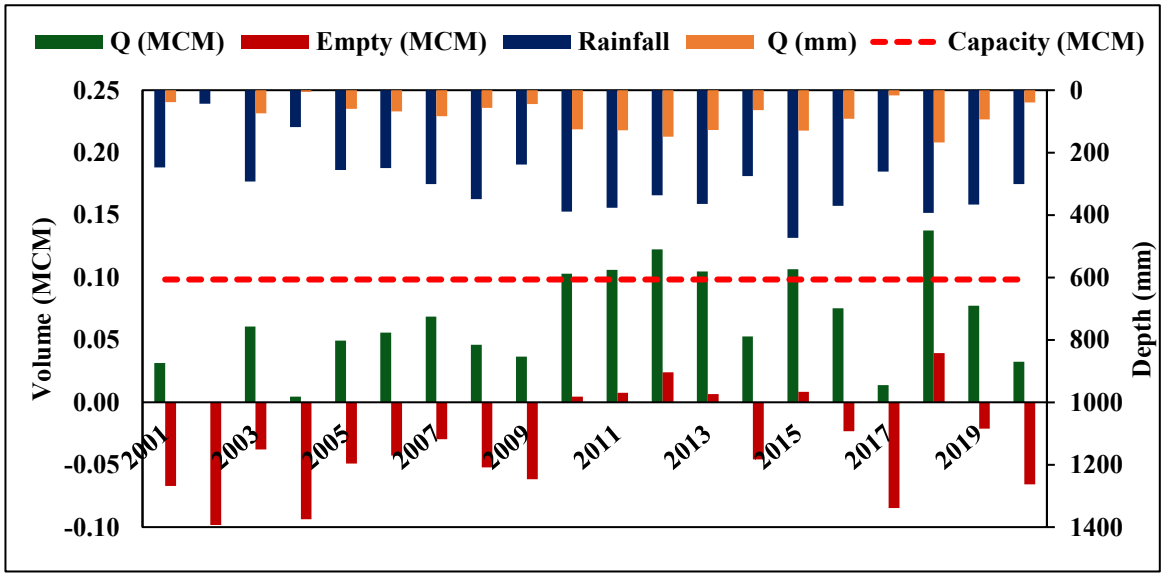

Figure 56:Status of water availability in Harsolav pond

Foolnath catchment

The average rainfall and runoff over the catchment during the period was estimated as 300.1 mm and 73.7 mm respectively (Table), indicating a runoff-rainfall ratio of approximately

24.5%. Generally, years with higher rainfall result in higher runoff, reflecting the relationship between precipitation and hydrological response in the catchment. Years with high rainfall, such as 2010, 2011, 2012, and 2018, saw significant runoff, indicating that intense or prolonged rainfall exceeded the catchment's absorption capacity. Conversely, in years like 2002 and 2004, very low runoff despite some rainfall suggests high evaporation. Anomalies, such as in 2008 and 2015, where significant rainfall did not lead to proportionately high runoff, highlights how antecedent soil moisture conditions and weather patterns impact the hydrological response.

Table 31 Annual rainfall and runoff over the Foolnath catchment

Year	Rainfall (mm)	Runoff (mm)	Year	Rainfall (mm)	Runoff (mm)
2001	247.4	34.8	**2012**	337.1	141.4
2002	43	0.0	**2013**	364.5	120.9
2003	292.6	69.8	**2014**	275.5	60.2
2004	118.6	5.1	**2015**	472.9	120.6
2005	255.6	55.4	**2016**	370.4	84.4
2006	249.3	64.3	**2017**	261.1	14.6
2007	300.3	80.1	**2018**	393.6	159.7
2008	349.4	51.1	**2019**	366.9	90.3
2009	237.8	41.3	**2020**	300.8	36.8
2010	389	118.2	**Average**	300.1	73.7
2011	376.2	124.2			

The overland flow from the catchment during 2001-2020 indicates significant fluctuations in runoff relative to its capacity of 1,804.1 m^3, with numerous instances of overflow and some years of deficit. Overflows were particularly notable in years such as 2018, 2012, 2011, 2010, 2013, and 2015, where the pond exceeded its capacity by substantial margins (**Fig.**). The most significant overflow occurred in 2018, with an excess of 15,312.5 m^3, highlighting extreme conditions of high precipitation or runoff. Other notable overflow years include 2012 with 13,350.7 m^3 and 2011 with 11,506.5 m^3. In contrast, the years 2002, 2004, and 2017 were marked by deficits, with 2002 having the most significant deficit of 1,804.1 m^3 due to no runoff, underscoring potential drought conditions or minimal rainfall.

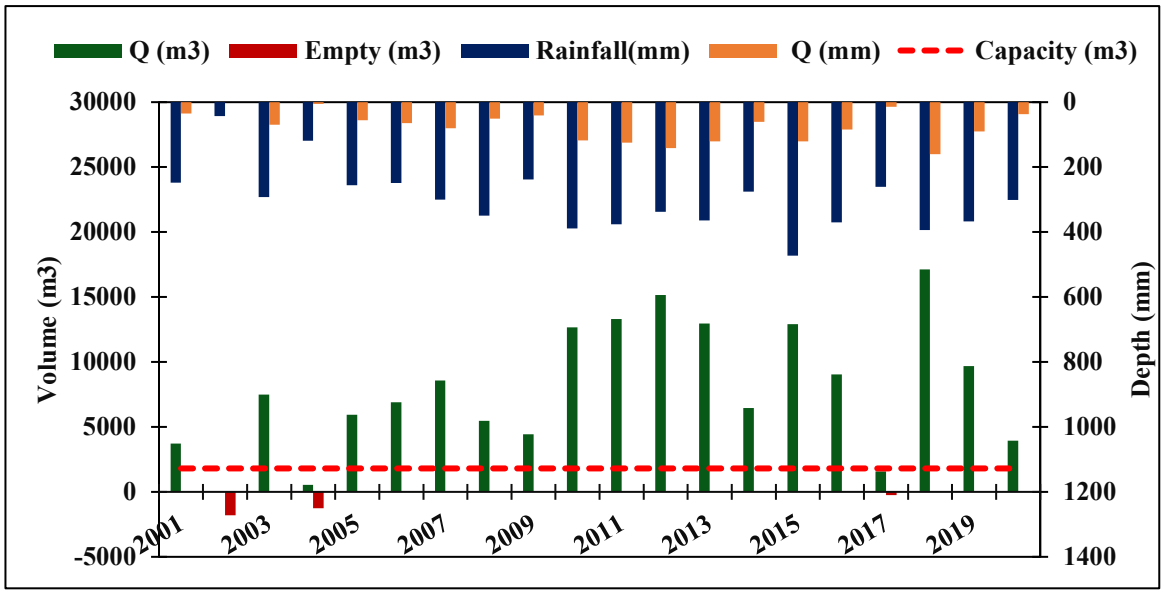

Figure 57:Status of water availability in Foolnath pond

Darbari catchment

The relationship between rainfall and runoff in different catchments can vary significantly due to several factors, including soil type, land use, topography, vegetation cover, and the intensity and duration of rainfall events. Analyzing the data from 2001 to 2020, the average annual rainfall and runoff over the catchment was estimated as 300.1 mm and 64.2 mm respectively **(Table)**. It was observed that annual rainfall and runoff do not always follow a linear relationship. The correlation between the rainfall and runoff was obtained as 0.63. For instance, in 2002, the recorded rainfall was only 43.0 mm with no runoff, indicating extremely dry conditions. Conversely, in 2018, a substantial rainfall of 393.6 mm resulted in a high runoff of 142.4 mm, which suggests either saturated soil conditions or heavy rainfall over a short period, leading to increased surface runoff. In 2014, despite a high rainfall of 472.9 mm, the runoff was relatively low at 101.7 mm due to several factors. It could be due to high infiltration capacity, allowing more water to be absorbed rather than contributing to runoff. Additionally, if the rainfall was spread over a longer period with moderate intensity, it would have had more time to infiltrate.

Table 32 Annual rainfall and runoff over the Darbari catchment

Year	Rainfall (mm)	Runoff (mm)	Year	Rainfall (mm)	Runoff (mm)
2001	247.4	27.9	**2012**	337.1	125.3
2002	43	0.0	**2013**	364.5	106.8
2003	292.6	61.7	**2014**	275.5	52.2

2004	118.6	3.8	**2015**	472.9	101.7
2005	255.6	45.6	**2016**	370.4	69.5
2006	249.3	56.7	**2017**	261.1	11.5
2007	300.3	72.6	**2018**	393.6	142.4
2008	349.4	41.7	**2019**	366.9	82.1
2009	237.8	34.8	**2020**	300.8	31.3
2010	389	103.3	**Average**	300.1	64.2
2011	376.2	114.0			

The analysis of the Darbari pond from 2001 to 2020 reveals several years with notable overflow and deficit. Overflow occurred in 16 of the 20 years (**Fig.**), with significant overflows in 2018, 2012, 2011, 2013, 2010, and 2015, indicating periods of heavy precipitation and runoff that exceeded the pond's capacity of 183,279.2 m^3. The most significant overflow occurred in 2018, with 723,954.7 m^3 of excess water. In contrast, deficit years like 2002, 2017, and 2004 highlight periods of reduced runoff, with 2002 experiencing the most severe deficit as there was no runoff.

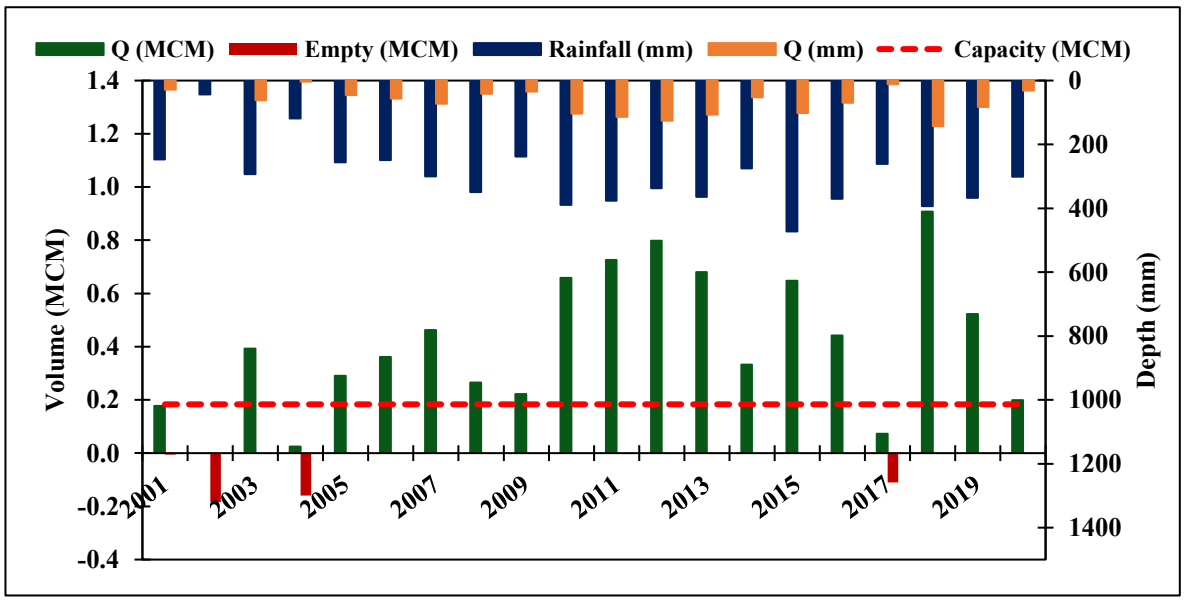

Figure 58:Status of water availability in Darbari pond

Gajner catchment

Based on the simulated runoff data from 2001 to 2020 for the Gajner catchment, a complex relationship between rainfall and runoff was observed. The average annual rainfall was 300.1 mm, while the average runoff was 52.5 mm. There is a general correlation between higher rainfall and increased runoff, as seen in years like 2010, 2011, 2012, and 2018, where rainfall

was above average and runoff was significantly higher (84.1 mm, 100.3 mm, 104.3 mm, and 119.9 mm, respectively) as given in **Table**. This suggests that intense or prolonged rainfall leads to increased surface runoff, overwhelming the catchment's absorption capacity. However, some years, such as 2008 and 2015, had relatively high rainfall but lower runoff, indicating factors like soil saturation, infiltration capacity, or rainfall intensity impacting runoff levels. Additionally, years with low rainfall, such as 2002 and 2004, resulted in minimal runoff, reflecting effective infiltration and absorption by the soil.

Table 33 Annual rainfall and runoff over the Gajner catchment

Year	Rainfall (mm)	Runoff (mm)	Year	Rainfall (mm)	Runoff (mm)
2001	247.4	20.0	**2012**	337.1	104.3
2002	43	0.0	**2013**	364.5	88.8
2003	292.6	51.9	**2014**	275.5	42.3
2004	118.6	2.5	**2015**	472.9	78.8
2005	255.6	34.0	**2016**	370.4	51.8
2006	249.3	46.6	**2017**	261.1	8.2
2007	300.3	62.7	**2018**	393.6	119.9
2008	349.4	30.9	**2019**	366.9	71.0
2009	237.8	26.8	**2020**	300.8	24.4
2010	389	84.1	**Average**	300.1	52.5
2011	376.2	100.3			

The overland flow analysis to the pond, having a capacity of 3,597,064.6 m^3, revealed a series of deficits and a few instances of overflow, underscoring significant variability in water availability. Many years experienced deficits, indicating periods of insufficient runoff to meet the pond's capacity. The most pronounced deficits occurred in 2002, 2004, and 2017, with 2002 having the most substantial deficit at 3,597,064.6 m^3 due to no runoff **(Fig.)**. Other years with significant deficits include 2001, 2003, and 2008. In contrast, overflow years were less frequent but notable when they occurred, highlighting periods of abundant runoff. The years 2010, 2011, 2012, 2013, 2015, and especially 2018 experienced overflow. The most significant overflow occurred in 2018, with a surplus of 2,212,286.5 m^3, followed by 2012 with an overflow of 1,458,576.2 m^3.

Diyatra catchment

The average rainfall over the period (2001-2020) is estimated as 300.1 mm, with an average runoff of 78.1 mm, suggesting a runoff-to-rainfall ratio of approximately 26% (Table). The relationship between rainfall and runoff in the Diyatra catchment is influenced by a combination of rainfall intensity, duration, antecedent soil moisture, and catchment characteristics. While there is a general trend of increased runoff with higher rainfall, the variability in data highlights the complexity of hydrological responses. The years 2010, 2011, 2012, and 2018 showed high runoff (125.2 mm, 128.9 mm, 148.9 mm, and 167.6 mm, respectively) correlated with high rainfall (above 337 mm). These instances highlight the catchment's limited infiltration capacity during intense or prolonged rainfall events, leading to significant surface runoff. Year 2018 stands out with the highest runoff of 167.6 mm, despite not having the highest rainfall, which implies possibly saturated soil conditions or intense rainfall events. In the year 2002, no runoff has occurred due to very low rainfall (43 mm). In the year 2017 low runoff (16.5 mm) compared to its rainfall of 261.1 mm have observed, suggesting conditions of high absorption or low-intensity rainfall. The variability in the runoff-to-rainfall ratio across different years points to dynamic catchment responses, where periods of intense rainfall lead to saturation and increased runoff, while dry spells or gradual rainfall allow for more infiltration.

Table 34 Annual rainfall and runoff over the Diyatra catchment

Year	Rainfall (mm)	Runoff (mm)	Year	Rainfall (mm)	Runoff (mm)
2001	247.4	38.2	**2012**	337.1	148.9
2002	43	0.0	**2013**	364.5	127.6
2003	292.6	73.7	**2014**	275.5	64.1
2004	118.6	5.7	**2015**	472.9	129.7
2005	255.6	60.0	**2016**	370.4	91.6
2006	249.3	67.8	**2017**	261.1	16.5
2007	300.3	83.6	**2018**	393.6	167.6
2008	349.4	56.1	**2019**	366.9	94.0
2009	237.8	44.5	**2020**	300.8	39.5
2010	389	125.2	**Average**	300.1	78.1
2011	376.2	128.9			

The pond frequently experienced significant overflows, particularly in the years 2010, 2011, 2012, 2013, 2015, and 2018, highlighting periods of excessive runoff and potential flooding risk (**Fig.**). The year 2018 marked the most extreme overflow, suggesting an exceptionally wet period. Conversely, deficit years like 2002, 2004, and 2017 indicate times of insufficient runoff, with 2002 experiencing the most severe deficit due to no runoff.

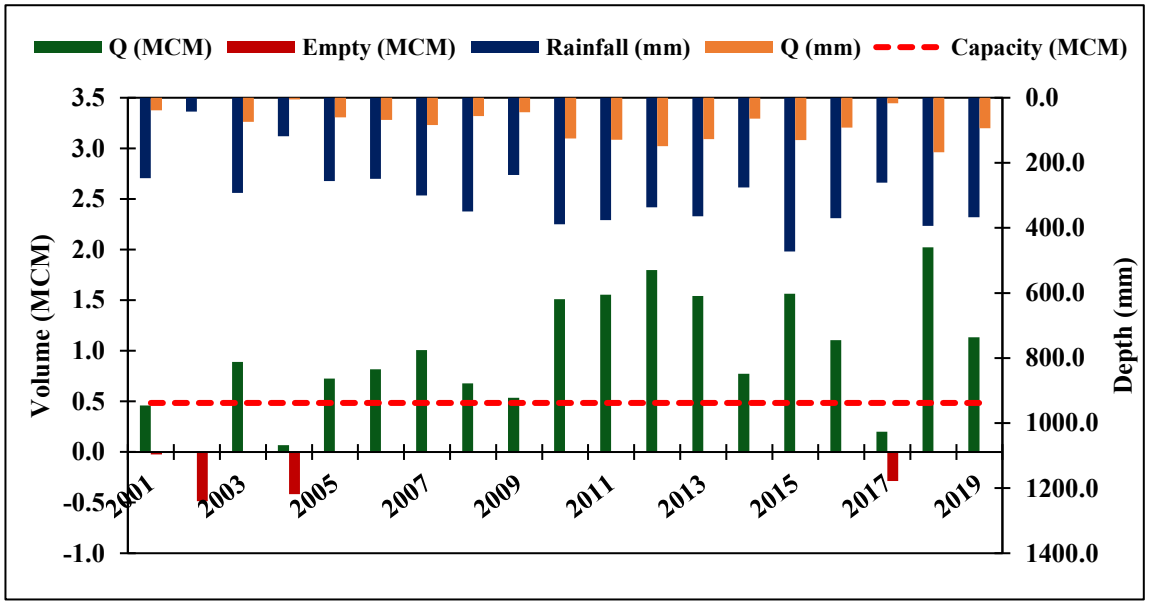

Figure 59:Status of water availability in Diyatra pond

Kodamdesar catchment

The rainfall and runoff pattern spanning from 2001 to 2020 over the Kodamdesar catchment showed that on an average, the catchment receives 300.1 mm of rainfall annually, with 73.7 mm of runoff. The rainfall-runoff ratio of 24.5%, indicates that approximately a quarter of the rainfall becomes runoff. The data shows considerable variability year-to-year; for instance, 2015 experienced the highest rainfall of 472.9 mm, which produced a substantial runoff of 120.7 mm, reflecting high runoff efficiency. Conversely, 2002 had the lowest rainfall at 43 mm and recorded no runoff, which might suggest exceptional conditions such as very dry soil or lack of significant surface runoff. The highest recorded runoff occurred in 2018 at 159.7 mm, despite rainfall not being the highest that year, suggesting that factors such as rainfall intensity and antecedent moisture content also play a critical role in runoff generation. Overall, there appears to be a general trend of increasing rainfall over the years, although runoff patterns remain highly variable.

Table 35 Annual rainfall and runoff over the Kodamdesar catchment

Year	Rainfall (mm)	Runoff (mm)	Year	Rainfall (mm)	Runoff (mm)
2001	247.4	34.8	**2012**	337.1	141.5
2002	43	0.0	**2013**	364.5	121.0
2003	292.6	69.8	**2014**	275.5	60.2
2004	118.6	5.1	**2015**	472.9	120.7
2005	255.6	55.4	**2016**	370.4	84.4
2006	249.3	64.3	**2017**	261.1	14.7
2007	300.3	80.1	**2018**	393.6	159.7
2008	349.4	51.3	**2019**	366.9	90.3
2009	237.8	41.3	**2020**	300.8	36.9
2010	389	118.3	**Average**	300.1	73.7
2011	376.2	124.2			

The overland flow analysis to a pond having a capacity of 237,642.2 m^3 revealed a consistent pattern of deficits in runoff, with no years of overflow, underscoring continuous underfilling. Each year recorded a shortfall, indicating insufficient runoff to meet the pond's capacity. The most significant deficit occurred in 2002, with a deficit of 237,642.2 m^3, as there was zero runoff (**Fig.**). Other years with significant deficits include 2004 with a shortfall of 233,546.5 m3 and 2017 with a deficit of 225,714.8 m^3. The least deficit year was 2018, with a shortfall of 108,296.6 m^3, indicating a relatively better runoff compared to other years.

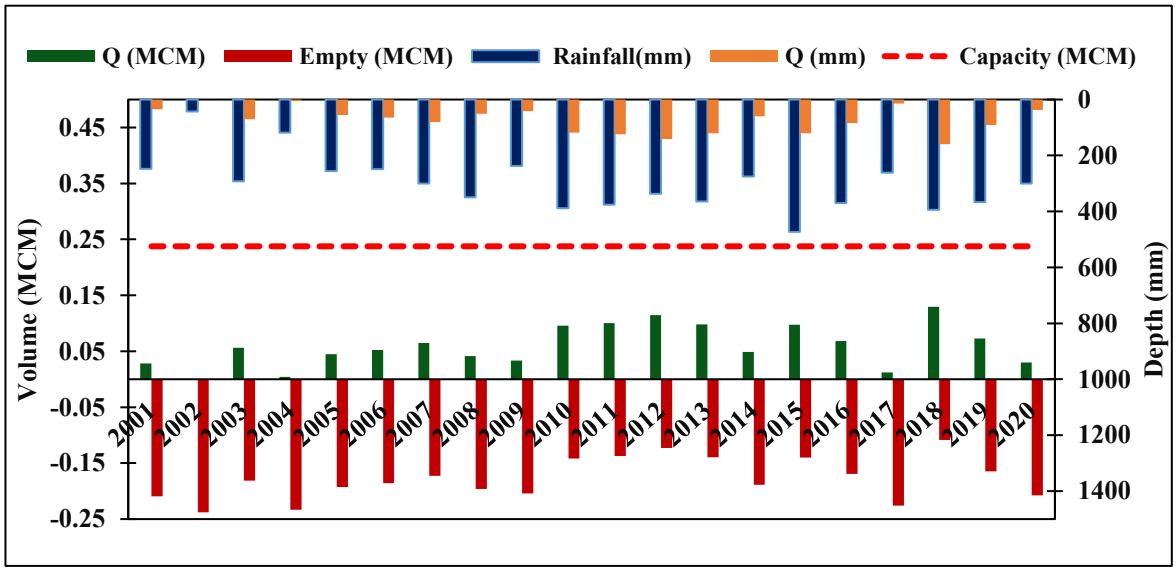

Figure 60:Status of water availability in Kodamdesar pond

Kolayat catchment

Based on the simulated runoff data from 2001 to 2020 for the kolayat catchment, a complex relationship between rainfall and runoff was observed. The average annual rainfall was estimated as 298.8 mm, while the average runoff was 68.1 mm. For instance, the year 2015 experienced the highest rainfall at 490 mm, which corresponded to a relatively high runoff of 129.3 mm. In contrast, 2002 recorded the lowest rainfall of only 49.3 mm, resulting in no measurable runoff. This suggests a good correlation between rainfall and runoff in the catchment area. In some years, such as 2003 and 2012, there was a noticeable discrepancy between rainfall and runoff. In 2003, despite a high rainfall of 318.8 mm, the runoff was 77.6 mm, indicating potential factors such as soil absorption, evaporation, or terrain characteristics affecting runoff efficiency. Similarly, 2012 had a rainfall of 334.8 mm with a significantly high runoff of 146.3 mm, possibly due to saturated ground conditions or other hydrological factors enhancing runoff. Years like 2018 having rainfall of 391.8 mm and the highest runoff recorded at 172.5 mm, emphasizing the catchment's response to heavy rainfall events. Conversely, 2004 and 2006 show very low runoff of 0.2 mm and 28.5 mm, respectively, despite moderate rainfall, suggesting periods of drought or soil conditions that retain moisture.

Table 36 Annual rainfall and runoff over the Kolayat catchment

Year	Rainfall (mm)	Runoff (mm)	Year	Rainfall (mm)	Runoff (mm)
2001	264.5	47.8	**2012**	334.8	146.3
2002	49.3	0.0	**2013**	378.3	116.0

2003	318.8	77.6	**2014**	292.3	62.5
2004	133.1	0.2	**2015**	490	129.3
2005	224.7	30.5	**2016**	368.6	82.8
2006	232.1	28.5	**2017**	239.6	10.2
2007	293.9	67.1	**2018**	391.8	172.5
2008	308.2	26.2	**2019**	345.4	72.0
2009	195.3	23.6	**2020**	332.2	40.5
2010	410.1	121.6	**Average**	298.7	68.1
2011	371.6	107.2			

The overland flow analysis to the pond having capacity of 28,341.6 m^3 showed fluctuations between overflow and deficit. The pond experienced overflow in several years, with the most significant overflow occurring in 2018, when the runoff exceeded the pond capacity by 40,351.5 m^3 (**Fig.**). Other years with notable overflow include 2012, 2011, and 2010, with overflows of 32,828.1 m^3, 24,266.7 m3, and 23,280.1 m3, respectively. Conversely, the years 2002, 2004, 2009, and 2017 witnessed significant deficits, with 2002 having the largest deficit of 28,336.8 m^3 due to no runoff.

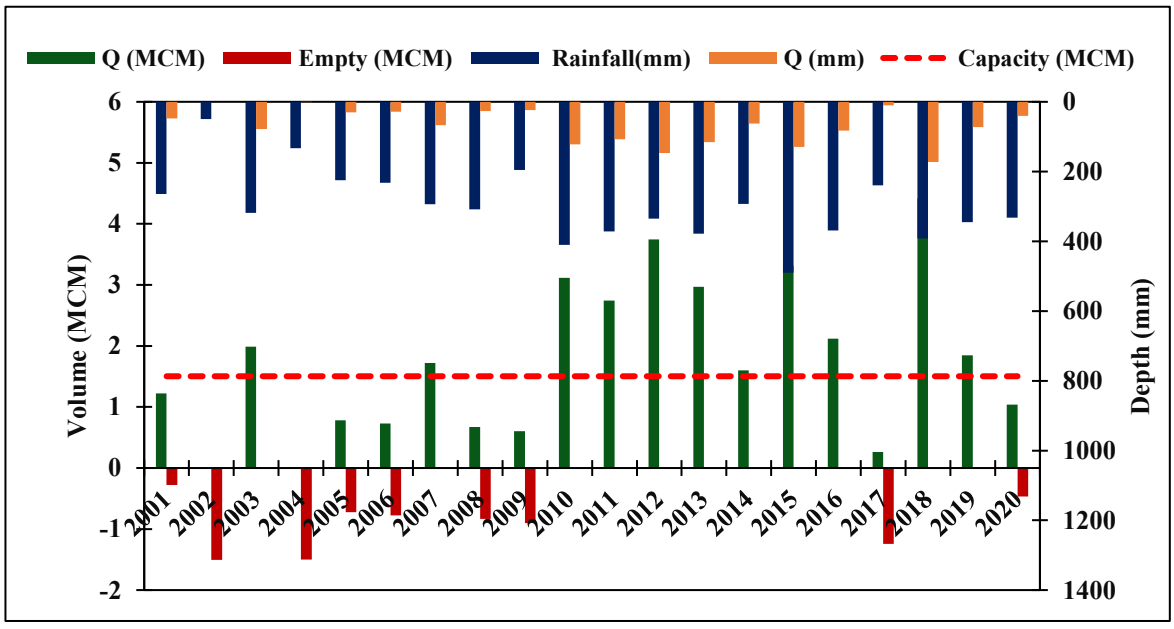

Figure 61:Status of water availability in Kolayat pond

Swarupdesar catchment

The rainfall and runoff analysis for the Swarupdesar catchment from 2001 to 2020 revealed significant patterns and variations in the hydrological response of this region. Over the past

two decades, the average annual rainfall was 300.1 mm, with an average runoff of 71.6 mm, indicating a moderate conversion of rainfall into runoff, though the efficiency of this conversion varies across the years. For instance, 2018 experienced the highest runoff at 156 mm following a substantial rainfall of 393.6 mm. This year reflects the catchment's responsiveness to increased precipitation, possibly due to factors such as soil saturation, reduced infiltration rates, or effective drainage systems. On the other hand, 2002 recorded the lowest rainfall at just 43 mm, resulting in no measurable runoff, indicating drought conditions, where limited precipitation is insufficient to generate any runoff. The year 2017 also recorded relatively low runoff (13.9 mm) despite receiving 261.1 mm of rainfall, which might be due to dry antecedent soil conditions that absorbed more water than usual. Some years displayed significant discrepancies between rainfall and runoff, suggesting the influence of other hydrological factors. For example, 2008 had a high rainfall of 349.4 mm but only 49.1 mm of runoff, indicating potential issues like high evaporation rates, increased soil retention, or improvements in water conservation practices within the catchment. Similarly, in 2015, despite receiving the highest rainfall of the data set at 472.9 mm, the runoff was only 116.5 mm, perhaps indicating enhanced groundwater recharge or storage in the catchment's natural features.

Table 37 Annual rainfall and runoff over the Swarupdesar catchment

Year	Rainfall (mm)	Runoff (mm)	Year	Rainfall (mm)	Runoff (mm)
2001	247.4	33.3	**2012**	337.1	138.0
2002	43	0.0	**2013**	364.5	117.9
2003	292.6	68.0	**2014**	275.5	58.4
2004	118.6	4.8	**2015**	472.9	116.5
2005	255.6	53.2	**2016**	370.4	81.1
2006	249.3	62.7	**2017**	261.1	13.9
2007	300.3	78.5	**2018**	393.6	156.0
2008	349.4	49.1	**2019**	366.9	88.6
2009	237.8	39.9	**2020**	300.8	35.6
2010	389	115.0	**Average**	300.1	71.6
2011	376.2	122.0			

The overland flow from the catchment to the pond having a capacity of 21,048.1 m^3 showed significant variability in overflow and deficit levels. Notable overflow years include 2018, with

an excess of 12,629.3 m^3, and several other years where overflow occurred, such as 2010, 2011, 2012, and 2015 (Fig.). Conversely, the pond faced substantial deficits in multiple years, with the most severe deficit in 2002, totaling 21,048.1 m^3. Other significant deficit years include 2004, 2007, 2008, 2009, and 2017.

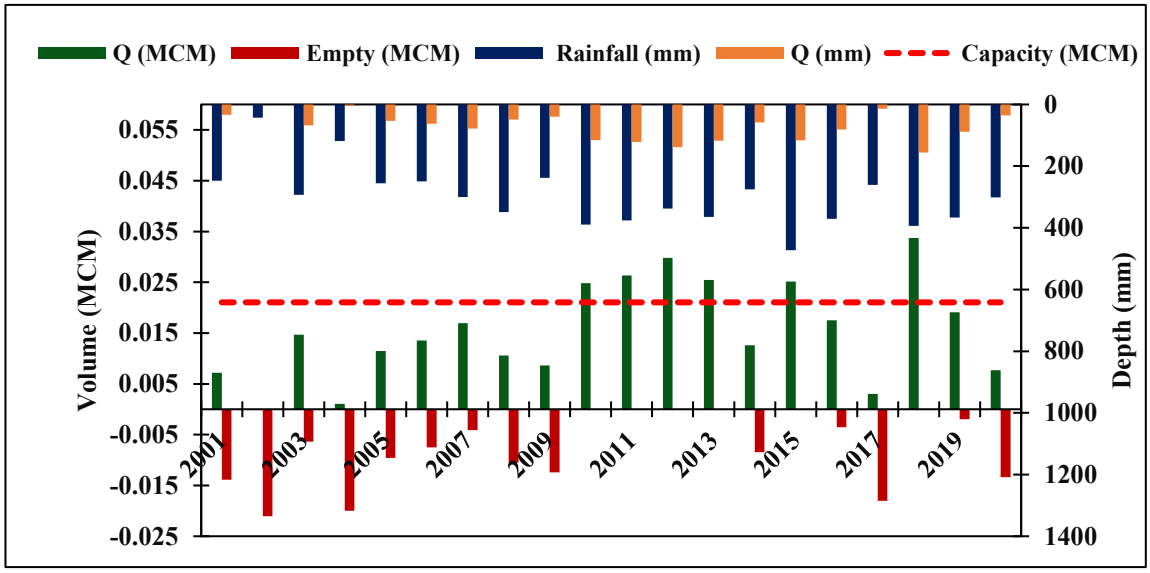

Figure 62:Status of water availability in Swarupdesar pond

Miscellaneous

The simulated runoff for the period from 2001 to 2020 across different catchments, including Darbari, Dayatra, Foolnath, Gajner, Harsolav, Kodam, Kolayat, Sonsolav, and Swarupdesar, revealed complex hydrological pattern. Across all catchments, there is significant variability in runoff, with the Sonsolav catchment experiencing the highest average runoff at 80.7 mm, while the Gajner catchment recorded the lowest average at 52.5 mm. This discrepancy in runoff suggests diverse catchment characteristics, such as soil type, vegetation cover, and topography, influencing water retention and absorption capacity. Years like 2010, 2011, 2012, and 2018 showed increased runoff across most catchments, indicating periods of intense rainfall that exceeded soil absorption capacity. Conversely, years such as 2002 and 2004 experienced minimal runoff due to insufficient rainfall or efficient absorption by dry soil. Some years, like 2008 and 2015, exhibited significant rainfall but comparatively lower runoff, suggesting factors like increased vegetation, improved soil permeability, or even distribution of rainfall events. The results underscores that rainfall is a primary driver of runoff, other factors, such as soil saturation, land cover, and rainfall intensity, also play crucial roles in determining hydrological responses. Each catchment's unique geographical and climatic conditions contribute to its specific runoff patterns, highlighting the importance of water management practices for effective water resource utilization.

The analysis of pond data across various locations from 2001 to 2020 reveals distinct patterns of overflow and deficit, reflecting the variability in water management and precipitation. At Darbari, significant overflow years, particularly 2018, 2012, and 2011, highlight periods of excessive runoff, while deficits in 2002 and 2017 illustrate dry years with minimal runoff. Diyatra similarly shows overflow in 2018, 2012, and 2011, with notable deficits in 2002 and 2004. Foolnath experienced substantial overflows in 2018, 2012, and 2011, but faced significant deficits in 2002 and 2017. Gajner's data points to frequent deficits, especially in 2002, 2004, and 2017, with overflow observed in years like 2018 and 2012. Harsolav predominantly showed deficits, particularly in 2002 and 2017, with overflow noted in 2018. Kodamdesar consistently faced deficits, with 2002 marking the most severe shortfall, and no years of overflow. Kolayat's data indicates a mix of overflow and deficit, with significant overflow in 2018 and 2012 and deficits in 2002 and 2004. Sonsolav experienced notable overflow in 2018 and several other years, but also significant deficits in 2002 and 2004. Lastly, Swarupdesar shows considerable variability, with overflow in 2018 and deficits in 2002 and 2017.

Overall, the percentage of time each pond experienced deficits varies significantly. Darbari, Foolnath, and Kolayat experienced more years of overflow compared to deficits, indicating generally more abundant water availability. In contrast, Gajner, Harsolav, Kodamdesar, and Swarupdesar faced a higher percentage of deficit years, particularly Gajner and Kodamdesar, which experienced deficits in almost every year. These fluctuations underscore the challenges of managing water resources effectively. The pond experienced both extreme overflow and deficit conditions, suggesting a need for adaptive management strategies to handle variable water inflows and ensure stable water storage throughout the year.

Soil Loss Assessment

In the present study, Universal soil loss equation is applied on Remote Sensing (RS) and Geographical Information System (GIS) platform for spatial soil erosion modeling to predict the average annual rate of soil loss from the catchment. The results obtained in this study are presented below.

Development of a database for USLE

Rainfall Erosivity factor (R)

Among the factors used in the USLE model, rainfall erosivity is of great importance as rainfall is the main driver for the erosion of soil by water and has a straight impact on the soil particles detachment, the failure of aggregates and the transport of eroded soil particles through runoff. The R-Factor measures the erosive force of rainfall and its potential to cause soil erosion, varies significantly among the catchments,

For the study area, the Rainfall erosivity (R) factor was calculated from available daily rainfall data of last 20 years (2001-2020) over the Bikaner district of Rajasthan. Moreover, sub-hourly rainstorm data was not available for Jodhpur region to calculate the summative kinetic energy rainstorm events in a year. Instead, we used an empirical equation relating R factor with Fournier index (F) developed for arid region in having annual rainfall less than 600 mm (Irvem et al., 2007). The average annual rainfall data (mm) and R-factor ($MJ \cdot mm \cdot ha^{-1} \cdot hr^{-1} \cdot yr^{-1}$) values in the study area are presented in the following Table 6.18

Station	Longitude	Latitude	FI	R-Factor	Station	Longitude	Latitude	FI	R-Factor
1	73	27.5	64.9	1406.1	23	73	28.25	50.7	806.9
2	73.25	27.5	74.1	1891.1	24	73.25	28.25	55.8	1001.6
3	73.5	27.5	75.8	1987.8	25	73.5	28.25	59.6	1159.4
4	72.25	27.75	49.3	758.1	26	73.75	28.25	49.6	768.4
5	72.5	27.75	50.3	792.5	27	74	28.25	70.9	1713.8
6	72.75	27.75	55.7	995.9	28	72.25	28.5	39.8	469.9
7	73	27.75	59.4	1152.7	29	72.5	28.5	39.2	453.6
8	73.25	27.75	71.5	1747.5	30	72.75	28.5	39.4	457.8
9	73.5	27.75	69.4	1633.4	31	73	28.5	41.9	526.9
10	73.75	27.75	71.5	1745.6	32	73.25	28.5	54.6	953.3
11	72	28	47.7	705.3	33	73.5	28.5	59.8	1170.2

12	72.25	28	47.7	704.1	34	73.75	28.5	60.8	1214.5
13	72.5	28	47.6	702.1	35	74	28.5	66.7	1496.7
14	72.75	28	50.5	800.6	36	72.5	28.75	38.4	433.3
15	73	28	54.0	928.8	37	72.75	28.75	38.6	439.1
16	73.25	28	51.7	844.0	38	73.25	28.75	47.6	701.7
17	73.5	28	57.3	1064.9	39	73.5	28.75	56.3	1023.9
18	73.75	28	57.1	1056.6	40	73.75	28.75	56.9	1044.6
19	74	28	56.9	1047.0	41	74	28.75	63.3	1328.5
20	72.25	28.25	43.8	581.2	42	73.5	29	41.0	503.0
21	72.5	28.25	41.8	524.3	43	73.75	29	42.8	552.8
22	72.75	28.25	45.8	642.3					

The assessed R-factor values range from 877.4 to 1136.8 MJ.mm.ha^{-1}.hr^{-1}.yr^{-1}. The lowest R-factor was observed in the Foolnath catchment, whereas, highest R-factor was observed in the Swarupdesar catchment **(Fig)**. The distribution of R-factor values varied and reliable with annual rainfall across the study area. These findings indicate varying levels of rainfall erosivity over different catchments, which reflects the potential for soil erosion. Foolnath and Sonsolav have relatively stable and moderate R-Factor values, suggesting consistent rainfall with lower erosive potential. In contrast, Kodamdesar, Darbari, and Gajner show higher maximum and average values, indicating more intense rainfall events that could increase erosion risks. Kolayat and Swarupdesar have the highest R-Factor values, suggesting the most intense and erosive rainfall conditions, likely requiring targeted soil and water management strategies to mitigate erosion.

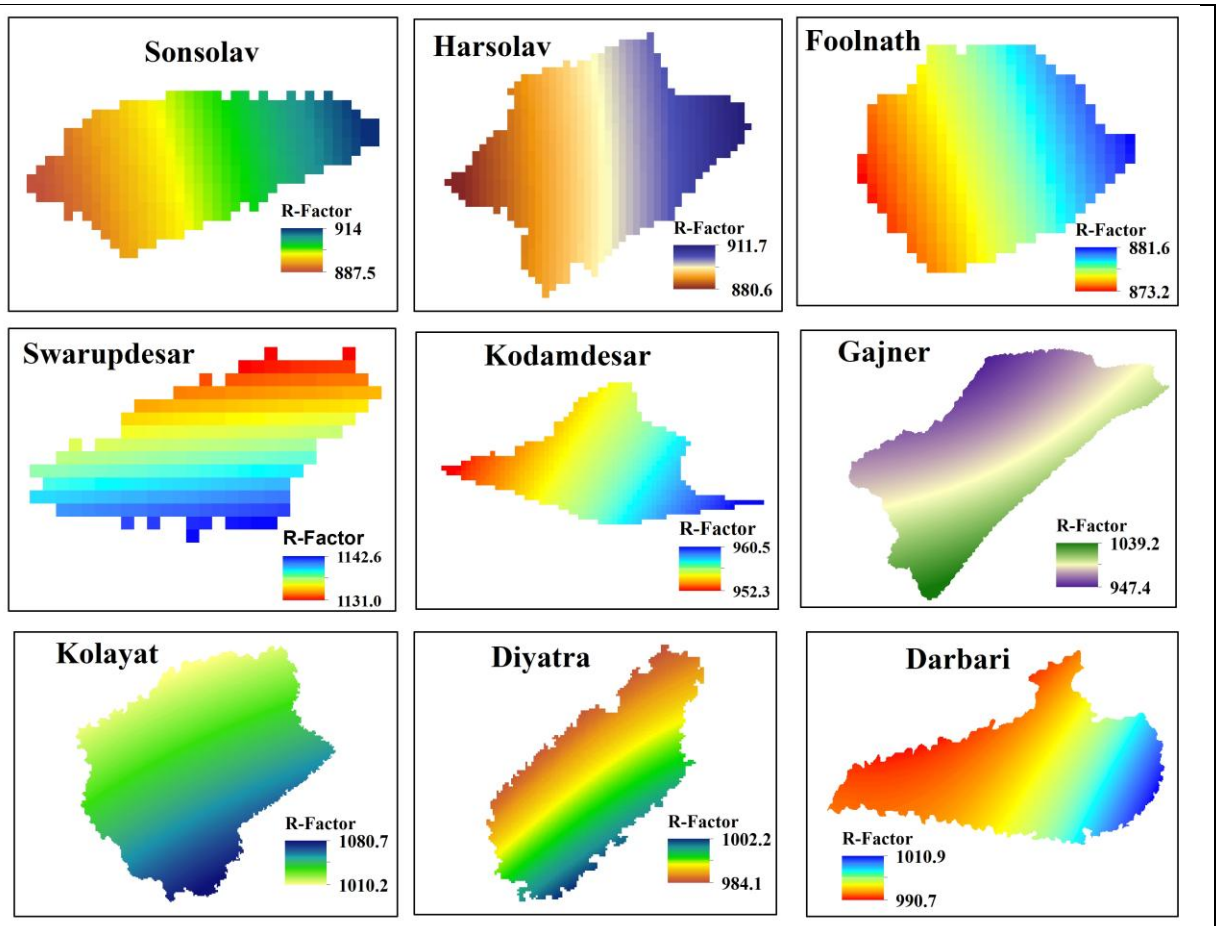

Figure 63:Spatial distribution of R-Factor values over different catchments

Soil Erodibilty Factor (K)

Soil erodibilty signifies the susceptibility or vulnerability of the soil erosion, it is the most significant fundamental property reliant on soil type. Different soil type is a function of grain size, structural integrity, organic content, drainage potential and cohesiveness (Young et al., 1987). A soil map of the study area is prepared with the downloaded data of The Digital Soil Map of the World (DSMW) from the FAO site (www.fao.org). From **Fig.** it is cleared that the soil map of the study area consists of 2 different soil type classes i.e. loam and sandy loam. Majority of the catchments consist of loamy type soil except Kodamdesar, Diyatra, and Gajner. Kodamdesar catchment wholly consist of sandy loam type soil whereas, Diyatra and Gajner contains both loam and sandy loam soil. The soil map of different catchments is presented in **Fig**. In this study, the soil type according to percentage of sand, silt and clay, organic carbon (OC) has been identified by using the SWAT soil database. The soil texture with Proportion of sand, silt, clay, and OC in the study area are given in **Table**.

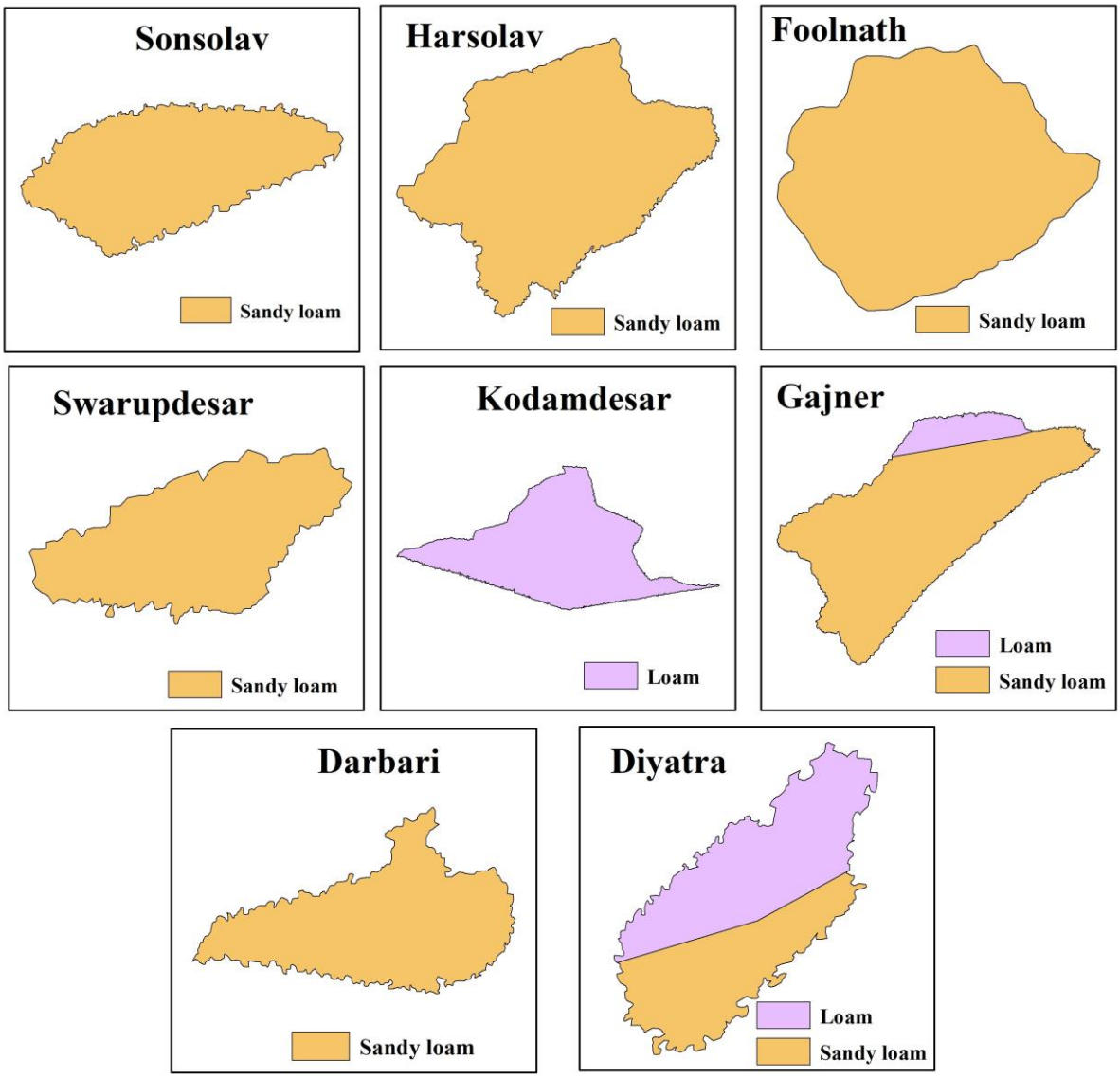

Figure 64:Soil map of the study area

Table 38 Proportion of sand, silt, clay, and OC

S. No.	Soil unit	Sand (%)	Silt (%)	Clay (%)	OC (%)
1.	Loamy sand	9	12	79	0.39
2.	Loam	27	39	34	0.35

Using the methodology described earlier, the K-factor (t ha h ha-1MJ-1mm-1) was estimated using equations. Here, **Table** is showing the different soil that are found in different catchments, the area under particular soil type and the K-factor value.

Table 39 K-Factor over different catchments

S. No.	Catchment	Soil type	Area (Ha)	Area(%)	K-Factor

1.	Sonsolav	Loam	40.0015	100%	0.3212
2.	Harsolav	Loam	82.1988	100%	0.3212
3.	Foolnath	Loam	10.7154	100%	0.3212
4.	Kodamdesar	Sandy loam	80.9733	100%	0.3339
5.	Darbari	Loam Sandy loam	358 279	56.20 43.80	0.3339 0.3212
6.	Gajner	Loam Sandy loam	470.19 4375.15	9.70 90.30	0.3339 0.3212
7.	Kolayat	Loam	2561.83426	100%	0.3212
8.	Diyatra	Loam	1206.9215	100%	0.3212
9.	Swarupdesar	Loam	21.5842	100%	0.3212

The observed data from the Table indicates, Sonsolav, Harsolav, Foolnath, Kolayat, Diyatra, and Swarupdesar catchment areas are entirely composed of loam soil. Loam soil type is known for its fertility and good drainage, which generally supports moderate erosion resistance. Each of these areas shows a K-Factor of 0.3212, indicating similar erodibility and resistance to erosion across these locations. The sizes of these catchments vary, with Kolayat being the largest at 2,561.83 Has and Foolnath the smallest at 10.72 Has. Kodamdesar catchment entirely composed of sandy loam soil, covering 80.97 Has. Sandy loam typically has larger particles, which may lead to a higher tendency for erosion when compared to regular loam. The K-Factor here is 0.3339, slightly higher than in other areas, suggesting a greater susceptibility to erosion. Darbari and Gajner catchments have mixed soil types, leading to varied erosion potentials within the same catchment. In Darbari, 56.2% of the area consists of loam soil with a K-Factor of 0.3339, while the remaining 43.8% consists of sandy loam with a K-Factor of 0.3212. This diversity in soil type affects how water interacts with the landscape, influencing both the fertility and erodibility of the land. Gajner has a majority of sandy loam soil, making up 90.3% of its area (4375.15 Has) with a K-Factor of 0.3212, while the remaining 9.7% is loam, with a K-Factor of 0.3339. The presence of predominantly sandy loam increases the potential for soil movement and water absorption in the catchment area.

Topographic Factor (LS)

Length of slope factor (L) and gradient of slope factor (S) in combination is called topographic factor (LS), both of the factors are determined by using Digital Elevation Model (DEM). The study area DEM raster was used for calculation of LS-factor for the USLE model using

Equation (Wischmeier and Smith, 1962). The DEM (digital elevation model) of the catchments were clipped out from the downloaded Shuttle Radar Terrain Mapper (SRTM) data and after filling the sinks in the study area has been presented in **Fig**.

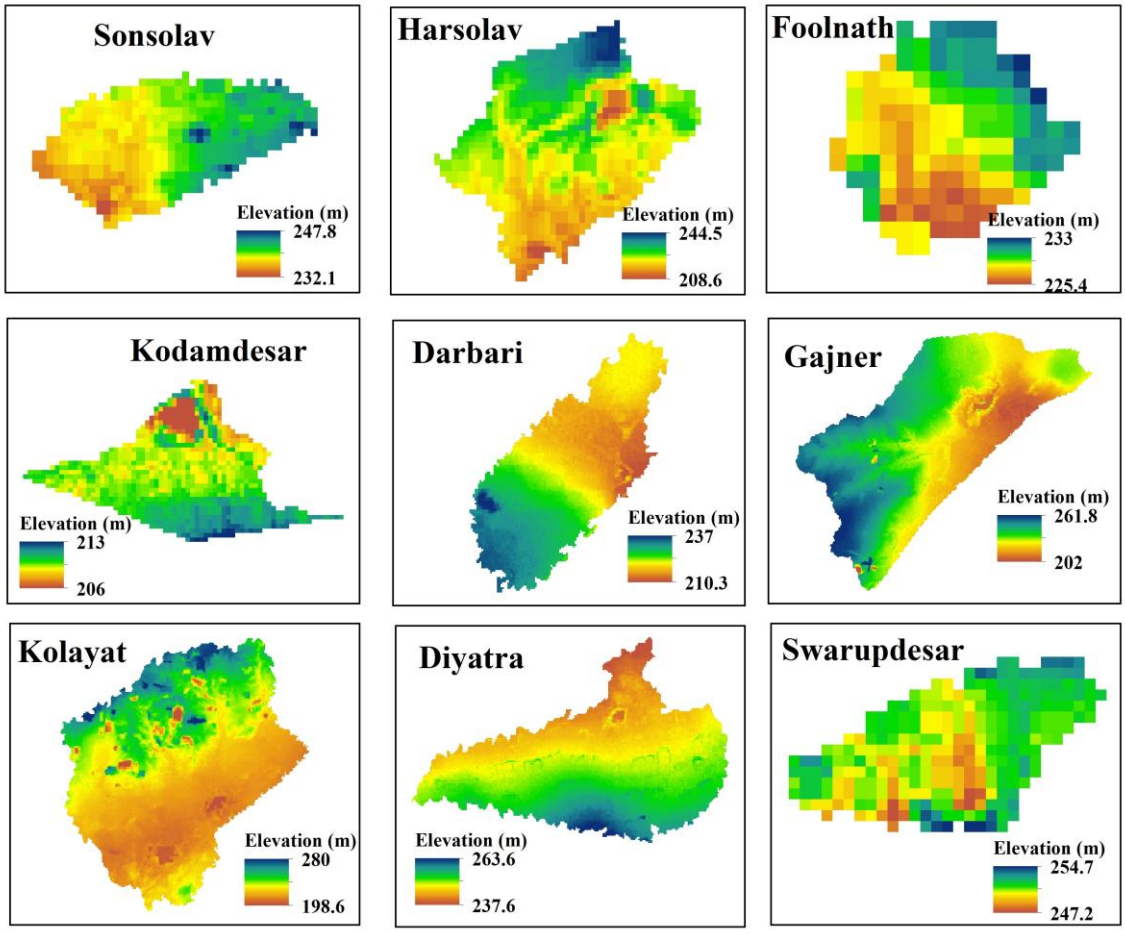

Figure 65:Digital elevation model (DEM) of study area

The analysis of slope percentages and LS factors across various catchments provides a deeper understanding of potential soil erosion risks and the need for effective land management strategies. The **LS factor**, which combines slope length and steepness, serves as a critical indicator of erosion potential, as steeper and longer slopes typically contribute to increased soil loss. The slope map was prepared by inserting filled digital DEM data as input. The topographic LS- factor was computed using ArcGIS 10.2 software by multiplying L-factor and S-factor maps in Geographical Information System (GIS) environment. Analysis revealed that Sonsolav and Darbari have moderate LS factors, 0 to 0.60 and 0 to 0.52 respectively, with slopes of up to 12.5% and 11.4%, indicating some erosion risk, especially in steeper sections. Harsolav and Foolnath show higher LS factors, up to 0.97 and 0.90, with slopes reaching 24% and 18.5%, reflecting significant erosion potential that requires targeted soil conservation practices. Kodamdesar and Swarupdesar have gentle slopes of up to 7.1% and 6.1%, with low LS factors

of 0 to 0.38 and 0 to 0.28, indicating minimal erosion risk and suitability for agriculture. Gajner and Kolayat present the highest erosion potentials, with steep slopes up to 40.4% and 60.6%, and high LS factors of 0 to 1.88 and 0 to 2.75. These catchments require comprehensive erosion control strategies to prevent soil degradation. Diyatra has a moderate slope of up to 11% and an LS factor of 0 to 0.50, suggesting some erosion risk that requires attention in steeper sections. The slope map and LS-Factor map of the catchments are presented in **Fig. and Fig**.

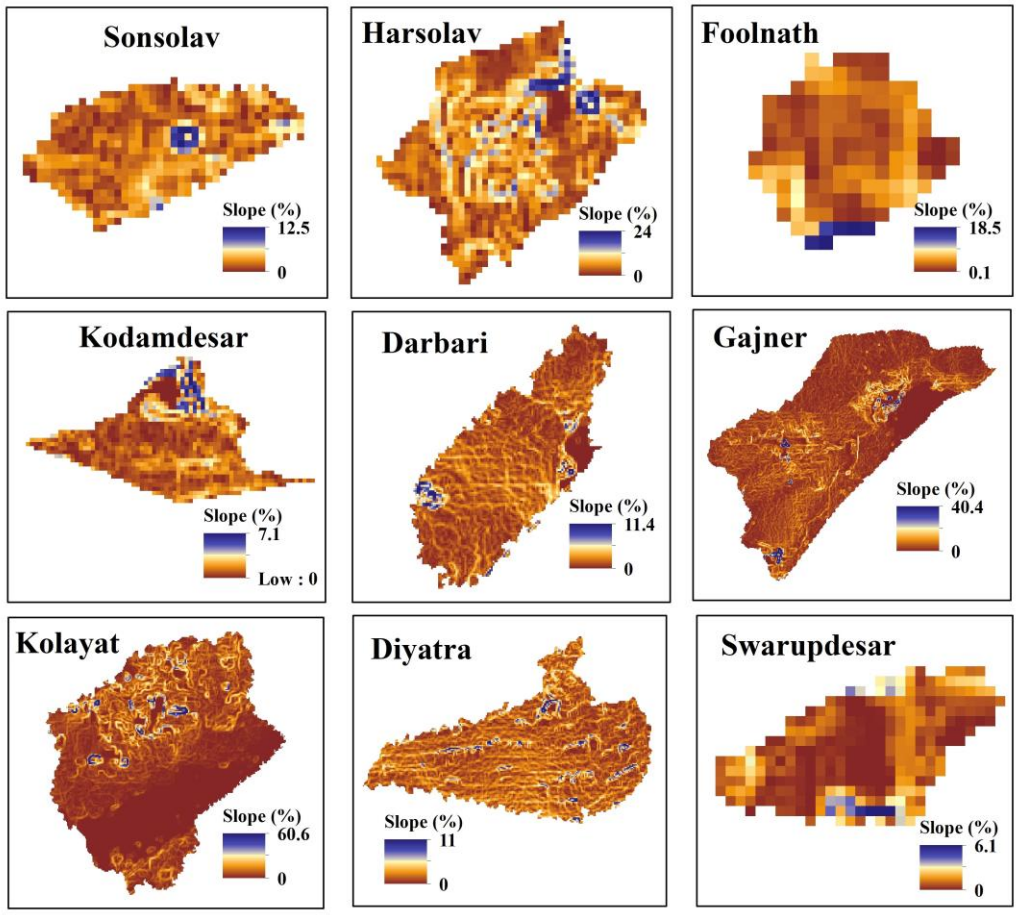

Figure 66:Slope map of the study area

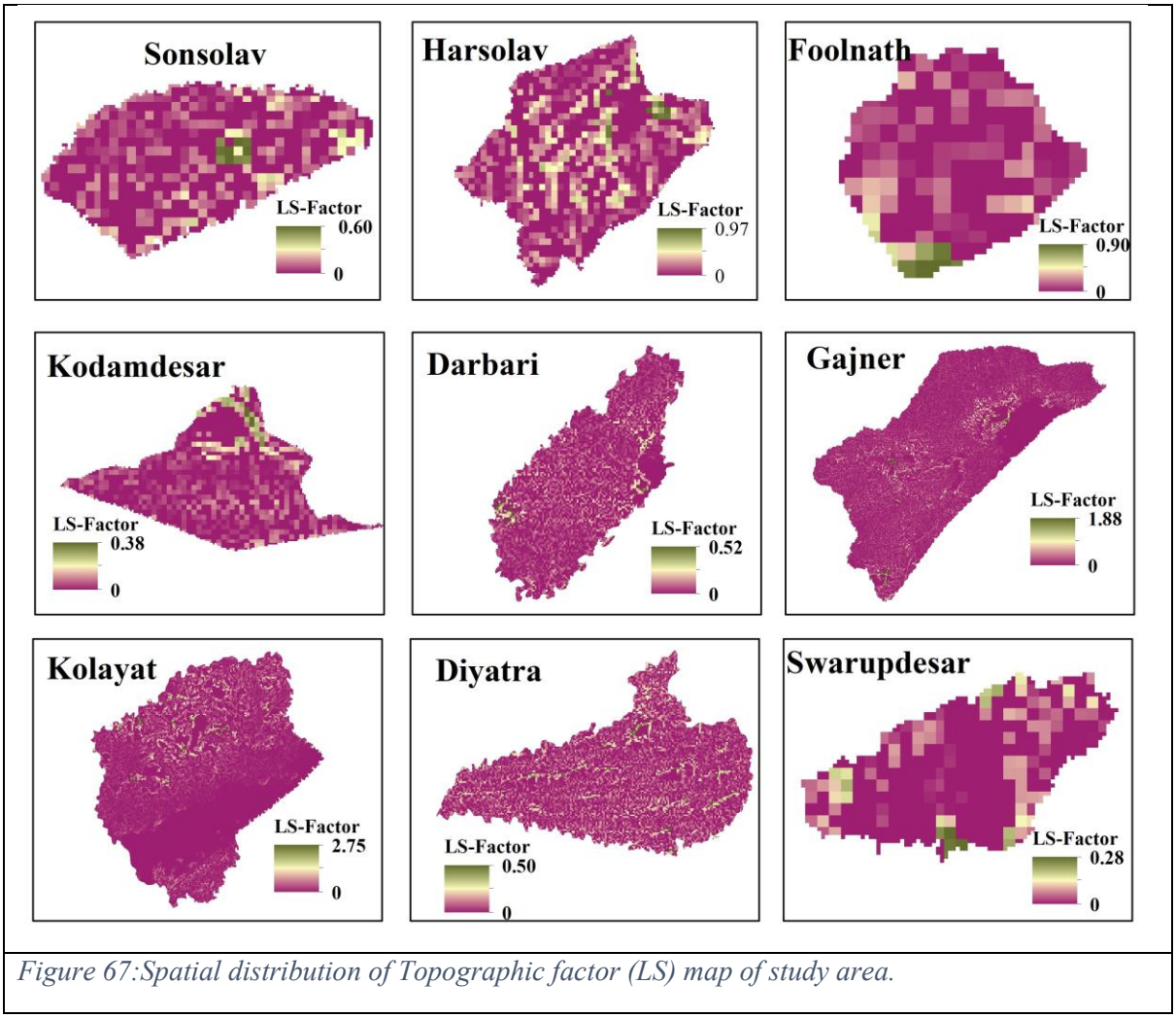

Figure 67:Spatial distribution of Topographic factor (LS) map of study area.

Crop management factor (C)

The C-factor is called as the crop management factor. It depends on land use/cover information of the study area. It is the expected ratio of soil loss from a cropped land under specific condition to soil loss from clean tilled fallow on identical soil and slope under the same rainfall conditions. The type of the land cover, the manner in which it is managed and the changes that have taken place over time form the basic premise for evaluating sediment yield from a watershed., redirects the effects of cropping and management performs on erosion rates as the loss of soil declines with an increase in the plants/vegetation cover (Lu et al., 2004). The C-factor measures the combined outcome of all interrelated cover and management factors that are most readily altered by human activities. In the present study, high resolution (5 meter) satellite images IRS-R2A LISS-IV FMX are employed for LULC map preparation for the year 2020. It functioned as a guiding tool in the allocation of (C) and (P) factors for different land use categories. The C-factor values were the typical values for allocating the land cover and management variables corresponding to each vegetation/crop condition for the USLE model. The C factor values were the representative values for allocating the USLE land cover and

management factors corresponding to each crop/vegetation condition. The study area has been classified into five land use classes namely; water, built up, trees, agriculture, and barren land. Finally, crop management factor was assigned for different land use patterns using **Table.** The magnitude and the spatial distribution of crop management factor are given in **Fig.** Crop management factor was found to be in the range of 0.01 to 1.

Table 40 Crop management factor for different land use/land cover classes

S. No.	Land Use Type	C-Factor
1.	Waterbodies	0.01
2.	Built up	0.03
3.	Trees	0.05
4.	Agriculture	0.128
5.	Barren land	1

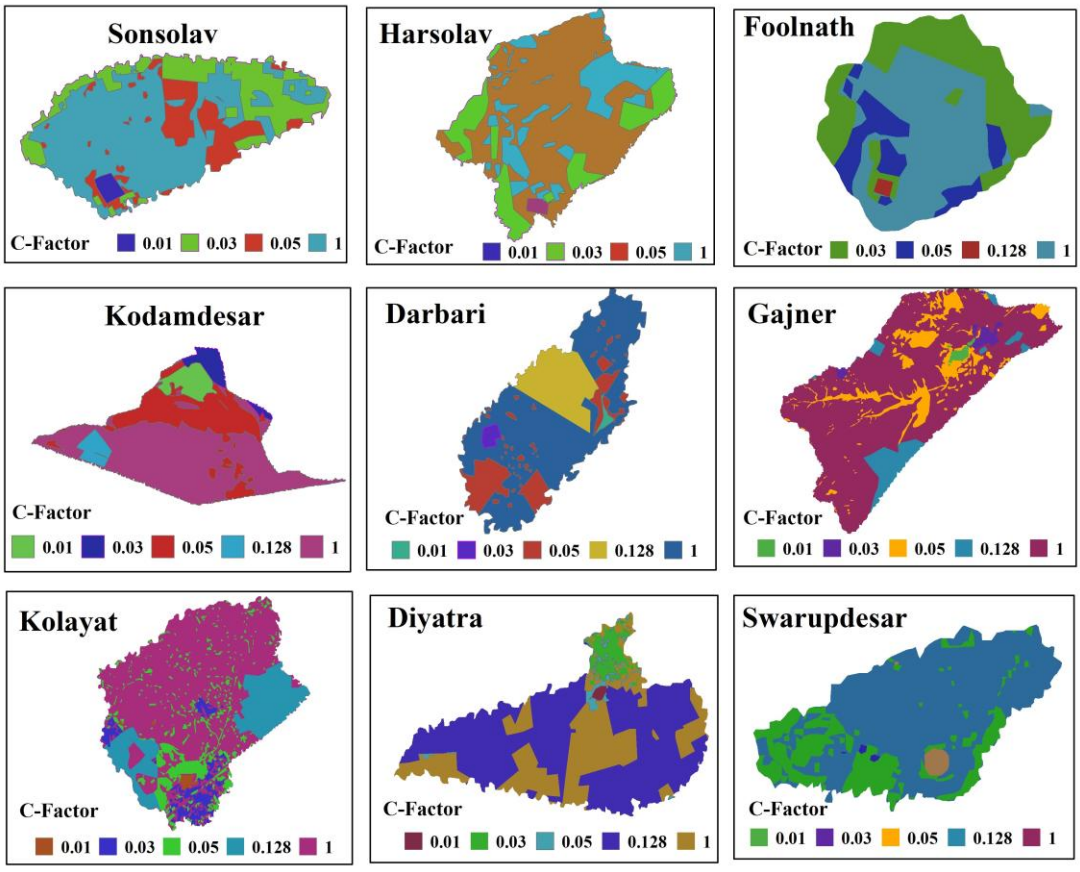

Figure 68:Spatial distribution of crop management factor

Based on the land use statistics of different catchments, the C-factor for each area can provide valuable insights into their potential soil erosion risks. Gajner, with the most extensive barren land covering 3,473.67 Has and significant tree cover of 1,054.04 Has, exhibits a high C-factor

due to the vast barren areas, indicating a greater susceptibility to soil erosion. However, the substantial tree cover helps mitigate this risk by providing natural protection against erosion. Foolnath, on the other hand, has minimal barren land at 5.39 Has, suggesting a lower C-factor in terms of exposed land but also limited vegetative protection against erosion. Diyatra, predominantly agricultural with 506.35 Has, presents a moderate C-factor, as agricultural practices can contribute to erosion if not managed sustainably. Conversely, Sonsolav, Harsolav, Foolnath, and Swarupdesar, with no agricultural land, might exhibit lower C-factors concerning this specific land use. Darbari has the largest built-up areas at 188 Has, reflecting a low C-factor as impervious surfaces protect against soil erosion, while Swarupdesar, with only 0.07 Has of built-up areas, might be more prone to erosion if not properly managed. The presence of water bodies is generally minimal across all catchments, with Gajner having 32.85 Has, which contributes to a low C-factor due to the lack of soil exposure. Overall, Gajner stands out with a high C-factor due to its extensive barren land, indicating a high potential for erosion. Diyatra has a moderate C-factor because of its predominant agricultural use, while Darbari exhibits a lower C-factor due to significant urbanization.

Conservation practice factor (P)

The conservation /support practice factor (P) is fundamentally the ratio between soil loss with a particular support practice and the corresponding soil loss with upslope and down slope tillage. These support practices dominantly affect soil erosion by improving the flow pattern, slope, or surface runoff direction and reducing the amount of runoff rate. In the present study P-values are assigned to the particular class of land use/land cover which is done as in the case of the C-factor for the USLE model. Finally P-Factor values suggested by soil and water conservation society (2013) were allocated to different land use categories. The P-Factor for different land use/land cover classes are shown in **Table**. The spatial distribution of conservation /support practice factor (P) in the study area is given in **Fig**. Conservation practice factor (P) was found in the range of 0.92 to 1.

Table 41 Conservation practice factor for different land use/land cover classes

S. No.	Land Use Type	P-Factor
1.	Waterbodies	0.92
2.	Built up	1
3.	Trees	1
4.	Agriculture	1
5.	Barren land	1

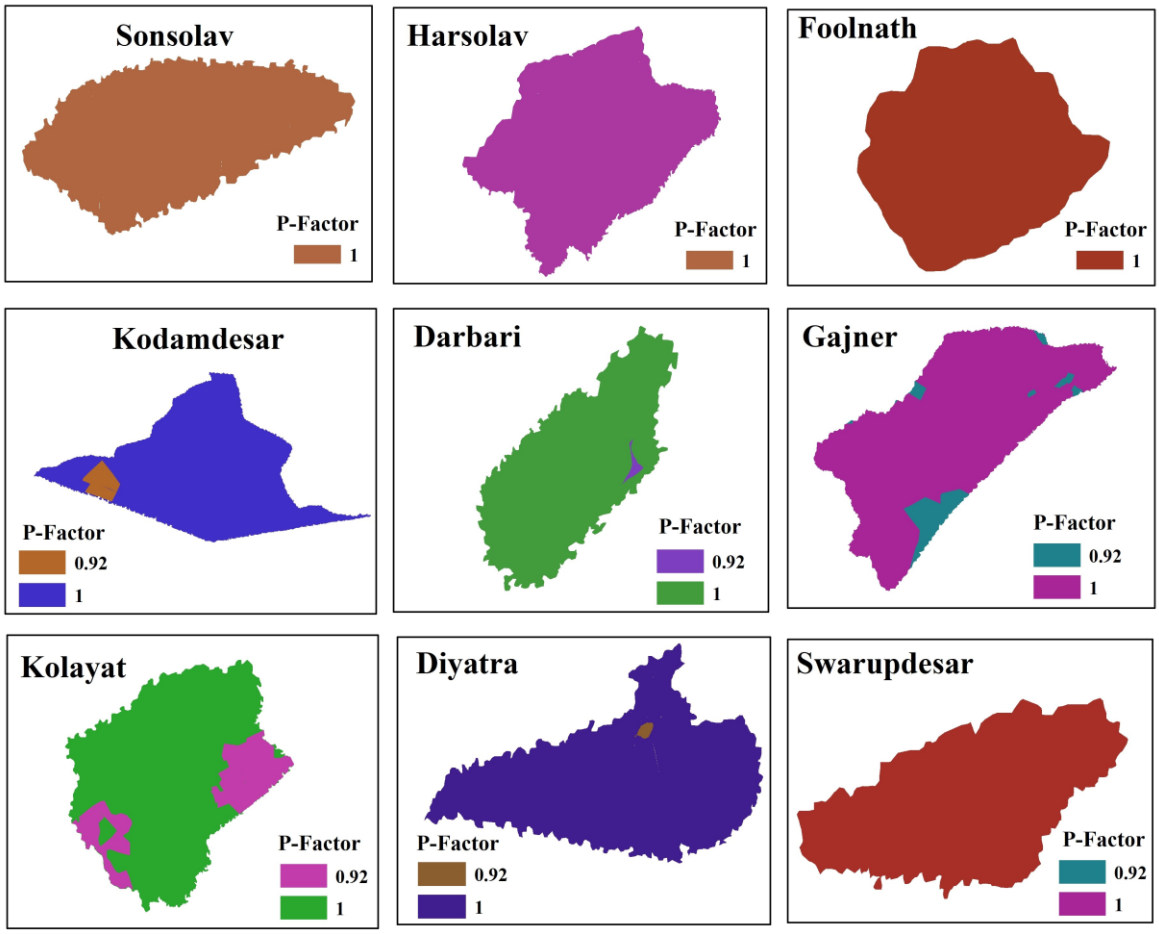

Figure 69:Spatial distribution of Conservation practice factor

Based on the land use statistics across different catchments, the P-factor, or conservation practice factor, revealed the effectiveness of erosion management strategies in each area. Gajner, with its extensive barren land totaling 3,473.67 Has, has a high P-factor of 1, signifying a lack of conservation practices and a high vulnerability to erosion. Diyatra, characterized by 506.35 Has of agricultural land, has a slightly lower P-factor of 0.92, suggesting the presence of some erosion control practices, such as contour farming or strip cropping, though there is still potential for improvement. Darbari, with its extensive built-up areas of 188 Has, also has a P-factor of 1, reflecting that urban environments with impervious surfaces generally do not implement traditional soil conservation practices. Foolnath, with minimal barren land (5.39 Has) and tree cover (2.67 Has), has limited opportunities for conservation practices, underscoring the need for careful land management to mitigate erosion.

Assessment of annual rate of soil erosion

The USLE (Wischmeier and Smith, 1965) was combined with the ArcGIS 10.2 to compute the average annual soil loss rate (A) occurring within the different catchments of Bikaner district.

Raster layers of rainfall erosivity factor (R), soil erodibility factor (K), topographic factor (LS), crop management factor (C) and conservation practice factor (P) were generated, stored and analyzed within the ArcGIS 10.2 software. The average annual soil erosion potential (A) is computed by multiplying the developed raster data from each USLE analysis (A= R K L S C P). Using USLE, the annual rate of soil erosion was estimated for the years 2001 to 2020

Average annual soil loss was estimated on the grid/cell basis and all the grids/cells of catchments were classified based on severity measure of soil erosion as shown in **Table**. These erosion groups are as per the guidelines recommended by Singh et al., (1992) for Indian conditions. The consequences show that majority of the catchments fall under slight risk of erosion and the highest soil erosion values are spatially interrelated with the steep slopes.

Table 42 Priority scales for soil erosion

S. No.	Soil loss (t/Ha/year)	Soil erosion class
1.	<5	Slight
2.	5-10	Moderate
3.	10-20	High
4.	20-40	Very high
5.	40-80	Severe
6.	>80	Very severe

Soil loss from Sonsolav catchment

The soil loss data from the Sonsolv catchment shows a minimum of 0 ton/Ha/year, a maximum of 36.8 ton/Ha/year, and an average of 2.8 ton/Ha/year, indicating varying degrees of soil erosion across the catchment. The erosion class statistics further elaborate on the spatial distribution of this soil loss **(Table)**. The "Slight" erosion class, covering 31.75 Ha, represents 79.41% of the catchment area. This suggests that the majority of the land experiences minimal erosion, likely due to favourable conditions such as dense vegetation, effective land management, or stable topography that mitigates soil erosion. The "Moderate" erosion class accounts for 6.7 Ha or 16.75% of the area, which indicates some level of concern, it is manageable with appropriate erosion control measures such as improved land management practices and vegetation maintenance. The presence of 1.17 Ha in the "High" erosion class, which constitutes 2.92% of the area, highlights sections of the catchment experiencing more severe erosion. This level of soil loss could result from factors such as steeper slopes or reduced vegetation cover, necessitating targeted interventions to prevent further degradation and loss

of soil fertility. The "Very High" erosion class, covering 0.36 Ha or 0.9%, represents the areas most at risk within the catchment. These zones require immediate and robust conservation measures to control erosion and stabilize the land, ensuring sustainable land use and productivity.

The catchment has no area falling into the "Severe" or "Very Severe" erosion classes, suggesting that erosion has not reached the most critical levels. This absence is a positive indicator, reflecting effective erosion control practices or natural protective factors already in place. However, the presence of "High" and "Very High" classes still warrants attention, as they can escalate if not managed properly. Overall, while the Sonsolav catchment experiences a range of erosion levels, the substantial area classified as "Slight" erosion reflects a generally stable landscape. However, continued monitoring and implementation of soil conservation strategies are essential to maintain and improve the current soil health status, especially in areas identified as vulnerable to higher erosion rates.

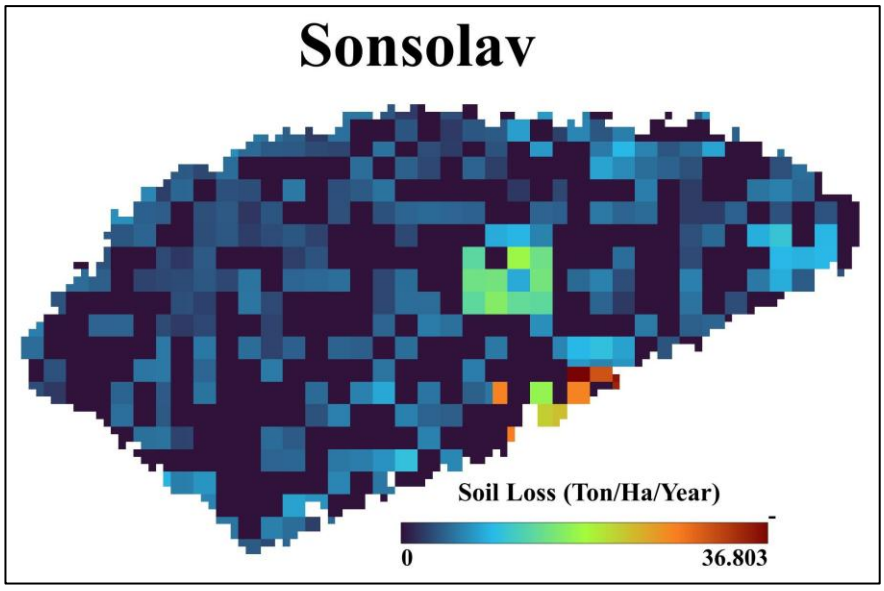

Figure 70:Spatial distribution of soil loss from Sonsolav catchment

Soil loss from Harsolav catchment

The soil loss data from the Harsolav catchment revealed significant variations in erosion, with a minimum of 0 ton/Ha/year, a maximum of 144.2 ton/Ha/year, and an average of 10.4 ton/Ha/year. This wide range indicates substantial differences in erosion rates across different parts of the catchment. The erosion class statistics provide further insights into the spatial distribution of this soil loss. The "Slight" erosion class encompasses 46.77 Ha, accounting for 56.82% of the catchment area. This suggests that more than half of the region experiences minimal erosion, likely due to factors such as effective ground cover, stable soil structures, or

gentle slopes that reduce soil displacement. In contrast, the "Moderate" erosion class covers 13.38 Ha, representing 16.26% of the area. This indicates a noticeable level of soil erosion in certain sections of the catchment, which may require some attention to prevent further degradation. The "High" erosion class, with 10.21 Ha or 12.40% of the area, highlights parts of the catchment that are experiencing more significant erosion. This level of erosion could be due to less vegetation cover, which accelerates soil loss. The "Very High" erosion class accounts for 6.01 Ha or 7.30% of the area. This category signifies areas where erosion is becoming increasingly problematic, potentially impacting soil fertility and land productivity. The "Severe" erosion class, covering 4.31 Ha or 5.24% of the area, and the "Very Severe" class, with 1.63 Ha or 1.98%, indicate regions within the catchment that are most at risk. These areas are experiencing critical levels of soil loss, which could lead to significant environmental and agricultural impacts if not addressed.

Overall, the Harsolav catchment exhibits a range of erosion levels, with a notable portion of the area falling into higher risk categories. While a majority of the land is classified under "Slight" erosion, indicating relative stability, there is a considerable amount of land under "High," "Very High," "Severe," and "Very Severe" classes. These findings highlight the need for continued monitoring and potential intervention to manage erosion effectively, ensuring sustainable land use and soil conservation in the catchment.

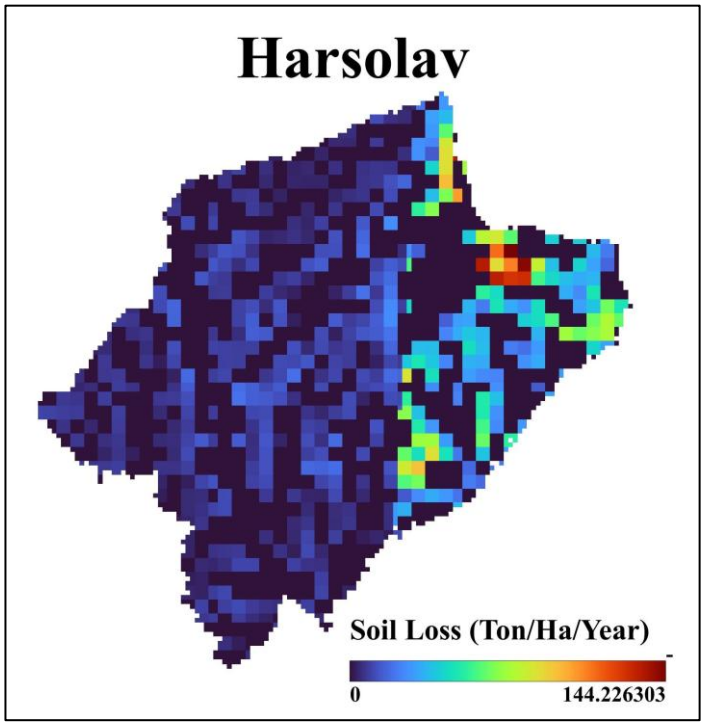

Figure 71:Spatial distribution of soil loss from Harsolav catchment

Soil loss from Foolnath catchment

The soil loss data from the Foolnath catchment shows a minimum of 0 ton/Ga/year, a maximum of 131.3 ton/Ga/year, and an average of 11.3 ton/Ha/year, indicating substantial variation in erosion rates across the area. The majority of the catchment is classified under the "Slight" erosion class, covering 6.7 Ha and accounting for 62.91% of the total area. This suggests that a significant portion of the catchment experiences minimal erosion, which may be due to favourable conditions such as effective vegetation cover or stable terrain that helps prevent soil displacement. In contrast, the "Moderate" erosion class includes 1.04 Ha, representing 9.77% of the area, indicating areas where soil erosion is more pronounced but not severe. The "High" erosion class covers 0.65 Ha, about 6.10% of the catchment area, pointing to portion where erosion is more significant, potentially due to factors like less vegetation or steeper slopes. The "Very High" erosion class accounts for 1.44 Ha, which is 13.52% of the catchment. This indicates areas where erosion is becoming a serious concern, potentially affecting soil fertility and land use. Additionally, the "Severe" erosion class, covering 0.62 Has or 5.82% of the area, and the "Very Severe" class, encompassing 0.2 Ha or 1.88%, highlight regions experiencing critical level of soil loss. These areas face significant risks to environmental stability and agricultural productivity.

Overall, the Foolnath catchment exhibits a range of erosion levels. While a majority of the area falls under the "Slight" erosion category, the presence of land in "Very High," "Severe," and "Very Severe" classes underscores the importance of ongoing monitoring and management. Addressing these higher-risk areas is crucial to preserving soil health and ensuring sustainable land management in the region.

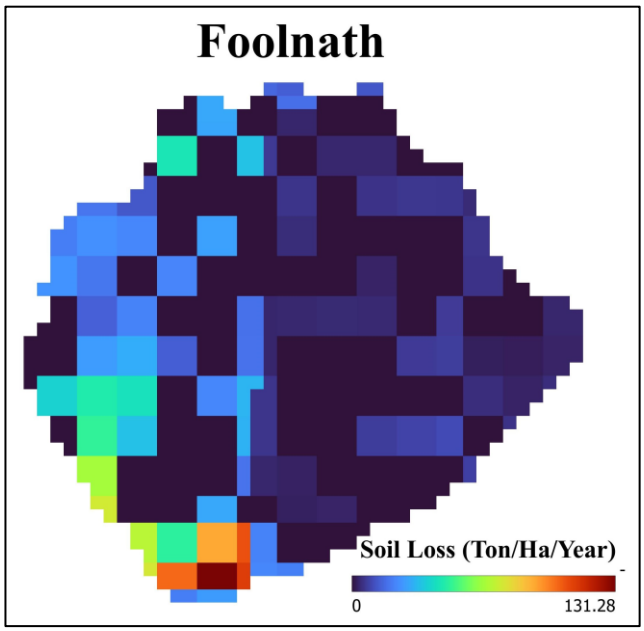

Figure 72:Spatial distribution of soil loss from Foolnath catchment

Soil loss from Kodamdesar catchment

The soil loss data from the Kodamdesar catchment reveals a range of erosion rates, with a minimum of 0 ton/Ha/year, a maximum of 40.9 ton/Ha/year, and an average of 6.9 ton/Ha/year. This data suggests moderate soil erosion across the area. Over half of the catchment, or 54.60% (44.18 Ha), falls under the "Slight" erosion class, indicating that the majority of the land experiences minimal soil loss. The "Moderate" erosion class covers 5.14% (4.16 Ha) of the area, suggesting some noticeable erosion but not at critical levels. However, a significant portion of the catchment, 35.85% (29.01 Ha), is classified under the "High" erosion class, indicating areas where soil erosion is more pronounced and could potentially impact soil health and agricultural productivity. This could be due to steeper slopes or reduced vegetation cover that accelerate soil loss. Additionally, the "Very High" erosion class comprises 4.34% (3.51 Ha), indicating zones where erosion may be becoming a more serious concern. The "Severe" erosion class extends over small area 0.06 Has covers 0.07% of the catchment and highlights areas experiencing significant soil loss, which could lead to environmental degradation if left unaddressed. Notably, there is no area classified as "Very Severe," suggesting that the most extreme erosion levels are currently not present in the catchment.

Overall, the Kodamdesar catchment exhibits a range of erosion levels, from slight to severe. While the majority of the area experiences minimal erosion, the presence of high and very high erosion zones emphasizes the importance of ongoing monitoring and potential management strategies to mitigate soil loss and ensure sustainable land use.

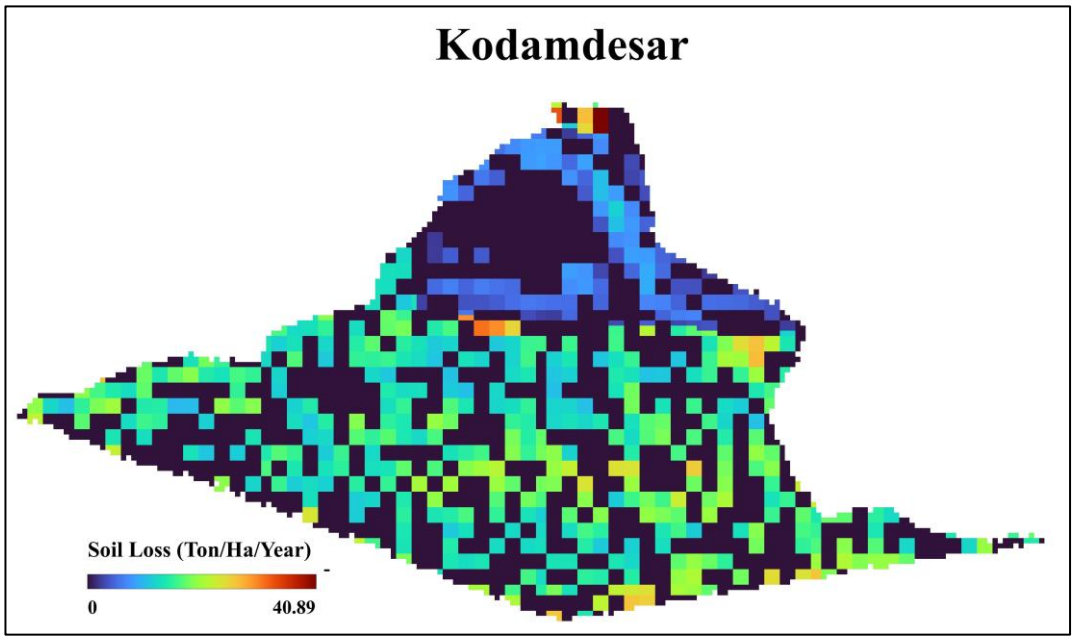

Figure 73:Spatial distribution of soil loss from Kodamdesar catchment

Soil loss from Darbari catchment

The soil loss data from the Darbari catchment indicates a significant range of erosion levels, with a minimum of 0 ton/Ha/year, a maximum of 79.6 ton/Ha/year, and an average of 7.9 ton/Ha/year. This variation highlights the diverse erosion dynamics present across the catchment. The majority of the area, 52.93% (337.14 Ha), falls under the "Slight" erosion class, suggesting that more than half of the land experiences minimal erosion. In contrast, a substantial portion of the catchment, 37.53% (239.07 Ha), is classified under the "High" erosion class, indicating significant soil erosion in these areas. This high rate of erosion could be due to factors such as steep terrain or sparse vegetation, which can increase the susceptibility of soil to erosion processes. The "Moderate" erosion class accounts for 1.55% (9.86 Ha) of the catchment, showing regions with noticeable but manageable soil loss levels. The "Very High" erosion class, covering 7.31% (46.56 Ha), indicates areas where erosion is becoming a severe concern, potentially affecting soil fertility and land usability. Additionally, the "Severe" erosion class, although a small portion of the catchment at 0.68% (4.32 Ha), highlights regions facing critical soil loss, which could lead to significant environmental and agricultural challenges if not addressed. Notably, there are no areas classified as "Very Severe," indicating that the most extreme erosion levels are currently absent from the catchment.

Overall, while the Darbari catchment predominantly experiences slight erosion, the presence of extensive areas under high and very high erosion classes underscores the need for careful monitoring and management. Addressing these areas is crucial to maintain soil health and ensure the sustainability of agricultural activities and natural habitats within the region.

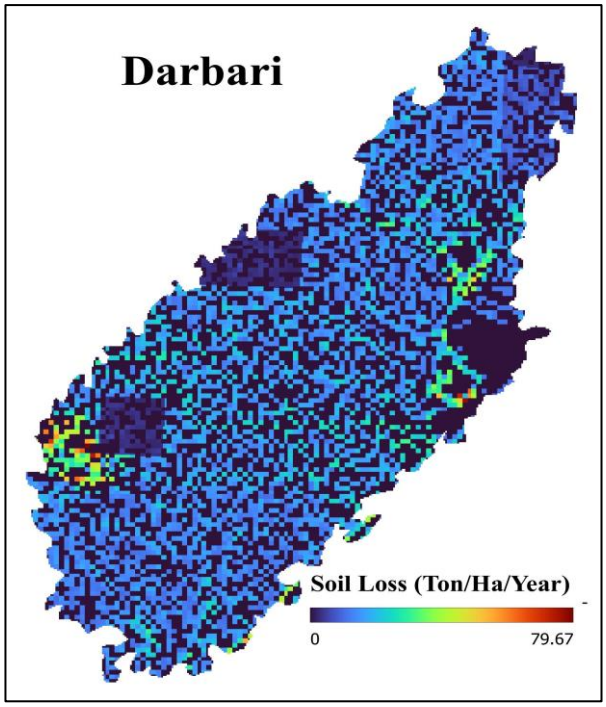

Figure 74:Spatial distribution of soil loss from Darbari catchment

Soil loss from Gajner catchment

The soil loss within the Gajner catchment exhibits considerable variability, with estimates ranging from a minimum of 0 tons/Ha/year to a maximum of 292.1 0 tons/Ha/year, and an average of 8.9 0 tons/Ha/year. This variation underscores the heterogeneous nature of erosion within the catchment area. The distribution of soil erosion across different classes reveales a significant portion of the area experiencing slight erosion. Specifically, 54.02% of the catchment, encompassing 2617.53 Ha, falls into the slight erosion category, which might be due to factors such as vegetation cover, soil type, or land management practices that help protect the soil from extensive erosion. In contrast, a relatively small fraction of the catchment, 0.88%, or 42.41 Ha, is classified as having moderate erosion. More notably, the high erosion class affects 30.85% of the area, which translates to 1494.63 Has. The very high erosion class, covering 12.86% of the area (623.18 Ha), and the severe class, encompassing 1.12% (54.32 Ha), indicate areas with more pronounced erosion issues. The very severe erosion class, though limited in extent, covers 0.28% of the catchment area, equivalent to 13.51 Has, representing areas where soil erosion is critically affecting the landscape. Although severe and very severe classes cover a smaller proportion of the catchment, the intensity of soil loss in these areas is very high, potentially leading to significant environmental and agricultural impacts

Overall, the findings from the Gajner catchment underscore the importance of targeted erosion management strategies. While a substantial portion of the catchment experiences only slight erosion, the presence of high, very high, and severe erosion classes highlights areas that may

require more intensive intervention to prevent further soil degradation and to maintain soil health and productivity.

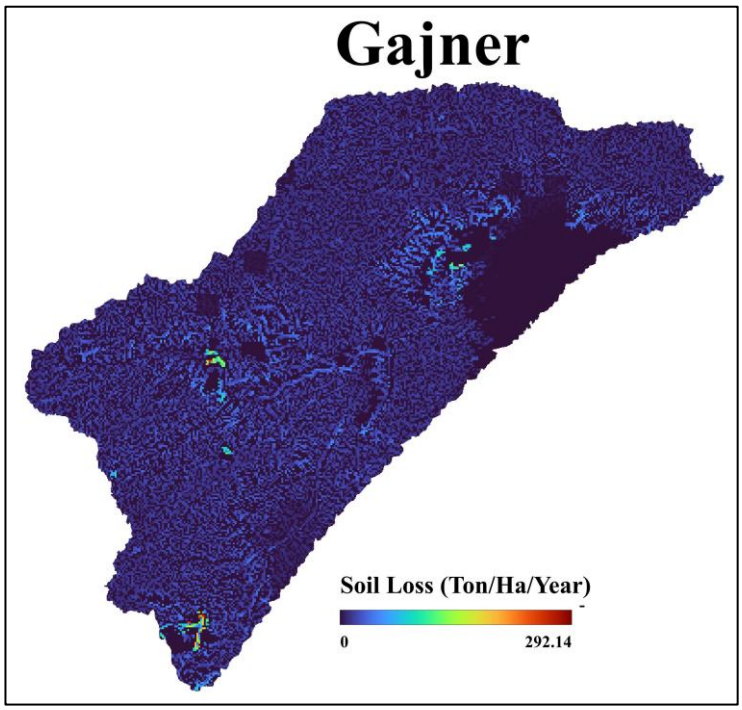

Figure 75:Spatial distribution of soil loss from Gajner catchment

Soil loss from Kolayat catchment

The soil loss data for the Kolayat catchment reveals a wide spectrum of erosion intensities, with estimates ranging from a minimum of 0 tons/Ha/year to a maximum of 428. tons/Ha/year, and an average loss of 11.7 tons/Ha/year. This broad range indicates significant variability in erosion conditions across the catchment, suggesting that some area experiences minimal soil loss while others face extreme erosion challenges. The distribution of soil erosion across different classes highlights a predominance of slight erosion, affecting 65.24% of the catchment area, or 1671.1 Ha. Moderate erosion is less prevalent, impacting only 2.85% of the catchment area (73 Ha). This indicates that moderate erosion is limited and confined to specific areas. In contrast, the high erosion class affects 10.20% of the catchment area (261.2 Ha), reflecting regions where soil loss is more pronounced. The very high erosion class, which covers 13% of the catchment (333.08 Ha), reveals areas with severe soil loss, suggesting more critical erosion issues that could have significant impacts on land productivity and environmental stability. The severe erosion class encompasses 6.68% of the catchment area (171.09 Ha), highlighting regions where soil loss is particularly intense and likely to have

substantial negative effects. Very severe erosion class, though covering a smaller area of 2.03% (51.95 Ha), indicates regions experiencing the most extreme levels of soil erosion, which may result in severe ecological and agricultural consequences.

Overall, the findings underscore the importance of implementing targeted erosion management strategies to address both localized and extensive erosion issues within the Kolayat catchment, aiming to mitigate soil loss and protect land and environmental resources.

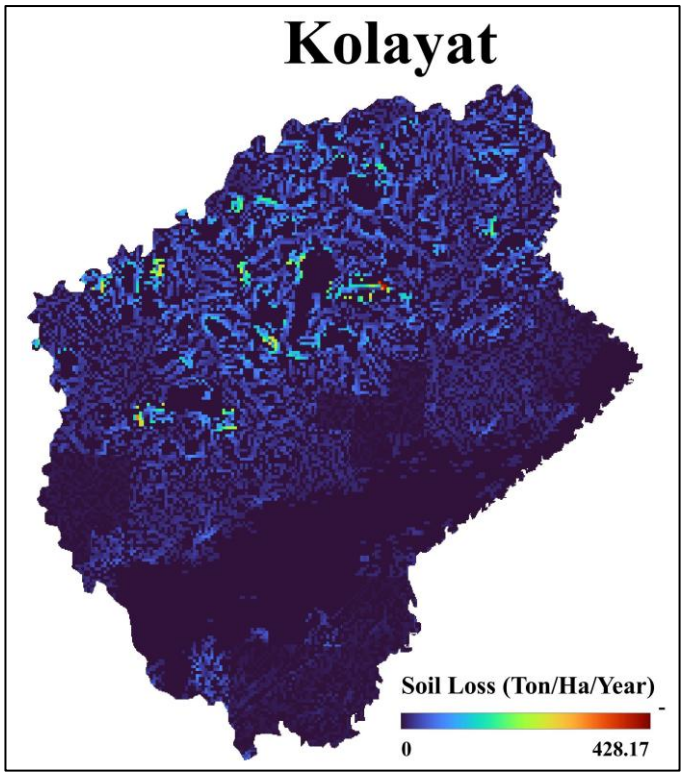

Figure 76:Spatial distribution of soil loss from Kolayat catchment

Soil loss from Diyatra catchment

The soil loss assessment from the Diyatra catchment provides insights into the range and distribution of erosion across the area. The estimates indicate a minimum soil loss of 0 tons/Ha/year, a maximum of 51.9 tons/Ha/year, and an average loss of 6.1 tons/Ha/year. This range reflects the variability in erosion conditions within the catchment, with some areas experiencing minimal erosion and others facing more significant soil loss. The distribution of soil erosion across different classes highlights that the majority of the catchment experiences slight erosion. Specifically, 55.03% of the catchment area falls into the slight erosion category. Moderate erosion affects 13.41% of the catchment area (161.8 Ha), indicating that this level of erosion is more localized and affects a smaller proportion of the total area. High erosion impacts 27.43% of the catchment area (331.05 Ha), revealing a significant portion of the catchment experiencing notable soil loss that could impact land use and environmental conditions. Very

high erosion is less prevalent, covering 4.04% of the catchment area (48.7 Ha), pointing to regions with more severe soil degradation. The severe erosion class, though minimal, covers 0.09% of the catchment area (1.14 Ha), indicating some areas with intense soil loss. Notably, there are no regions classified as experiencing very severe erosion, suggesting that the most extreme levels of soil loss are not present in this catchment.

Overall, the findings indicate that while the Diyatra catchment predominantly experiences slight to moderate erosion, there are areas with higher levels of soil loss that may require attention. The absence of very severe erosion suggests that, while erosion is a concern, it has not reached the most extreme levels seen in other catchments.

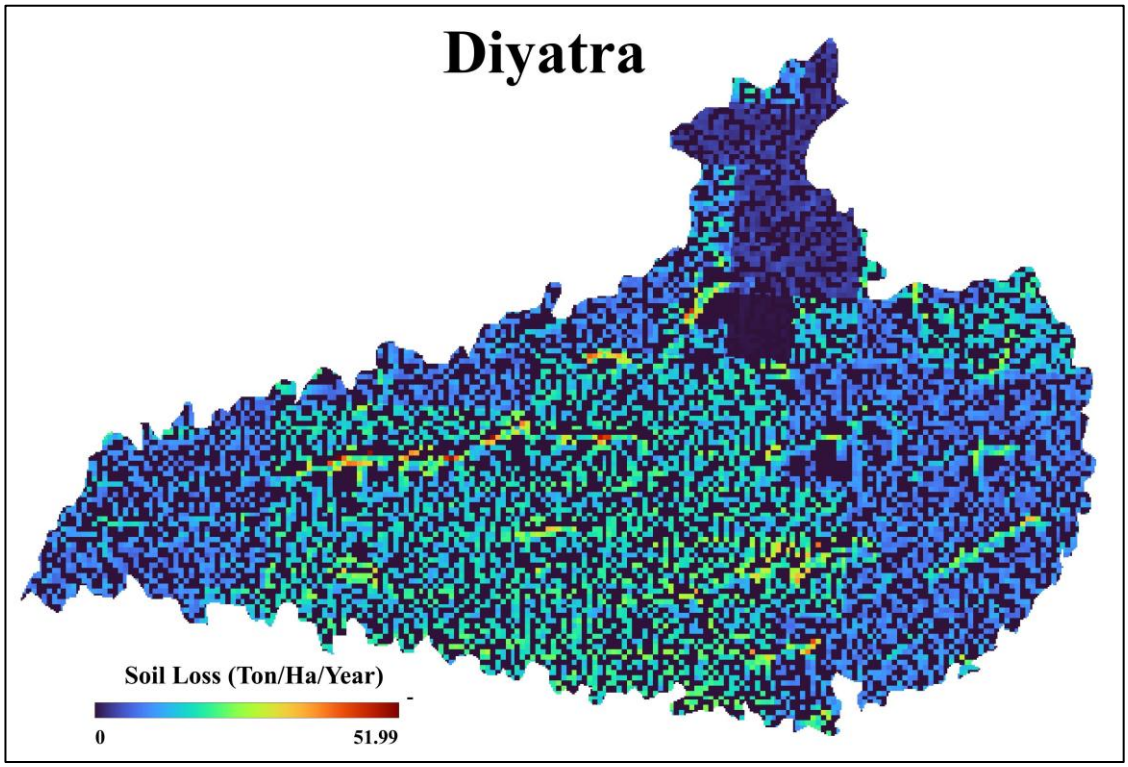

Figure 77:Spatial distribution of soil loss from Diyatra catchment

Soil loss from Swarupdesar catchment

The soil loss data for the Swarupdesar catchment reveals relatively low erosion levels across the area. The estimated soil loss ranges from a minimum of 0 tons/Ha/year to a maximum of 27.9 tons/Ha/year, with an average loss of 2.9 tons/Ha/year. The distribution of erosion classes further highlights the minimal impact of soil loss in the catchment. A substantial 80.73% of the catchment area is classified under slight erosion, suggesting that most of the area experiences minimal soil loss. Moderate erosion affects 7.97% of the catchment area (1.72 Ha), indicating that this level of erosion is present but limited to a small portion of the catchment. High erosion is observed in 10.10% of the catchment area (2.18 Ha), reflecting some regions with more

pronounced soil loss. Very high erosion covers only 1.20% of the catchment area (0.26 Ha), pointing to a small number of areas with severe erosion issues. Notably, there are no areas classified under severe or very severe erosion, indicating that the catchment does not experience the most extreme levels of soil degradation.

Overall, the results suggest that the Swarupdesar catchment is relatively stable with minimal soil loss. The major portion of the catchment is characterized by slight erosion, with only a small proportion affected by higher levels of erosion. This indicates that erosion management practices in the area are effective, and the soil erosion issues present are manageable.

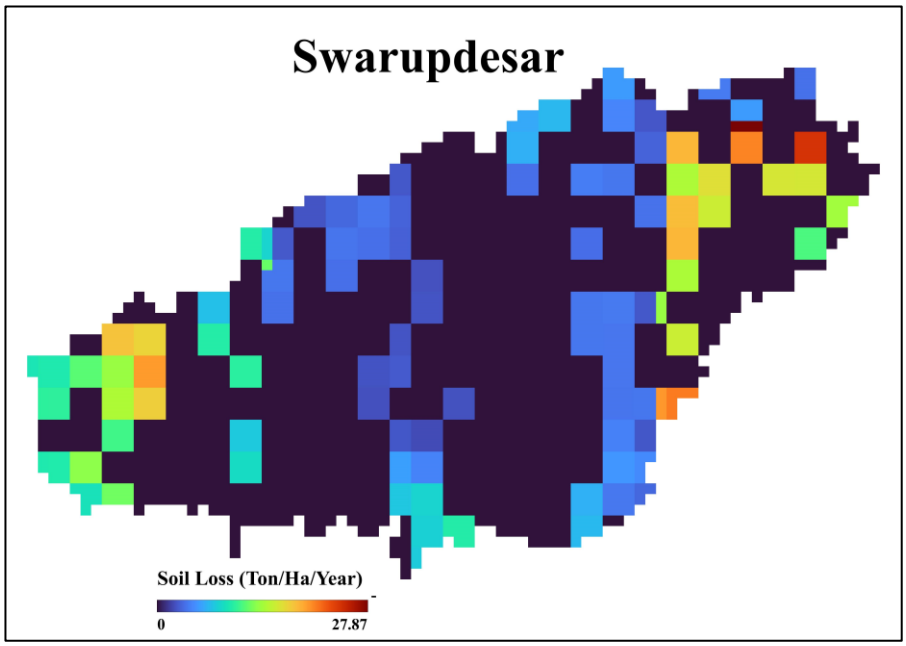

Figure 78:Spatial distribution of soil loss from Diyatra catchment

Conclusion

The results indicate that slight erosion class is widespread across all catchments, but, there is considerable variation in the extent of more severe erosion classes. In catchments such as Sonsolav and Swarupdesar, a high percentage of the area is classified as having slight erosion, indicating relatively stable soil conditions and suggesting effective erosion control measures. These catchments show minimal severe erosion, reflecting a lower risk of significant soil degradation. On the other hand, catchments like Foolnath and Kodamdesar exhibit significant proportions of high and very high erosion, highlighting areas with critical erosion issues that could impact agricultural productivity and environmental sustainability. These areas may require more intensive management strategies to mitigate the effects of erosion. The variation in severe and very severe erosion across catchments further underscores the need for targeted approaches to erosion management. For example, Harsolav, with notable percentages of severe

and very severe erosion, may benefit from specialized interventions focused on these hotspots to prevent further land degradation. Meanwhile, catchments like Darbari and Kolayat show a mix of erosion classes, indicating that while much of the area remains relatively stable, there are portion having significant erosion that need attention. This diverse erosion profile suggests that proper erosion management strategies are necessary, emphasizing the importance of localized assessments and interventions. Overall, the results highlight the critical importance of understanding the specific erosion dynamics within each catchment to implement effective soil conservation practices. Addressing areas with severe and very severe erosion is crucial to maintaining land productivity and ecological balance, while ongoing monitoring and adaptation of erosion control measures are essential to ensure long-term sustainability across the catchments.

Water Quality Assessment

Premonsoon and psot monsoon water sampoles were collected for the various waterbodies namely Sursagar, Sonsolav, Harsolav, Dharnidhar, Foolnath, Kalyansagar, Naal Badi, Kodamdesar, Darbari, Gajner, Kolayat, Diatra, Swarupdesar were collected during the field visits and were analysed in the NIH laboratory at Roorkee. Total 17 water samples from these surface water bodies and 2 groundwater samples were collected for physico-chemical parameters, demand parameters, heavy metals and pesticides. Parameters such as pH, EC, Oxidation-Reduction Potential (ORP), Total Suspended Solids (TSS), DO, BOD, COD, Silica, Major cations, Major anions, Heavy metal, and Alkalinity were analysed.

The analysis of physico-chemical parameters DO, BOD, COD were performed as per standard methods (APHA, 2017). Parameters like pH and EC, and ORP were measured with the help of pH meter, EC meter and ORP meter. Major Cations (Na, K, Ca, Mg), Moreover, major Anions (HCO_3, Cl, SO_4, NO_3), and Minor Ions (F, PO_4) were analysed using Ion Chromatograph.

Water quality assessment showed that almost all physico-chemical parameters in almost all water bodies except Dharnidhar (SW4) were observed within the permissible limit of BIS (2012) for drinking water (IS: 10500). Safe BOD level (>2.0 mg/L) is observed in almost all water bodies. Heavy metal concentrations show Al, Fe, Mn, Pb and B exceeded the prescribed permissible limit of BIS (2012) for drinking water (IS: 10500) in few of the samples. The details of water quality is shown in Figure 6.38

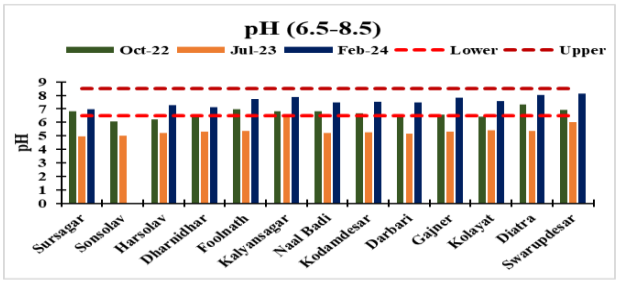
pH (6.5-8.5)
Oct-22
Jul-23
Feb-24
Lower
Upper
pH
Sursagar
Sonsolav
Harsolav
Dharnidhar
Foolnath
Kalyansagar
Naal Badi
Kodamdesar
Darbari
Gajner
Kolayat
Diatra
Swarupdesar

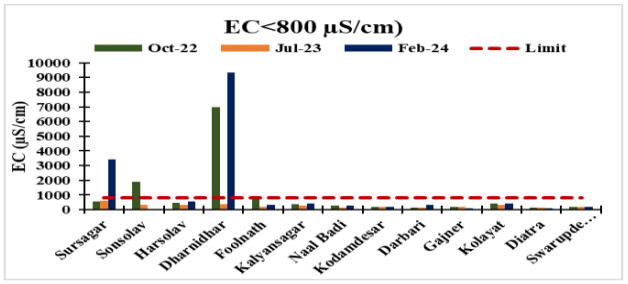
EC<800 µS/cm)
Oct-22
Jul-23
Feb-24
Limit
EC (µS/cm)

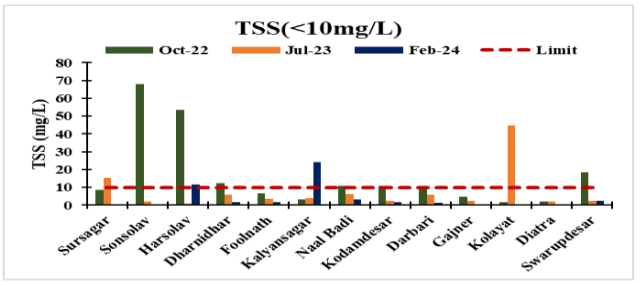
TSS(<10mg/L)
Oct-22
Jul-23
Feb-24
Limit
TSS (mg/L)

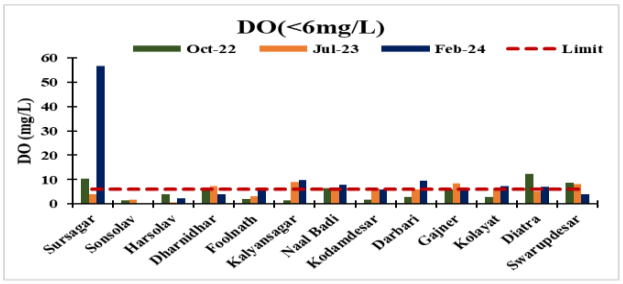
DO(<6mg/L)
Oct-22
Jul-23
Feb-24
Limit
DO (mg/L)

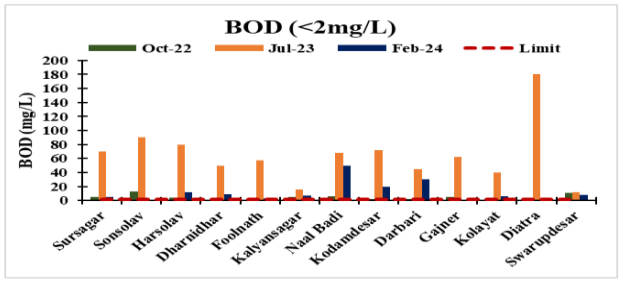
BOD (<2mg/L)
Oct-22
Jul-23
Feb-24
Limit
BOD (mg/L)

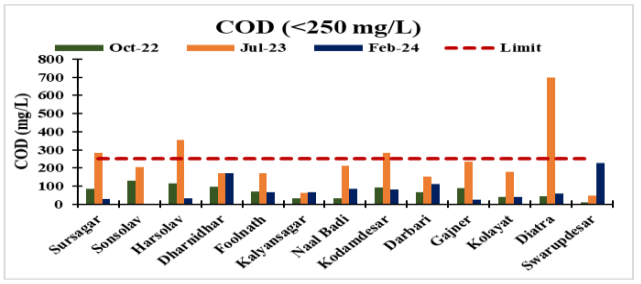
COD (<250 mg/L)
Oct-22
Jul-23
Feb-24
Limit
COD (mg/L)

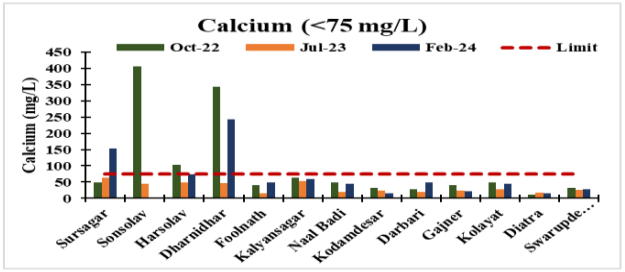
Calcium (<75 mg/L)
Oct-22
Jul-23
Feb-24
Limit
Calcium (mg/L)

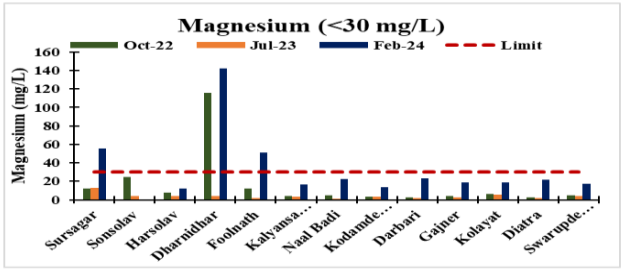
Magnesium (<30 mg/L)
Oct-22
Jul-23
Feb-24
Limit
Magnesium (mg/L)

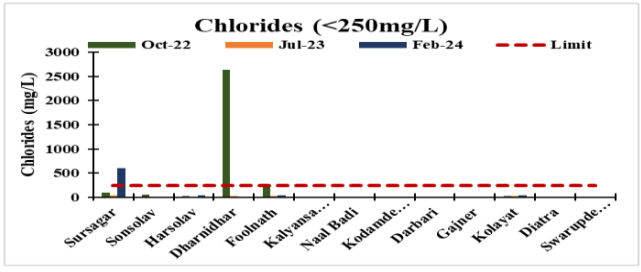
Chlorides (<250mg/L)
Oct-22
Jul-23
Feb-24
Limit
Chlorides (mg/L)

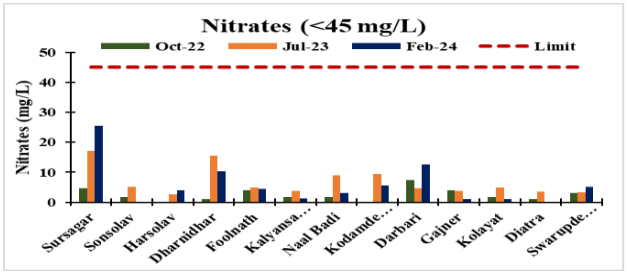
Nitrates (<45 mg/L)
Oct-22
Jul-23
Feb-24
Limit
Nitrates (mg/L)

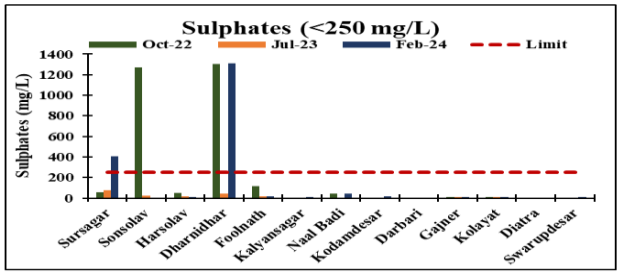
Sulphates (<250 mg/L)
Oct-22
Jul-23
Feb-24
Limit
Sulphates (mg/L)

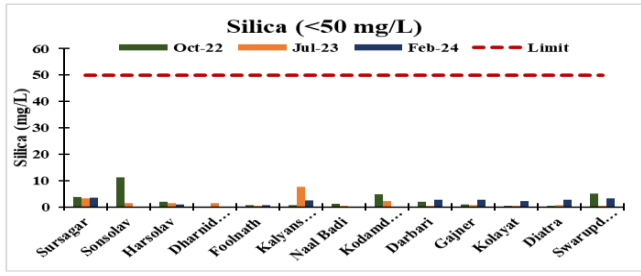
Silica (<50 mg/L)
Oct-22
Jul-23
Feb-24
Limit
Silica (mg/L)

CHAPTER 7

STRATEGIES AND MEAURES ON POND REJUVENATION

Ponds are experiencing severe neglect and deterioration, impacting water security and public health. In rural villages, ponds, which were once vital for water security, irrigation, and groundwater recharge, have fallen into disrepair. These ponds are often filled with various forms of waste, including domestic wastewater and solid refuse, leading to stagnant, foul-smelling water that poses serious health risks. The improper disposal of waste into these ponds not only creates unsightly conditions but also spread waterborne diseases. As a result, ponds have become dump yard and are no more used for drinking or bathing purposes or any other useful purpose. Pond rejuvenation is vital for enhancing environmental health, supporting economic growth, and improving community well-being. It improves water quality by reducing pollutants and sediment, supports diverse wildlife habitats, and aids groundwater recharge. Economically, it boosts agricultural productivity, lowers water treatment costs, and increases property values. Socially, it enhances public health by providing clean water, recreational spaces, and educational opportunities. Additionally, rejuvenated ponds help control erosion, mitigate flood risks, and contribute to climate resilience, making them essential for sustainable water management and overall ecological balance.

Benefits of pond rejuvenation

Pond rejuvenation offers a wide range of environmental, economic, and social benefits. Here are some of the key advantages:

1. Environmental Benefits:

- Improved Water Quality:

o Rejuvenated ponds can have better water quality due to reduced siltation and the removal of pollutants. This helps in sustaining aquatic life and maintaining ecological balance.

- Enhanced Biodiversity:

o Healthy ponds support diverse ecosystems, providing habitat for various species of fish, birds, amphibians, and plants, thereby increasing local biodiversity.

- Groundwater Recharge:

o Properly managed ponds facilitate groundwater recharge by allowing water to percolate into the soil, helping to replenish aquifers and maintain local water tables.

- Soil Erosion Control:

o Rejuvenated ponds, especially with stabilized embankments e.g. stone pitching and surrounding vegetation, help in preventing soil erosion and reducing sediment laden runoff into water bodies.

- Microclimate Regulation:

o Ponds contribute to local microclimate regulation by providing cooling effects and increasing humidity, which can benefit surrounding vegetation and agriculture.

2. Economic Benefits:

- Enhanced Agricultural Productivity:

o Ponds provide a reliable source of water for irrigation during deficit, improving crop yields and enabling farmers to grow multiple crops throughout the year.

- Cost Savings:

o By improving water management and reducing the need for expensive water treatments, rejuvenated ponds can lower water-related costs for communities and agricultural enterprises.

- Increased Property Value:

o Well-maintained ponds can enhance the aesthetic value of properties nearby and increase their market value, benefiting landowners.

- Supporting Local Livelihoods:

o Healthy ponds can support fishing, provide fodder, and create opportunities for eco-tourism and recreational activities, benefiting local economies.

3. Social Benefits:

- Community Well-being:

o Rejuvenated ponds improve access to clean water for drinking, sanitation, and domestic use, contributing to better health and quality of life for local communities.

- Educational Opportunities:

o Ponds can serve as outdoor classrooms for environmental education and awareness, providing learning experiences related to ecology, water management, and conservation.

- Employment Generation:

o Ponds desilting and maintenance activities funded under the National Rural Employment Guarantee Act (NAREGA) generate employment opportunities for rural communities, providing wages and improving local infrastructure.

- Cultural and Recreational Value:

o Ponds often have cultural significance and can be sites for community gatherings, festivals, and recreational activities, which promotes social cohesion and cultural heritage.

- Aesthetic and Psychological Benefits:

o Well-maintained ponds enhance the beauty of the landscape, offering scenic views and recreational spaces.

4. Ecological Restoration:

- Habitat Restoration:

o Rejuvenation efforts restore critical habitats for aquatic and semi-aquatic species, supporting ecosystem resilience and function.

- Natural Flood Control:

o Ponds act as natural buffers during heavy rains by capturing and storing excess water, helping to reduce flooding and manage stormwater.

• Carbon Sequestration:

o Vegetation around rejuvenated ponds can sequester carbon dioxide, contributing to climate change mitigation efforts.

 Suggestive measures of pond rejuvenation based on Rural and Urban area

Pond rejuvenation is essential for maintaining ecological balance, supporting biodiversity, and ensuring sustainable water resources in both urban and rural areas. However, the strategies for rejuvenation may differ based on the specific needs and challenges of urban as well as rural environments. Here are some suggested measures for each:

Urban Areas

1. Pollution Control and Waste Management:

o Wastewater Treatment: Ensure that untreated sewage and industrial effluents are not discharged into ponds. Implement decentralized wastewater treatment systems (like Constructed Wetlands) to treat wastewater before it reaches water bodies.

o Solid Waste Management: Install litter traps and ensure regular cleaning to prevent solid waste from accumulating in ponds. Promote community awareness to reduce littering.

2. Catchment Area Management:

o Green Infrastructure: Implement green roofs, rain gardens, and permeable pavements to reduce runoff and improve water quality entering the pond.

o Stormwater Management: Develop rainwater harvesting systems and recharge wells to reduce surface runoff and increase groundwater recharge.

3. Desilting and Deepening:

o Sediment Removal: Regular desilting of ponds is crucial to maintain depth and water holding capacity. This also helps in removing pollutants accumulated in the sediments.

o Pond Deepening: If feasible, deepen the pond to increase its water retention capacity, which can help during dry periods.

4. Biodiversity Enhancement:

o Plantation of Native Species: Introduce native aquatic plants around the pond to create a buffer zone, which can help in filtering pollutants entering into pond.

o Fish Stocking: Introduce fish species that are compatible with the pond's ecosystem to maintain ecological balance.

5. Community Involvement and Awareness:

o Public Participation: Engage local communities and organizations in the maintenance and monitoring of ponds. Organize awareness campaigns to educate people about the importance of pond conservation.

o Urban Planning Integration: Integrate pond conservation into urban planning processes, ensuring that ponds are protected from encroachment and are considered in development projects.

Rural Areas

1. Agricultural Runoff Management:

o Buffer Strips: Establish vegetation buffer strips around ponds to reduce the flow of fertilizers, pesticides, and sediments from agricultural fields and other non-point sources into the water bodies.

o Contour Ploughing and Terracing: Implement soil conservation practices like contour ploughing, water absorption trenches (WAT), terracing, etc. to reduce soil erosion and damaging surface runoff contributing to erosion.

2. Traditional Water Management Practices:

o Suitable cropping pattern: Re-introducing traditional water management practices, such as the Ahar-Khejri system in Rajasthan, to channelize water into ponds, ensuring both irrigation and groundwater recharge.

o Check Dams and Bunding: Construction of small check dams and bunds to slow down the flow of water, and increasing the opportune time to recharge the groundwater.

3. Desilting and Capacity Enhancement:

o Regular Desilting: Conduct periodic desilting operations to maintain the pond's storage capacity and prevent the buildup of nutrients that could lead to eutrophication.

o Increasing Water Holding Capacity: Expand the pond area where feasible or increase depth to enhance water storage, which can be critical during droughts.

4. Biodiversity and Livelihood Integration:

o Agroforestry: Promote agroforestry practices around ponds to improve soil fertility, enhance biodiversity, and provide additional income to farmers.

o Aquaculture: Introduce sustainable fish farming practices that do not harm the pond ecosystem, providing a livelihood option for local communities.

5. Community-Based Management:

o Pond Management Committees: Establish and empower local pond management committees to oversee the maintenance and rejuvenation of ponds, ensuring community ownership and responsibility. Public-Private Partnership (PPP) mode of pond restoration and rejuvenation should also be promoted in the area.

o Awareness and Training: Conduct training programs for farmers and villagers on sustainable water management practices and the importance of pond conservation and rejuvenation.

 Suggestive measures based on short term and long term approaches

Short-Term Measures for Pond Rejuvenation:

1. Desilting and Cleaning:

o Remove accumulated silt, debris, and vegetation from the pond bed to restore water holding capacity and improve water quality.

o Impact: Immediate increase in pond storage capacity and better water quality.

2. Repair and Strengthening of Bunds:

o Repair any damaged bunds (embankments) to prevent leaks and enhance the pond's structural strength and integrity.

o Impact: Prevents water loss and ensures the pond can hold water effectively during the rainy season.

3. Inlet and Outlet Channel Maintenance:

o Clear and repair inlet and outlet channels to ensure proper water flow into and out of the pond.

o Impact: Facilitates the natural flow of rainwater into the pond and prevents overflow or waterlogging issues.

4. Community Awareness and Engagement:

o Conduct awareness campaigns and involve local communities in pond cleaning and maintenance activities.

o Impact: Immediate engagement of the community ensures better upkeep and protection of the pond with a sense of belongingness.

5. Planting Grass and Shrubs on Embankments:

o Plant grass, shrubs and medicinal herbs on the bunds to prevent soil erosion and reduce siltation in the pond. This also provide nutrional and health benefits to the community.

o Impact: Quickly stabilizes soil, reducing erosion and sedimentation in the pond.

6. Temporary Check Dams and Contour Trenches:

o Construct temporary check dams, contour trenches and WAT upstream to reduce the flow of sediments into the pond.

o Impact: Reduces the amount of silt and debris entering the pond, improving water quality and storage capacity.

7. Water Quality Testing and Treatment:

o Regularly test the water quality and take immediate corrective measures like adding lime or organic matter to neutralize pH and improve water health.

o Impact: Ensures that the pond water is suitable for irrigation, drinking (if applicable), and aquatic life.

Long-Term Measures for Pond Rejuvenation:

1. Watershed Management:

o Implement comprehensive watershed management practices, including afforestation, silvipasture, agro-forestry, contour bunding, WAT, and check dams, to improve the overall eco-hydrology of the area. Livestock management through social fencing is also another important aspect towards upkeep of ponds.

o Impact: Enhances groundwater recharge, reduces soil erosion, and ensures sustainable water availability in the pond over the long term.

2. Reforestation and Agroforestry:

o Plant trees and adopt agroforestry practices around the pond and in the catchment area to improve soil stability and water infiltration.

o Impact: Long-term improvement in water retention and soil health, supporting sustained pond rejuvenation.

3. Establishment of Buffer Zones:

o Create vegetative buffer zones around the pond to filter pollutants and reduce runoff of sediments and nutrients into the pond.

o Impact: Maintains water quality and reduces the frequency of desilting, ensuring the pond remains healthy over time.

4. Rainwater Harvesting Structures:

o Construct permanent rainwater harvesting structures such as check dams, percolation tanks, and recharge wells in the catchment area to increase water availability and groundwater recharge.

o Impact: Enhances the long-term sustainability of the pond by increasing water inflow during the rainy season.

5. Sustainable Agricultural Practices:

o Promote sustainable agricultural practices in the catchment area, such as organic farming, crop rotation, and reduced use of chemical fertilizers and pesticides.

o Impact: Reduces agricultural runoff, which can contaminate the pond, ensuring cleaner and healthier water over time.

6. Legal Protection and Policy Support:

o Advocate for legal protection of ponds and implementation of policies that encourage pond conservation and prevent encroachment.

o Impact: Ensures the long-term preservation of ponds as vital water resources.

7. Community-Based Management Systems:

o Establish community-led management committees for regular monitoring, maintenance, and decision-making related to pond management. Public-Private Partnership (PPP) mode of pond restoration and rejuvenation should also be promoted in the area.

o Impact: Empowers local communities to take ownership of pond rejuvenation efforts, ensuring long-term sustainability and protection.

8. Biodiversity Conservation:

o Promote the conservation of native aquatic and terrestrial species in and around the pond to enhance ecological balance.

o Impact: Supports a healthy ecosystem that contributes to the overall stability and functionality of the pond.

 In-Situ and Ex-Situ Treatment for Pond Rejuvenation

In-Situ Treatment:

In-situ treatment refers to interventions applied directly within the pond or its immediate surroundings. These methods aim to improve the pond's condition without removing the water or disturbing the pond's existing structure.

1. Desilting and Excavation:

o Remove accumulated silt and debris from the pond bed to restore its storage capacity and improve water quality.

o Benefits: Increases water depth, reduces nutrient loading, and enhances aquatic habitat.

2. Aquatic Plant Management:

o Control the growth of invasive aquatic plants like water hyacinth and algae by manual removal or using natural predators.

o Benefits: Improves water quality, increases oxygen levels, and enhances habitat for native species.

3. Nutrient Management:

o Apply natural or organic amendments such as lime or alum to reduce excess nutrients (like phosphorus) in the water.

o Benefits: Controls algal blooms, improves water clarity, and reduces eutrophication.

4. Bio-remediation:

o Introduce beneficial microorganisms or use natural processes to break down organic pollutants and improve water quality.

o Benefits: Reduces harmful substances, enhances nutrient cycling, and improves overall pond health.

5. Water Aeration:

o Use aerators or fountains to increase oxygen levels in the water, which helps to reduce stratification and improve overall water quality.

o Benefits: Supports aerobic decomposition of organic matter and promotes a healthier aquatic environment.

Ex-Situ Treatment:

Ex-situ treatment involves interventions that occur outside of the pond. These methods often include removing materials from the pond for treatment or management.

1. Silt Disposal and Management:

o Remove silt and sediment from the pond and treat or dispose of it appropriately, such as by using it for land reclamation or composting.

o Benefits: Reduces sediment load in the pond and can be used for beneficial purposes like improving soil fertility.

2. Water Filtration:

o Use filtration systems to remove suspended solids and contaminants from pond water before returning it to the pond or using it for irrigation.

o Benefits: Improves water quality and reduces pollution levels in the pond.

3. Sediment Traps:

o Install sediment traps or catchment basins in inflow areas to capture and settle out sediments before they enter the pond.

o Benefits: Reduces sediment load in the pond and improves water quality.

4. Constructed Wetlands:

o Create artificial wetlands designed to treat water before it flows into the pond. These wetlands use plants and natural processes to filter and cleanse water.

o Benefits: Enhances water quality and reduces nutrient and pollutant levels entering the pond.

5. Contour Bunding and Check Dams:

o Construct bunds and small check dams around the pond catchment area to manage runoff and prevent sediment from entering the pond.

o Benefits: Reduces sedimentation, controls erosion, and improves water quality entering the pond.

6. Green or Buffer Zone:

o Buffer Zone around a lake or pond (at least 50 to 100 m periphery) should be maintained as green belt zone. Within the buffer zone, no impervious cover is allowed and mainly plantation with a dense population of deeply rooted plants, trees, shrubs and grasses should be created so as to absorb nutrients that comes directly from the anthropogenic activities.

o Benefits: Quickly stabilizes soil, reducing erosion and sedimentation in the pond.

7. Suitable Agricultural activities:

o Crop management, crop residue management and creation of shelter belts, good Irrigation practices, run off control provisions from agriculture runoff laden with excess fertilizers and pesticides

o Benefits: Reduces agricultural runoff, which can contaminate the pond, ensuring cleaner and healthier water over time.

 Do’s and Don’ts for pond rejuvenation

Do's for Pond Rejuvenation:

1. Implement Integrated Watershed Management programme:

o Manage the surrounding watershed to prevent erosion and reduce runoff into the pond. Practices like afforestation, contour bunding, and check dams help improve water quality and quantity. Ensure implementation of Govts. Programmes through converging local agencies and departments.

2. Desilt the Pond:

o Regularly remove silt and debris from the pond to increase its water-holding capacity and improve water quality.

3. Plant Native Vegetation:

o Introduce native plants and trees such as Khejri, Neem, Babul, Lemon Grass, etc. around the pond to stabilize soil, reduce erosion, and enhance biodiversity.

4. Maintain Inlets and Outlets:

o Ensure that inlets and outlets are clear and functional to allow for the proper flow of water into and out of the pond.

5. Use Organic Methods for Water Treatment:

o Utilize natural or organic methods to treat the pond water, such as using lime to balance pH or adding organic matter to improve water quality.

6. Create Buffer Zones:

o Establish vegetative buffer zones around the pond to filter pollutants and reduce the impact of runoff.

7. Monitor and Maintain Regularly:

o Set up a regular monitoring and maintenance schedule to address issues like siltation, water quality, and structural integrity promptly.

8. Promote Sustainable Agriculture:

o Encourage the adoption of sustainable agricultural practices in the surrounding area to minimize runoff of chemicals and sediments into the pond.

9. Engage the Community:

o Involve local communities in planning, implementing, and maintaining pond rejuvenation projects. Community participation ensures long-term success and sustainability. Promoting PPP mode of implementation.

Don’ts for Pond Rejuvenation:

1. Avoid Encroachment:

o Do not allow encroachment on pond areas or surrounding buffer zones, as it can lead to reduced water capacity and increased pollution.

2. Don't Use Harmful Chemicals:

o Avoid using chemicals such as pesticides, herbicides, or synthetic fertilizers near the pond, as they can contaminate the water and harm aquatic life.

3. Prevent Waste Disposal:

o Do not dispose of solid waste, sewage, or industrial effluents into the pond, as this can severely degrade water quality.

4. Avoid Excessive Construction and mining activities in the catchment:

o Avoid constructing permanent structures and mining activities too close to the pond, as it can disrupt natural water flow and contribute to pollution.

5. Don't Neglect Water Inlets and Outlets:

o Ensure inlets and outlets are not blocked or damaged. Ignoring these can lead to water stagnation and reduced pond functionality.

6. Avoid Non-Native Species:

o Do not introduce non-native or invasive plant species, as they can disrupt the pond's ecosystem and outcompete native species.

7. Don't Over-Desilt:

o Avoid excessive desilting, which can disturb the pond's natural ecosystem. Balance is key to maintaining a healthy pond environment.

8. Prevent Over-Extraction of Water:

o Do not over-extract water from the pond, especially during dry seasons, as it can lead to drying up of the pond and loss of aquatic life.

9. Don't Ignore Local Knowledge:

o Avoid overlooking traditional knowledge and practices related to pond management. Local wisdom can be valuable in effective pond rejuvenation.

 Integration of Government Schemes with Pond Rejuvenation Measures

The suggested measures for pond rejuvenation can be effectively linked to various government schemes that focus on water conservation, rural development, environmental sustainability, and employment generation. Some of these measures align with specific government initiatives are as follows:

1. Desilting and Deepening

• Linked Scheme: MGNREGA (Mahatma Gandhi National Rural Employment Guarantee Act)

- MGNREGA provides employment opportunities for desilting and deepening ponds, enhancing their water storage capacity and contributing to groundwater recharge. The scheme funds labor-intensive activities, making it ideal for such projects.

2. Vegetative Buffer Zones

- Linked Scheme: National Afforestation Programme (NAP) and Green India Mission (GIM)

- These schemes focus on increasing forest cover and promoting afforestation, which can be applied to creating vegetative buffer zones around ponds. They provide resources for planting native trees and shrubs, helping to stabilize soil and prevent erosion.

3. Check Dams and Contour Bunding

- Linked Scheme: Pradhan Mantri Krishi Sinchayee Yojana (PMKSY) – Watershed Development Component

- PMKSY supports the construction of check dams, contour bunding, and other water conservation structures in catchment areas. These measures help in reducing runoff, controlling soil erosion, and improving water availability in ponds.

4. Bio-remediation and Aeration

- Linked Scheme: National River Conservation Plan (NRCP)

- These programs aim at improving water quality through the treatment of polluted water bodies, including ponds. Bio-remediation and aeration techniques are supported under these schemes to rejuvenate aquatic ecosystems and reduce pollution.

5. Wastewater Management

- Linked Scheme: Swachh Bharat Mission (SBM) – Urban and Rural

- Swachh Bharat Mission focuses on the management of solid and liquid waste in rural and urban areas. The scheme can be linked to preventing untreated wastewater from being dumped into ponds and promoting proper sanitation practices.

6. Community Participation and Awareness

- Linked Scheme: Amrit Sarovar Scheme, Jal Shakti Abhiyan and Atal Bhujal Yojana (Atal Jal)

- Amrit Sarovar scheme emphasizes the holistic development and rejuvenation of ponds with a strong focus on community involvement and long-term sustainability. Jal Shakti Abhiyan emphasizes water conservation through community participation and awareness programs. Atal Bhujal Yojana also encourages community involvement in managing groundwater resources, which can be extended to pond rejuvenation activities.

8. Renewable Energy Integration (for Aeration)

- Linked Scheme: KUSUM (Kisan Urja Suraksha Evam Utthaan Mahabhiyan)

- The KUSUM scheme promotes the use of solar energy in agricultural activities. Solar-powered aerators can be implemented under this scheme to improve oxygen levels in ponds, enhancing water quality and supporting aquatic life.

9. Sustainable Agriculture Practices

- Linked Scheme: Paramparagat Krishi Vikas Yojana (PKVY)

- PKVY promotes organic farming and sustainable agriculture. The practices encouraged under this scheme, such as organic farming around pond catchment areas, help in reducing chemical runoff into ponds, thereby maintaining water quality.

Based on the field visits conducted to few existing ponds and findings from the laboratory-based water quality assessment, the following Table 1 provides a summary of the associated problems, its causes and suggestive local measures in rejuvenating the ponds.

Pond name	Problems	Causes	Solutions
Sonsolav, **Harsolav,** **Foolnath**	• Profuse growth of aquatic plants • Algal bloom	The disposal of left-over materials (including flowers, leaves, fruits, grains, oil, rice balls, polythene, etc.) into pond	Restrictions on the disposal of waste matter after any rituals. Alternate arrangements for disposal of solid wastes and arrangements to transfer to goshala (cattle-sheds). This could provide nourishment to milking cattle. Mass sensitization programme involving people.
		Poor management by the local authorities	Provision of constructed wetlands at the entry of the pond. This will facilitate removal of the contaminants entering the pond through run-off.
		Non-maintenance of the pond	• Periodical removal of water plants • Periodical removal of silt
Sursagar	Foul odour	• Enrichment of nutrients especially carbon and nitrogen due to organic and inorganic • Lack of aeration	• Restrictions on the disposal of organic and inorganic matter • Introduce ducks, which will aid in aeration and control of water plants, algae, etc. • Installation of aerator fountains to increase the amount of dissolved oxygen.
	Entry of dirty water into pond	• Overflow from surrounding areas during rainy season.	• Proper drainage facility should be developed. • Rooftop rainwater harvesting from nearby urban infrastructure.
Kodamdesar	Limited water supply to pond	• Issue of encroachment	• Provision of boundary/fencing around the pond for safety purposes • Inlet and outlet of the waterbody to be identified for smooth flow of water to the pond.
	Siltation	• Light texture soil in the area • Idol submersion during the festival	• Management of watershed – arrest deforestation. Planting of native species in the catchment/watershed. • Provision of constructed wetlands at the entry of the pond

			• Complete ban on immersion of idols (painted, plaster of paris idols, etc.) in the pond.
	Abundant growth of aquatic plants	Dumping of organic inorganic waste after Pooja rituals	• Restrictions on the waste disposal into pond. • Regular partial removal of water plants twice a year.
Diyatra	Overflow during rainy season	Siltation Deforestation • Idol submersion during festival (Ganesha, etc.).	• In-situ measures such as desilting, deweeding should be adopted. • Construction of silt trap structure at the pond inlet • Proper inlet and outlet of waterbody to be identify • Provision of wetlands at the entry of the pond which will remove the contaminants entering the pond during run-off • Alternate arrangements for idol immersion
Darbari, Swarupdesar	Seepage	Light texture soil	• Lining should be done
	Siltation	• Deforestation, • Idol immersion	• Planting of natives species in the catchment/watershed. • Alternate arrangements for idol immersion
Dharnidhar	Presence of bad odour	• Enrichment of nutrients (Sodium, Phosphorous) – due to Bathing (soap, etc.) • Washing of clothes with detergents – introduces phosphorous into the ponds, which trigger algal growth	• Sensitizing local people to avoid using soaps and detergents •

Kolayat	Health problems (of people using water), turbidity in water, algal bloom, and bad odour.	• Disposal of organic,inorganic and left-over materials (including flowers, leaves, fruits, grains, oil, rice balls, polythene, etc.) into the pond. • Leakages from the nearby septic tanks/ community drains.	• Restriction on disposal of waste into pond • Conservation measures for stabilizing and plugging cracks and other defects in the embankments.
	Accumulation of heavy metals	Mining activity in the catchment	Ensuring implementation of non-damaging, non-hazardous and environment-friendly mining activities particularly in the catchment area draining into the pond
Gajner	Abundant Growth of aquatic plants	Effluent disposal from nearby area	Proper water treatment measures before disposal

Chapter 8

CONCLUSION AND SUMMARY

This study investigates Hydrological Study for Revival and Restoration of Traditional Water Bodies in Bikaner, Rajasthan, with the aim to tackle the issues and challenges focusing three dimensions namely recognition (inventory), restoration (hydrological study) and protection (suggestive measures) of the traditional waterbodies in the Bikaner falling in an arid region part of Thar Desert region of Rajasthan, and further developing strategies for their revival and restoration. Thirteen representative pilot water bodies were selected for detailed investigation by integrating the remote sensing, GIS techniques, field surveys, and laboratory analysis**.** Multi-temporal satellite imagery in GIS environment, and field observations were supportive in the processing the digital elevation model (DEM) for catchment delineation of the water bodies, extracting land use/land cover (LULC) and soil erosion dynamics. Moreover, in the present study rainfall and temperature trends, groundwater dynamics, infiltration rates, runoff estimation, soil erosion modeling, and water quality assessments were undertaken. Results indicate a non-significant rise in rainfall and maximum temperature, but a significant increase in minimum temperature from 1951–2020. LULC analysis revealed an expansion of built-up areas and vegetation, with relatively stable water body extents. Groundwater showed rising trends near the IGNP command area but declining levels in southern blocks. Most water quality parameters were within permissible limits, though heavy metal concentrations (Al, Fe, Mn, Pb, B) exceeded standards in some samples. Soil analysis showed sandy texture with moderate infiltration capacity. Socio-cultural and anthropogenic practices such as idol immersion, waste dumping, and agricultural runoff were found to contribute significantly to degradation. The study emphasizes adaptive management measures such as wetland construction, catchment treatment, waste regulation, and community participation for sustainable restoration. The revival and restoration efforts must be holistic, combining the (a) Hydrological Interventions involving construction of recharge structures, desilting, and catchment treatment (b) Ecological Measures by creation of constructed wetlands, biodiversity restoration, and protection of natural inflows (c) Community Engagement which may involve public awareness programs, involvement of local stakeholders, and regulation of idol and related organic offerings immersion and waste disposal and (d) policy Integration which in necessary for linking rejuvenation efforts with government schemes Atal Mission for Rejuvenation and Urban Transformation (AMRUT), National Plan for Conservation of Aquatic Ecosystems (NPCA) Jal Shakti Abhiyan (JSA). Adopting these measures will be helpful for the revival and

restoration of Bikaner's traditional waterbodies and serve as sustainable sources of water, ecological buffers, and cultural heritage sites, thereby strengthening resilience in this arid district.

Limitations

Despite providing a comprehensive hydrological assessment, the study has certain limitations. Higher resolution digital elevation model may be more helpful especially for delineating the watershed of water bodies located in urban area or having the physical survey. The consistent monitoring of water bodies for data on like the pond surface area, inflow and out flows, seasonal water quality and social-cultural usage.

REFERENNCES

Homogeneity and Trend assessment

Basseville, M., & Nikiforov, I. V. (1993). *Detection of abrupt changes: theory and application* (Vol. 104).

Lai, T. L. (1995). Sequential changepoint detection in quality control and dynamical systems. Journal of the Royal Statistical Society: Series B (Methodological), 57(4), 613-644.

Chen, J., & Gupta, A. K. (2001). On change point detection and estimation. Communications in statistics-simulation and computation, 30(3), 665-697.

Liao, T. W. (2005). Clustering of time series data—a survey. Pattern recognition, 38(11), 1857-1874.

Silvestrini, A., & Veredas, D. (2008). Temporal aggregation of univariate and multivariate time series models: a survey. Journal of Economic Surveys, 22(3), 458-497. https://doi.org/10.1111/j.1467-6419.2007.00538.x

Yue, S., & Hashino, M. (2003). Long term trends of annual and monthly precipitation in Japan 1. JAWRA Journal of the American Water Resources Association, 39(3), 587-596. https://doi.org/10.1111/j.1752-1688.2003.tb03677.x

Buishand, T. A. (1984). Tests for detecting a shift in the mean of hydrological time series. Journal of hydrology, 73(1-2), 51-69.

Serra, C., Burgueno, A., & Lana, X. (2001). Analysis of maximum and minimum daily temperatures recorded at Fabra Observatory (Barcelona, NE Spain) in the period 1917–1998. International Journal of Climatology: A Journal of the Royal Meteorological Society, 21(5), 617-636.

Basher, M. A., Stiller-Reeve, M. A., Saiful Islam, A. K. M., & Bremer, S. (2018). Assessing climatic trends of extreme rainfall indices over northeast Bangladesh. Theoretical and Applied Climatology, 134, 441-452. https://doi.org/10.1007/s00704-017-2285-4

Patakamuri, S. K., Muthiah, K., & Sridhar, V. (2020). Long-term homogeneity, trend, and change-point analysis of rainfall in the arid district of Ananthapuramu, Andhra Pradesh State, India. Water, 12(1), 211. https://doi.org/10.3390/w12010211

Yildirim, G., & Rahman, A. (2022). Homogeneity and trend analysis of rainfall and droughts over Southeast Australia. Natural Hazards, 112(2), 1657-1683. https://doi.org/10.1007/s11069-022-05243-9

Marengo, J. A., & Camargo, C. C. (2008). Surface air temperature trends in Southern Brazil for International Journal of Climatology, 28, 893-904.

Mann HB (1945) Nonparametric tests against trend. Econometrica. 13:245. https://doi.org/10.2307/1907187

Kendall MG (1957) Rank correlation methods. Biometrika. 44:298. https://doi.org/10.2307/2333282

Mauget, S. A. (2004). Low frequency streamflow regimes over the central United States: 1939–1998. Climatic Change, 63(1), 121-144. https://doi.org/10.1023/B:CLIM.0000018502.86522.57

Su, J. G., Brauer, M., Ainslie, B., Steyn, D., Larson, T., & Buzzelli, M. (2008). An innovative land use regression model incorporating meteorology for exposure analysis. Science of the total environment, 390(2-3), 520-529. https://doi.org/10.1016/j.scitotenv.2007.10.032

Fealy, R., & Sweeney, J. (2005). Detection of a possible change point in atmospheric variability in the North Atlantic and its effect on Scandinavian glacier mass balance. International Journal of Climatology, 25(14), 1819-1833. https://doi.org/10.1002/joc.1231

Elsner, J. B., Niu, X., & Jagger, T. H. (2004). Detecting shifts in hurricane rates using a Markov chain Monte Carlo approach. *Journal of climate*, *17*(13), 2652-2666. https://doi.org/10.1175/1520-0442(2004)017%3C2652:DSIHRU%3E2.0.CO;2

Bates, B. C., Chandler, R. E., Charles, S. P., & Campbell, E. P. (2010). Assessment of apparent nonstationarity in time series of annual inflow, daily precipitation, and atmospheric circulation indices: A case study from southwest Western Australia. Water resources research, 46(3). https://doi.org/10.1029/2010WR009509

Hirsch, R. M., Slack, J. R., & Smith, R. A. (1982). Techniques of trend analysis for monthly water quality data. Water resources research, 18(1), 107-121. https://doi.org/10.1029/WR018i001p00107

Parthasarathy, B., & Dhar, O. N. (1974). Secular variations of regional rainfall over India. Quarterly Journal of the Royal Meteorological Society, 100(424), 245-257. https://doi.org/10.1002/qj.49710042411

IPCC, 2001: Climate Change 2001: The Scientific Basis. Contribution of Working Group I to the Third Assessment Report of the Intergovernmental Panel on Climate Change [Houghton, J.T., Y. Ding, D.J. Griggs, M. Noguer, P.J. van der Linden, X. Dai, K. Maskell, and C.A. Johnson (eds.)]. Cambridge University Press, Cambridge, United Kingdom and New York, NY, USA, 881pp.

Martínez Santafé, M. D., Serra de Larrocha, C., Burgueño, A., & Lana Pons, F. J. (2010). Time trends of daily maximum and minimum temperatures in Catalonia (ne Spain) for the period 1975-2004. International Journal of Climatology, 30, 267-290. https://doi.org/10.1002/joc.1884

Salarijazi, M., Akhond-Ali, A. M., Adib, A., & Daneshkhah, A. (2012). Trend and change-point detection for the annual stream-flow series of the Karun River at the Ahvaz hydrometric station. African Journal of Agricultural Research, 7(32), 4540-4552. https://doi.org/10.5897/AJAR12.650

Adarsh, S., & Reddy, M. J. (2015). Trend analysis of rainfall in four meteorological subdivisions of southern India using nonparametric methods and discrete wavelet transforms. International journal of Climatology, 35(5). https://doi.org/10.1002/joc.4042

Chakraborty, I., & Pradeep, T. (2017). Atomically precise clusters of noble metals: emerging link between atoms and nanoparticles. Chemical reviews, 117(12), 8208-8271. https://doi.org/10.1021/acs.chemrev.6b00769

Deoli, V., & Rana, S. (2019). Seasonal trend analysis in rainfall and temperature for Udaipur district of Rajasthan. Current World Environment, 14(2), 312. http://dx.doi.org/10.12944/CWE.14.2.15

Sharma, S. K., Sharma, D. P., Sharma, M. K., Gaur, K., & Manohar, P. (2021). Trend analysis of temperature and rainfall of Rajasthan, India. Journal of Probability and Statistics, 2021(1), 6296709. https://doi.org/10.1155/2021/6296709

Mehta, D., Waikhom, S., Yadav, V., Lukhi, Z., Eslamian, S., & Furze, J. N. (2022). Trend analysis of rainfall: A case study of Surat City in Gujarat, Western India. In Earth Systems Protection and Sustainability: Volume 2 (pp. 191-202). https://doi.org/10.1007/978-3-030-98584-4_8

Mehta, D. J., & Yadav, S. M. (2022). Long-term trend analysis of climate variables for arid and semi-arid regions of an Indian State Rajasthan. International Journal of Hydrology Science and Technology, 13(2), 191-214. https://doi.org/10.1504/IJHST.2022.120639

Nath, S., Mathew, A., Khandelwal, S., & Shekar, P. R. (2023). Rainfall and temperature dynamics in four Indian states: A comprehensive spatial and temporal trend analysis. HydroResearch, 6, 247-254. https://doi.org/10.1016/j.hydres.2023.09.001

- **Waterbody inventory**

Roberts, N., Taieb, M., Barker, P., Damnati, B., Icole, M., and Williamson, D. (1993). Timing of the Younger Dryas event in East Africa from lake-level changes. Nature, vol.366, pp. 146–148.

Voeroesmarty, C. J., Meybeck, M., Fekete, B., & Sharma, K. (1997). The potential impact of neo-Castorization on sediment transport by the global network of rivers. IAHS Publication, 246, 261-273.

Bastiaanssen, W. G., Molden, D. J., & Makin, I. W. (2000). Remote sensing for irrigated agriculture: examples from research and possible applications. Agricultural water management, 46(2), 137-155. https://doi.org/10.1016/S0378-3774(00)00080-9

Prasad, S. N., Ramachandra, T. V., Ahalya, N., Sengupta, T., Kumar, A., Tiwari, A. K., Vijayan, V.S. and Vijayan, L. (2002). Conservation of wetlands of India-a review. *Tropical Ecology*, *43*(1), 173-186.

Suresh, K. J. (2016). Utilization of remote sensing and gis for mapping of natural resource-on water resource action plan and prioritization for Yagachi watershed Hassan district. ATMECE.

Verpoorter, C., Kutser, T., Seekell, D. A., & Tranvik, L. J. (2014). A global inventory of lakes based on high-resolution satellite imagery. Geophysical Research Letters, 41(18), 6396-6402. https://doi.org/10.1002/2014GL060641

Terasmaa, J., Bartout, P., Marzecova, A., Touchart, L., Vandel, E., Koff, T., Choffel, Q., Kapanen, G., Maleval, V., Vainu, M. and Millot, C. (2019). A quantitative assessment of

the contribution of small standing water bodies to the European waterscapes–case of Estonia and France. Heliyon, 5(9).

Tyagi, N., & Sahoo, S. (2022). Assessing the status of changing regimes of water bodies in Gorakhpur District, Uttar Pradesh, India. Environmental Monitoring and Assessment, 194(2), 67. https://doi.org/10.1007/s10661-021-09630-w

Subramaniam, S., Babu, A. S., & Roy, P. S. (2010). Automated water spread mapping using ResourceSat-1 AWiFS data for water bodies information system. IEEE Journal of Selected Topics in Applied Earth Observations and Remote Sensing, 4(1), 205-215.

- **Land Use Land Cover Detection**

Singh, N. P., Mukherjee, T. K., & Shrivastava, B. B. P. (1997). Monitoring the impact of coal mining and thermal power industry on landuse pattern in and around Singrauli coalfield using remote sensing data and GIS. Journal of the Indian Society of Remote Sensing, 25, 61-72.

Sarma, K., & Kushwaha, S. P. S. (2005, March). Coal mining impact on land use/land cover in Jaintia hills district of Meghalaya, India using remote sensing and GIS technique. In Conference Proceeding of National Conference on Geospatial Technologies, Geomatrix (Vol. 9, No. 2005, pp. 28-43).

Mundia CN, Aniya M (2006). Dynamics of land use / cover changes and degradation of Nairobi city, Kenya. Land Degrad. Dev., 17: 97-108. https://doi.org/10.1002/ldr.702

Abbasi, H. U., Baloch, M. A., & Memon, A. G. (2011). Deforestation analysis of riverine forest of sindh using remote sensing techniques. Mehran University Research Journal of Engineering & Technology, 30(3).

Elhag, M., Psilovikos, A., & Sakellariou-Makrantonaki, M. (2013). Land use changes and its impacts on water resources in Nile Delta region using remote sensing techniques. Environment, development and sustainability, 15, 1189-1204. https://doi.org/10.1007/s10668-013-9433-5

Vorovencii, I. (2014). Assessment of some remote sensing techniques used to detect land use/land cover changes in South-East Transilvania, Romania. Environmental monitoring and assessment, 186, 2685-2699. https://doi.org/10.1007/s10661-013-3571-y

Patra, S., Sahoo, S., Mishra, P., & Mahapatra, S. C. (2018). Impacts of urbanization on land use/cover changes and its probable implications on local climate and groundwater level. Journal of urban management, 7(2), 70-84. https://doi.org/10.1016/j.jum.2018.04.006

Vivekananda, G. N., Swathi, R., & Sujith, A. V. L. N. (2021). Multi-temporal image analysis for LULC classification and change detection. European journal of remote sensing, 54(sup2), 189-199. https://doi.org/10.1080/22797254.2020.1771215

Patel, A., Vyas, D., Chaudhari, N., Patel, R., Patel, K., & Mehta, D. (2024). Novel approach for the LULC change detection using GIS & Google Earth Engine through spatiotemporal analysis to evaluate the urbanization growth of Ahmedabad city. Results in Engineering, 21, 101788. https://doi.org/10.1016/j.rineng.2024.101788

Gupta, P., Singh, S. K., Gupta, P., Kanga, S., & Mishra, V. N. (2023). Application of Remote Sensing and GIS Techniques for Identification of Changes in Land Use and Land Cover (LULC): A Case Study. Indian Journal of Science and Technology, 16(46), 4456-4468. https://doi.org/10.17485/IJST/v16i46.2530

Chauhan, N., Paliwal, R., Kumar, V., Kumar, S., & Kumar, R. (2022). Watershed prioritization in lower Shivaliks region of India using integrated principal component and hierarchical cluster analysis techniques: A case of upper Ghaggar watershed. Journal of the Indian Society of Remote Sensing, 50(6), 1051-1070. https://doi.org/10.1007/s12524-022-01519-6

- **Runoff Estimation using Curve Number**

Banasik K. (1994). Model sedymentogramu wezbrania opadowego w małej zlewni rolniczej (Sedimentgraph Model of Rainfall Event in a Small Agricultural Watershed) (in Polish with an English summary), Publication of Warsaw Agricultural University – SGGW, p. 120.

Chormanski, J., Okruszko, T., Ignar, S., Batelaan, O., Rebel, K. T., & Wassen, M. J. (2011). Flood mapping with remote sensing and hydrochemistry: A new method to distinguish the origin of flood water during floods. Ecological Engineering, 37(9), 1334-1349. https://doi.org/10.1016/j.ecoleng.2011.03.016

Soil Conservation Service (1972). National Engineering Handbook Section 4: Hydrology.

Schneiderman, E. M., Steenhuis, T. S., Thongs, D. J., Easton, Z. M., Zion, M. S., Neal, A. L., Mendoza, G.F. and Todd Walter, M. (2007). Incorporating variable source area hydrology into a curve-number-based watershed model. Hydrological Processes: An International Journal, 21(25), 3420-3430. https://doi.org/10.1002/hyp.6556

Ali, S., Ghosh, N. C., & Singh, R. (2010). Rainfall–runoff simulation using a normalized antecedent precipitation index. Hydrological Sciences Journal–Journal des Sciences Hydrologiques, 55(2), 266-274. https://doi.org/10.1002/hyp.6556

Sahu, R. K., Mishra, S. K., & Eldho, T. I. (2012). Performance evaluation of modified versions of SCS curve number method for two watersheds of Maharashtra, India. ISH Journal of Hydraulic Engineering, 18(1), 27-36. https://doi.org/10.1080/09715010.2012.662425

Williams, J. R., Kannan, N., Wang, X., Santhi, C., & Arnold, J. G. (2012). Evolution of the SCS runoff curve number method and its application to continuous runoff simulation. Journal of Hydrologic Engineering, 17(11), 1221-1229. https://doi.org/10.1061/(ASCE)HE.1943-5584.0000529

Kim, N. W., & Shin, M. J. (2018). Estimation of peak flow in ungauged catchments using the relationship between runoff coefficient and curve number. Water, 10(11), 1669. https://doi.org/10.3390/w10111669

Verma, S., Mishra, S. K., & Verma, R. K. (2020). Improved runoff curve numbers for a large number of watersheds of the USA. Hydrological Sciences Journal, 65(16), 2658-2668. https://doi.org/10.1080/02626667.2020.1832676

Neitsch, S. L., Arnold, J. G., Srinivasan, R., & Grassland, S. (2002). Pesticides fate and transport predicted by the soil and water assessment tool (SWAT). Atrazine, Metolachlor and Trifluralin in the Sugar Creek Watershed: BRC Report, 3.

Gassman, P. W., Sadeghi, A. M., & Srinivasan, R. (2014). Applications of the SWAT model special section: overview and insights. Journal of Environmental Quality, 43(1), 1-8. https://doi.org/10.2134/jeq2013.11.0466

Arnold, J. G., Moriasi, D. N., Gassman, P. W., Abbaspour, K. C., White, M. J., Srinivasan, R., Santhi, C., Harmel, R.D., Van Griensven, A., Van Liew, M.W. and Kannan, N. (2012). SWAT: Model use, calibration, and validation. *Transactions of the ASABE*, *55*(4), 1491-1508. https://doi.org/10.13031/2013.42256

Krysanova, V., & White, M. (2015). Advances in water resources assessment with SWAT—an overview. Hydrological Sciences Journal, 60(5), 771-783. https://doi.org/10.1080/02626667.2015.1029482

Hawkins, R. H. (1979). Runoff curve numbers form partial area watersheds. Journal of the Irrigation and Drainage Division, 105(4), 375-389.

Hjelmfelt Jr, A. T. (1991). Investigation of curve number procedure. Journal of Hydraulic Engineering, 117(6), 725-737.

Boughton, W. C. (1989). A review of the USDA SCS curve number method. Soil Research, 27(3), 511-523.

Bhola, P., & Singh, A. (2010). Rainfall-runoff modeling of River Kosi using SCS-CN Method and ANN (Doctoral dissertation).

Somashekar, R. K., Ravikumar, P., Sowmya, S. V., Dar, M. A., & Ravikumar, A. S. (2011). Runoff estimation and morphometric analysis for Hesaraghatta watershed using IRS–1D LISS III FCC satellite data. Journal of the Indian Society of Remote Sensing, 39, 95-106. https://doi.org/10.1007/s12524-011-0074-6

Nagarajan, N., Poongothai, S., & Arutchelvan, V. (2013). Impact of land use/land cover changes on surface runoff from a rural watershed, Tamilnadu, India. International Journal of Water, 7(1-2), 122-141. https://doi.org/10.1504/IJW.2013.051982

Dwivedi, P., Mishra, A., Karwariya, S., Goyal, S., & Thomas, T. (2017). SCS-CN method for surface runoff calculation of agricultural watershed area of Bhojtal. SGVU Journal of Climate Change and Water, 1(2), 9-12.

Ponce, V. M., & Hawkins, R. H. (1996). Runoff curve number: Has it reached maturity?. Journal of hydrologic engineering, 1(1), 11-19.

Mishra, S. K., Singh, V. P., Sansalone, J. J., & Aravamuthan, V. (2003). A modified SCS-CN method: characterization and testing. Water Resources Management, 17, 37-68. https://doi.org/10.1023/A:1023099005944

Bonta, J. V. (1997). Determination of watershed curve number using derived distributions. Journal of Irrigation and Drainage Engineering, 123(1), 28-36.

Jain, M. K., Mishra, S. K., & Singh, V. P. (2006). Evaluation of AMC-dependent SCS-CN-based models using watershed characteristics. Water Resources Management, 20, 531-552. https://doi.org/10.1007/s11269-006-3086-1

- **Water Quality Assessment**

Fokmare A. K. and Musaddiq M. (2001): Comparative studies of physicochemical and Bacteriological quality of surface and ground water at Akola (M.S.), Pollution Research, Vol. 20 (4) PP. 651-665.

Sood, A., Singh, K. D., Pandey, P., & Sharma, S. (2008). Assessment of bacterial indicators and physicochemical parameters to investigate pollution status of Gangetic river system of Uttarakhand (India). Ecological Indicators, 8(5), 709-717. https://doi.org/10.1016/j.ecolind.2008.01.001

Rajkumar, B., & Sharma, G. D. (2013). Seasonal bacteriological analysis of Barak River, Assam, India. Applied Water Science, 3, 625-630. https://doi.org/10.1007/s13201-013-0120-3

Bartone, C. R., Bernstein, J., & Leitmann, J. (1992, November). Managing the environmental challenge of Mega-Urban Regions. In International Conference on Managing the Mega-Urban Regions of ASEAN Countries: Policy Challenges and Responses. Bangkok: Asian Institute of Technology (Vol. 30).

Sharma, U. C. (2003). Impact of population growth and climate change on the quantity and quality of water resources in the northeast of India. International Association of Hydrological Sciences, Publication, 281, 349-357.

Robertson, P. (2006). The influence of Agricultural land use and the mediating effect of Riparian vegetation on water quality in Jones Creek, Alberta, Canada. Enquiries Journal of Interdisciplinary Studies for High School Students, 2(1), 13-24.

Huang, J., Zhan, J., Yan, H., Wu, F., & Deng, X. (2013). Evaluation of the impacts of land use on water quality: a case study in the Chaohu Lake Basin. The Scientific World Journal, 2013(1), 329187. https://doi.org/10.1155/2013/329187

Chauhan, S., & Bhardwaj, S. K. (2017). Effect of different land use on quality of water in Solan Block of Himachal Pradesh. Indian Journal of Ecology, 44(4), 808-812.

Ghosh, M. K., Ghosh, S., & Tiwari, R. (2013). A study of water quality index assessment of ground water and pond water in Sirsakala village of bhilai-3, Chhattisgarh, India. International Journal of Civil, Structural, Environmental and Infrastructure Engineering Research and Development, 3(5), 65-76.

Lawniczak, A. E., Zbierska, J., Nowak, B., Achtenberg, K., Grześkowiak, A., & Kanas, K. (2016). Impact of agriculture and land use on nitrate contamination in groundwater and running waters in central-west Poland. Environmental monitoring and assessment, 188, 1-17. https://doi.org/10.1007/s10661-016-5167-9

Pandey, J., Shubhashish, K., & Pandey, R. (2010). Heavy metal contamination of Ganga river at Varanasi in relation to atmospheric deposition. Tropical Ecology, 51(2), 365-373.

Dev, R., & Bali, M. (2019). Evaluation of groundwater quality and its suitability for drinking and agricultural use in district Kangra of Himachal Pradesh, India. Journal of the Saudi society of agricultural sciences, 18(4), 462-468. https://doi.org/10.1016/j.jssas.2018.03.002

Saini, D., & Dube, K. K. To study the water quality status of river Narmada with special reference to BOD and COD at Jabalpur region in MP (India).

Chen, Q., Lu, Z., Zhang, X., Wang, Q., & Xin, S. (2019). Study on the accumulation characteristics and conduction trend of water environment risk from Taizihe River Basin, China. Ecotoxicology, 28, 619-630. https://doi.org/10.1007/s10646-019-02058-6

Khan, I. I., & Hazarika, A. K. (2012). Study of some water quality parameters of Kolong riverine system of Nagaon, India. The Clarion-International Multidisciplinary Journal, 1(2), 121-129.

Arora, N. K., Tewari, S., & Singh, S. (2013). Analysis of water quality parameters of river Ganga during Maha kumbha, Haridwar, India. Journal of environmental biology, 34(4), 799-803.

Rout, C., & Sharma, A. (2011). Assessment of drinking water quality: A case study of Ambala cantonment area, Haryana, India. International journal of environmental sciences, 2(2), 933-945.

Singh, S., Tanvir Hassan, S. M., Hassan, M., & Bharti, N. (2020). Urbanisation and water insecurity in the Hindu Kush Himalaya: insights from Bangladesh, India, Nepal and Pakistan. Water Policy, 22(S1), 9-32. https://doi.org/10.2166/wp.2019.215

Downing, J. A., Prairie, Y. T., Cole, J. J., Duarte, C. M., Tranvik, L. J., Striegl, R. G., McDowell, W.H., Kortelainen, P., Caraco, N.F., Melack, J.M. and Middelburg, J. J. (2006). The global abundance and size distribution of lakes, ponds, and impoundments. Limnology and oceanography, 51(5), 2388-2397. https://doi.org/10.4319/lo.2006.51.5.2388

Riley, W. D., Potter, E. C., Biggs, J., Collins, A. L., Jarvie, H. P., Jones, J. I., Kelly-Quinn, M., Ormerod, S.J., Sear, D.A., Wilby, R.L. and Siriwardena, G. M. (2018). Small Water Bodies in Great Britain and Ireland: Ecosystem function, human-generated degradation, and options for restorative action. Science of the total environment, 645, 1598-1616. https://doi.org/10.1016/j.scitotenv.2018.07.243

Ministry of Jal Shakti. (2023). Annual Report 2023-24: Department of Water Resources, River Development and Ganga Rejuvenation. Government of India.

United Nations World Water Development Report 2018: Nature-Based Solutions for Water. Paris, UNESCO.

Yadav, S., Yoneda, M., Tamura, M., Susaki, J., Ishikawa, K., & Yamashiki, Y. (2017). A satellite-based assessment of the distribution and biomass of submerged aquatic vegetation in the optically shallow basin of Lake Biwa. Remote Sensing, 9(9), 966. https://doi.org/10.3390/rs9090966

Wang, Y., Lu, S., Zi, F., Tang, H., Li, M., Li, X., Fang, C. and Ikhumhen, H. O. (2022). Artificial and Natural Water Bodies Change in China, 2000–2020. Water, 14(11), 1756. https://doi.org/10.3390/w14111756

Guareschi, S., Laini, A., Viaroli, P., & Bolpagni, R. (2020). Integrating habitat-and species-based perspectives for wetland conservation in lowland agricultural landscapes. Biodiversity and Conservation, 29(1), 153-171. https://doi.org/10.1007/s10531-019-01876-8

Doi, H., & Nakamura, K. (2023). Environmental DNA as a practical tool for aquatic conservation and restoration. Landscape and Ecological Engineering, 19(1), 1-2. https://doi.org/10.1007/s11355-022-00534-6

Moore, T. L., & Hunt, W. F. (2012). Ecosystem service provision by stormwater wetlands and ponds–a means for evaluation?. Water research, 46(20), 6811-6823. https://doi.org/10.1016/j.watres.2011.11.026

Oertli, B., & Parris, K. M. (2019). Toward management of urban ponds for freshwater biodiversity. Ecosphere, 10(7), e02810. https://doi.org/10.1002/ecs2.2810

Yadav, S., & Goyal, V. C. (2022). Current status of ponds in India: a framework for restoration, policies and circular economy. *Wetlands*, *42*(8), 107. https://doi.org/10.1007/s13157-022-01624-9